University of Bath

PHD

Development of a Novel PVA-PLGA Hollow Fibre Bioreactor for Tissue Engineering

Meneghello, Giulia

Award date:
2010

Awarding institution:
University of Bath

Link to publication

Alternative formats
If you require this document in an alternative format, please contact:
openaccess@bath.ac.uk

Copyright of this thesis rests with the author. Access is subject to the above licence, if given. If no licence is specified above, original content in this thesis is licensed under the terms of the Creative Commons Attribution-NonCommercial 4.0 International (CC BY-NC-ND 4.0) Licence (https://creativecommons.org/licenses/by-nc-nd/4.0/). Any third-party copyright material present remains the property of its respective owner(s) and is licensed under its existing terms.

Take down policy
If you consider content within Bath's Research Portal to be in breach of UK law, please contact: openaccess@bath.ac.uk with the details. Your claim will be investigated and, where appropriate, the item will be removed from public view as soon as possible.

Download date: 06. May. 2023

DEVELOPMENT OF A NOVEL PVA-PLGA HOLLOW FIBRE BIOREACTOR FOR TISSUE ENGINEERING

Giulia Meneghello

A thesis submitted for the Degree of Doctor of Philosophy

University of Bath

Department of Pharmacy and Pharmacology

July 2010

COPYRIGHT

Attention is drawn to the fact that copyright of this thesis rests with its author. A copy of this thesis has been supplied on condition that anyone who consults it is understood to recognise that its copyright rests with the author and they must not copy it or use material from it except as permitted by law or with the consent of the author.

This thesis may be available for consultation within the University Library and may be photocopied or lent to other libraries for the purposes of consultation.

Table of Contents

Acknowledgements

I would like to thank Dr Paul De Bank for his supervision, support and guidance thoughout all my experiments and during my thesis drafting and Dr Marianne Ellis for advice on the engineering aspects of the project. I also acknoledge all the members from the tissue engineering group, and in particular Dr Richard Forsey, Dr Holly Shearer, Dr Ben Ainsworth and Dr Chris Gribbon for their suggestions and help during the first stage of my PhD, and the PhD students Steve Wu, Marina Kramer and Adam Davidson for the wonderful time we spent together at work but also outside the lab. I also would like to thank the Marie Curie fellows Luca Orlando and Michael Buchholz because their help has been fundamental during the last stage of my experimental work. I finally would like to acknowledge the technicians that have helped me with the learning of new techniques, in particular Fernando Acosta in the Department of Chemical Engineering, Anne O'Reilly and Adrian Rogers in the centre for Electron and Optical Studies, and Richard Weston in the Department of Mechanical Engineering.

I thank the Marie Curie fellowship for the financial support that has made this work possible and Dr Alan Wheals for coordinating the Marie Curie program.

I thank my parents for supporting me for my entire time abroad, I am eternally grateful to them for everything they have done and do for me.

I finally would like to thank all the wonderful friends that have made during my time at the University of Bath, as they have made my last years the most unforgettable period of my life.

Abstract

Tissue engineering offers a potential alternative therapy to overcome the limitations of organ transplantation, by employing biomaterials as scaffold for cell growth. For example, poly-lactic-co-glycolic acid (PLGA) is a synthetic biomaterial widely used in tissue engineering. However, the hydrophobicity of PLGA results in scaffolds that are poorly wettable, and which, therefore, possess poor mass transfer properties for the delivery of nutrients and the removal of waste. The present work aimed to develop more hydrophilic PLGA scaffolds, specifically hollow fibre membranes, within a bioreactor system, which enables co-culture of cells in order to direct stem cell differentiation. Large quantities of costly growth factors are required over long periods for stem cell differentiation. Therefore, this project also aimed to use a cell line as a "factory" for the inexpensive, *in situ* growth factor production. Hollow fibres were fabricated by wet spinning and a hydrophilic polymer, polyvinyl alcohol (PVA), was added to the PLGA solution at three different concentrations (1.25, 2.5, 5% w/w) in order to obtain a more hydrophilic membrane. Results indicated that 5% PVA-PLGA hollow fibres were the only membranes which allowed permeation of water, BSA and cell-secreted hepatocyte growth factor (HGF), thus indicating that they are the most suitable membranes for use in bioreactor devices. However, these membranes failed to improve cell-attachment. Cell secreted HGF was shown to be more stable in a dynamic culture environment than commercial HGF, thus suggesting its suitability for applications in bioreactor devices. However, using both commercial and cell-secreted HGF, mesenchymal stem cell differentiation was unsuccessful. In conclusion, this work has developed a hollow fibre membrane which is more permeable to water and proteins for a higher mass transfer of nutrients, and has realised a model system for the inexpensive production of growth factors for use in bioreactor devices and the differentiation of stem cells.

List of abbreviations

ANOVA	Analysis of variance
BMP	Bone morphogenetic protein
BSA	Bovine serum albumin
CFDA SE	Carboxyflurescein diacetate succinimidyl ester
CO_2	Carboxyl dioxide
dbcAMP	Dibutyryl cyclic adenosine monophosphate
DMEM	Dulbecco's modified Eagles's medium
DMSO	Dimethyl sulfoxide
ECM	Extracellular matrix
EDTA	Ethylenediamine tetraacetic acid
ESCs	Embryonic stem cells
FCS	Foetal calf serum
FDA	Food and Drug Administration
FITC	Fluorescein Isothiocyanate
FGF	Fibroblast growth factor
HGF	Hepatocyte growth factor
HL60s	Human leukaemia cells
HFM	Hollow fibre Membrane
IGF	Insulin-like growth factor
IgG	Immunoglobulin G
iPSCs	induced pluripotent stem cells
MG63	Human osteosarcoma cells
MHC	Major histocompatibility complex
MSCs	Mesenchymal stem cells
MWCO	Molecular weight cut off
NaOCl	Sodium hypochlorite
NaOH	Sodium hydroxide
NMP	*N*-methyl-2-pyrrolidinone
PBS	Phosphate buffered saline
PCL	Polycaprolactone
PE	Phycoerythrin

PEG	Poly(ethylene glycol)
PGA	Polyglycolic acid
PLA	Polylactic acid
PLGA	Polylactic-co-glycolic acid
PVA	Polyvinyl alcohol
PVP	Polyvinyl pyrrolidone
SEM	Scanning electron microscope
TE	200 mM Tris-HCl, 20 mM EDTA
TGF-β	Transforming growth factor β
TPA	12-O-tetradecanoylphorbol-13-acetate
UGT	UDP-glucoronosyltransferase
UV	Ultraviolet light
VEGF	Vascular endothelial growth factor

Nomenclature

A	Membrane surface area (m^2)
A_0	Membrane cross-sectional area (m^2)
d	Hollow fibre diameter (m)
E	Young's modulus (Pa)
F	Force applied to the membrane (N)
J	Flux ($l\ m^{-2}\ h^{-1}$)
L	Length (m)
L_p	Permeability ($l\ m^{-2}\ h^{-1}\ Pa$)
N	Molar flow rate ($mol\ s^{-1}$)
Q	Volumetric flow rate ($m^3 s^{-1}$)
S	Hoop tension (N)
t	Time (min, hr)
v	Fluid mean velocity (m/s)
V	Volume of permeate collected (l)

ε	Tensile strain
ΔL	Change in length (m)
ΔP	Transmembrane pressure (Pa)
θ	Contact angle (°)
μ	Fluid viscosity (Pa s)
ρ	Fluid density (kg/m^3)
σ	Tensile/Hoop stress (Pa)
τ	Shear stress (Pa)

1. Tissue engineering as a promising alternative therapy to transplantation

1.1 Introduction

Failure of organs is one of the main causes of death in intensive care units, and, at present, organ transplantation often represents the only possible treatment for end-stage organ disease patients. However, although organ transplantation has been shown to be a very successful therapy for the treatment of organ failure, it presents several major limitations. As the demand for transplantation increases, there is shortage of available donors, which results in most patients dying while waiting for transplantation, thus suggesting that transplantation procedures alone will probably never be able to meet the increasing demand. Furthermore, problems with the immune system lead to organ rejection, and immunosuppressive treatments can cause new tumour formation. It is clear that alternative strategies which could provide a therapy for patients without need of transplantation need to be investigated.

Tissue engineering offers a great potential towards the development of an alternative therapy to transplantation. The principle of tissue engineering consists in the design and development of functional three-dimensional tissues by culturing cells on biodegradable 3D supports (scaffolds), in an *in vitro* environment (bioreactor) that resembles as closely as possible that found *in vivo*, prior to implantation into the patient. The implant will generate natural tissue and the components of the scaffold will be degraded. Therefore, the main issues in tissue engineering include the selection of the following:

1. A suitable cell source for tissue regeneration
2. A biocompatible and biodegradable biomaterial scaffold that will allow an appropriate mass transfer of nutrients and support cell growth and proliferation and tissue formation
3. A bioreactor system that will recreate *in vitro* an environment as close as possible to that found *in vivo* by the specific tissue to be engineered.

This thesis investigates these three main aspects of tissue engineering by the development of a novel scaffold for cells, the design and characterization of a novel bioreactor system module, and the study of the ability of stem cells to differentiate into hepatocytes under opportune stimulation with liver-specific factors.

1.2 Thesis outline

This thesis is divided into 7 chapters, including this chapter, which presents the need for the research described in this thesis as well as a general overview of the project with aims and objectives.

Chapter 1 reviews the literature in the field of tissue engineering, including the characteristics and types of biomaterials and bioreactors and the cell sources for tissue engineering with a special focus on stem cells.

Chapter 2 gives details of the materials and experimental methods used to carried out the research.

Chapter 3-6 are the results chapters.
Chapter 3 focuses on the scaffold used in the project, and in particular describes the development and characterisation of novel PVA-PLGA hollow fibre membranes to be used as a scaffold for stem cells in a hollow fibre bioreactor. Chapter 4 describes the cell adhesion and proliferation on the novel PVA-PLGA blended membranes. Chapter 5 focuses on the release of the hepatocyte growth factor by cell lines and analyses the stability of the protein and its permeability across the PVA-PLGA hollow fibre membrane inside the hollow fibre bioreactor. The viability and metabolic activity of the cell line within the bioreactor is also analysed. Chapter 6 focuses on mesenchymal stem cells differentiation into hepatocytes with liver-specific growth factors and in particular with the hepatic growth factor secreted by the cell line.

Chapter 7 provides the overall conclusions for the work and outlines the future work that is required both in the short and in the long term.

1.3 An insight into tissue engineering

The term *tissue engineering* was defined for the first time in the mid 1980s as "an interdisciplinary field that applies the principles of engineering and life sciences toward the development of biological substitutes that restore, maintain, or improve tissue function or a whole organ" [1].

Tissue engineering aims to solve the problem of shortage of donor tissues associated with transplantation, by engineering tissues *in vitro* that resemble as closely as possible natural tissues and that will be implanted into the body of the patient. Thus tissue engineering involves the design and development of functional three-dimensional tissues by culturing cells extracted from a donor on biodegradable 3D supports (scaffold), in an *in vitro* environment (bioreactor) that resembles as closely as possible that found *in vivo*, prior to implantation (fig.1.1). The implant will generate natural tissue and the components of the scaffold will be degraded in a time scale ranging from hours to years.

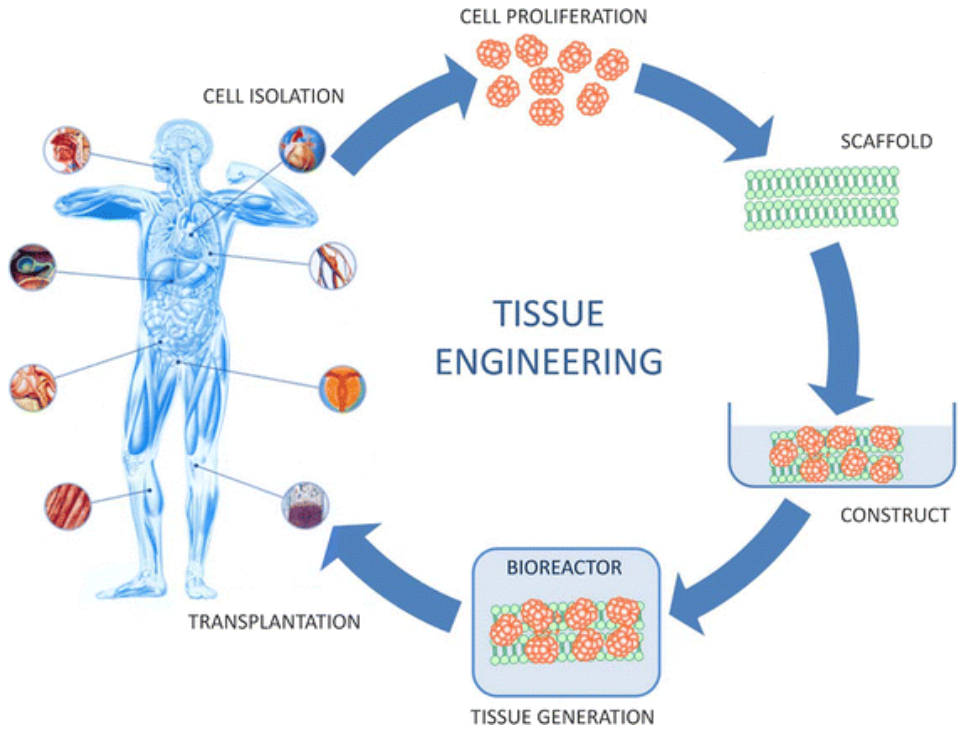

Fig. 1.1.The principle of tissue engineering: cells are extracted from the patient and cultured *in vitro* on biodegradable and biocompatible scaffolds that support cell growth. The scaffold with the cells can be cultured in bioreactors to recreate an environment as close as possible to that *in vivo*. The ultimate goal of tissue engineering is to implant the newly formed tissue back into the patient. From [2].

However, in order to imitate natural tissues, it is necessary to understand the basic biology of the tissues or organs of interest. The growing interest in the fields of embryology and stem cell biology have then led to a new broader term, *regenerative medicine*, to indicate either tissue engineering or repair/regeneration. In this new approach, by knowing the biological processes occurring in the tissue of interest, it will be possible to control them in order to develop strategies (*e.g.* the use of specific growth factors and cytokines to stimulate the production or the function of endogenous cells) either to engineer tissue substitutes or to enhance tissue repair or/and regeneration [3, 4].

The greatest successes of tissue engineering to date can be found in the engineering of relatively simple tissues, *e.g.* skin and cartilage, with Dermagraft (Smith & Nephew), Apligraf (Organogenesis) and Epicel (Genzyme) being among the approved bioengineered skin products and Carticel (Genzyme) a bioengineered cartilage product [4]. However, several limitations still have to be overcome, especially in the recreation of more complex structures such as liver, kidney and heart. A major challenge is represented by the oxygen and nutrient delivery to neo-tissues both *in vitro* and post implantation, especially for highly metabolic tissues like liver, kidney and pancreas. Furthermore, the design of bioreactors able to maintain large masses of viable cells *in vitro* presents an additional challenge [3]. Finally, further issues are represented by the integration of the engineered tissue into the living system. There is a lack of appropriate animal models for the evaluation of the integration of the engineered implant. Immunoacceptance is probably the most challenging issue related to transplantation, especially in the case of non autologous cells. Also, once the tissue has been implanted into the patient, it might not grow at the same rate of the other tissues [3]. These are some of the most important challenges that tissue engineering has to face at present for the reconstruction of tissues/organs that resemble natural ones. Below the three key aspects of engineering tissues will be discussed further: the selection of the appropriate cell types to give rise to the required tissue, the design of an appropriate scaffold to support cell adhesion and growth and, finally, the creation of a controlled environment to allow the cells to proliferate and create tissue structures.

1.4 Cell sources for tissue engineering

The first step of any attempt to engineer a tissue or organ substitute is to decide whether the source to be employed is given by autologous, allogenic or xenogenic cells. An autologous source is represented by the patient's own cells, so there are no problems associated with immune rejection or disease transmission. The use of autologous cells, although overcoming the immunologic barrier, presents some problems. Autologous approaches require obtaining the patient's own cells, expanding them in vitro in large quantities over several weeks, and reintroducing the cells in a site-specific manner. Thus, each treatment is an individualized and non-scalable process which is subject to individualised culture, quality control testing and preparation for delivery to the patient [4, 5]. Furthermore, providing the patient with their own cells is quite a difficult and expensive procedure, therefore allogenic (cells from other human sources) and xenogenic (cells from different species) cell sources have been considered. Allogenic therapies have the aim to deliver functional cells "ready to use", providing more immediate clinical benefit to the patient. Allogenic cell preparation would allow culturing of one batch of cells to treat multiple patients and multiple diseases, thus reducing the expense [4]. However, allogenic and xenogenic sources present some problems, *in primis* the risk of immunorejection. With xenogenic sources there are also problems associated with animal virus transmission [3]. Furthermore, the use of primary cells from donated organs and tissues is often limited by the scarcity of donors.

1.5 Types of cells that can be used in tissue engineering

Cells with different differentiation potential have been used for tissue engineering purposes. Cells can be classified as totipotent, pluripotent, multipotent or differentiated, depending on their source and differentiation capacity (fig. 1.2), Totipotent cells are cells found in the zygote that have the ability to produce any cell type in the embryo, including the extraembryonic tissue. Pluripotent cells can differentiate into any of the cells in the three germ layers (endoderm, mesoderm, ectoderm) and therefore into any type of tissue in the body but cannot produce extraembryonic tissue. Multipotent cells have the potential to differentiate into

multiple but limited number of cell types while differentiated cells have reached the final stage of development and have a specific function in a specific tissue.

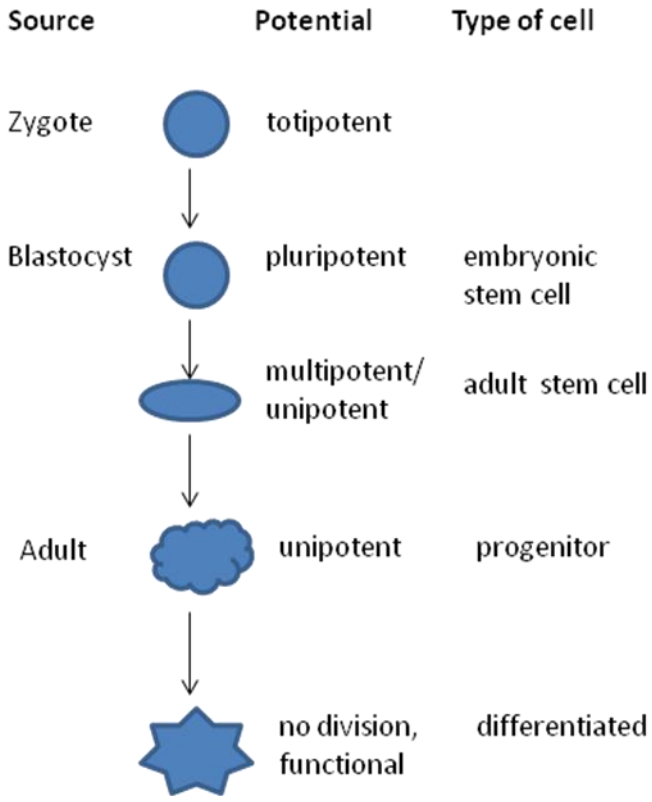

Fig. 1.2: Differentiation capacity of cells. According to their source and differentiation potential cells can be classified as embryonic stem cell, adult stem cells, progenitor cells and differentiated cells.

1.5.1 Primary cells

Primary cells are mature cells that are harvested from a specific tissue removed by surgical procedure. An example is given by primary human osteoblasts harvested from the femoral heads removed during total hip replacement operations [6]. Primary cells do not present immunological issues if they are harvested from the same patient, but they tend to proliferate slowly and to de-differentiate when cultured *in vitro* [6]. These limitations have stimulated researchers to find alternative cell types for tissue engineering strategies.

1.5.2 Cell lines

Cell lines are immortalised cells that have been artificially modified (*e.g.* through random mutation or artificial expression of the telomerase gene) in order to acquire the ability to proliferate indefinitely in culture. Different cell lines have been the most popular alternative to primary cells so far, but there is concern about metastasis of tumour-derived cell lines and the transmission of uncharacterized infectious agents from tumour or animal-derived cells to the patient [3]. However cell lines are useful for non-clinical experiments given the ease of culture and the high proliferation *in vitro.*

1.5.3 Stem cells

A promising cell source for tissue engineering strategies is at present represented by stem cells, for their potential to differentiate into mature cell types that may have therapeutic benefit in the support, repair and regeneration of damaged tissues [7]. Depending to the clinical application, stem cells can be from either an allogenic or autologous cell source, added exogenously or recruited from the host, and then expanded *in vitro.*

Stem cells are undifferentiated, "blank" cells that do not yet have a specific function. They are characterised by the capacity to maintain an undifferentiated status *in vitro* (self-renewal) and the ability to differentiate under appropriate conditions into specialised cell types and form specialised tissues and organs (plasticity) [8]. They can also give rise to progenitor cells, which can differentiate into tissue-specific cell types. Depending on their source, two types of stem cells exist: embryonic stem cells (pluripotent) and adult stem cells (can be multipotent or unipotent).

1.5.3.1 Embryonic stem cells (ESCs)

Embryonic stem cells are cells isolated from the inner cell mass of the blastocyst, an early (4-5 days) stage of the embryo. They have the ability to proliferate *in vitro* for extended periods of time in an undifferentiated state (self-renewal capacity) and they are pluripotent, *i.e.* they have the potential to differentiate into any of the three germ layers: endoderm (interior stomach lining, gastrointestinal tract, the lungs),

mesoderm (muscle, bone, blood, urogenital), or ectoderm (epidermal tissues and nervous system) but cannot become an entire human being because they lack the potential to contribute to extraembryonic tissue, such as the placenta (fig. 1.3). This degree of plasticity represents at the same time a strong advantage and a major limitation in the use of ESCs for tissue engineering purposes: the same plasticity that permits ESCs to differentiate into so many cell types makes difficult to maintain a large number of ESCs in an undifferentiated state and subsequently direct their differentiation to a desired lineage with high efficiency [9]. To induce differentiation *in vitro* ESCs usually form aggregates called embryoid bodies (EBs), where later cell types of many different lineages will be generated. EBs mimic the structure of the developing embryo and therefore create better conditions for the differentiation of cells into the three germ layers compared to cells cultured in 2D monolayers [3].The formation of embryoid bodies has been used to produce neural cells [10], cardiomyocytes [11] hematopoietic precursors [12], β-like cells [13], hepatocytes [14] and germ cells [15].

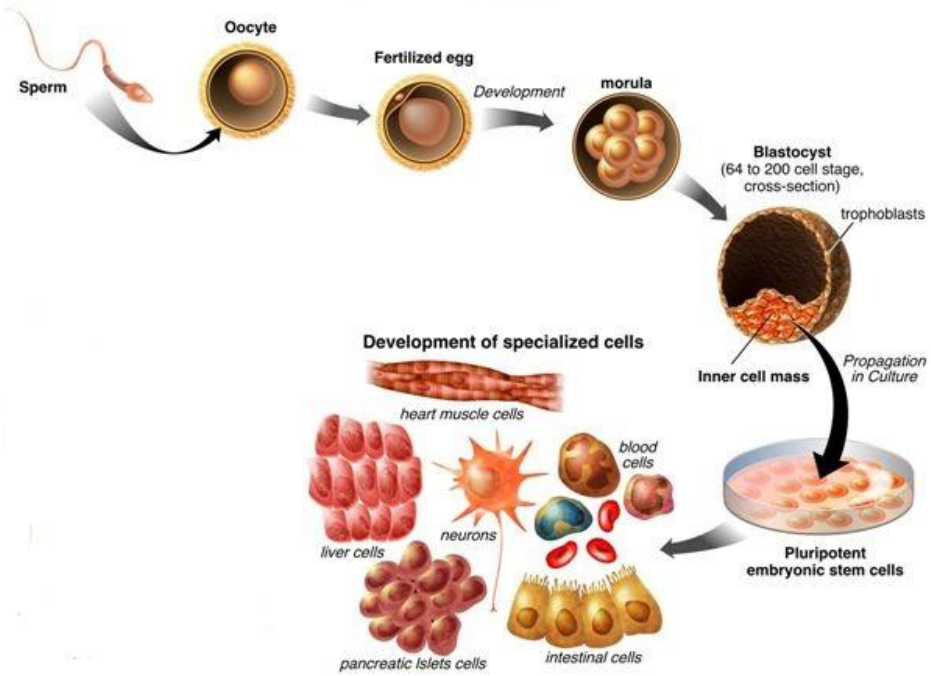

Fig. 1.3: Pluripotency of embryonic stem cells. Adapted from [16], with permission from the author.

However, the ESCs differentiation processes are in general characterised by quite low efficiency and are not syncronised among the cells [4]. The selection of specific

lineages requires sequential exposure to several inducing factors but most cells do not progress to a full terminally differentiated phenotype or often they differentiate incontrollably into undesired cell phenotypes [4]. Methods to obtain a more controlled differentiation of ESCs to specific lineages include co-culture with differentiated cells [17, 18] or differentiation in presence of specific growth factors [19, 20]. Furthermore, ESCs present safety issues as they have the potential to form tumours once transplanted *in vivo*: if ESCs remain undifferentiated after implantation in the body, they will spontaneously differentiate into multiple cell types and form a type of tumour derived from all three germ layers and called teratoma [21].Therefore ESCs should be guided to differentiate into a specific lineage before implantation in order to avoid teratoma formation.

Another issue arising with transplantation of ESCs is immune rejection: there is clear evidence that once the differentiated ESCs are transplanted, they express high levels of major histocompatibility complex (MHC) class I antigens and any allogenic ES-cell based construct would be rejected [22]. This problem could be solved by therapeutic cloning or somatic cell nuclear transfer, which consists in the transfer of the nucleus of a somatic cell into an enucleated oocyte, generating a blastocyst, and then culturing the inner mass to obtain an ES cell line with identical MHC to that of the host tissue [23]. However, the reliability and efficiency of the process has to be improved. A further immunological issue is related to the fact that human ESCs have been typically cultured in medium containing animal sera and/or with mouse feeder layers, which may induce an immuno-response or transfer cross-species pathogens. Therefore, these human ES cell lines grown with xenogenic components are very unlikely to be ever used in clinical applications. Progress has been made in the derivation and expansion of cells with human feeder cells [24] or, better, feeder-free [25]. Another option is offered by tissue engineering: ESCs can be cultured on polymer scaffolds, instead of using the feeder layer. Both natural and synthetic scaffold have been shown to support ESCs growth and differentiation into different lineages [26-29].

Finally, one of the most debated arguments about the use of embryonic stem cells regards the ethical issues which arise from the isolation of these cells from an

embryo. ESC isolation from the inner cell mass of the blastocyst results in the destruction of the pre-implantation embryo, which would otherwise form a living human being. Some approaches have tried to circumvent the ethical problem, like Chung and colleagues for example, who have shown that a single cell embryo biopsy could be used to generate an ES cell line, without the destruction of the embryo [30].

1.5.3.2 Adult stem cells

At present, a very promising stem cell type for tissue engineering is represented by adult stem cells. Adult stem cells are undifferentiated cells found in specific organs, where their primary role is to maintain and repair the tissue in which they are found [31]. These cells have a capacity for self-renewal in culture and are multipotent, since they have more limited differentiation potential than ESCs, although researchers have recently started reviewing this definition. Initially it was thought that adult stem cells could only be found in a limited selection of tissues and could differentiate only in those lineages from the originating tissues. Recent studies have demonstrated that adult stem cells can be derived from bone marrow [32], blood [33], brain [34], fat [35], liver [36], muscle [37], pancreas [38], and umbilical cord blood [39] and also that some adult stem cells have a greater plasticity and they are able to generate other cell types from the same embryonic germ layer or even cells of other germ layers [40] (fig. 1.4). Hematopoietic stem cells, for example, are adult stem cells found in the bone marrow which give raise mainly to blood cells, but they also can differentiate into other cell types from the mesoderm (skeletal and cardiac muscle, endothelium) [41-43] or even into different cell types of the endoderm (lung epithelium, intestinal epithelium, kidney epithelium, pancreas, liver, bile ducts) [44-49] and of ectoderm (epidermis and neural cells) [50, 51]. There is also evidence that hepatic stem cells may be able to generate different cells from the endodermal lineage, like pancreas cells [52, 53]. Another example is offered by mesenchymal stem cells (MSCs), particularly abundant in the bone marrow and adipose tissue, which can differentiate into osteoblasts, chondrocytes and adipocytes, but can also give rise to cells of cardicac tissue and vascular system, skeletal muscle, nerve, liver and pancreas [4, 54] (fig. 1.4). An explanation of the plasticity of adult stem cells could be cell fusion between the stem cells and some host cells [4] or that there might be stem cells with more pluripotent characteristics that persist into adulthood or that

adult stem cells could be reprogrammed via a process of de-differentiation and then re-differentiation to another lineage via trans-differentiation [4].

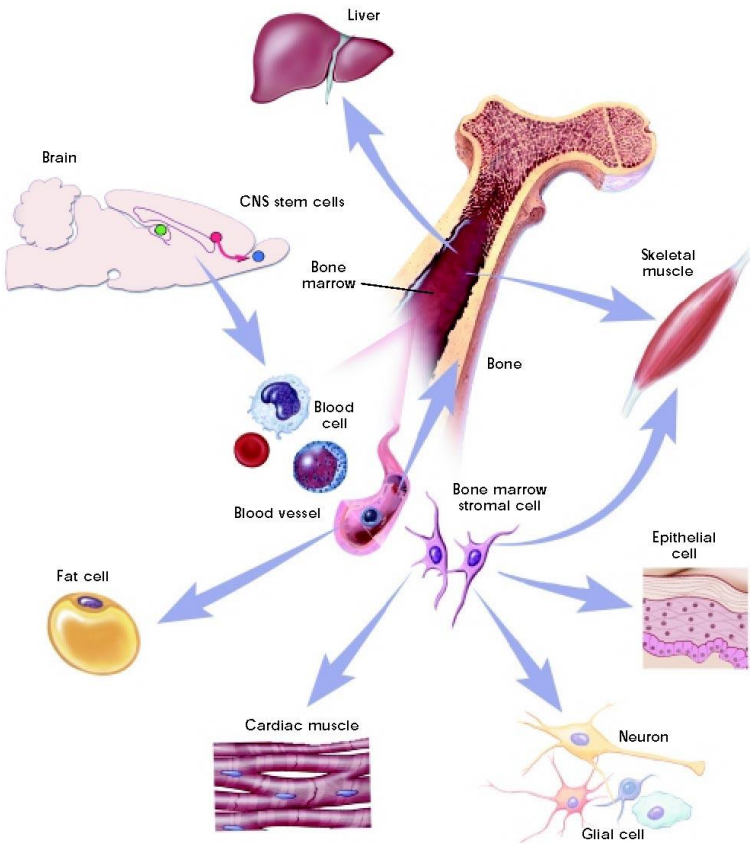

Fig. 1.4: Plasticity of adult stem cells. Bone marrow stem cells can differentiate into bone cells but also into completely different tissues like liver, skeletal muscle, neural cells under opportune stimulation with cytokines and growth factors. From [55], with permission from the author.

MSCs are among the most characterised adult stem cells, as they can be easily expanded in culture and, as mentioned above, they can differentiate into multiple lineages. Also, MSCs from bone marrow and adipose tissue have been shown to be non-immunogenic [56]: they express very low levels of MHC class I molecules on their cell surface and they lack MHC class II expression [4], a characteristic which makes them very attractive for clinical applications as they would not cause rejection when implanted into the body of the patient. Furthermore, MSC differentiation can be more easily predicted and controlled compared to ESCs. For these reasons MSCs at present are more suited than ESCs for tissue engineering applications. MSCs can also be derived from umbilical cord blood, which offers an abundant source of stem cells with large proliferation capacity *in vitro*, thus an attractive resource for

regenerative medicine applications [57]. Other abundant sources of MSCs are placenta and amniotic fluid. In't Anker et al reported that MSCs derived from these two sources exhibited a phenotype and multilineage differentiation potential similar to that of bone marrow-derived MSCs [58]. However, large interest is focused on fat as an alternative to bone marrow as an autologous MSC source: lipoaspirates have been shown to provide an abundant, easy and accessible source of these cells with less discomfort for the patient compared to the painful and risky MSCs extraction from bone marrow. Furthermore, lipoaspirate-derived MSCs have the ability to differentiate into multiple phenotypes [59-61] which makes them an attractive alternative to bone-marrow MSCs.

In addition, in a recent study conducted at Imperial College, London, researchers were able to mobilize mesenchymal stem cells from bone marrow into the bloodstream by treating healthy mice with VEGF followed by a new drug called Mozobil [62]. This work could lead to new treatments which work by mobilising a person's own stem cells into the blood circulation and it is potentially very important for tissue engineering purposes as a simple blood drawing from the patient could provide a population of mesenchymal stem cells to be used for regeneration of the damaged tissue to be re-implanted back into the same patient without any risk of rejection.

Adult stem cells are at present more suited than embryonic stem cells for tissue engineering purposes because their use would not raise ethical issues, as they are not derived from an embryo. Furthermore, they would be more committed to a specific lineage, non-tumourigenic and non-immunogenic, therefore they could be transplanted into the patient without problems of rejection. Regenerative medicine approaches using stem cells for the regeneration of functional tissue could be: 1) transplants of stem cells or their derivatives; 2) use of stem cells or their derivatives to construct bioartificial tissues (tissue engineering) for implantation into the body; and 3) induction or enhancement *in vivo* of resident stem cell proliferation and differentiation to regenerate tissues at the site of damage [3]. Adult stem cells, and in particular mesenchymal stem cells, have been used for clinical applications, especially in orthopaedical applications [63-65]. In 2008 the first full transplant of a human trachea grown from adult stem cells was carried out at the Hospital Clínic of Barcelona. Researchers harvested a section of trachea and removed all the cells

thus leaving a non-immunogenic acellular scaffold. The section was then seeded with stem cells taken from the patient's bone marrow and a new section of trachea was grown in the laboratory over four days. The new section of trachea was then transplanted into the left main bronchus of the patient. Because the stem cells were harvested from the patient's own bone marrow, the patient's immune system did not show signs of rejecting the transplant [66].

Despite these promising results, the use of adult stem cells is not free from obstacles: their availability decreases with age in most tissues and also, once extracted and cultured *in vitro*, they tend to grow slowly. To be useful for transplant purposes, stem cells must proliferate extensively and generate sufficient quantities of tissue, differentiate into the desired cell type(s), survive in the recipient after transplant, integrate into the surrounding tissue after transplant, function appropriately for the duration of the recipient's life, and avoid harming the recipient in any way [67]. Furthermore, in order to take full advantage of stem cell technology for tissue engineering applications, it is necessary to acquire a better understanding of stem cell biology, and in particular of their response not only to biological factors and scaffolds, but also to the microenvironment (niche) in which they must survive and function. In addition, the isolation techniques must be improved in order to obtain a pure stem cell population.

1.5.3.3 Induced pluripotent stem cells (iPSCs)

A recent discovery could bring the focus of researchers to a new, pluripotent stem cell type. In August 2006 Takahashi and Yamanaka announced that somatic cells can be reprogrammed to a pluripotent state by the viral transfection of four transcription factors (Oct4, Sox2, Klf4 and c-myc) into mouse fibroblasts [68]. They called these cells "induced pluripotent stem cells" (iPSCs), as they have the ability to differentiate into virtually all types of cells like ESCs. One year later they also reported the generation of human iPSCs (fig 1.5). In 2008 Nakagawa *et al* showed that iPSCs can be generated with only three factors [69], and Huangfu *et al* later demonstrated that just two factors (Oct4 and Sox2) in combination with a valproic acid (VPA), are sufficient to reprogram fibroblasts to an embryonic state [70]. In the same year, Aoi *et al* showed that iPSCs can be generated not only from fibroblasts but also from adult mouse hepatocytes and gastric epithelial cells [71]. In 2009 Kim *et al.* reported

that Oct4 alone is sufficient to reprogram adult mouse neural stem cells into iPSCs [72].

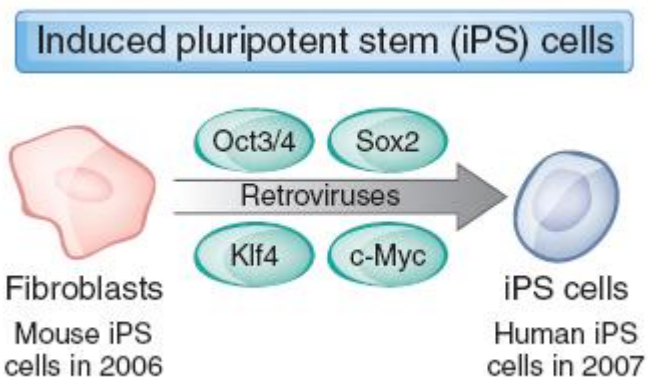

Fig. 1.5: Induced pluripotent stem cells (iPS) can be generated by introducing genes encoding four transcription factors (Oct4, Sox2, Klf4 and c-myc) into fibroblasts. From [73].

iPSCs would solve two main problems associated with ESCs, *in primis* the ethical issues as they do not require the destruction of an embryo instead being isolated from somatic cells, and secondly they don't cause immune rejection when transplanted into the patient [73]. For these reasons iPSCs research has become one of the hottest areas in life sciences, as these cells are expected to be used for generating disease models, drug screening, toxicology and regenerative medicine (fig. 1.6). At the same time the technology is still at the beginning, and there are many challenges to be overcome before iPSCs can be applied into clinics. One main challenge is that the reprogramming methods involve the expression of oncogenes by retroviral vectors, which may cause cancer by integrating into the genome [74]. A few alternative reprogramming methods have been developed to avoid genome integration by retroviral vectors: Stadtfeld *et al*, for example, generated iPSCs from mouse hepatocytes through an adenoviral vector, which does not integrate into the host genome. However, the efficiency of reprogramming was much lower than that obtained by retroviral infection [75]. Simple transfection, another alternative method developed by Okita et al [76], also resulted in low reprogramming efficiency, while a third strategy which employs small molecules that can replace the reprogramming transgenes, like VPA instead of klf4, has been shown to dramatically increase the efficiency of reprogramming in both human and mouse cells [70]. From these

examples it is clear that, although the potential of iPSCs in medicine, drug discovery and toxicology is immense, long-term studies must still be carried out in order to fully characterise them and eliminate any potential safety concern about their use.

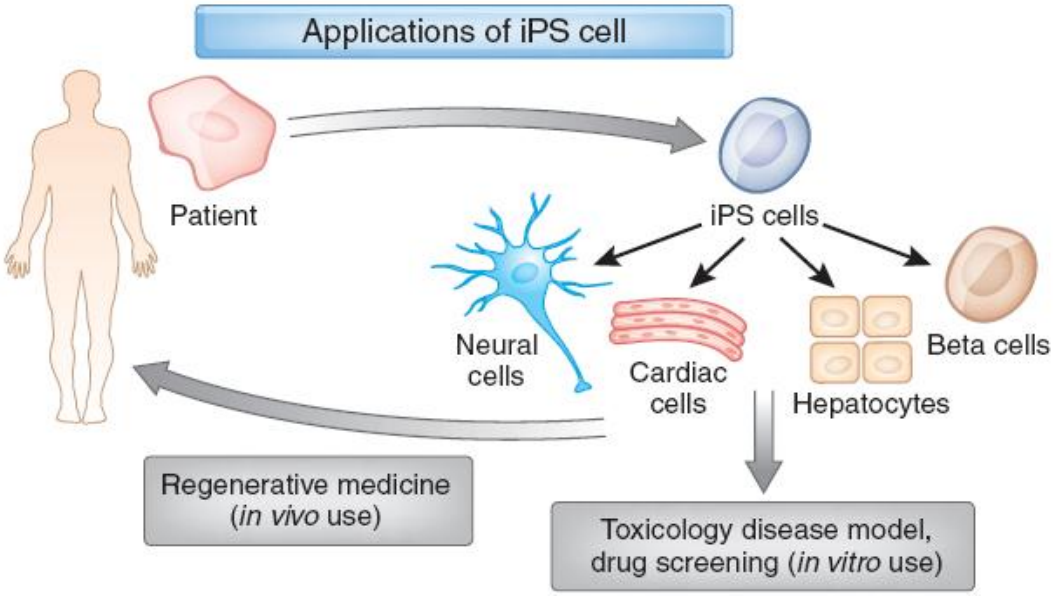

Fig. 1.6: Possible applications of iPS cells. iPS cells could be used *in vivo* for regenerative medicine applications, as well as in vitro for toxicology, disease models, and for drug screening. From [73].

However, in 2010 Vierbuchen *et al* identified three neuron-specific transcription factors (Ascl1, Brn2 and Myt1l) that were sufficient to directly convert mouse fibroblasts into functional neurons *in vitro* [77]. From this finding it appears to be possible to directly covert one differentiated cell type into another differentiated one with no more need of the induced pluripotent stem cells intermediate step. This strategy would eliminate the safety risks associated with pluripotent stem cells, and possibly open a new era of investigation which would provide advances not only in cellular and molecular biology, but also in drug discovery and regenerative medicine.

1.6 Biomaterials as scaffolds for cells

With the selection of a source of cell, the next challenge in tissue engineering is the development of an organised three-dimensional support or delivery vector for the cells. Tissue engineering involves the use of biomaterials as scaffolds to support and induce tissue formation *in vitro* and *in vivo*. According to the definition proposed at

the Consensus Conference of the European Society for Biomaterials, Chester, England, March 1986, biomaterials are *"any substance, other than a drug, or combination of substances, synthetic or natural in origin, which can be used for any period of time, as a whole or as a part of a system which treats, augments, or replaces any tissue, organ, or function of the body."* [78].
Biomaterials have been employed in tissue engineering as scaffolds to support cell growth and proliferation. The properties that need to be considered when designing a scaffold for tissue engineering will be discussed in the following section.

1.6.1 Scaffold design properties

A scaffold is defined as *"the support, delivery vehicle, or matrix for facilitating the migration, binding, or transport of cells or bioactive molecules used to replace, repair or regenerate tissues"* [79]. Unlike permanent implants, tissue-engineered scaffolds serve as temporary devices to facilitate the tissue repair and regeneration process [3]. The scaffolds employed in tissue engineering must be capable of promoting cell-biomaterial interactions, cell adhesion and extracellular matrix deposition, allowing sufficient transport of gases, nutrients and regulatory factors in order to permit cell survival, proliferation and differentiation, of provoking a minimal degree of inflammation toxicity when implanted *in vivo* (biocompatible) and of biodegrading at a controllable rate close to that of tissue regeneration, assuring in this way the complete integration of the engineered construct (biodegradable). Also, in the design of a scaffold it is important to consider a cell's microenvironment since the cell *in vivo* is exposed to a series of signals (mechanical signals, signals from the extracellular matrix and from the neighbouring cells) that direct its function, and therefore the scaffold has to reproduce as close as possible the characteristics of the tissue where the cell is found. For this scope at present several scaffolds incorporate into the biomaterial bioactive molecules such as growth factors, anti-inflammatory drugs or gene delivery vectors to elicit the same cellular responses occurring *in vivo* [3]. Finally, adequate mechanical properties such as strength and stiffness, sterilizability, long-term storage, manufacturability and appropriate engineering design are also to be considered in the development of a scaffold for tissue

engineering [80]. Below are described some of the fundamental parameters to be considered during scaffold design.

1.6.1.1 Scaffold structure

At the macroscopic level, scaffolds can be formed into a number of different geometries which try to mimic the tissue/organ anatomical features (fig. 1.7). For example, hollow fibres have been employed for liver regeneration purposes as they resemble the liver lobule [81], while nanofibres have been employed as artificial nerve guidance channels for nerve regeneration [82, 83]. Fibres are attractive for tissue engineering as they provide a large surface area to volume ratio for large cell attachment and also they allow the rapid diffusion of nutrients to cells and waste products from cells [84]. Hydrogels are another macro-structure type of scaffold used especially for cell encapsulation and drug delivery for their capacity of absorbing a high amount of water, thus creating an ideal aqueous environment [85-88]. They are easy to inject, and in situ forming hydrogels that solidify on external stimuli have been designed as injectable scaffolds for minimally invasive cell and biomolecule transplantation [89]. However, they showed weak mechanical properties and they are difficult to sterilise. Highly porous foam and sponge scaffolds provide a template for cells to form into a 3D tissue structure and they can be processed with different techniques in order to obtain porous constructs. Macroporous scaffolds prepared with gas foaming method, for example, exhibited a porosity of over 90% and pore size of about 200 μm, thus allowing cell infiltration into the pores [90].

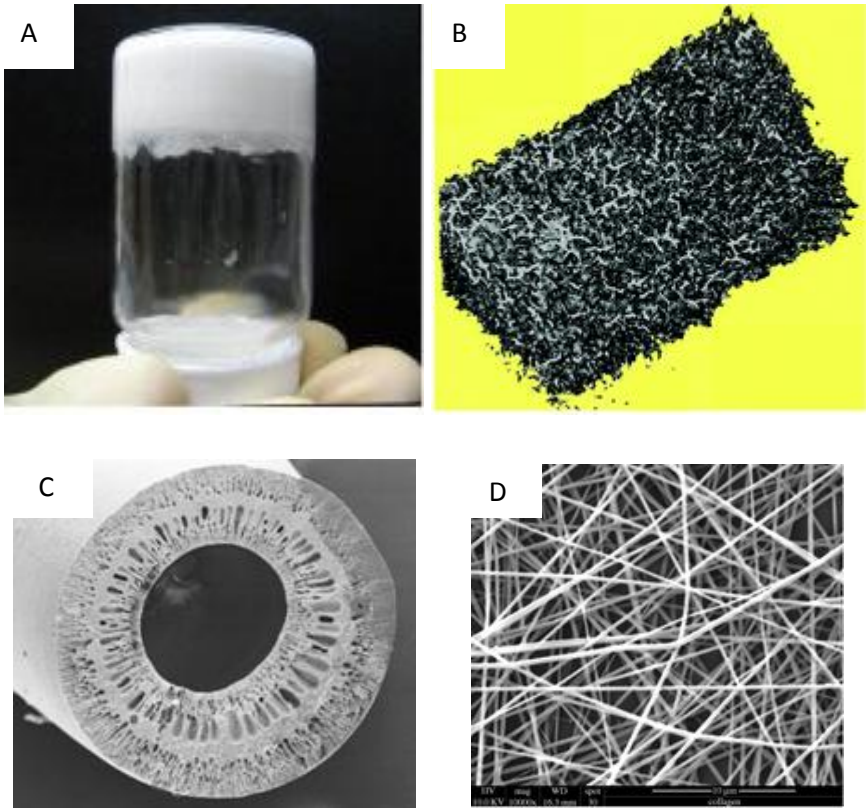

Fig. 1.7: Different scaffold macro-structures: A) composite hydrogel [88], B) gelatine foam [91], D) PLGA hollow fibre [92], C) nanofibres [93].

1.6.1.2 Mass transport and scaffold micro-structure

Mass transport is the movement of fluids, solutes and cells through a tissue construct and it is one of the most significant challenges in tissue engineering. Cells located further than 200 μm from a blood supply are exposed to low oxygen tension and as a result they become either metabolically inactive or necrotic [94]. The mass transport in a scaffold is related to the scaffold's chemical composition and the structural characteristic of its pores, defined mainly by pore size, porosity, pore interconnectivity/tortuosity, and surface area. These scaffold characteristics can affect the diffusion or convection of nutrients, growth factors and cytokines through the engineered tissue [3]. Once cells are seeded on the scaffold, the distribution and density of cells on the scaffold highly influence the distribution and availability of nutrients to the cells within the scaffold interior, thus affecting mass transport [95]. Since most cells are anchorage dependent, the scaffold should possess properties that facilitate cells' growth and attachment [96, 97]. One main parameter affecting the

initial cell attachment and distribution is the pore size of the scaffold. Optimal scaffold pore sizes have been shown to positively affect tissue regeneration *in vivo* [98-100].

In addition to pore size, other parameters that influence cell attachment and mass transport are porosity, pore interconnectivity and available surface area. Highly porous scaffolds allow a greater number of cells to infiltrate the scaffold's void space and also an easy diffusion of nutrients to and waste products from the implant, which is a major requirement for the regeneration of highly metabolic organs like pancreas and liver. Also, the continuity of the pores is important for an adequate transport of nutrients and cell migration. It is also an advantage for a scaffold to possess a large surface area to volume ratio, in order to achieve an optimal cell density on the scaffold. This ratio depends on the density and average diameter of the pores [84]. However, while high porosities can improve the mass transport capabilities of a scaffold, they can also compromise the mechanical integrity of the scaffold. Therefore, the challenge in the design of an optimal tissue engineered scaffold is to find the right balance between the scaffold's surface area, void space and mechanical strength [101].

1.6.1.3 Mechanical strength

Since tissues are subjected to mechanical forces, the mechanical properties of the engineered construct have to be taken into account during the scaffold design, especially for weight-bearing tissues like bone. In these tissues the scaffold must be capable of sustaining the forces applied to it and to the surrounding tissues. Mechanical properties of scaffolds should resemble those of the native tissues. For bone regeneration, for example, mechanically stiff biomaterials are required to support cell expansion and the production of bone matrix [102], while soft biomaterials such as hydrogels are suitable for soft tissue engineering for their similarity to native soft tissues like muscle, nerves, blood vessels, fat and connective tissue [103]. Furthermore, the scaffold should be able to retain its mechanical properties until the new tissue is engineered completely [3, 101]. The mechanical properties of the scaffold are determined in part by the bulk properties of their constituent materials (*e.g.* Young's modulus, degradation rate). For example, hydrophobic polymers tend to resist water adsorption and therefore exhibit a higher

mechanical strength than hydrophilic polymers or hydrogels. Because of the high porosity and of the consequent low material content, the mechanical properties of the scaffold are often determined by the structural arrangement of their constituent materials (*e.g.* pore size, fibre diameter and orientation).

1.6.1.4 Surface properties

The chemical and topographical features of the surface are the ones that determine the interaction between the scaffold and the cells. The surface chemistry refers to the chemical environment that the scaffold surface presents to the cells. To tailor the scaffold chemical properties, the interactions of the scaffolds with different factors, such as protein adsorption from biological fluids to the scaffold surface, need to be considered. Studies have been carried out to understand how the adsorption and denaturation of proteins can lead to different cellular responses at the material surface [104], such as cell adhesion. Scaffolds that are derived from natural materials, such as collagen, fibrin, hyaluronic acid, already contain innate biological molecules to aid cell attachment and proliferation, while the surface chemistry of synthetic scaffolds has often been modified in order to improve cell attachment either by direct surface treatment/modification or by incorporating bioactive molecules into the scaffold bulk. For example, hydrophobic polymers such as polylactic acid (PLA) and polylactic-co-glycolic acid (PLGA) can be wet by two-step immersion in ethanol and water in order to facilitate the entry of water into the pores thus promoting cell attachment [105]. Another strategy of surface modification consists in coating the scaffold surfaces with specific extracellular matrix-derived adhesion proteins. For example, PLGA scaffolds and polyvinyl alcohol (PVA) hydrogels have been coated with fibronectin in order to improve cell adhesion and proliferation [26, 106]. Finally, an alternative strategy for improving cell attachment consists of using electrically charged surfaces in order to improve adsorption of specific adhesive proteins that promote cell adhesion. This can be achieved by modulating the isoelectric point of the surface or of the adhesive protein, *i.e.*, the pH at which a protein or surface carries no net electrical charge. A protein/surface can then exhibit different charges according to the pH of the surrounding environment: at pH values above the isoelectric point the surface/protein will be negatively charged, while at pH values below the isoelectric point the surface/protein will be positively charged.

Surface charge plays an important role in cell adhesion: the surface charge of a polymer affects protein adsorption to its surface, which is thought to improve cell attachment. Many proteins have a net negative surface charge, which promote their adsorption to a positively charged surface, while negatively charged surfaces will promote adsorption of positively charged proteins [4]. The other major strategy of surface chemistry modification consists in incorporating into the scaffold pepetide ligands derived from the active domains of ECM adhesion proteins. For example, the incorporation the peptide Arg-Gly-Asp (RGD) into the scaffold, is a common technique to enhance cell adhesion [107].

Surface topographical features include pores, nodes, ridges, steps, grooves and have been shown to be responsible for changes in cell morphology, cell activities, and with the production of autocrine/paracrine regulatory factors compared to smooth surfaces [108]. In general surface roughness increases cell adhesion, migration and the production of ECM. Therefore, many fabrication and surface modification techniques aim to generate different topographical surfaces to improve cell attachment. For example, nanostructured PLGA scaffolds treated with sodium hydroxide have shown to increase the chondrocyte adhesion, proliferation and ECM production, due to increased porosity and nanoscale roughness [109]. At present, there is a growing interest in the fabrication of nanostructured scaffolds and in particular in developing synthetic nanofibrous scaffolds, with nanofibres of diameters ranging from a few to hundreds nanometers as the differential topography created by the nanofibres has been shown to support cell and tissue growth [110, 111].

1.6.1.5 Biodegradability

As opposed to permanent implants, tissue engineered scaffolds are designed to provide temporary support for the cells in order to facilitate tissue engineering processes. Therefore, tissue engineered scaffolds have to be biodegradable and the degradation rate of the scaffold should ideally correspond to the rate of new tissue formation. However, it is difficult to match the degradation rate with the wound healing and new tissue regeneration rate, which may vary between different patients. Therefore, designing scaffolds with appropriate degradation properties, especially combining the properties of the scaffold with the aspects of a specific tissue formation still remains a challenge. For example, scaffolds used for bone implants

need to support mechanical forces and at the same time allow new bone formation [112]. In order to tailor the degradation of the scaffolds, wound healing and tissue-regeneration mechanisms have to be further explored. Many factors can influence the degradation profile of scaffolds *in vitro* such as the polymer molecular weight, polydispersity, crystallinity, glass transition temperature, scaffold porosity, pH of medium, and *in vivo*, such as presence of enzymes or proteins, cellular activity and cell-induced pH changes [113]. There are two types of scaffold degradation: surface and bulk degradation. Surface degradation is characterised by a gradual decrease in the dimensions of the scaffold with no changes in its mechanical properties. Bulk degradation is characterised by loss of material throughout the scaffold's volume with loss of mechanical strength while maintaining an intact surface. Therefore bulk degrading scaffolds might allow a better cell attachment than surface eroding scaffolds [101]. Many polyester scaffolds made of lactic and glycolic acid, *e.g.* PLGA and hydrophilic scaffolds like hydrogels, undergo bulk degradation. However, in bulk degradation, the accumulation of degradation products may have negative effects on the tissue, *e.g.* the release of acidic products from PLGA degradation.

Once described the main properties of the scaffolds, the main classes of biomaterials will be now discussed, with a particular focus on polymers.

1.6.2 Biomaterials classification

Biomaterials can be classified into five groups (table 1) [114]:

1) metals
2) ceramics
3) glasses
4) polymers (natural and synthetic)
5) composites

In the past century metals and ceramics have contributed to major advances in medicine, especially in orthopedic tissue replacement. However, they have two major

disadvantages for tissue engineering applications: they are not biodegradable (except biodegradable ceramics such as tricalcium phosphate) and their processability is very limited. For these reasons polymeric materials have received an increasing attention over recent years [84].

Table 1: Characteristics of the three major groups of biomaterials: polymers, metals, ceramics. Adapted from [80].

Biomaterials	Examples	Advantages	Disadvantages
Metals (Ti, Co-Cr, stainless steels, Au, Ag, Pt etc.)	Joint replacements, bone plates and screws, dental root implants	strong, tough, ductile	may corrode: biocompatibility issue, difficult to process, not biodegradable
Ceramics (aluminum oxide, calcium phosphates including hydroxyapatite, carbon)	Dental implants, femoral head or hip replacement, coating of dental and orthopedic implants	very biocompatible, inert, strong in compression	Brittle, difficult to process, not resilient, not biodegradable
Glasses (phosphate based glasses, silicate based glasses, bioactive glasses)	Orthopaedic implants	biocompatible, biodegradable, bioactive	Brittle, difficult to process, limited solubility
Polymers (collagen, fibrin, chitosan, alginate, PLA, PGA, PLGA....)	Sutures, blood vessels, soft tissues	easy to fabricate, can be tailored to suit specific functions, resilient	not strong, deform with time, might degrade into acidic products

1.6.2.1 Polymeric biomaterials

The main advantages of polymeric biomaterials compared to metal or ceramic materials are the ease of manufacturability to produce various shapes (films, sheets, fibres etc), biodegradability, reasonable cost and availability with desired physical and mechanical properties.

Polymeric materials used in tissue engineering applications can be divided into two main classes:

1) Natural: those most employed are usually from proteic (*e.g.* collagen, fibrin, gelatin, silk) or polysaccaridic *(e.g.* alginate, hyaluronic acid, chitosan) origin. Natural materials are usually biocompatible and enzymatically biodegradable. They have the advantage of possessing bio-functional molecules that aid the attachment, proliferation and differentiation of cells. However, these scaffolds present some drawbacks: the degradation rate might not be easily controlled, as it would be different according to the host, and therefore the lifespan of these materials would vary *in vivo.* Also, natural materials possess weak mechanical properties [101] and batch to batch variations.

2) Synthetic: they present many advantages over natural polymers, *e.g.* they are available in unlimited quantities, they can be prepared with controlled physical and chemical properties and the degradation rate and mechanical properties can be chemically modified. A disadvantage is that some of them degrade into acid products which might increase the local acidity and this might result in adverse responses such as inflammation. The most common synthetic polymers are polyesters such as polyglycolic acid (PGA), polylactic acid (PLA) and and their copolymer polylactic-co-glycolic acid (PLGA), or polycaprolactones. Other types include polyanhydrides, polycarbonates and polyphosphazenes [101].

Since a synthetic polymer, PLGA, has been used in this project as scaffold for cells, the group of poly(α-hydroxy acids), to which PLGA belongs to, will be discussed in more detail in the next section.

1.6.2.1.1 Poly(α-hydroxy acids)

Polylactic (PLA), polyglycolic (PLGA) and poly(lactic-co-glycolic) (PLGA) acids are bioresorbable polyesters belonging to the group of poly-α-hydroxy acids. They have been extensively used for over 30 years in a wide range of biomedical applications and especially in surgical sutures thanks to their biocompatibility, biodegradability and processability, characteristics with which they received

approval from the Food and Drug Administration (FDA) for clinical use [80]. These polymers degrade by non-specific hydrolysis of their ester bonds, which results in a decrease in the polymer molecular weight [115]. The degradation rate of these polymers is determined by initial molecular weight, exposed surface area, crystallinity and, in the case of co-polymers, by the ratio of the monomers. The degradation of these polymers is also thought to be linked to macrophage/material interactions that stimulate macrophage activation which, in turn, leads to the macrophage production of the growth factors required to initiate tissue regeneration [80]. Within this family of polyesters, PGA has the simplest structure (fig. 1.8). Because it is a highly crystalline polymer, it has a high melting point and low solubility in organic solvents. Due to its hydrophilicity, PGA tends to degrade and therefore to lose its mechanical properties usually between two to four weeks post implantation [116].

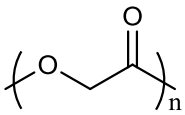

Fig. 1.8: Chemical structure of polyglycolic acid (PGA).

Due to the presence of an extra methyl group on the α-carbon, PLA is a chiral molecule and thus D (fig. 1.9 a), L (fig. 1.9 b) and D,L (fig. 1.9 c) isomers are possible. The polymers derived from the optically active D and L monomers are semicrystalline and relatively hard materials with extremely slow biodegradation rate, therefore they are employed in applications where high mechanical strength is required, such as sutures and orthopaedic devices [117], while the optically inactive D,L-PLA is always amorphous, with a faster degradation rate compared to the optically active isomers, and therefore is preferred for drug delivery applications, where a homogeneous dispersion of the active species within a monophasic matrix is required [3]. Because of its methyl group, PLA is more hydrophobic than PGA, and this results in a lower hydrolysis rate than PGA. Also, PLA is more soluble in organic solvents than PGA.

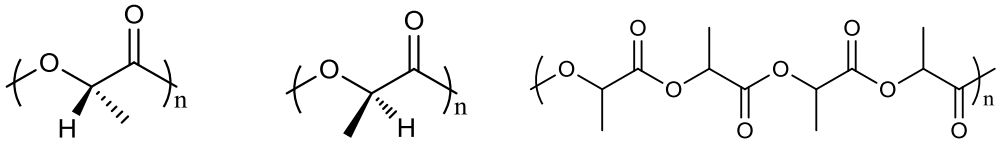

a) L-PLA **b) D-PLA** **c) D,L-PLA**

Fig. 1.9: Chemical structure of polylactic acid isomers: L- PLA, D-PLA, and D,L-PLA.

Although these polymers have been considered biocompatible and safe and therefore FDA approved, a delayed inflammatory reaction has been observed in orthopaedic implants made from PGA and/or PLA, which is probably due to the acidic products (glycolic acid for PGA and lactic acid for PLA) released by the polymer during degradation [118], that have the potential to significantly lower the pH of the local environment and this leads to an accelerated acid-catalysed hydrolysis in the tissue surrounding of the implant. This, in turn, could cause a faster loss of mechanical properties. A controlled slow release of degradation products in a manner that the surrounding area could metabolise them could be a solution to the acidity problem.

PLGA is the co-polymer of glycolic acid and lactic acid (fig. 1.10), synthesized by means of random ring-opening co-polymerization of lactide and glycolide. During polymerisation, successive monomeric units of glycolic or lactic acid are linked together by ester linkages, leading to a linear aliphatic polyester.

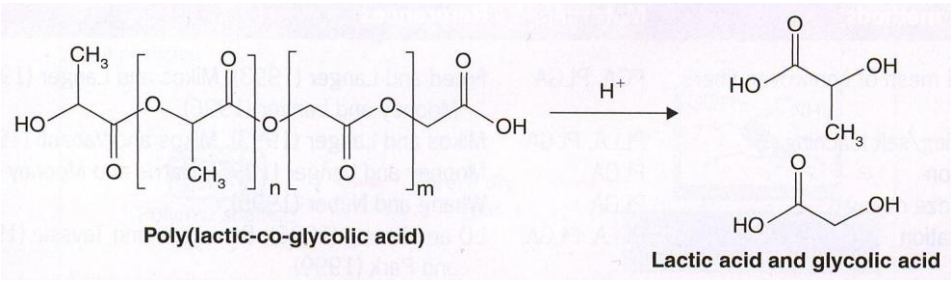

Fig. 1.10: Structure of polylactic-co-glycolic acid and its decomposition in lactic and glycolic acid. From [4].

PLGA degrades by hydrolysis or enzyme catalysed hydrolysis in four steps: 1) water penetrates the amorphous region and disrupts the secondary forces; 2) cleavage of the

covalent bonds in the polymer back-bone by hydrolysis; 3) significant mass loss begins to occur by massive cleavage of the backbone covalent bonds; 4) erosion: polymer weight loss [119]. Degradation rates of PLGA differ according to the proportion of lactic versus glycolic acid content (fig. 1.11): the higher the proportion of the more hydrophilic glycolic acid, the faster the degradation time of PLGA. For example, over 4 weeks time PLGA 85:15 was found to lose 10% of its mass, compared to 50% for PLGA 75:25 and 70% for PLGA 50:50 [120]. Furthermore, the degradation of PLGA is affected by the polymer crystallinity, and by significant changes in temperature and pH [121].

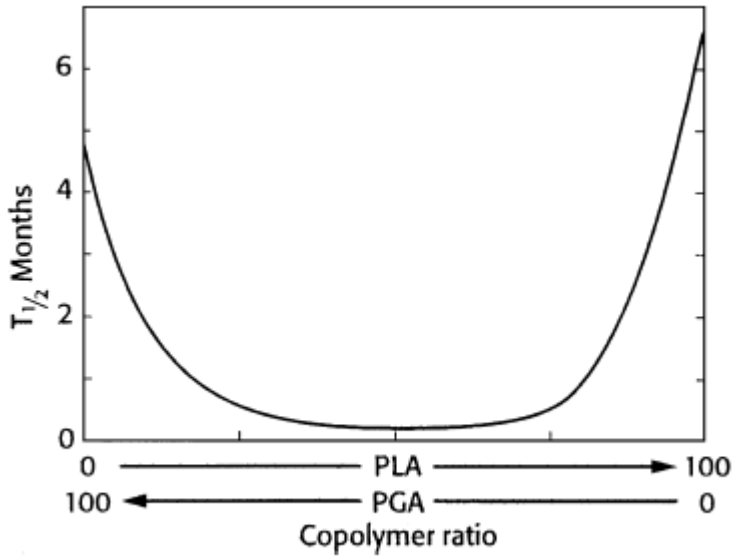

Fig. 1.11: Half-life of PLA and PLGA homopolymers and copolymers. From [122].

Several processing methods can be used to produce PLGA tissue scaffolds, *e.g.* solvent casting/particulate leaching technique, phase separation, emulsion freeze-drying, gas foaming, electrospinning and 3D printing [123] (fig. 1.12). PLGA is used for the fabrication of different forms of scaffolds, such as fibres, mesh, membranes, sponges.

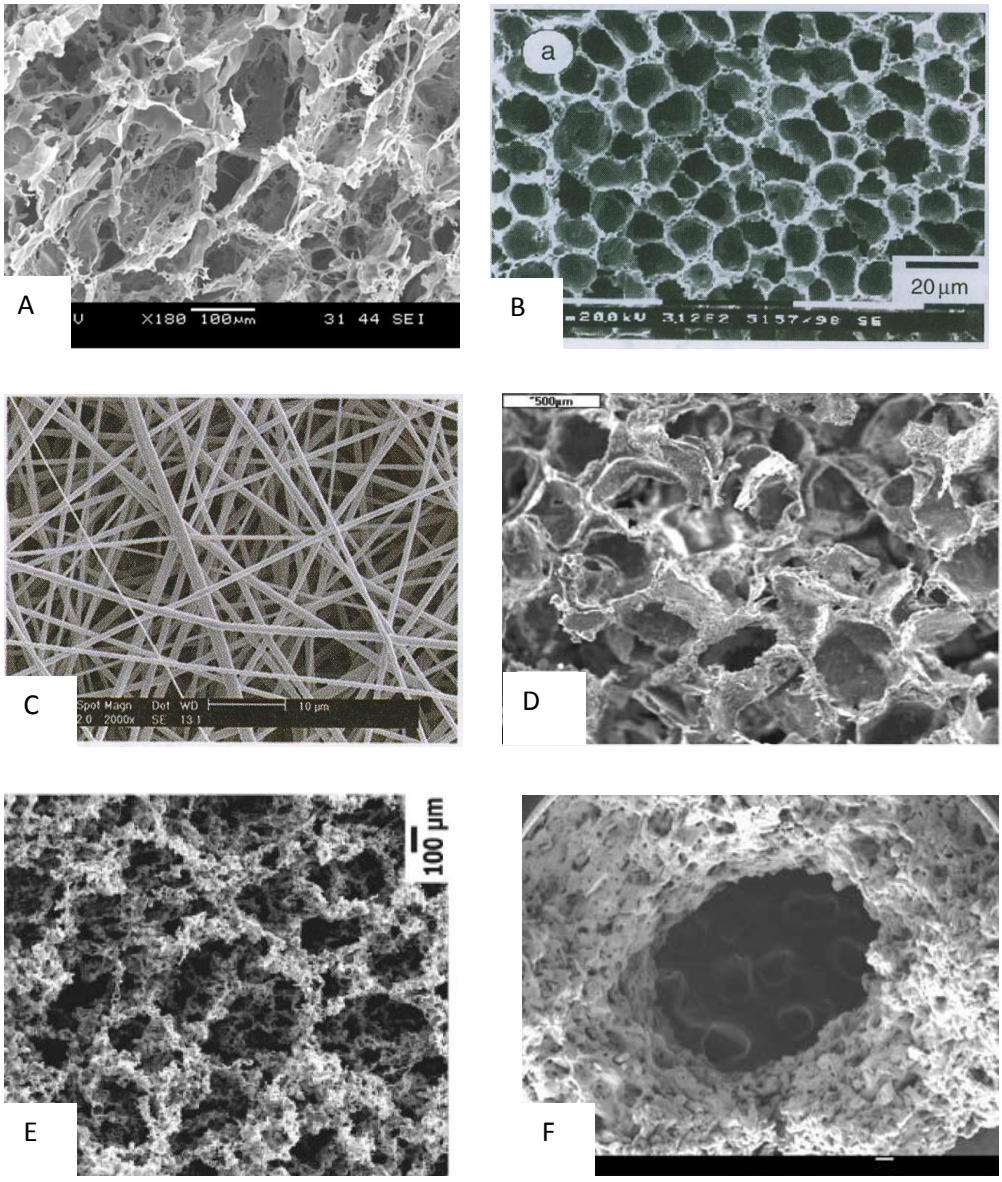

Fig. 1.12: Morphology of PLGA scaffolds prepared with different processing methods: A) gas foaming/salt leaching for cartilage regeneration [124], B) thermally induced phase separation for mesenchymal stem cell culture [4], C) electrospinning for nerve regeneration [4], D) solvent casting for *in vitro* and *in vivo* degradation studies [125], E) emulsion freeze drying for smooth muscle reconstruction [126], F) 3D printing for bone reconstruction [127].

Hollow fibre PLGA membranes have proved to be a good scaffold for cells, especially bone and cartilage derived cells, because they offer a large surface area to volume ratio in order to obtain large cell numbers when incorporated into a hollow fibre perfusion bioreactor [92]. High cell seeding and cell affinity are important factors to be considered in the fabrication of a scaffold. One of the major limitations in the use of PLGA for tissue engineering scaffolds is its hydrophobic character, resulting in sub-optimal adhesion, spreading and growth of cells on the surface of the

material [128], and also resulting in low hydraulic permeability through the scaffold. Hydraulic permeability is important for mass transfer studies as cell culture medium contains proteins which support the growth of cells (albumin, transferrin, fibronectin, fetuin), but also growth factors and proteins released by the cells themselves. Some techniques to make membranes more hydrophilic include pre-wetting the material with ethanol before cell seeding [105], hydrolysis with NaOH [129], protein-coating [130] and plasma treatment [131]. Blending with hydrophilic polymers is another way of improving the properties of polymeric membranes, especially their permeability and hydrophilicity [132-135]. Water-soluble porogens such as poly(ethyleneglycol) (PEG) [136, 137], polyvinylpyrrolidone (PVP) [138-142] and polyvinylalcohol (PVA) [139, 143-146] have been reported to improve the permeability of membranes. PVA is a water-soluble polyhydroxy polymer formed by hydrolysis of polyvinyl acetate [147] and degrades mostly by oxidative or thermal degradation (pyrolysis) [148], but also by photodegradation [149]. The degradation of PVA is pH dependent: alkaline hydrogen peroxide solutions, for example, can cause complete dissolution of PVA in 10 minutes at 95º C. Thanks to its hydrophilicity, excellent chemical resistance (e.g. long term temperature and pH stability), non-toxicity and biodegradability, PVA has been used in various pharmaceutical, medical, cosmetic and food products [150-152]. For the same reasons PVA is an attractive polymer for tissue engineering applications. For example, Oh *et al* have demonstrated how blended PVA-PLGA blend scaffolds made by the particulate-leaching method improved porosity, hydrophilicity and wettability of the material resulting in better cell adhesion and growth [147].

1.7 Bioreactors for tissue engineering

With the selection of the appropriate cell source and scaffold, the third challenge in tissue engineering is the ability to recreate an environment *in vitro* which mimics as closely as possible the environment that the cells experience *in vivo*, in order to allow their growth and expansion. In order to achieve this goal, bioreactors, *i.e.* systems for the cultivation of cells by controlling supplies of nutrients and gases, have been applied in tissue engineering. A bioreactor is a simulator, a device that should ideally create an environment that allows the cells to proliferate and differentiate as *in vivo*,

establish uniform cell distribution on 3D scaffolds, maximise the mass transfer of nutrients and oxygen to the tissue, and expose the tissues to physical stimuli, if required. The aim of the most recent bioreactors is then to mimic the cell's microenvironment in a living organism while allowing for a strict control over the cell environment and a real-time insight into cellular events, such as cell proliferation and differentiation [153].

1.7.1 Bioreactors employed in tissue engineering

Several types of bioreactor have been applied so far in tissue engineering. The choice of the bioreactor depends on the tissue to be engineered and its functional biomechanical environment. Below are described some of the most common bioreactors used in tissue engineering.

1.7.1.1 Spinner flask

The spinner flask (fig. 1.13) represents one of the first bioreactor models. Scaffolds seeded with cells are attached to needles hanging from the cover of the flask and medium is added in order to cover the scaffolds. A magnetic stirrer bar at the bottom of the flask continuously mixes the media thus providing the cells with a homogeneous distribution of oxygen and nutrients [154]. Spinner flasks have been shown to increase the efficiency of scaffold cell seeding and survival compared to static culture [155]. Cartilage constructs have been grown in these devices with good results, however the thickness of the tissue was found to be far thinner than native one, probably due to the poor mass transfer capacity of the reactor [156]. Another issue related to spinner flasks is that the fluid flow is turbulent and characterised by relatively high shear forces that could cause damage to the cells. Furthermore, the non uniformity of the shear forces may negatively influence the homogeneity of cell distribution on the scaffold [101].

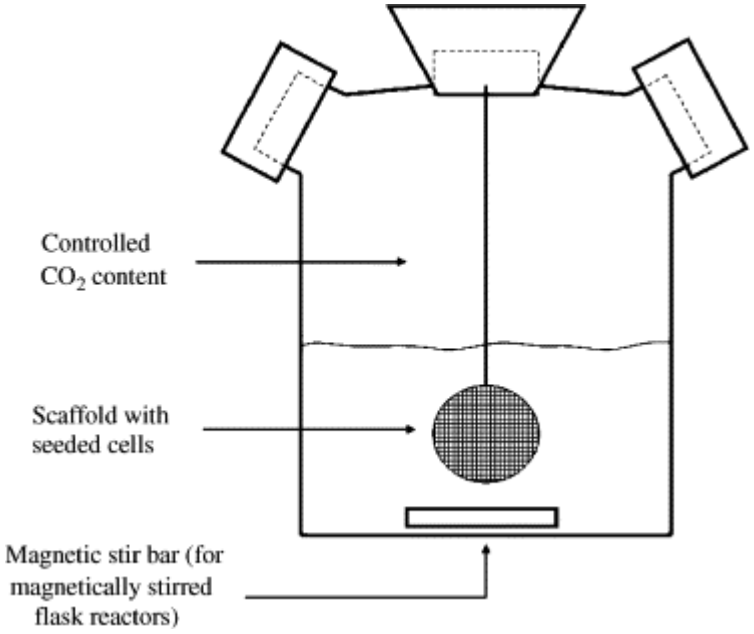

Fig. 1.13: The spinner flask, one of the first bioreactor models. From [156].

1.7.1.2 Rotating-wall vessel bioreactor (RWV)

Since high shear stresses can cause cell damage, bioreactors with low shear stresses have been developed. The most common system that operates at low shear stress is the rotating-wall vessel (RWV), where the cells are grown in a microgravity environment [157]. This device, first introduced by NASA, consists of two concentric cylinders whose annular space contains the cell culture medium (fig. 1.14). The inner cylinder is static and permeable to allow gas exchange for oxygen supply. The outer cylinder is impermeable and rotates horizontally at a speed that causes centrifugal forces that balance the gravitational forces thus generating a microgravity environment. In contrast to the spinner flask, the fluid flow is laminar and the shear stresses generated by the flow decrease in the direction of the flow [101]. The efficacy of RWV bioreactors has been demonstrated for cartilaginous [158] osteogenic [159], neuroendocrine [160], hepatic [161], adipose [162], vascular [163] and cardiac tissues [164]: tissues grown for a few weeks in the RWV showed characteristics very close to those of native tissue and were structurally and functionally superior compared to those cultured in static conditions or spinner flasks. One disadvantage of the RWV system is that the growth of the tissue is usually not uniform: the centrifugal force causes the scaffold to frequently collide

with the bioreactor wall, thus inducing cell damage and disrupting cell attachment [165].

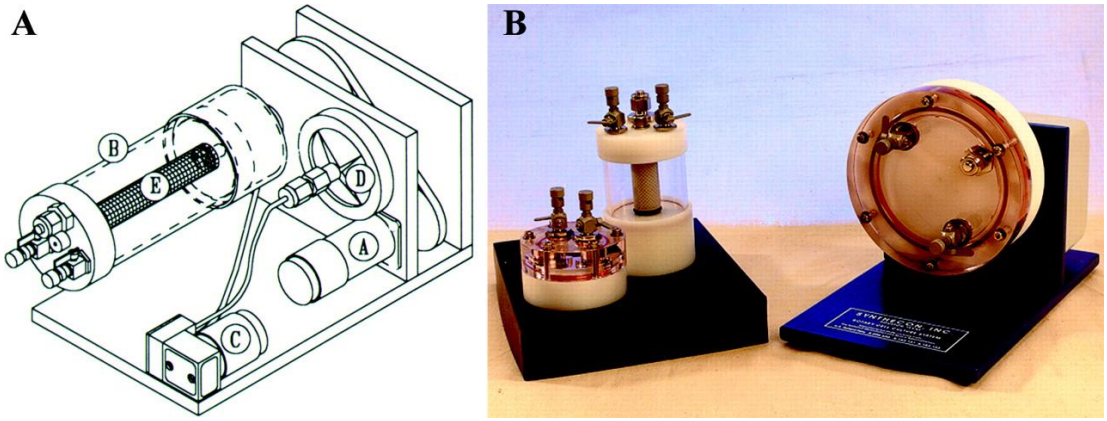

Fig. 1.14: Schematic draw (A) and picture (B) of the rotating wall vessel bioreactor. From [166].

1.7.1.3 Flow perfusion bioreactor

Flow perfusion bioreactors offer enhanced transport of nutrients to the interior of the scaffold and also a more uniform cell distribution compared to static culture and spinner flasks as they allow medium to be transported throughout the entire structure (external and internal) of the material (fig. 1.15), reducing in this way both external and internal diffusional limitations of 3D-scaffolds. In these systems a pump is used to perfuse medium continuously through the interconnected pores of the scaffold, thus maximising the mass transfer of nutrients. Furthermore, they expose the cells to mechanical forces by fluid shear stress, which can be varied by simply changing the flow rates in the system [154]. Perfusion bioreactors are the ideal culture systems for highly metabolic cells, *e.g.* hepatocytes, thanks to the increased mass transport of oxygen and nutrients to the cells [167].

Perfusion bioreactors can be used for seeding and/or culturing three-dimensional constructs. During seeding, cells are transported directly into the scaffold pores, while during culture, medium flows continuously through the internal pores thus enhancing the mass transfer of nutrients though the whole construct [168]. Perfusion bioreactors have been designed in different configuration, *e.g.* column, hollow fibre

and microfluidic bioreactors. For the purposes of this thesis, only hollow fibre bioreactors will be described.

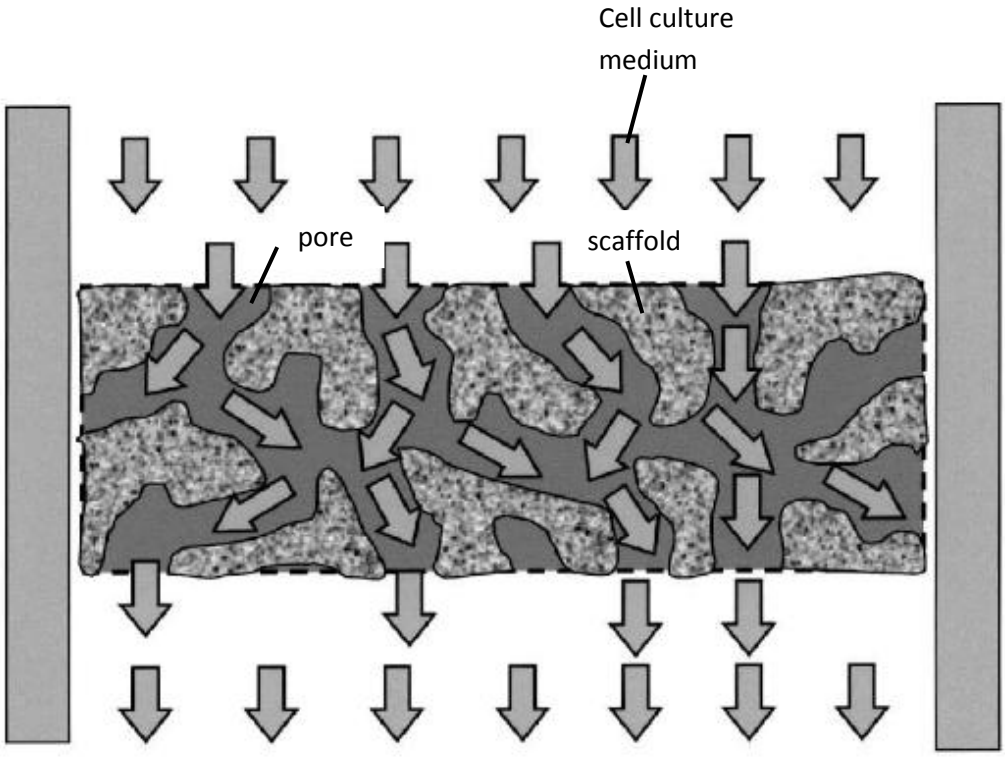

Fig. 1.15: Flow perfusion system: the culture medium is forced through the internal porous network of the scaffold, enhancing in this way nutrient delivery to and waste removal from the cells [154].

1.7.1.3.1 Hollow fibre bioreactor

A hollow fibre bioreactor consists of a bundle of hollow fibres encased in a cylindrical shell with ports for flow of media around the fibres. It is a two compartment module with an intracapillary and an extracapillary space (fig. 1.16). The fibres are fabricated from a porous material that permits the passage of nutrients and low molecular weight species but excludes cells and high molecular weight cellular products such as antibodies. Cells can be seeded either on the outer or in the inner surface of the fibre, with intracapillary or extracapillary media perfusion, respectively.

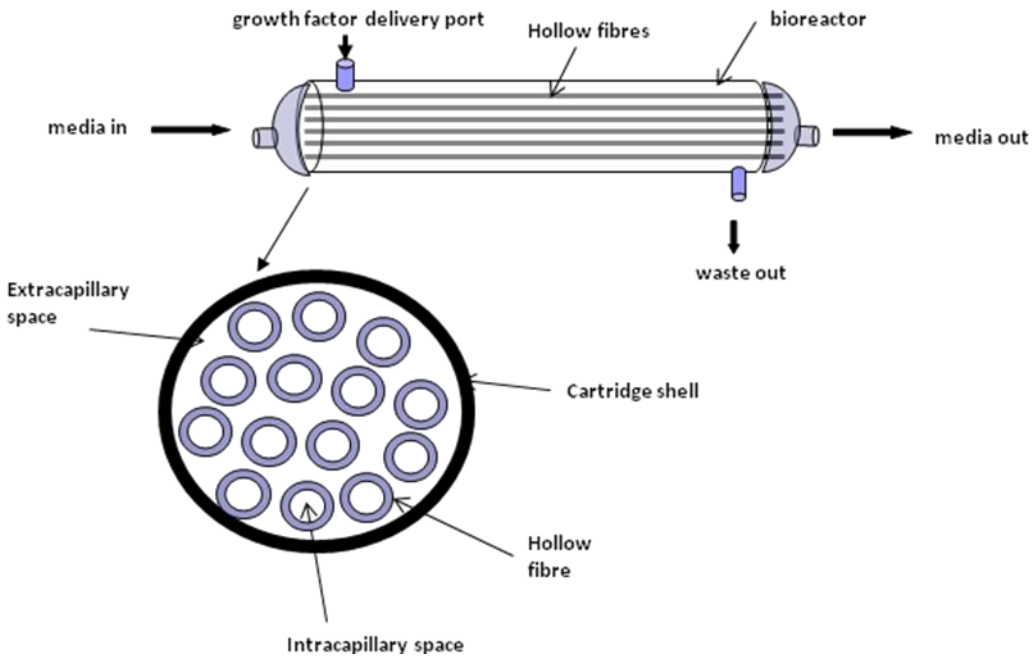

Fig. 1.16: Lateral and front view of a hollow fiber bioreactor. Adapted from [169, 170].

Flow inside the lumen of the fibre has a parabolic velocity profile, so that the cells grown on the inner surface of the fibre are subjected to a uniform shear stress which is directly proportional to the intracapillary flow rate [155]. The hollow fibres, by providing nutrients to the cells and eliminating their waste, mimic *in vivo* blood vessels. The main advantage of using this type of bioreactor is that it provides nutrients at the centre of the growing tissues, while oxygen delivery is the main factor limiting cell growth in hollow fibre bioreactors, as cell distributions and morphologies were found to vary with the distance from the oxygen supply. Hollow fibre systems have been employed for cell expansion [171], gene transfer [172], production of recombinant protein and viruses [173, 174], dialysis [175] and extracorporeal hepatic devices [176]. The most widespread use of hollow fibre for biomedical application is renal dialysis, where blood is passed through the intracapillary space of a hollow fibre membrane dialyser with a low molecular weight cut-off (< 10 kDa).

1.8 Co-cultures, scaffolds, growth factors and bioreactors to direct stem cell differentiation: potentials and limitations

As discussed in the previous sections, cells with different differentiation potential have been employed for tissue engineering purposes. For their ability of self-renewal and differentiation into different mature cell types, stem cells are becoming one of the most promising cell sources for tissue engineering strategies. For their capacity of differentiation toward different lineages, stem cells have been employed in this project, and this section will discuss the different strategies that researchers have explored in order to direct stem cell fate.

Soluble factors, cell-cell and cell-matrix interactions and cell microenvironment can be considered the most important effectors of stem cell fate (fig. 1.17) [177]. The following paragraph will discuss in more depth these four effectors with a focus on tissue engineering applications.

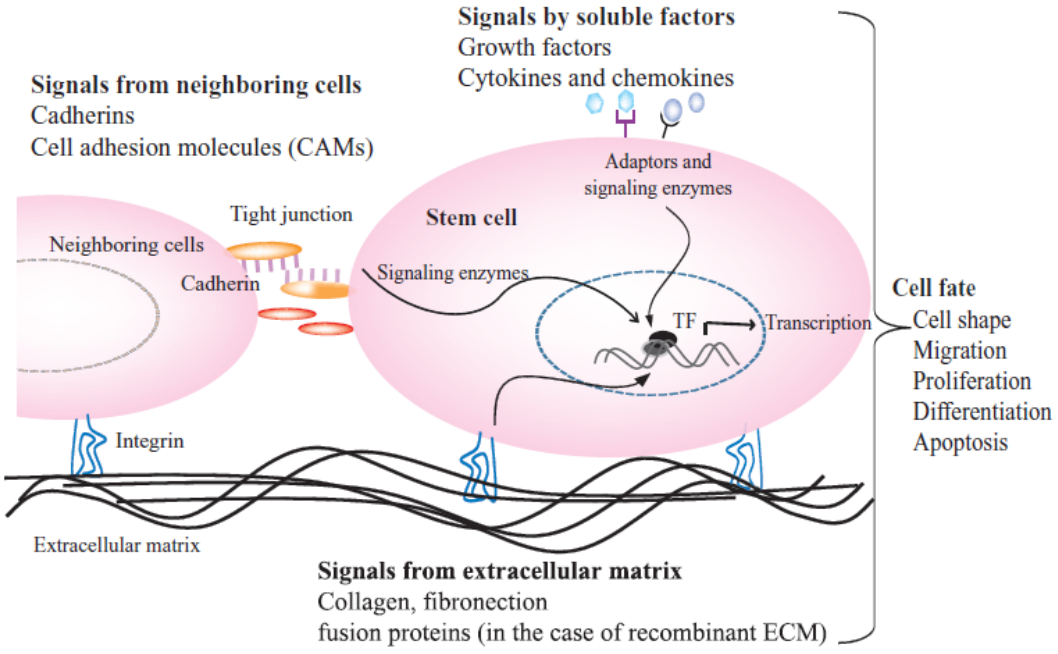

Fig. 1.17: Stem cell fate is influenced by interaction of soluble factors, extracellular matrix and signals from neighbouring cells. From [177].

1.8.1 Cell-cell interactions

Cell-cell interactions consist of specific binding of signalling molecules to cell-surface receptors (cadherins, cell adhesion molecules) which induces specific signalling pathways affecting gene expression, self-renewal and differentiation [177]. Cell-cell contact based signalling provides in fact important cues for development, morphogenesis and phenotypic stabilisation of stem cells [178]. Furthermore, cell-cell interactions have been shown to play a critical role in tissue regeneration *in vitro* [179]. For example, high mesenchymal stem cell densities have been shown to induce higher chondrogenic differentiation rates due to soluble factors and to signals from the neighbouring cells [180, 181].

Numerous studies have also shown that tissue specific cells may promote and enhance differentiation of stem cells towards a specific lineage by promoting dynamic cell-cell interactions. Therefore several studies focused on co-cultures systems, where stem cells were cultured in direct or indirect contact with tissue specific cells. For example, co-culture of hepatocytes with embryonic stem cells or mesenchymal stem cells was shown to enhance stem cell proliferation and differentiation towards the hepatic lineage [182-184]. Similarly, Csaki et al demonstrated that primary osteoblasts co-cultured with MSCs actively made cell-cell contacts, which strongly promoted the proliferation of MSCs and their differentiation into osteoblasts [185]. This was further confirmed by the observation that high-density co-cultures of primary osteoblasts and MSCs increased the MSC differentiation rate [185]. In high density co-culture systems, the expression of integrins (adhesion molecules that mediate cell-cell and cell-matrix interactions) is high, thus confirming the cell-cell communications that are taking place [185]. Another example is given by differentiation into neural lineage by co-culture with stromal cell lines or cerebellar neurons or astrocytes [186-191]. Despite co-culture systems have shown a great potential for the differentiation of stem cells, they still produce a heterogeneous population of cells, which raises the issue of the retrieval of the differentiated stem cells from the culture. Furthermore, they fail to induce terminal differentiation, suggesting that co-cultures alone might lack factors which are required to induce complete differentiation and therefore they are not sufficient to adequately replicate the complexity of the in vivo environment [192].

1.8.2 Cell-matrix interactions

Cell-matrix interactions also play an important role in regulating stem cell differentiation. Components of the ECM, such as collagen, laminin and fibronectin, are recognised by the transmembrane integrin receptors, and induce specific signalling pathways, which lead to changes in gene expression, cell growth and differentiation [177] (fig. 1.17).

Biomaterials have been the most important tool so far to recreate *in vitro* the extracellular matrix and they can provide signals to the cells that are missing in 2D cultures. Biomaterials can provide both chemical and physical stimuli that can influence stem cells fates. In particular, it was found that scaffolds can promote embryonic and adult stem cell self-renewal [29, 193], proliferation [194] and differentiation [26]. MSCs cultured on agarose gels with different stiffness, for example, differentiated into neural, muscle, or bone lineage according to the stiffness of the scaffold, which closely resembled that of brain, muscle or bone respectively [193]. Both biologically derived and synthetic biomaterials have been investigated as an extracellular matrix (ECM) in regenerative medicine and tissue engineering. In general materials from natural sources are advantageous for stem cells adhesion and differentiation because of the presence of specific ECM biofunctional molecules recognisable by the cells [177]. Fibrin scaffolds, for example, have been shown to significantly improve neural and chondrogenic differentiation of ESCs [195, 196]; hyaluronic acid hydrogels have been shown to maintain the pluripotency and undifferentiated state of human ESCs and to direct their differentiation towards specific lineages when soluble growth factors were added [27]; alginate, a natural polysaccharide derived from algae walls, has also been used for stem cell culture: Maguire and colleagues, for example, reported that mouse ESCs encapsulated in alginate poly-L-lysine supported cell proliferation and differentiation into hepatocytes [28]; collagen has been shown to direct chondrogenesis from human MSCs and to sustain umbilical cord stem cells expansion, viability and hematopoietic function [197]; silk has also been used to differentiate MSCs into bone and cartilage [198]. However, issues related to natural materials, e.g. purification, immunogenicity and pathogen transmission have driven the design of synthetic biomaterials which mimic the ECM, which have gained particular interest due to their excellent

mechanical properties, processability and low cost [177]. The development of artificial ECM should enable more efficient and scalable culture of stem cells, as well as greater control over stem cells behaviour [177].

Among synthetic materials, PGA, PLA and PLGA have been shown to support ESCs growth and differentiation [26]. Taqvi et al have also demonstrated that mESCs differentiation into the hematopoietic lineage was increased by decreasing PLA scaffold pore size and increasing the polymer concentration [199]. Nanofibrous scaffolds from poly(ε-caprolactone) (PCL) have also been found to enhance both MSCs and ESCs proliferation and adipogenic, chondrogenic and osteogenic differentiation [200, 201]. Finally, poly(ethylene glycol) (PEG) hydrogels have been studied as scaffolds for both MSC and ESCs cultures and have been shown to promote chondrogenic differentiation of mESCs [202].

Scaffold materials have also been chemically modified in order to improve adhesion, proliferation and differentiation of stem cells. Incorporation or deposition of simple chemical modifications within/on a material offers a great potential to control stem cell differentiation. Scaffolds modified with methyl, amino, hydroxy and carboxy groups, for example, have been shown to trigger differentiation of MSCs into chondrocytes and osteoblasts when cultured in the appropriate medium [203]. However, these modifications only directed the differentiation of a limited number of stem cells. Emerging technologies associated with nanotopography, *e.g.* nanopatterned chemically modified surfaces, have shown promising results in terms of controlling initial cell responses and offer a great potential for the induction and control of cell functionality [203].

1.8.3 Growth factors

The third type of effector on stem cell differentiation is represented by soluble factors (growth factors, cytokines, chemokines), which, by binding to specific cell receptors, can induce intracellular signalling pathways which can cause stem cells to differentiate into specific lineages. Different factors have been reported for their capacity to induce stem cell differentiation into specific lineages. The transforming growth factor β (TGF-β), for example, is a multifunctional growth factor involved in

tissue development and repair. It exists in three different isoforms (TGF-β1, 2, 3) and belongs to a superfamily of proteins called TGF-β superfamily. Among the proteins of the TGF-β superfamily, TGF-β1 and bone morphogenetic protein (BMP) are considered two key factors in chondrogenic differentiation [181]. It has in fact been reported that TGF-β1 and BMP proteins induce mesenchymal stem cells towards chondroblastic and osteoblastic differentiation [181, 204]. Weiss et al demonstrated that TGF-β1 alone can induce chondrogenesis, thus highlighting the pivotal role of this protein in chondrogenic differentiation, and the supportive role of other factors (BMPs, insulin-like growth factor 1 (IGF-1) and fibroblast growth factor (FGF)), which act synergistically with TGF-β in the differentiation of stem cells towards the chondrogenic lineage [205]. BMPs, FGFs and TGF-β are also involved in liver differentiation [206]. In particular, FGFs and BMPs are essential for selective differentiation in hepatic cells from definitive endoderm [207], and Touboul et al reported the induction of definitive endoderm by adding activin A, FGF-2 and BMP-4 to cell culture medium, while the subsequent addition of FGF-10 induced the differentiation of the cells of the definitive endoderm into the hepatic progenitor cells [208]. FGF proteins have also a key role in neural differentiation [209], and this is confirmed by the fact that when FGF activity is disrupted, neural induction is inhibited [210]. The multifunctional growth factor TGF-β is also implicated in neural differentiation, and in particular in the development of dopaminergic neurons [211, 212].

From these examples it is clear that some factors are involved in several signalling pathways that lead to the differentiation of stem cells into different lineages, therefore the accurate programming of stem cells toward a specific lineage might require not only the activation of some specific pathways but also the inhibition of other signalling pathways. Therefore there is a need for a better understanding of which factors maintain or induce stem cell differentiation toward a specific lineage during development, and in what time sequence. Indeed it was reported that when growth factors were delivered to the cells in a time sequence that resembled that occurring during the specific tissue development, the differentiation rate was higher compared to that of cells treated with simultaneous delivery of the same growth factors [181, 204, 206-208, 213]. Snykers *et al*. for example, reported that mesenchymal stem cells differentiated toward the hepatic lineage with a higher

efficiency when cells were exposed to liver-specific factors in a time-sequence that mimicked the *in vivo* liver embryogenesis (FGF-4 to induce endoderm, followed by hepatocyte growth factor (HGF), insulin-transferrin-selenium, dexamethasone and trichostatin A to induce liver specification), compared to those treated with a "cocktail" of the all factors at the same time-points [213], while Touboul et al differentiated hESCs into hepatocytes using a differentiation protocol that followed the key stages of liver development and showed that the cells expressed some liver markers and displayed hepatic functions [208]. Similarly, Raiche *et al*. showed that the sequential delivery of IGF-1 and BMP to MSC cells resulted in a even more increased alkaline phosphatase activity and bone formation compared to simultaneous release [214], while Yilgor et al found a higher chondrogenic differentiation rate by means of sequential delivery of BMP-2 and BMP-7 to MSCs compared to simultaneous or individual release [215]. The sequential exposure of cells to growth factors seems therefore to be a successful approach for differentiation of stem cells as it mimics more closely the gradual and sequential process of tissue development that is found in nature.

1.8.3.1 Growth factor delivery systems

Once identified which growth factors are needed for directing the fate of stem cells toward a specific lineage, and with which time sequence, another issue arising is represented by the mean of delivery of the growth factors. In most current differentiation protocols growth factors are supplemented directly into the cell culture medium at regular intervals. However, cells often need a prolonged exposure to growth factors in order to achieve terminal differentiation and maintain *in vitr*o the specific functions of differentiated cells. Therefore other systems for growth factor delivery have been employed. Recent advances in tissue engineering have led to the development of new systems of growth factor delivery: the growth factor can be incorporated into the biomaterial, thus creating a scaffold releasing growth factors that elicit specific cellular responses, such as differentiation (fig. 1.18). Park *et al*, for example, developed a hyaluronic acid-based hydrogel scaffold containing brain-derived neurotropic factor. The controlled delivery of the factor from the hydrogel facilitated the differentiation into neural lineages of mesenchymal stem cells that had been incorporated into the material [216]. However, hydrogel-based scaffolds have

limitations such as cell death in the depths of the scaffolds as well as poor mechanical properties [217]. For these reasons more solid scaffolds such as PLGA have been preferred for growth factor delivery. Sahoo et al, for example, developed PLGA nanofibers capable of continuous release of bFGF to direct the differentiation of MSCs towards the fibroblastic lineage [217]. The growth factors can also be encapsulated into biodegradable nano/microparticles which release them in a time-controlled manner. PLGA nano/microparticles releasing BMP have, for example, been shown to enhance bone formation [218, 219]. The particles can be then incorporated into the biomaterial, thus creating a scaffold releasing growth factors.

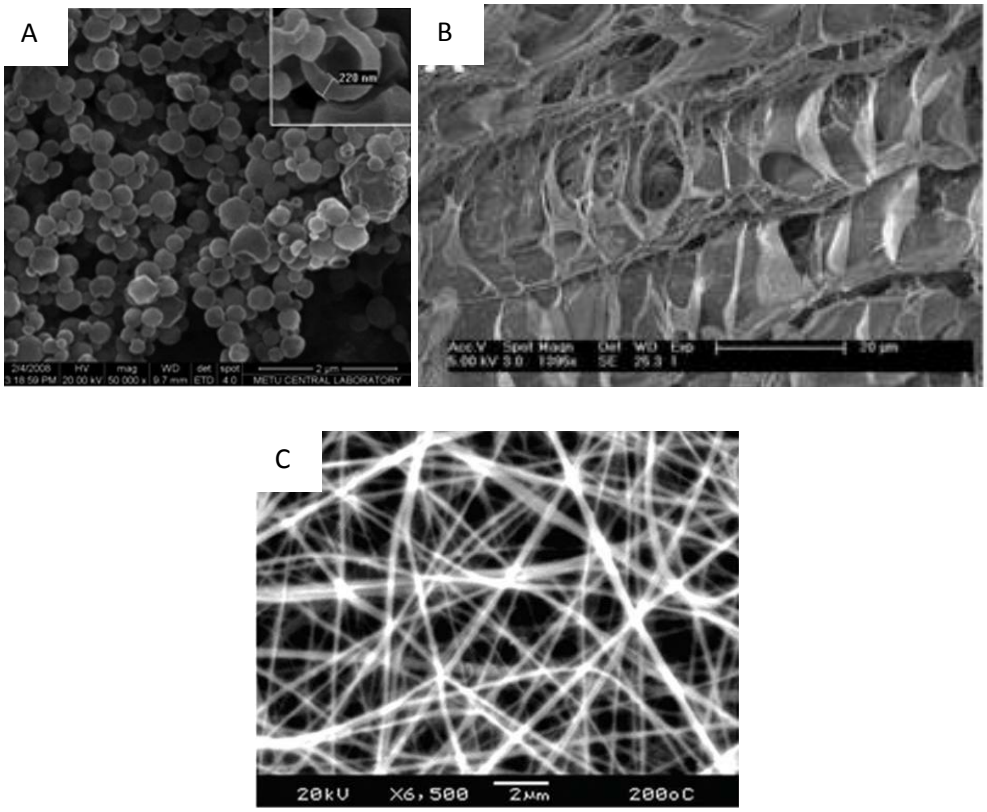

Fig. 1.18: Different biomaterials for growth factor delivery. A: PLGA nanoparticles releasing BMP [204]; B: poly-L-lysine PEG hydrogel for neurotropic factor delivery [220]; C: PLGA nanofibres delivering bFGF [217].

Although these three strategies allow for the prolonged delivery of growth factors, biomaterials incorporate commercial growth factors, which are often expensive, especially if the cells need to be exposed to them for a sustained period of time. Stem

cells differentiated into hepatocytes, for example, started losing their characteristic morphology and expression of liver-specific markers after a few days [221]. Similarly, a loss of chondrogenic phenotypes at late stages of differentiation was observed [222], indicating that cells needed to be treated with the specific growth factors for a longer period of time.

Furthermore, current differentiation protocols do not lead to enough cells differentiated: most cells are still critically limited by insufficient differentiation and only exhibit a progenitor phenotype [206, 207, 222]. If embryonic stem cells are used, there are also safety issues as they can give rise to tumors known as teratomas. Hence, it is critical for any therapeutic strategy employing a stem cell–based approach to ensure complete and irreversible differentiation of stem cells into the desired terminal target cell type. This could be achieved for example by extending the timing of differentiation protocols in order to allow a greater mass of differentiated cells to be produced. In contrast to artificial release of growth factors from biomaterials, co-culture systems would make the protein continuously available for the stem cells for extended periods of time and at no additional costs. The neighbouring cells might also provide, through cell-cell contacts, additional signals required for differentiation that would not occur with the delivery of exogenous synthetic growth factors. The co-culture system would be the strategy that mimics more closely nature. Co-culture systems and biomaterials-systems might lead to different degrees of differentiation, *e.g.* different phenotypes and different markers expression. The factors and signalling pathways regulating tissue development still have not been completely clarified and therefore there is a need for a deeper understanding of the mechanisms of tissue specification in the embryo in order to reproduce *in vitro* the steps of stem cells differentiation that occur in nature.

1.8.4 Bioreactors for stem cells expansion and differentiation

Another issue related to stem cell differentiation is that the number of cells that need to be expanded *in vitro* and then differentiated for clinical use is still a limitation, and, as a consequence, current differentiation protocols do not lead to enough cells for clinical use [206, 207]. This suggests that there is a need for systems that are able

to expand progenitor cells in order to obtain large yields of more differentiated cells which can remain more stable for longer periods of time. Traditional static cell culture systems like flasks and multi-well plates are not ideal for stem cell expansion as they do not provide adequate nutrient and oxygen distribution [223], and it is difficult to control some of the key regulatory factors of stem cells, especially shear stress and oxygen levels [3], which have been found to play an important role in stem cell proliferation and differentiation [224, 225]. In addition, static 2D systems cannot provide large volumes of media required for stem cells expansion. Furthermore, these systems fail to reproduce *in vitro* the dynamic environment experienced by the cells *in vivo*. Therefore dynamic cell cultures systems need to be designed and tested for the *in vitro* expansion and maintenance of stem cells. The use of bioreactors that create a shear stress and provide continuous oxygenation in the culture medium represents an advance from static flasks as they enable a precise control of the cellular microenvironment. MSCs subjected to fluid perfusion, for example, showed an increased cell density and more uniform distribution [226] and those subjected to compression differentiated towards the chondrogenic lineage [61] compared to static cultures. Some fluid shear stress-based bioreactors have been also used with ESCs to study the embryoid body model and to promote differentiation toward a specific lineage [227-229].

As can be seen from these examples, substantial progress has been made in directing differentiation of stem cells toward lineage-specific cells. However, in order to bring these findings to clinical applications, large-scale robust and totally controlled culture systems capable of expanding and differentiating stem cells, as fast and pure as possible, are needed [230, 231]. Stirred suspension bioreactors have gained special interest for stem cell expansion, as they have been shown good results in the expansion of different types of stem cells and in their differentiation into pancreatic and neural lineages [231, 232]. However researchers have to face many challenges in scaling-up stem cell cultures. For example, if cells are cultured in suspension, they might aggregate and this would result in a limited diffusion of nutrients, growth factors, and gases within the aggregates [230]. Another problem is the heterogeneity in the culture environment due to gradients in dissolved oxygen and metabolites. Thus it is important to ensure that the culture is adequately mixed while limiting shear forces that could damage the cells [230]. The maintenance of embryonic stem

cells in the self-renewal state presents a further problem, as it requires growth factors and extracellular matrices that are very expensive. Another issue related to ESCs is related to the potential genetic instability of these cells through many divisions, which might present safety issues for clinical applications [230]. Finally, since the current systems to differentiate stem cells do not produce a completely homogeneous population of differentiated cells, monitoring the differentiation status of the cells during the scale-up process is another challenge, and selection processes might be needed in order to select the differentiated cells from the immature ones [230]. Ultimately, each clinical application will require a bioreactor with different properties in order to recreate the most suitable environment for the differentiation of the stem cells into a specific lineage.

1.9 Conclusions

Stem cell differentiation is a complex process that still has not been fully understood. The result obtained by several studies indicate soluble factors, cell-cell and cell-matrix interactions as the most important effectors of stem cell fate. Advances in tissue engineering have allowed the fabrication of different scaffolds that mimic the natural extracellular matrix, thus allowing cell growth and proliferation, and in some cases, directing stem cell differentiation. Cell-cell interactions play an important role in stem cells differentiation and different co-culture systems have been employed to direct the stem cell fate toward the desired lineage. Soluble cytokines and growth factors have also been shown to be required for stem cell differentiation, and different systems of delivery to the cells have been investigated. However, for clinical applications, large numbers of differentiated cells are needed over time, requiring large amounts of costy growth factors and rising the issue of high costs. Finally, a dynamic microenvironment that mimics as closely as possible that found *in vivo* needs to be recreated *in vitro* in order to promote stem cell growth, proliferation and differentiation. To achieve this, different bioreactor designs have been realised, for the expansion and differentiation of stem cells *in vitro*. Although each of these factors have been shown to induce some degree of stem cells differentiation, the appropriate combination of all of them might be required in order to achieve an adequate stem cell expansion and a terminally differentiated cell stem cell-derived phenotype, for clinical applications.

Therefore this project aims to combine the development of a suitable bioreactor, and scaffold for stem cells growth and of co-culture systems for the cheap production of growth factors for stem cell differentiation. The next paragraph will describe in further details the aims and objectives of the project.

1.10 Aims and objectives

The major aim of this project is to develop a suitable bioreactor to enable the co-culture of cells in order to direct stem cell differentiation. Several aspects of the system need to be considered in order to achieve the goals of the project. In the first place, the type of bioreactor that will be used for the optimal growth of stem cells and the appropriate mass transfer of nutrients must be selected. It is known that hollow fibres offer a greater surface area to volume ratio for the culture of higher cell numbers compared to flat sheets and also act as a barrier between the cells and the medium that flows inside the lumen of the fibre, thus allowing high flow rates with no risk of cell damage due to mechanical forces caused by the flow [92]. Therefore the hollow fibre bioreactor was selected for the purposes of this project. The system that this project aims to realise is represented in fig. 1.19. Stem cells are seeded on the outer surface of the hollow fibre, and medium containing growth factors is continuously circulated inside the lumen of the fibre. Because the fibre is porous, the growth factors can permeate through the pores of the membrane and differentiate the stem cells.

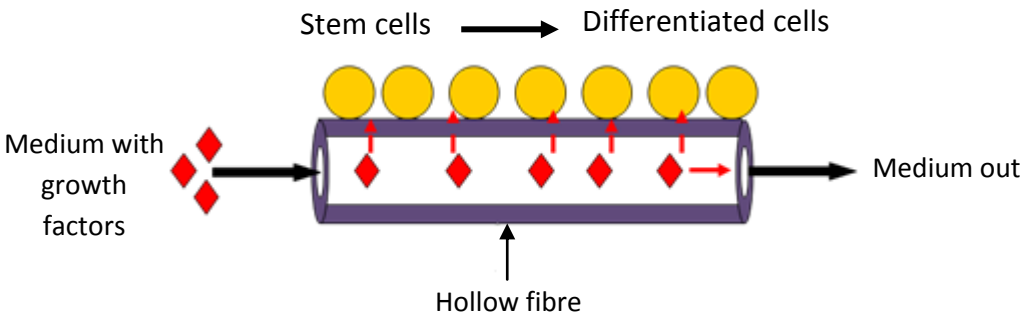

Fig. 1.19: Schematic representation of the system that this project aims to realise: stem cells are seeded on the outer surface of a PLGA hollow fibre membrane and medium containing specific growth factors is continuosly circulated inside the lumen of the fibre. Growth factors permeate across the pores of the fibre thus reaching the stem cells and causing their differentiation.

When considering this system, the next aspect that should be investigated concerns the choice of the material from which to fabricate hollow fibres. The synthetic polymer PLGA has been widely used in tissue engineering as it is biocompatible, biodegradable and FDA approved [80]. For these reasons, PLGA was selected for this project. However, despite these advantages, PLGA presents a major issue: its hydrophobic character makes the membrane poorly wettable by water and aqueous solutions *e.g.*. cell culture medium, thus reducing cell adhesion and transfer of nutrients across the membrane, which is extremely important for appropriate *in vitro* tissue reconstruction [128]. Therefore strategies to improve hydrophilicity of PLGA need to be investigated.

The last part of the project will focus on the differentiation of stem cells by means of growth factors and co-culture systems. Growth factors are among the most important effectors in stem cell differentiation. However, the use of commercial growth factors would imply high costs as large quantities of protein would be required for the differentiation of the stem cells and for the maintenance of their differentiated state. Therefore, a system for the continuous and inexpensive production of growth factors needs to be investigated. Cells can release proteins into the cell culture medium, either spontaneously or when engineered to do so. Therefore a cell line capable of releasing one or more growth factors at the concentrations needed for stem cell differentiation and that is stable in dynamic culture systems must be selected. In this way, a growth factor-secreting "cell factory" would be developed, which would continuously provide the growth factors to the cells within the system, thus reducing the cost of the experiment.

Finally, In order to explore a clinically relevant application of the system, the differentiation of stem cells into one specific cell type must be investigated. Liver disease is one of the big killers in the world and tissue engineering might offer a valid therapy to overcome the issues related to liver transplantation. Therefore the hollow fibre bioreactor system will be tested for a potential application in liver tissue engineering. A cell line capable of releasing liver specific growth factors that can permeate across the pores of the hollow fibre membranes and differentiate the stem cells into hepatocytes needs to be selected.

In summary, this research aims to:

- Improve the hydrophilicity of PLGA
- Develop a bioreactor system that allows optimal stem cell growth and transfer of nutrients
- Develop a system for the continuous and inexpensive production of growth factors
- Develop a system for the differentiation of stem cells by means of growth factors and co-cultures
- Differentiate stem cells into hepatocytes by means of liver-specific growth factors and co-culture systems as a potential application

2. Materials and methods

2.1 Materials

All materials were purchased from Sigma Aldrich, except from those listed in the following table:

MATERIAL	COMPANY
PLGA, Resomer RG 756S	Boehringer Ingelheim
NMP	Acros Organics
Compressed nitrogen gas	BOC Gases
HL60 cells	ECACC
Vybrant CFDA SE Cell Tracer Kit	Invitrogen
Quant-iT™ Pico Green dsDNA quantitation assay kit	Invitrogen
HGF ELISA Development system kit	R&D Systems
Sodium Pyruvate	Gibco
FGF-4	Peprotech
HGF	R&D Systems
Blocking reagent for immunostaining	Roche
Goat anti-rat transferrin antibody	Insight Biotechnology
Sheep anti-rat albumin antibody	AbD Serotech
Sheep anti-rat UGT antibody	Cypex
Fluorescein anti-sheep IgG	Vector Laboratories
Fluorescein anti-goat IgG	Vector Laboratories
99% Isopropanol	Fisher Scientific
Haematoxylin stain	Fisher Scientific

2.2 Membrane preparation

The polymer used to fabricate the membranes was poly (lactic-co-glycolic) acid (PLGA) with 75:25 lactide-glycolide ratio.
The process of membrane preparation can be divided into two steps: 1) polymer solution preparation and 2) membrane fabrication.

2.2.1 Polymer solution preparation

Polymer solutions were prepared from PLGA blended with polyvinyl alcohol (PVA) (0, 1.25, 2.5, 5% w/w) by dissolution in N-methyl-2-pyrrolidinone at a total polymer concentration of 20% w/w. The mixture was placed on a roller mixer (SRT9D, Bibby Stuart, UK) and left under ambient conditions (8-20°C) overnight, to ensure complete dissolution.

2.2.2 Flat sheet fabrication

Flat sheet membranes were fabricated by the phase inversion method. 2-3 ml of polymer solution were cast over the surface of a flat glass plate (10 cm x 15 cm) with a 1 cm diameter glass pipette kept at a height of 200 μm from the plate using 200 μm wire wrapped around it. The plate was then submerged in deionised water (non-solvent) at 10-20º C for a few minutes to allow the phase-inversion process to take place. The resulting membrane could then be peeled from the surface of the plate and was soaked in water for 3 days. The water was changed twice a day for solvent removal. The membranes were then left to dry in ambient conditions for at least 24 h prior to use.

2.2.3 Hollow fibre fabrication

Polymer solutions were degassed under a vacuum for 1 hour to remove air bubbles and then extruded through a double-orifice spinneret to produce hollow fibre membranes through a process called wet-spinning, using the method optimised by Shearer [233]. A schematic representation of the spinneret and of the spinning apparatus used to fabricate the fibres can be seen in fig 2.1 and 2.2, respectively. It consists of a spinneret, three water tanks and motorized rollers. The first two tanks

(coagulation bath and wash bath) were filled with tap water (non-solvent) and the temperature of the coagulation bath set at 25º C. After setting up the spinning rig, the polymer solution was pumped through the spinneret outer annulus (1.0 mm outer diameter, bore 0.7 mm inner diameter) while distilled water was extruded through the inner orifice (inner diameter 0.4 mm) at a flow rate of 200 ml/h. As soon as the polymer solution contacted the water from the spinneret it precipitated forming a fibre. The newly formed hollow fibre was collected by a roller located at the bottom of the first tank (the coagulation bath) to ensure that the fibre dropped vertically. The fibre was fed through the other rollers and washed in the second tank and finally collected in the last tank, where it was left for 24h before drying in ambient conditions (10-20°C).

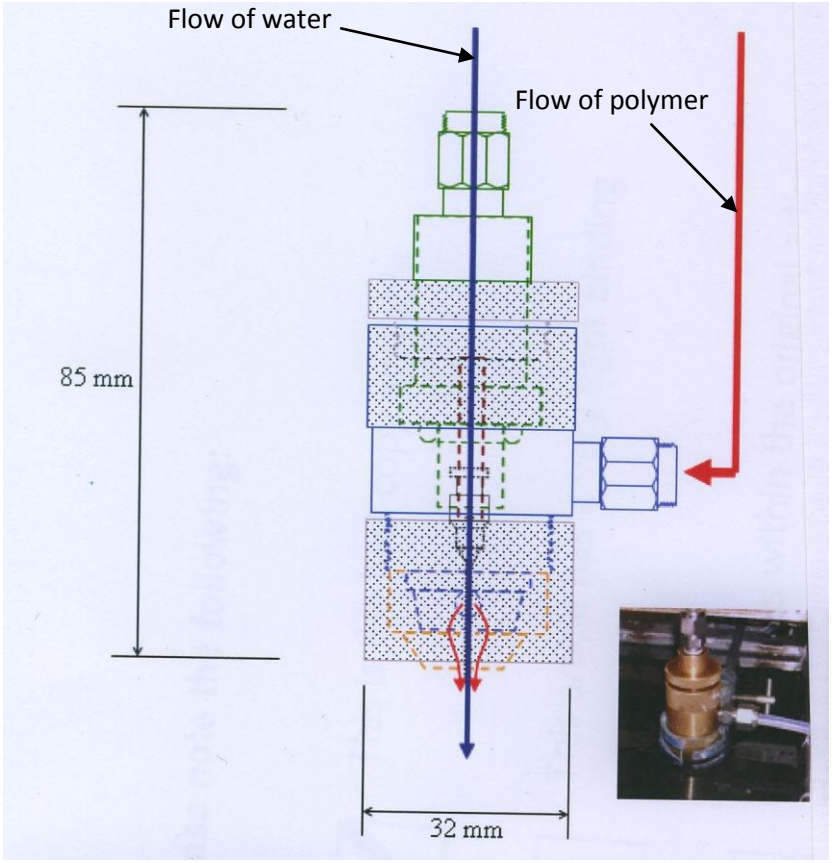

Fig. 2.1: Picture and schematic representation of the double orifice spinneret. Adapted from Shearer H., 2007 [233].

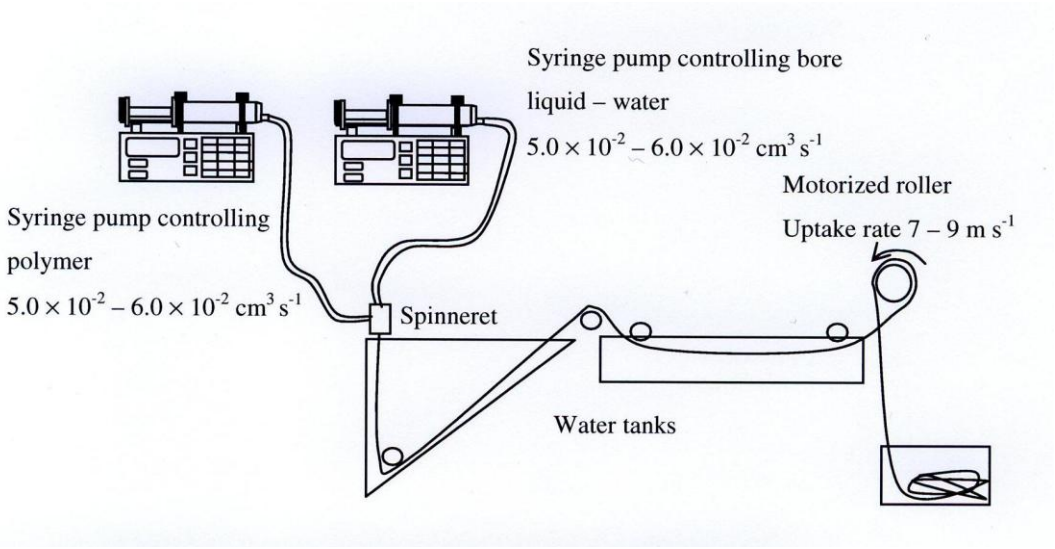

Fig. 2.2: Representation of the spinning apparatus. Distilled water and polymer solution were pumped by means of two different syringe pumps through the orifice of a spinneret. The hollow fibre formed by precipitation was collected in the first tank and then transferred by means of motorised rollers to a second tank and finally collected in a third tank and left for 24 h prior to drying. From Shearer H., 2007 [233].

2.3 Treatment of hollow fibre membranes with sodium hypochlorite

Fibres were incubated for 24 hours in 5% v/v sodium hypochlorite (NaOCl) or in distilled water at 37° C in order to study the effect of NaOCl on the morphology, hydrophilicity, permeability and mechanical properties of the fibres. After 24 hrs the fibres were washed for one hour with distilled water to remove any residual NaOCl.

2.4 Membrane characterization

2.4.1 Morphological analysis

Morphological analysis of the membranes was conducted using scanning electron microscopy (SEM). Hollow fibres were cut into pieces of approximately 5 mm in length. The membranes were sputter coated with gold (Edwards Sputter Coater 5150B) and subsequently analyzed by SEM (JEOL JSM-6480LV) with an acceleration voltage of 15 kV at the Centre for Electron Optical Studies (CEOS), University of Bath. Images of the inner and outer surfaces and of cross-sections of hollow fibre membranes were obtained.

2.4.2 Mean pore size and porosity

Mean pore size and overall porosity of hollow fibre membranes were determined by gas permeation using a single-fibre dead-end module with purified nitrogen (BOC, UK) as the test gas. A schematic representation of the gas permeation module and apparatus used can be seen in fig. 2.3. A 12 cm long hollow fibre was glued into a 10 cm x 6 mm stainless-steel tube with epoxy resin. The excess length was trimmed, and at one end the lumen of the fibre was sealed while at the other end the shell side was sealed. The module was connected to a bubble-meter and nitrogen gas was passed into the module through the lumen, exiting through the fibre wall at a range of flow rates between 2 l/min and 6 l/min and the corresponding air pressures measured. The time required by the soap bubble inside the bubble-meter to reach 100 ml was recorded and the volumetric flow rate of gas flowing through the fibre calculated with equation 2.1:

$$Q = \frac{V}{t} \qquad (2.1)$$

where Q = volumetric gas flow rate (m^3s^{-1}), V= volume of gas timed (0.1 m^3), t = time taken (s).

The volumetric gas flow rate was then converted into molar gas flow rate with equation 2.2:

$$N = \frac{QP_{out}}{RT} \qquad (2.2)$$

Where N= molar gas flow rate (mol s^{-1}), P_{out} is the atmospheric pressure (1 x 10^5 Pa), R the molar gas constant (8.31 J mol^{-1} k^{-1}), T = temperature (298 K).

The gas permeability was then calculated using equation 2.3:

$$J = \frac{N}{AP_{in}} \qquad (2.3)$$

Where J = gas permeability (mol s^{-1} $Pa^{-1}m^{-2}$), A = membrane surface area (m^2), P_{in} = pressure inside the fibre (Pa).

Also, the mean pressure across the fibre P was calculated as:

$$P = \frac{P_{in} + P_{out}}{2} \qquad (2.4)$$

The gas permeability J values were then plotted against mean pressures P values across the fibre, thus obtaining the equation $y = P_0x + K_0$. The values of P_0 and K_0

obtained from the equation, were used to calculate the mean pore diameter using the method described by Li et al. [234] with the mean pore radius being calculated using equation 2.5:

$$r = \left(\frac{16}{3}\right)\left(\frac{P_0}{K_0}\right)\left(\frac{8RT}{\pi M_{N_2}}\right)^{0.5}\mu \qquad (2.5)$$

where r = pore radius (m), P_0 = gradient of flux versus mean pressure plot (mol m^{-2} Pa^{-1} s^{-1}), K_0= intercept of flux versus mean pressure plot (mol m^{-2} s^{-1}), R = Universal Gas Constant (8.314 JK^{-1} mol^{-1}), M_{N2}= molar mass of nitrogen (kg mol^{-1}) and μ = viscosity of nitrogen (Pa s).

Overall porosity was calculated with the following formula (equation 2.6):

$$\varepsilon_p = 1 - \frac{\nu_{polymer}}{\nu_{fibre}} \qquad (2.6)$$

where ε_p = porosity, $\nu_{polymer}$ = specific volume of the polymer, (m^3 kg^{-1}) and ν_{fibre} = specific volume of the fibre (m^3 kg^{-1}).

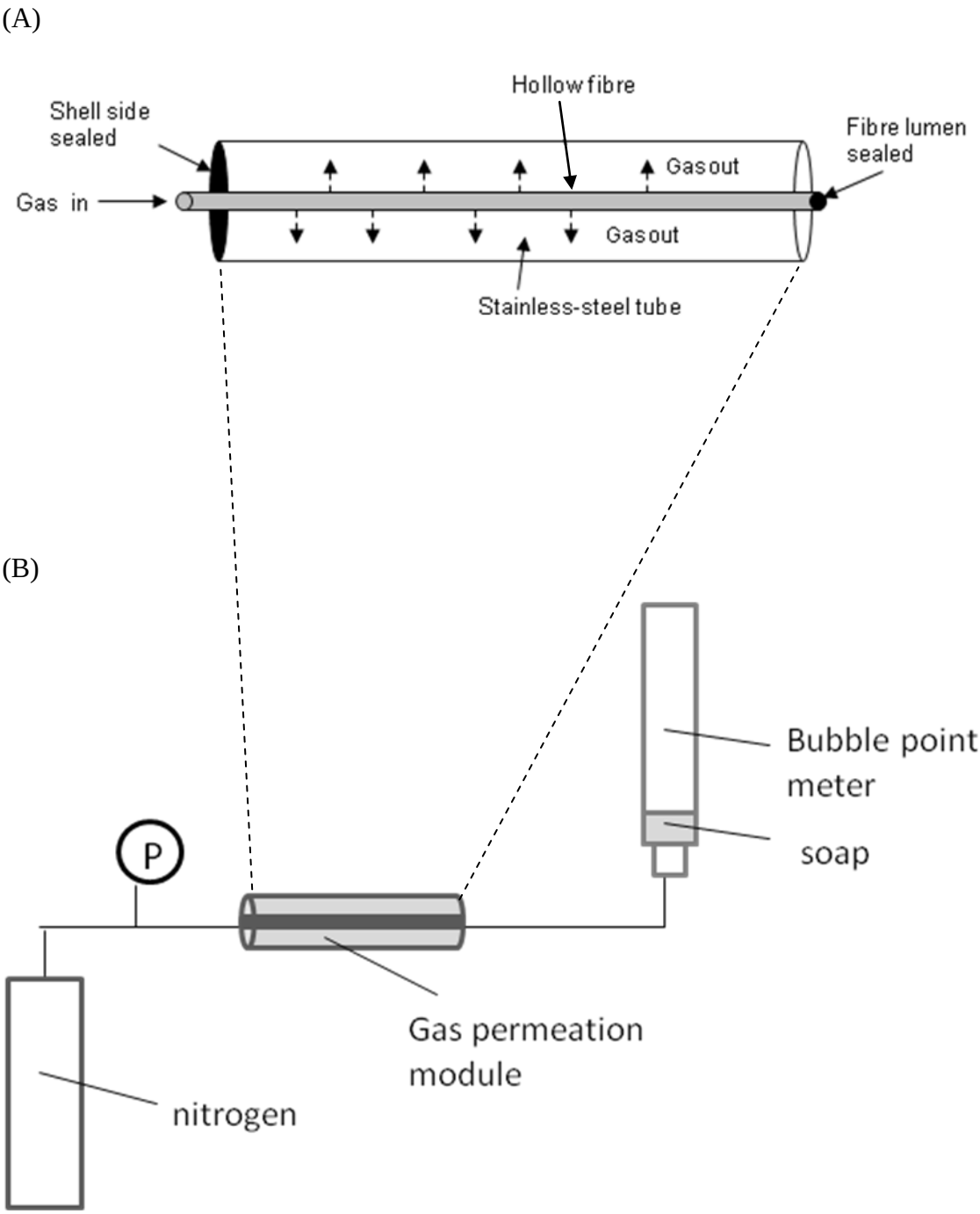

Fig. 2.3: Schematic representation of the gas permeation module (A) and apparatus ((B) used to determine the mean pore size of the fibres. Nitrogen gas flowed inside the lumen of the hollow fibre from the sealed shell end, while the other end of the fibre was sealed so that all the gas collected in the bubble meter had perfused through the wall of the fibre.

2.4.3 Mechanical properties

The mechanical properties of PLGA and PVA-PLGA hollow fibre membranes were tested with a mechanical test rig (Instron 3367 with 10N loadcell running Bluehill software). The membranes were cut in pieces of 6 cm in length and clipped into a grip attached to the Instron machine. A crosshead speed of 2 mm/min was set and the stress-strain curves were obtained from the samples. From the stress-strain curves Young's modulus (*E*) was calculated at the elastic limit using the following formula (equation 2.7):

$$E = \frac{\sigma}{\varepsilon} = \frac{FL_0}{A_0 \Delta L} \qquad (2.7)$$

where σ = stress (MPa), ε = strain, F = force applied to the membrane (N), A_0 = cross-sectional area of the membrane (m^2), ΔL = change in length (m) and L_0 = original length of the sample (m).

When a fluid was circulated inside the lumen of the hollow fibre, the membrane was subjected to an internal pressure, therefore the hoop stress, *i.e.* the stress acting in the circumference of the cylinder wall, should be considered in the calculation of the Young's modulus.

The hoop stress is expressed as:

$$\sigma = \frac{S}{A} \qquad (2.8)$$

where σ = hoop stress, S= circumferential hoop tension (N), A = cross sectional area of the membrane (m^2).

More specifically, the hoop stress in hollow fibre with membrane thickness > than $1/10^{th}$ of the internal radius r_i is given by the equation 2.9:

$$\sigma = \frac{p_i r_i^{\,2} - p_0 r_0^{\,2}}{r_0^{\,2} - r_i^{\,2}} - \frac{r_i^{\,2} r_0^{\,2} (p_0 - p_i)}{r^2 (r_0^{\,2} - r_i^{\,2})} \qquad (2.9)$$

where p_i = internal pressure in the hollow fibre, p_o= external pressure, r_i= hollow fibre internal radius, r_o= hollow fibre external radius, r = the radial variable.

2.4.4 Hydrophilicity

The contact angle method was used to evaluate the hydrophilicity of PLGA and PVA-PLGA flat sheet membranes. A schematic representation of the method is displayed in fig. 2.4. Drops of purified water (3 μl) were deposited onto the top side of 5 cm x 1 cm membranes positioned on the stage of a bench-type contact angle goniometer (NRL Goniometer Model 100-00), ensuring that the membrane was completely flat. Measurements were repeated at different positions on the flat sheet. Since hydrophobic materials are not easily wetted by water, in order to confirm the results obtained by contact angle measurements, the flat sheets were also placed in water to see whether they floated or sank.

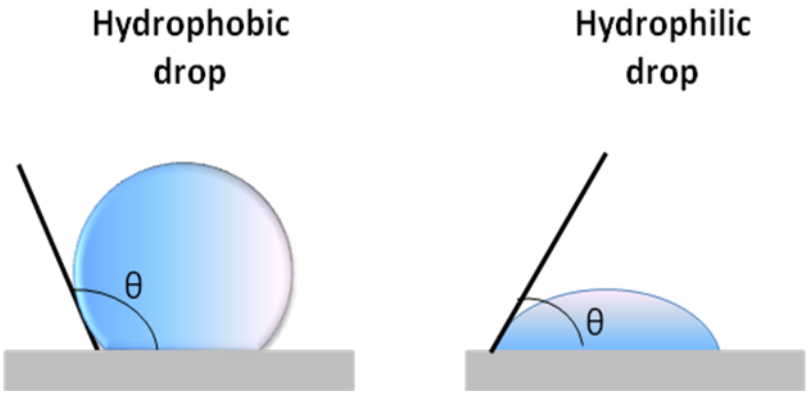

Fig. 2.4: Schematic representation of the contact angle method. A drop of water is deposited on the surface of the membrane. In a hydrophilic membrane the drop of water will easily spread out on the surface and the material will have a lower contact angle (θ). On the contrary a hydrophobic membrane is not easily wetted by water and the contact angle for that material will be higher, as the drop cannot easily spread out on the surface of the material.

2.4.5 Hydraulic and protein permeability: the single fibre hollow fibre bioreactor

In order to evaluate the permeability of the hollow fibre membranes to water and of bovine serum albumin (BSA), a single hollow fibre bioreactor module was used. Being an important component of serum, BSA was used as a model protein for the study of the permeability of the hollow fibre membranes to proteins.

2.4.5.1 Single fibre bioreactor setup

The bioreactor consisted of a borosilicate glass tube of 10 cm in length, 4 mm outer diameter and 2.4 mm inner diameter, with 2 side ports at a distance of 2 cm from the extremes of the bioreactor. A single fibre hollow fibre membrane (10 cm length) was inserted into the bioreactor, glued with silicone (or epoxy resin for experiments with cells) at the ends and left to dry overnight, so that the working length was 6 cm. A schematic representation of the module used in the project can be seen in fig. 2.5. This system intends to reproduce the concept of the Krogh's cylinder, which implies that organs are composed of many microcirculatory functional units (the Krogh's cylinders) organised in parallel and perfused by capillaries with each section of a capillary responsible for the supply to a corresponding cylindrical section of surrounding tissue. When this principle is applied to hollow fibre bioreactors, the entire hollow fibre bundle in the bioreactor can be described by one fibre surrounded by an annulus representing the extracapillary space (fig. 2.6). This approach assumes that all the fibres are identical in terms of properties and internal flow, perfectly straight and equally spaced. The interstitial spaces between adjacent Krogh's cylinders are ignored.

In the single fibre bioreactor flow was achieved using a peristaltic pump (Masterflex L/S™ model 7519-06) and two stop tubings (Masterflex Santoprene tubing, 2.06 mm internal diameter, Cole Parmer). Mean transmembrane pressure was controlled by a digital pressure transducer at the inlet and outlet of the bioreactor.

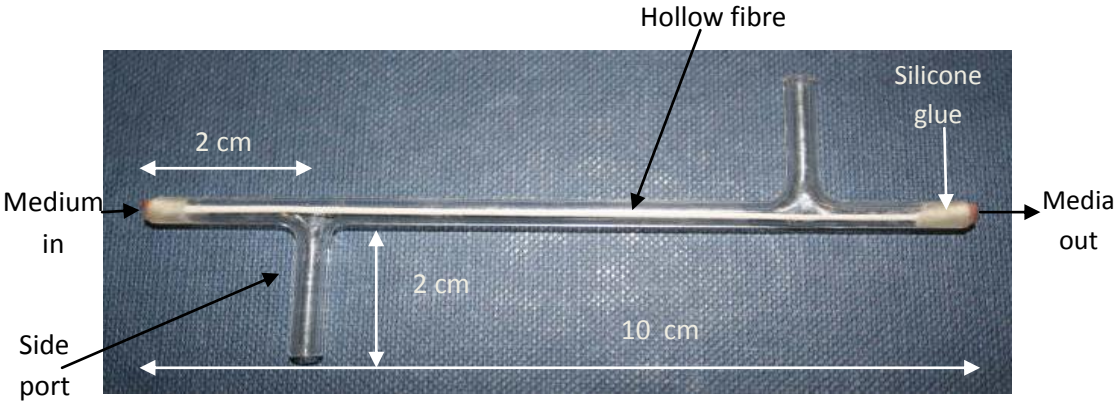

Fig. 2.5: Picture of the single fibre hollow fibre bioreactor module: it consists of a 10 cm long borosilicate glass tube with two side ports, one inlet for the flow of the medium inside the device, and of one outlet for the flow of the medium outside the device. One hollow fibre is inserted inside and glued at the side ports.

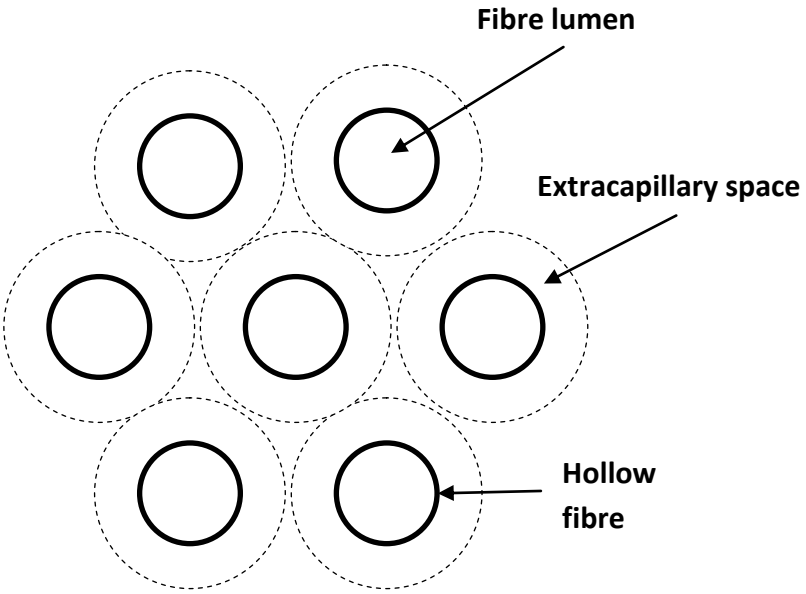

Fig. 2.6: The Krogh's cylinder model: the entire bundle of fibres can be described as one fibre surrounded by an annulus representing the extracapillary space.

2.4.5.2 Permeability experiments

Hollow fibre membranes were washed with either 5% NaOCl v/v or distilled water prior to permeability experiments. Distilled water was circulated for 24 hours through the lumen of the fibre and in the extra capillary space prior to the experiments to ensure both the inner and outer surfaces were completely wetted. In contrast, when sodium hypochlorite was used to wash the membrane, 5% NaOCl v/v solution was circulated for one hour in the lumen of the fibre and in the extra capillary space in order to open the pores of the membrane and subsequently the inner and outer surface of the fibre were washed with distilled water for 30 minutes in order to remove any NaOCl residual.

Fresh distilled water was subsequently circulated for seven hours through the lumen of the hollow fibre at a flow rate of 2.5 ml/min. Water permeate was collected from one side port (the other was closed) every hour and permeate flow rate measured, while retentate was collected from the lumen outlet (fig. 2.7). Permeate volume was used to calculate the volumetric water flux (J; equation 2.10) and the hydraulic permeability (L_P; equation 2.11):

$$J = \frac{V_P}{tA} \qquad (2.10)$$

$$L_p = \frac{J}{\Delta P} \qquad (2.11)$$

where V= volume of permeate collected (l), t = time (h), A = membrane surface area (m^2), ΔP = transmembrane pressure (Pa)

BSA solution (100 μg/ml in PBS; MW = 66,430 Da) was pumped through the lumen of the fibre at a flow rate of 2.5 ml/min. The system was allowed to reach steady state for 2 hours and then run for a further two hours, during which time samples were collected every 20 minutes. Permeate samples were collected from a side port and the retentate was collected from the lumen outlet. Samples were also taken from the feed bottle. BSA concentration was determined according to the method of Bradford [235] with absorbance read at 595 nm using a UV plate reader (Synergy™ HT Multi-detection Microplate reader, running Microplate Data collection and analysis software Gen5™).

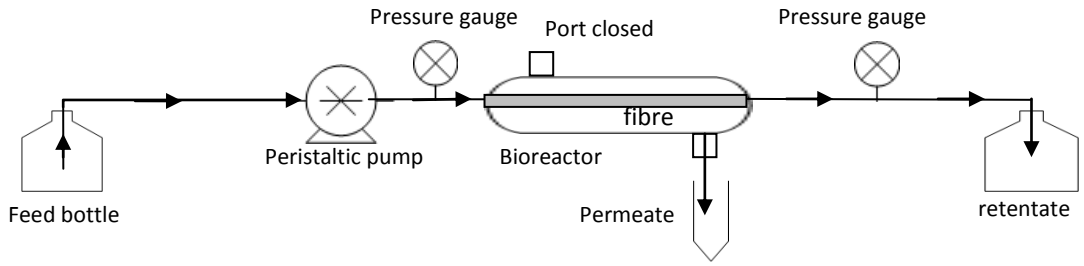

Fig. 2.7: Schematic representation of the module used in the permeation experiments. Water or BSA solution were pumped from a feed bottle through the lumen of the membrane inside the bioreactor, and collected in the permeate. The water or BSA solution that did not permeate through the membrane but exited the outlet of the bioreactor was collected in the retentate bottle.

2.5 Determination of Reynolds number (Re) and shear stress

Distilled water was circulated by means of a peristaltic pump (Masterflex L/S™ model 7519-06) inside the lumen of the hollow fibre, inserted into a single fibre hollow fibre bioreactor module at increasing flow rates, from 0.8 to 5 ml/min and the

difference in pressure between inlet and outlet was measured with a digital pressure transducer.

Reynolds number, which tells whether the flow is laminar (for Re < 2100) or turbulent (for Re > 2100), was calculated with the following formula (equation 2.12):

$$\mathrm{Re} = \frac{\rho v d}{\mu} \qquad (2.12)$$

Shear stress (τ) at the walls of the pipe was calculated with the following formula (equation 2.13):

$$\tau = \frac{8\mu v}{d} \qquad (2.13)$$

where d = hollow fibre diameter (m), v = fluid mean velocity (m/s), ρ = fluid density (kg/m^3), μ = fluid viscosity (Pa s).

2.6 Static cell cultures

Cell culture was performed according to good cell culture practice, under aseptic conditions and within a category II laminar flow containment hood (Kendro Laboratory Products Plc, Hertfordshire, UK). All reagents used for cell cultures were pre-warmed to 37° C before use.

2.6.1 HL60 cell culture

HL60 human promyelocytic leukemia cells were thawed and resuspended in a 25 cm^2 flask at a density of 3-5 x 10^5 cells/ml in RPMI-1640 medium containing 20% v/v foetal calf serum (FCS) and maintained in a humidified environment at 37°C and 5% CO_2 . Cells were counted daily with a haemocytometer to check their proliferation. Once they had reached the appropriate cell density, cells were centrifuged at 1000 rpm for 5 minutes, the supernatant aspirated and the pellet resuspended at a concentration of 3 x 10^5 cells/ml in RPMI-1640 medium with 10% FCS v/v and maintained in a humidified environment at 37° C and 5% CO_2. Medium was changed

three times a week and cells were counted twice a week to check that their number did not exceed 1 x 10^6 cells/ml, which may cause their spontaneous differentiation into mature myelocytes (monocytes, macrophage-like cells, eosinophils, or granulocytes) [236].

2.6.2 MG63 cell culture

MG63 human osteosarcoma cells were thawed and resuspended in a 75 cm^2 cell culture flask at a density of 1 x 10^4 cells/cm^2 in Dulbecco's modified Eagle's medium (DMEM) containing 10% v/v foetal calf serum (FCS), 1% v/v sodium pyruvate, 1% v/v non essential amino acids and 1% v/v antibiotic-antimicotic solution. Cells were maintained in a humidified environment at 37° C and 5% CO_2 and medium was replaced every 2-3 days. When cells reached confluence, they were washed with 10 ml of PBS and subsequently incubated with 3 ml of 1% v/v trypsin-EDTA at 37° C and 5% CO_2 in order to release the cells from the surface. Once all the cells were detached from the surface (cells were examined at the microscope to ensure that they were all floating) 6 ml of complete medium was added in order to inactivate the trypsin and cells were centrifuged at 1,200 rpm for 5 minutes. The supernatant was discarded and the cell pellet was resuspended in 2 ml of fresh medium. Cells were then plated at a concentration of 1 x 10^4 cells/cm^2 and maintained at 37° C and 5% CO_2.

2.6.3 Isolation and culture of rat mesenchymal stem cells (rMSCs)

Mesenchymal stem cells were isolated from the femur and tibia bone marrow of 2 month old Wistar rats using the method described by Cho et al [237]. The femur and tibia were removed and skin and muscles surrounding the bones were carefully removed. The bones were placed in 50 ml of sterile minimum essential Eagle's medium, alpha-modification (α-MEM). The epiphyses of the bones were removed, a hole was created in the knee joint end of each bone and a syringe full of PBS was used to flush out the marrow from the bones. The collected marrow was suspended in PBS in order to eliminate the blood and centrifuged at 400 g for 5 minutes. The resulting pellet was resuspended in α-MEM with 10% v/v FCS, 1% v/v antibiotic-

antimicotic solution and 1% v/v 200 mM L-Glutamine and incubated overnight in a 25 cm^2 culture flask (NUNC) at 37° C with 95% humidity and 5% CO_2. The following day the medium was removed in order to discard the non-adherent cells and it was replaced with fresh medium. When the cells had reached 80% confluence, they were washed twice with PBS and subsequently 1 ml of 0.25% v/v trypsin-EDTA was added and the flask was left at 37° C and 5% CO_2 for about 1 minute in order to release the cells from the surface. Once all the cells were detached from the surface (cells were examined at the microscope to ensure that they were all floating) they were resuspended in 6 ml of complete medium in order to inactivate the trypsin and centrifuged at 1,200 rpm for 10 minutes. The supernatant was discarded and the cell pellet was resuspended in 2 ml of fresh medium. Cells were then plated at a concentration of 5 x 10^3 cells/cm^2 and maintained at 37° C and 5% CO_2. Cells were used only at low passages, usually passage 2 or 3, in order to limit their spontaneous differentiation.

2.7 Dynamic cell cultures

2.7.1 HL60 culture in the single fibre hollow fibre bioreactor

All bioreactor components were autoclaved at 1 bar and 120º C for 20 minutes. The 75:25 PLGA hollow fibre was sterilized by soaking in penicillin-streptomycin solution (1% in PBS) overnight. The following day, the lumen of the fibre was sterilized by injecting into it the antibiotic solution with a 2 ml syringe. Inside the culture hood the ends of the single fibre bioreactor were glued and the antibiotic solution injected into the side ports of the bioreactor and left overnight in order to sterilize the extracapillary space of the bioreactor. The following day the antibiotic solution was pumped through the lumen of the hollow fibre with a peristaltic pump (Masterflex L/S™ model 7519-06) continuously for 24 hours at a flow rate of 2 ml/min in the cold room. RPMI 1640 medium was then pumped for a few minutes through the fibre to wash away the antibiotic solution. A schematic representation of the system can be seen in fig. 2.8. HL60 cells were prepared as described in section 2.6.1 and 20 ml of cells at a density of 3 x 10^5 cells/ml were continuously circulated

by means of a peristaltic pump through the lumen of the fibre for 48 hours at a flow rate of 2 ml/min or 4 ml/min. Samples of 1 ml of cell suspension were collected every 24 hours from the feed bottle for analysis and compared with the results obtained from cultures of HL60 cells grown in static flasks for the same period of time (controls).

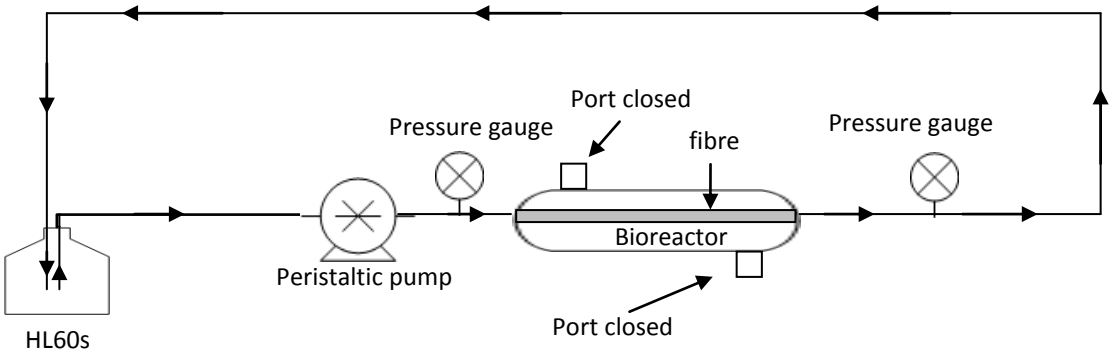

Fig. 2.8: System used to culture HL60 cells in a dynamic environment. Cells were pumped from a feed bottle into the lumen of a PLGA hollow fibre inserted into a single fibre bioreactor by means of a peristaltic pump and recycled into the same bottle.

2.7.2 Analysis of HL60 proliferation in the single fibre hollow fibre bioreactor

Analysis of HL60 proliferation within the single fibre bioreactor was carried out using the MTT cell proliferation test [238]. Samples of 1 ml of HL60 cells in RPMI medium were collected from the feed bottle of the system described in fig. 2.8 and 100 µl of HL60 cells were added in triplicate to each well of of a 96-well plate. 20 µl of MTT solution (2mg/ ml in PBS) were subsequently added to each well and the plate was incubated for 3 hours at 37°C and 5% CO_2. Plates were then centrifuged, the supernatant removed and 100 µl of dimethyl sulfoxide were added to each well. The plate was shaken for 30 minutes and the absorbance was read with a UV plate reader (Versa Max Microplate Reader, software Soft Max Pro) at a wavelength of 540 nm from which were subtracted the readings at 690 nm (background) for more accurate results. Results were compared with a standard curve of absorbance versus metabolically active cells and the number of metabolically active cells calculated (cells/ml). The absorbance measured was then divided by the viable cell number per well in order to obtain the absorbance per cell and have more comparable results.

The viability of the cells inside the bioreactor was assessed by the Trypan Blue method. 100 μl of Trypan Blue solution were added to 100 μl of cells, and 10 μl of this combined solution were placed into the chamber of a haemocytometer. Live (unstained) and dead (blue stained) cells were counted.

2.8 Cell seeding and attachment on PLGA and 5% PVA-PLGA flat sheet membranes

2.8.1 Seeding of MG63s and rMSCs

Flat sheets were sterilised prior to seeding with 5% antibiotic-antimicotic solution overnight at 4° C. The following day the membranes were cut into small circles of approximately the same area of the well (culture area 1.9 cm^2) and inserted into the wells of a 24 well plate. A silicon ring (1.48 cm internal diameter) was inserted on the top of the membrane in each well in order to keep the membrane at the bottom of the well. The membranes were then left in 5% antibiotic-antimicotic solution for one hour and subsequently washed with PBS. MG63s or rMSCs, cultured as described in section 2.6.3, were seeded on the top of membranes at a density of 5,000 cells/cm^2 for rMSCs and 10,000 cells/cm^2 for MG63s in a volume of 500 μl. The plates were then incubated at 37° C and 5% CO_2 for 4 days. Medium was changed at day 2 and samples of membranes with cells attached were removed every 24 hours for analysis. The analysis of cell attachment and proliferation on the two different types of membranes was compared with the attachment and proliferation of cells on plastic (control).

2.8.2 Qualitative analysis of cell attachment: live staining

Qualitative analysis of cell attachment was conducted by means of a live staining technique, using the Vybrant CFDA SE Cell Tracer kit. Carboxy-fluorescein diacetate, succinimidyl ester (CFDA SE) passively diffuses into the cells and its succinimidyl ester group reacts with intracellular amines, forming fluorescent conjugates.

Medium was removed from the wells and replaced by 500 µl of CFDA SE (5 µM solution in PBS). The cells were incubated at 37° C and 5% CO_2 for 15 minutes and subsequently washed with PBS. Cells were then incubated for 30 minutes with fresh complete medium at 37°C and 5% CO_2. Cells were then washed with PBS and fixed for 20 minutes with 10% v/v formalin solution. After fixation cells were washed twice with PBS and stored at 4° C prior to analysis. Analysis of morphology, attachment and distribution of the cells on the membranes was conducted using fluorescence microscopy (Leica DMI 4000B).

2.8.3 Quantitative analysis of cell attachment: Pico Green assay

A Quant-iT™ Pico Green® dsDNA Quantitation Assay Kit was used to determine the number of cells on PLGA and 5% PVA-PLGA flat sheets. Pico Green® dsDNA reagent is a fluorescent acid stain which quantifies double-stranded DNA in solution.

Medium was removed from the wells and cells were washed with PBS then incubated overnight at -80° C with 1 X TE buffer (10mM Tris-HCl, 1mM EDTA; pH 7.5) in molecular grade water in order to detach the cells from the membranes and lyse them. For the analysis, 100 µl of each sample were added to wells of a 96 well plate, three repeats being performed for each sample. In addition, DNA calibration was carried out using known concentrations of DNA in the range 0-2 µg/ml. 100 µl of Pico Green working solution diluted 200X in TE buffer was added to each well and the plate was read immediately with a fluorescent plate reader (Synergy™ HT Multi-detection Microplate reader, running Microplate Data collection and analysis software Gen5™, Biotek) with excitation wavelength set at 485 nm and emission wavelength at 530 nm.

2.9 Secretion of Hepatocyte Growth Factor (HGF) by HL60 and MG63 cell lines

2.9.1 Stimulation of HL60s to secrete HGF

HL60s were stimulated to secrete HGF by treatment with 12-*O*-tetradecanoylphorbol-13-acetate (TPA) or dibutyryl cyclic adenosine-monophosphate

(dbcAMP) as shown by Inaba and colleagues [239] or heparin, as shown by Matsumoto and colleagues [240].

HL60s (1 x 10^6 cells/ml) were treated with either DMSO, TPA (1 ng/ml), dbcAMP (100 nM in sterile water) or heparin (1 μg/ml in sterile water) or with a combination of the four and incubated for four days at 37° C and 5% CO_2. After this time the cells were centrifuged at 1000 rpm for 5 min and the supernatants collected and stored at -80° C prior to analysis. Cells treated with the compounds were compared with untreated cells, to see whether the addition of the chemicals had any effect on the increase of the amount of HGF secreted.

2.9.2 Secretion of HGF by MG63s

MG63s were seeded at density of 1 x 10^4 cells/ml in 24 well plates and incubated for three days at 37°C and 5% CO_2. After three day incubation the supernatants were collected from the cells and stored at -80° C for the analysis.

2.9.3 Quantification of HGF secretion by HL60 or MG63 cells

HGF secreted by MG63s or HL60s was quantified using a human HGF DuoSet® ELISA (Enzyme-Linked ImmunoSorbent Assay) Development System kit. A polystyrene 96 immuno-microwell plate (NUNC) was coated with 100 μl per well of mouse anti-human HGF capture antibody at a concentration of 1 μg/ml and the plate was sealed and incubated overnight at room temperature. The following day the solution was aspirated from every well and the plate was washed three times with 0.05% v/v Tween® 20 in PBS (wash buffer). 200 μl of 1% w/v BSA in PBS were added to each well and the plate was incubated at room temperature for one hour. The plate was washed three times with wash buffer, and 100 μl of samples or standards (serial dilutions of recombinant human HGF, 0-10 ng/ml) were added to each well and the plate was sealed and incubated for two hours at room temperature. The plate was washed three times with wash buffer, and 100 μl of biotinylated goat anti-human HGF detection antibody (200 ng/ml in 1% w/v BSA in PBS) were added to each well and the plate was sealed and incubated for two hours at room

temperature. The plate was washed three times with wash buffer, and 100 µl of Streptadividin conjugated to horseradish-peroxidase (diluted 1:200 in 1% w/v BSA in PBS) were added to each well and incubated for 20 minutes in the dark at room temperature. The plate was washed three times with wash buffer, and 100 µl of 3,3',5,5' tetramethylbenzidine were added to each well and incubated for 20 minutes in the dark at room temperature. 100 µl of 2N H_2SO_4 (stop solution) were added to each well and the optical density was determined immediately, using a microplate reader (Synergy™ HT Multi-detection Microplate reader, running Microplate Data collection and analysis software Gen5™, Biotek) with wavelength set at 450 nm and wavelength correction set at 540 nm.

2.9.4 Comparison of commercial and MG63s derived HGF in static and dynamic environment

Commercial HGF (recombinant human HGF, MW= 60-70 kDa) at initial concentration 2 ng/ml in DMEM + 10% FCS and HGF released by MG63 cells (diluted in order to obtain a concentration of 2 ng/ml) were placed in separate glass bottles and incubated for 3 hours at 37° C and 5% CO_2. Samples were collected from each bottle every 30 minutes and stored at -80° C until analysis. In order to compare samples in a static environment to those in a dynamic environment, commercial and MG63-derived HGF were also circulated inside platinum-cured silicone tubing (internal diameter 2.4 mm, Cole Parmer) by means of a peristaltic pump in a closed recycling system at 37° C and 5% CO_2. Samples were taken every 30 minutes from the feed bottle and stored at -80° C until analysis. For the analysis samples were thawed at 37° C and the amount of HGF present in the samples was quantified by an HGF ELISA kit as described in section 2.9.3.

2.9.5 Permeation of MG63-derived HGF through 5% PVA-PLGA hollow fibre membranes

In order to evaluate the permeability of the hollow fibre membranes to hHGF, a 5% PVA-PLGA single fibre hollow fibre bioreactor module was used. A description of the bioreactor system can be seen in section 2.4.5.2. HGF released by MG63 (initial

concentration 8 ng/ml in DMEM + 10% v/v FCS + 1% v/v sodium pyruvate + 1% v/v non essential aminoacids + 1% v/v antibiotic-antimycotic solution) was circulated through the lumen of the fibre at a flow rate of 2.5 ml/min, the system was allowed to reach steady state and then run for three hours, during which time samples were collected every 10 minutes. Permeate samples were collected from a side port and the retentate was collected from the lumen outlet. For a schematic representation of the system see fig. 2.7. Samples were also taken from the feed bottle. Samples were stored at -80° C until analysis. HGF concentration was determined with an ELISA kit as described in section 2.9.3.

2.10 Hepatic differentiation of rat mesenchymal stem cells

2.10.1 Analysis of stem cells markers

The presence of two positive MSC surface markers (CD44 and CD90) and absence of a negative MSC marker (CD45) was assessed by flow cytometry in order to check the purity of MSCs.

Rat MSCs were trypsinised, pelleted, resuspended in 0.1% BSA in PBS (incubation buffer) and divided between 1.5 ml eppendorf tubes. A minimum of 30,000 cells per surface marker were used for the experiment. Cells were centrifuged at 1200 rpm for 10 minutes, the supernatant was aspirated and cells were incubated for 30 minutes in ice with 50 µl of primary antibody (dilution 1:5 in incubation buffer). The primary antibodies used for the analysis were: mouse anti-rat CD44, mouse anti-rat CD45 and mouse anti-rat CD90, all purchased from Immunotools. The primary antibodies were conjugated to a fluorophore, and more specifically CD44 and CD45 were conjugated to fluorescein isothiocyanate (FITC) and CD90 to phycoerythrin (PE). Mouse IgG1 FITC-conjugated, mouse IgG1 PE-conjugated and mouse IgG2 FITC-conjugated were used as negative controls for the three different markers. Following incubation with the primary antibody, 1 ml of incubation buffer was added to each sample and cells were centrifuged for 10 minutes at 1200 rpm. Supernatant was discarded, pellets were resuspended in incubation buffer and samples centrifuged again. The procedure was repeated three times and subsequently 300 µl of each sample were transferred to

a flow cytometry tube and kept on ice until analysis. Samples were analysed within one hour by flow cytometry (Becton Dickinson FACSCanto I, running BD FACS Diva software) at the BioImaging Suite, University of Bath.

2.10.2 Hepatic differentiation of MSCs

Mesenchymal stem cells were differentiated into hepatocytes according to the protocol of Snykers et al. [213, 241]. rMSCs were plated on 24 well-plates at a density of 20,000 cells/cm^2 in α-MEM supplemented with 10% fetal calf serum, 2 mM L-glutamine and 1% antibiotic-antimicotic solution (basal medium). Once cells reached 100% confluency they were cultured for three days in basal medium supplemented with 0.25 mM sodium pyruvate and 10 ng/ml of fibroblast growth factor 4 (FGF-4). After this first differentiation step, cells were cultured for three days in basal medium supplemented with 0.25 mM sodium pyruvate and 20 ng/ml commercial HGF or 20 ng/ml of HGF secreted by MG63s. In the following 12 days cells were cultured in basal medium supplemented with 0.25 mM sodium pyruvate, 20 ng/ml commercial HGF or HGF secreted by MG63s, 1X insulin-transferrin-sodium selenite (ITS), 20 μg/l dexamethasone and 1μM trichostatin A (TSA). Differentiation media were changed every three days. Cells were checked for changes in morphology using light microscopy. At day 18 cells were fixed for 20 minutes at room temperature with 10% formalin solution, washed two times with PBS and kept at 4°C until analysis.

2.10.3 Analysis of hepatic markers

The presence of three hepatic markers (albumin, UGT and transferrin) was assessed by immonofluorescence to check the differentiation of rMSCs into hepatocytes.

600 μl of 0.1% v/v Triton X100 in PBS were added to each well and incubated for 20 minutes at room temperature in order to permeabilise the cells. The solution was then removed and replaced by 600 μl of blocking buffer: 1X blocking reagent in maleic acid buffer (100 mM maleic acid, 150 mM NaCl; pH 7.5). Plates were incubated for

one hour at room temperature. Blocking buffer was removed and 200 µl of primary antibody (dilution 1:100 in blocking buffer) were added to each well and plates were incubated overnight at 4° C. The primary antibodies used for the analysis were: goat anti-rat transferrin, sheep anti-rat albumin and sheep anti-rat UGT antibody. The following day the antibody solution was removed from the wells and plates were washed three times with PBS and left for 15 minutes on a shaker between every wash. PBS was then removed and 200 µl of secondary antibody (fluorescein anti-sheep IgG or fluorescein anti-goat IgG) diluted 1:100 in PBS were added to each well. Plates were incubated for two hours at room temperature and protected from light. After two hours the antibody solution was removed from the wells and plates were washed three times with PBS and left for 15 minutes on a rotator between every wash. Plates were then analysed immediately for hepatic markers using fluorescence microscopy (Leica DMI 4000B).

2.10.4 Staining of adipogenic cultures

Oil Red O staining was performed to detect mature adipocytes in culture. Cells were fixed for 20 minutes at room temperature with 10% v/v formalin solution and subsequently washed with PBS. 300 mg of Oil Red O powder were dissolved in 100 ml of 99% v/v isopropanol and 30 ml of this solution were mixed with 20 ml of distilled water. The working solution was incubated for 10 minutes at room temperature and filtered through a Whatman filter paper before use. 500 µl of 60% v/v isopropanol were added to each well and left for five minutes. The solvent was then removed and replaced by 500 µl of Oil Red O working solution and the plates were incubated at room temperature for five minutes. Oil Red O solution was removed and cultures were rinsed with distilled water until the water rinsed off clear. 500 µl of haematoxylin stain were then added to each well in order to stain the nuclei of the cells and left for 1 minute at room temperature. Haematoxylin solution was removed and then cultures were rinsed with distilled water until the water rinsed off clear. Plates were analysed using light microscopy (Leica DMI 4000B) for the presence of adipocytes in cultures (red stained).

2.11 Statistical analysis

Unless stated, data are represented as the mean value from n = 4 ± 1 standard deviation. Graphs were created using Graph Pad Prism Software. One-way analysis of variance (one-way ANOVA) was used to test significant differences between multiple samples. Since ANOVA does not identify which samples are different from one another, Tukey's post-hoc test was used to identify significant differences between independent samples. When appropriate, R^2 values are presented in graphs as an indication of the deviation from the trendline equation.

3. Characterization and improvement of the properties of PLGA hollow fibre membranes

3.1 Introduction

3D constructs require more efficient transport of nutrients, oxygen, growth factors, CO_2 and metabolites to and from the cells compared to 2D culture systems. Early studies showed that cellular spheroids larger than 1 mm in diameter usually contain a hypoxic necrotic centre, surrounded by viable cells [242]. Because engineered constructs should be at least a few millimetres in size to serve as grafts for tissue replacement, mass transfer limitations represent one of the greatest challenges to be addressed. A challenge in mass transport is represented by oxygen mass transport because of its extremely low solubility in aqueous media and because limitations in oxygen transfer are significant when cells adopt 3D structures [168]. Oxygen is one of the most important nutrients for cells, as it acts in all aerobic metabolic cycles. However, it is the factor that often limits cell survival and tissue growth [156]. All reactors designed for tissue growth are considered mass transfer limited relative to oxygen. Oxygen mass transfer can be described as the movement of molecules due to convective flow and diffusion. On the other hand, an excess of oxygen in medium causes the presence of free radicals, which are cytotoxic. Therefore oxygen concentrations are usually maintained at between 20% and 100% air saturation to maintain a balance between oxygen needs and tolerance of the cells to free radicals. It must also be taken into account that different tissue types have different oxygen requirements, depending on cell type, concentration and metabolic activity. For example the oxygen uptake of human skin fibroblasts seeded at a cell density of 10^6 cells/ml is 0.064 mmol O_2 /l h, while it is 0.30 mmol O_2/l h for human hepatocytes. It must be considered that oxygen has to be transferred from a gaseous phase to a liquid one before it can be used by the cells. While culture systems present maximal oxygen concentrations of 0.2 mmol O_2/ l h, blood of a healthy adult man can carry up to 9.5 mmol O_2/l h. The diffusive component will remain limited in vitro due to the small oxygen gradient compared to the in vivo situation. Diffusive transport will have to be

matched with an important convective effect to bring sufficient oxygen molecular flux to the growing cells.

The rate of diffusion of nutrients and oxygen is proportional to their concentration gradient, where the constant of proportionality is the diffusion coefficient (D) in the Stokes-Einstein equation:

$$D = \frac{kT}{6\pi r}$$

Where k is the Boltzmann's constant, T is the temperature and r is the particle radius. Since the volume of a sphere is equal to the cube of its radius, the diffusion coefficient is inversely proportional to the cube root of the molecular weight. This means that larger molecules such as growth factors will have a lower diffusion coefficient. In particular, the diffusion of growth factors is limiting at low concentrations, especially if a high density cell culture is not supplemented with additional growth factors [155].

The mass flux is also related to the stagnant boundary layer that can be generated at the cell/medium interface (Fick's law of diffusion). Mass transfer is then limited by the thickness of the stagnant layer and by the concentration at the boundary of the stagnant layer and can be increased by reducing the thickness of the stagnant boundary layer surrounding the cells. Therefore the role of convection generated in bioreactors is to reduce diffusion limitations imposed by stagnant boundary layers around the cells. External mass transfer (transport of molecules from medium to tissue surface) rates are dependent mostly on the hydrodynamic conditions in the bioreactor, while internal (transport through the tissue to the cells) rates may depend on the scaffold/tissue structure.

Hollow fibres are attractive macrostructures for tissue engineering as they provide a large surface area to volume ratio for higher cell attachment compared to flat sheets and also because they act as a solid barrier between the cells and the media, allowing high media flow rates to be selected for appropriate mass transfer of nutrients and waste products to and from the cells, without any cellular damage.

Despite the advantages of using PLGA hollow fibres compared to flat sheets, one of the major limitations in the use of PLGA as a tissue engineering scaffold in

bioreactor devices is its hydrophobic character, which results in low permeability of water and water-based solutions, such as cell culture media, through the scaffold. However, a modification of the chemical composition of the membrane might lead to a more hydrophilic fibre, which is likely to positively affect the hydraulic permeability and also cell adhesion. This could potentially solve the mass transfer limitations and allow for the employment of PLGA hollow fibres into bioreactors devices.

In order to improve the hydrophilicity of membranes, some techniques have been attempted in the past, including pre-wetting the material with ethanol before cell seeding [105, 128], hydrolysis with NaOH [128, 129] protein-coating [130] and plasma treatment [131]. In our research group there have been attempts to improve the hydrophilicity and permeability of PLGA membranes by ethanol pre-wetting or hydrolysis with NaOH, but both the methods resulted in distortion and/or breakage of the fibres after a very limited period of time [128, 233]. Blending with a hydrophilic polymer, *e.g.* poly(ethyleneglycol) [136, 137], polyvinylpyrrolidone [138-142] and polyvinyl alcohol (PVA) [139, 143-146], is another technique that has been shown to successfully improve the hydrophilicity and permeability of the membranes [132-135].

In this project, blending with the hydrophilic polymer polyvinyl alcohol (PVA) has been performed. Due to its hydrophilicity, excellent chemical resistance (*e.g.* long term temperature and pH stability), non-toxicity and biodegradability, PVA has been used in various pharmaceutical, medical, cosmetic and food products [150-152]. For the same reasons PVA is an attractive polymer for tissue engineering applications. For example, Oh *et al* have demonstrated that blended PVA-PLGA sponge scaffolds made by thermal compression molding, exhibited improved porosity, hydrophilicity and wettability, which resulted in better cell adhesion and growth [147].

In this project, blended PVA-PLGA hollow fibre membranes were fabricated by wet spinning in order to improve hydrophilicity, pore size and protein permeability of the membrane. In addition to blending PLGA with PVA, subsequent treatment of hollow fibres with 5% v/v sodium hypochlorite (NaOCl) for 24 hours was performed in order to optimise their properties, especially their permeability. NaOCl is one of the most popular chemical cleaning agents used to remove irreversible fouling [243] and the most common disinfectant for haemodialysis membranes [244]. Cleaning with

NaOCl has been largely employed on pure and blend polyethersulphone membranes in order to increase their degradation and therefore their pore size [245], their hydrophilicity [243, 245], their hydraulic permeability [140, 142, 243, 246-248] and in order to remove proteins deposited on or inside the membrane [244, 246]. Morphology, mechanical properties, hydrophilicity and permeability of PVA-PLGA blended hollow fibres untreated and treated with NaOCl were analysed.

3.2 PVA-PLGA blended membranes

Blended PVA-PLGA hollow fibre membranes (PVA content: 1.25%, 2.5% and 5% w/w) were fabricated by wet spinning as described in section 2.2.3. Morphology, mechanical properties, hydrophilicity and permeability of 1.25, 2.5 and 5% PVA-PLGA blended hollow fibres were studied to determine their potential suitability for tissue engineering applications.

The following results were published as: Meneghello G, Parker DJ, Ainsworth BJ, Perera SP, Chaudhuri JB, Ellis MJ, De Bank PA. "*Fabrication and characterization of poly(lactic-co-glycolic acid)/polyvinyl alcohol blended hollow fibre membranes for tissue engineering applications*" Journal of Membrane Science 344 (2009) 55-61 [249].

3.2.1 Morphological analysis

Fig. 3.1 illustrates the SEM images of PVA-PLGA blended membranes at three different concentrations of PVA: 1.25, 2.5 and 5%. The phase inversion process used to fabricate the fibres resulted in anisotropic membranes with skin layers on both the inner and outer surfaces, with large finger-like macrovoids in the sublayer, extending from the skin layers to the centre of the fibre wall. With increasing PVA content, the central core diminished and for the 5% PVA-PLGA hollow fibre membranes was completely replaced with macrovoids that extended over the middle half of the fibre. This is indicative of instantaneous demixing [250] and is a result of the change in thermodynamic and hydrodynamic interactions between PVA, NMP and water [251].

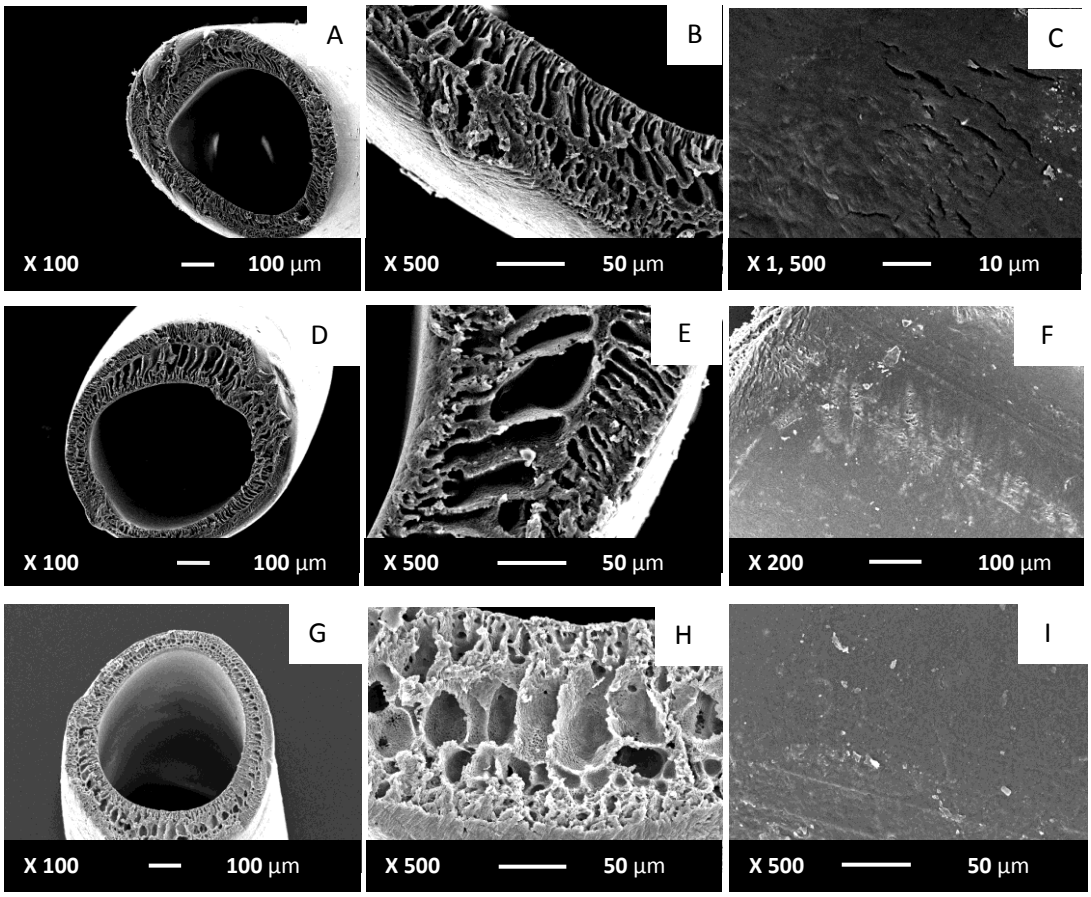

Fig. 3.1: Cross sections and surface views of PVA-PLGA hollow fibre membranes soaked in water for 24hrs. A-C: 1.25% PVA-PLGA HFMs; D-F: 2.5% PVA-PLGA HFMs, G-I: 5%PVA-PLGA HFMs. Fibres present large macrovoids in the centre and skin on the outer surfaces. From [249].

The morphology of blended PVA-PLGA hollow fibres is very similar to that of pure PLGA membranes (fig. 3.2): membranes present thin outer and inner skin layers (A, B) supported by a porous structure, with finger-like pores and macrovoids extending towards the centre of the fibre wall (B). Outer surfaces present some pores as well, but of smaller size and not regularly distributed (C).

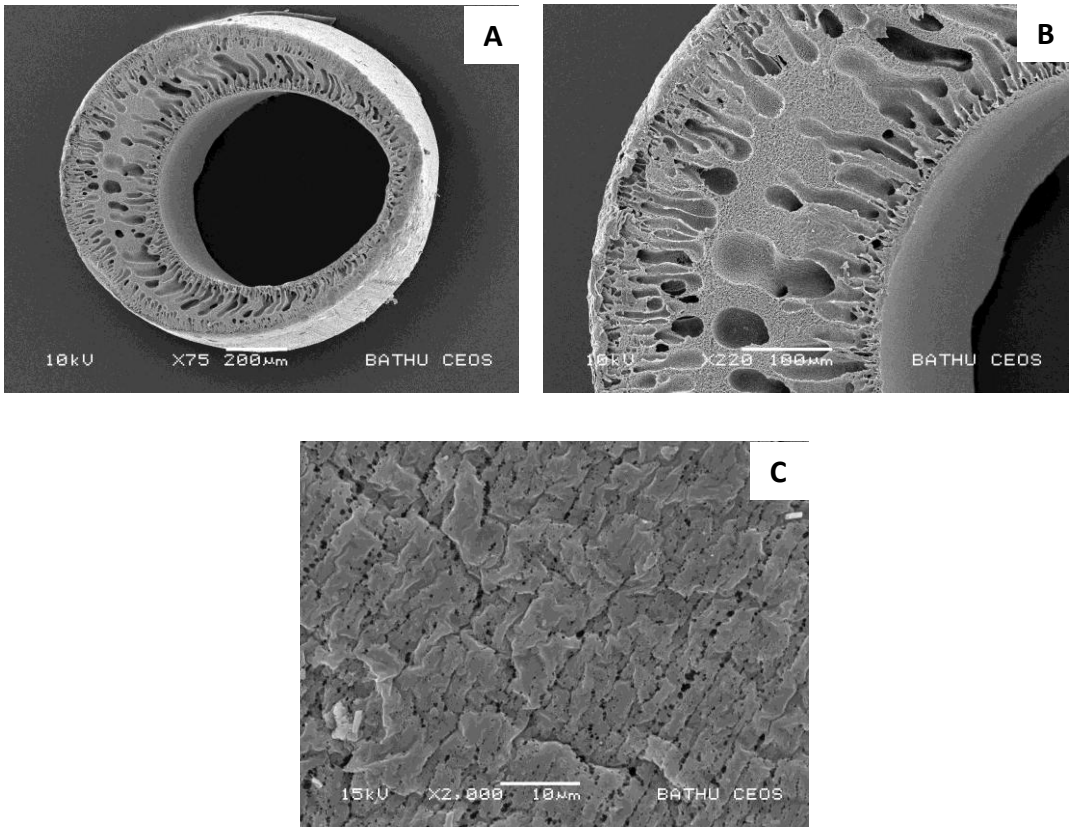

Fig. 3.2: Cross section (A, B) and outer surface (C) of 75:25 PLGA hollow fibre membranes.

3.2.2 Mean pore size and overall porosity

Mean pore size was obtained by gas permeation technique, as described in section 2.4.2. The aim of the experiment was to obtain membranes with an increased pore size and porosity which allowed a greater transfer of nutrients while still providing a suitable scaffold to support cells. The mean pore size calculated was 0.54± 0.11 µm for PLGA hollow fibres, 0.67± 0.15 µm for 1.25% PVA-PLGA hollow fibres, 0.89± 0.16 µm for 2.5% PVA-PLGA and 1.1± 0.1 µm for 5% PVA-PLGA hollow fibres. These data demonstrate an increase in pore size corresponding to an increase in PVA concentration (Fig. 3.3), with the coefficient of determination of 0.97 indicating an almost perfect linear relationship. These data indicate that the blended membranes are suitable as tissue engineering scaffolds as the size of the pores is big enough for the passage of molecules including large proteins across the scaffold, but small enough to prevent cells from infiltrating the fibre lumen.

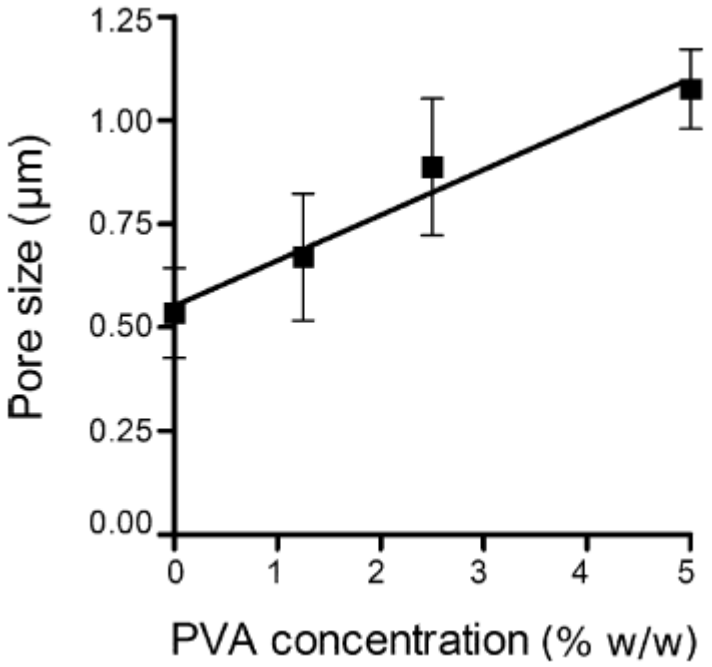

Fig. 3.3: Relationship between the PVA concentration and the pore size of PVA-PLGA hollow fibre membranes. Data represent the mean ± standard deviation (n= 4) and were fitted with linear regression using GraphPad Prism software. R^2= 0.97; y= 0.1099x + 0.5515. From [249].

By increasing the concentration of PVA in the polymer solution, overall porosity increased as well, although not linearly but reached a plateau at 2.5% PVA concentration (fig. 3.4): the overall porosity calculated for the fibres was respectively, 0.46± 0.01 for PLGA hollow fibres, 0.67± 0.026 for 1.25% PVA-PLGA, 0.76± 0.02 for 2.5% PVA-PLGA and 0.77± 0.03 for 5% PVA-PLGA fibres. Further studies should be performed in order to investigate the reason why the porosity did not increase at PVA concentrations higher than 2.5%.

These data indicate that PVA had a positive effect on the porosity of the scaffold, as not only could it contribute to increasing the size of the pores thus allowing for a better mass transfer of larger molecules across the scaffold, but also improved the overall porosity of the material. An increased porosity allows for higher cell adhesion, migration and for an adequate transport of nutrients and waste products across the scaffold, which are major requirements in bioreactors design for the regeneration of highly metabolic tissues.

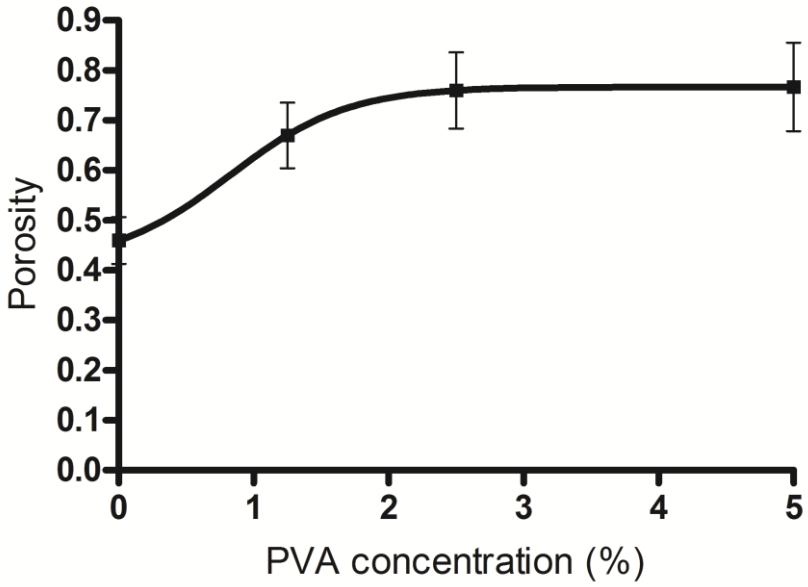

Fig. 3.4: Relationship between PVA concentration and porosity of PVA-PLGA hollow fibre membranes. Data represent the mean ± standard deviation (n= 4) and were fitted with non-linear regression (one site competition using GraphPad Prism software).

3.2.3 Mechanical properties

To investigate the mechanical properties of PLGA and PVA-PLGA membranes, and see whether the newly fabricated membranes that exhibited an increased porosity could still provide a suitable scaffold for the cells, load-displacement curves were obtained from the analysis of five samples for each type, and Young's modulus, tensile strengths at break, and yield strengths were calculated. From load displacement curves (Fig. 3.5), the lack of linearity suggests there is no defined elastic region for these membranes. The Young's modulus calculated for the samples considered the original cross sectional area of the sample (A_0) and the change in length ($L - L_0$). However, it is worth of notice that during tensile strength the hollow fibres exhibited a change in length but also in cross-sectional area: when stress reaches the maximum value, the cross section decreases due to "necking". Therefore it would be more accurate to consider the true sample cross-section in the Young's modulus calculation instead of the original dimensions of the cross section before tensile testing. The relative reduction of area, *i.e.* the ratio between the decrease of the specimen cross-section area before its rupture and its original cross-sectional area

(A_0) is given by: $\Delta A = \frac{A_0 - A_{min}}{A_0}$, where S_{min} is the minimum specimen cross sectional area.

Furthermore from the graph it can be noticed that pure PLGA fibres beared the highest load (1.9 N) while the tolerable load decreased upon increasing the PVA concentration, with 5% PVA-PLGA fibres bearing the lowest load (0.75 N).

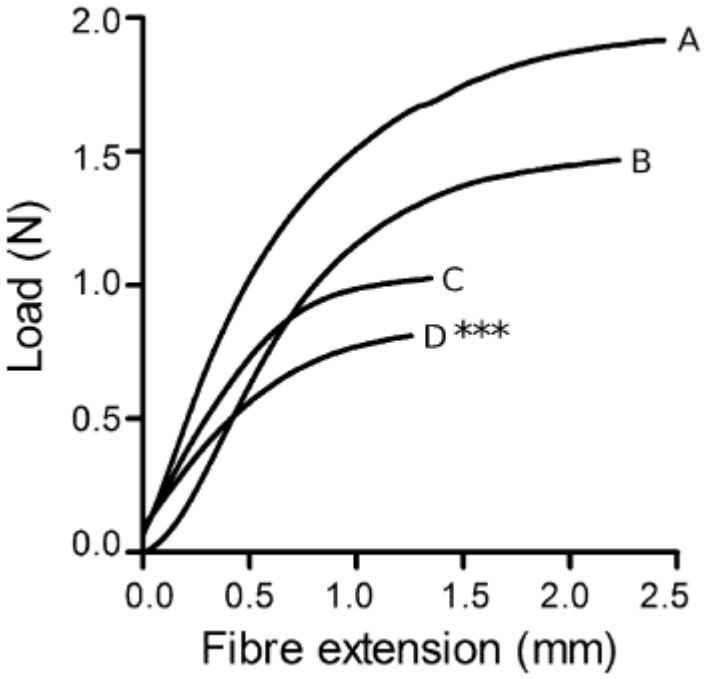

Fig. 3.5: Load displacement curves of PLGA (A) *versus* 1.25% (B), 2.5% (C) and 5% (D) PVA-PLGA hollow fibre membranes. n=5 *** P< 0.001. From [249]. One-way analysis of variance (one-way ANOVA) was used to test significant differences between multiple samples.

As shown in Table 4.1, it is clear that Young's modulus, tensile and yield strength decrease with increasing PVA concentration in the polymer solution, with a loss of 31% in Young's modulus when 5% PVA was added to the polymer solution compared to pure PLGA hollow fibre membranes.

Table 3.1: Young's Modulus, tensile strength at break and yield strength of PLGA and PVA-PLGA hollow fibre membranes. Data represents the mean± standard deviation (n=5). **P<0.01, *** P < 0.001. From [249]. One-way analysis of variance (one-way ANOVA) was used to test significant differences between multiple samples.

Fibre type	Young's modulus (MPa)	Tensile strength at break (MPa)	Yield strength (MPa)
PVA0% (pure PLGA)	109 ±2.50	3.88 ±0.36	2.58 ±0.64
PVA1.25%	106 ±4.00	2.77 ±0.15***	1.43 ±0.03***
PVA2.5%	101 ±3.40**	2.08 ±0.08***	1.26 ±0.41***
PVA5%	75 ±9.50***	1.68 ±0.09***	1.05 ±0.03***

The loss of mechanical strength was expected since PVA, being a hydrophilic polymer, tends to adsorb more water and therefore exhibits a lower mechanical strength compared to PLGA, which is hydrophobic. Therefore, the higher the PVA content in the solution, the higher the content of water adsorbed and the lower the mechanical strength of the fibre. Furthermore, PVA, by increasing the pore size and the porosity of the scaffold, contributes to a decrease in the mechanical properties of the material. However, the reduction in mechanical strength did not affect the handling of the fibres and was therefore deemed to be insignificant in practical terms.

3.2.4 Hydrophilicity

Hydrophilicity of a membrane scaffold is likely to affect its hydraulic permeability and cell adhesion. To evaluate whether the addition of PVA had an effect on the membrane surface hydrophilicity, the water contact angle on the pure PLGA and blended PVA–PLGA membranes was measured as described in section 2.4.4. However, since hollow fibres do not provide a suitable flat surface for testing the hydrophilicity with the water contact angle method, flat sheets were employed for this experiment. The water contact angle of pure PLGA membranes was 64± 0.5º, which indicates that the membrane surface is hydrophobic. By increasing the PVA in the polymer solution, the contact angle decreased, with 5% PVA–PLGA having the lowest value (50± 1.7º) and therefore being the most hydrophilic (Fig. 3.6). The

trendline obtained from the data shows that contact angle decreased exponentially with increasing PVA content in the solution, with 5% PVA–PLGA membranes having a value very close to that of the plateau (48.5º).

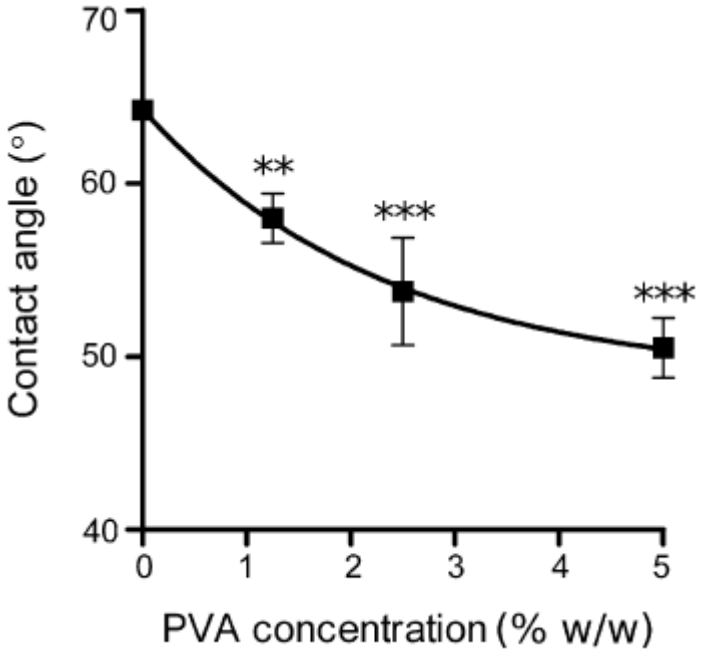

Fig. 3.6: Water contact angle values for PLGA and PVA-PLGA flat sheet membranes. Data represent the mean± SD (n= 4) and were fitted with non-linear regression (one phase exponential decay) using GraphPad Prism software. **P<0.01; ***P<0.001. One-way analysis of variance (one-way ANOVA) was used to test significant differences between multiple samples. From [249].

It was also observed that pure PLGA flat sheet membranes floated when immersed into water as PLGA, being a hydrophobic polymer, resists water adsorption, whereas 5% PVA–PLGA flat sheets sank, qualitatively indicating that they are more hydrophilic.

When combining this data with the mechanical properties data, it can be concluded that 5% is the optimal concentration of PVA to be added to PLGA in order to obtain the highest improvement in hydrophilicity with minor loss of mechanical properties. Hydrophilicity is very important when considering water flux, permeation of nutrients across the membrane and cell attachment [139, 145-147]. Hydrophobic materials are poorly wetted by cell culture medium, resulting in limited cell attachment to the scaffold and poor transfer of nutrients and waste products across the membrane. One common attempt to improve the wettability of scaffolds is pre-

wetting with ethanol, but this method has been shown to induce structural deformation of the material and the fibres have a tendency to stick together do to the ethanol acting as a plasticizer [128]. On the contrary, the addition of PVA to the polymer solution allows for the fabrication of hollow fibres without need of pre-treatment with a wetting agent.

3.2.5 Hydraulic and protein permeability

Mass transfer of nutrients through scaffolds is an important parameter in tissue engineering. One of the major limitations of PLGA is its hydrophobic character, which results in low permeability of water and water-based solutions (*e.g.* cell culture medium) through the scaffold. The addition of hydrophilic PVA to PLGA could lead to a more hydrophilic membrane, thus improving its permeability to water and nutrients.

The hydraulic and protein permeability of pure PLGA and blended PVA-PLGA membranes was assessed as described in section 2.4.5.

No pure water flux readings were obtained from PLGA membranes, confirming their hydrophobic character and need for a wetting agent. Interestingly, no measurable pure water flux readings were collected from 1.25 and 2.5% blended membranes during the experimental timeframe. However, a water flux of 7.0 l m^{-2} h^{-1} and a hydraulic permeability of 0.12 l m^{-2} h^{-1} Pa^{-1} were calculated at steady state for the 5% PVA–PLGA membranes. The increase in water flux over time observed in 5% PVA-PLGA membranes is probably caused by the combination of increased pore size, porosity and hydrophilicity reported for these membranes (fig. 3.7).

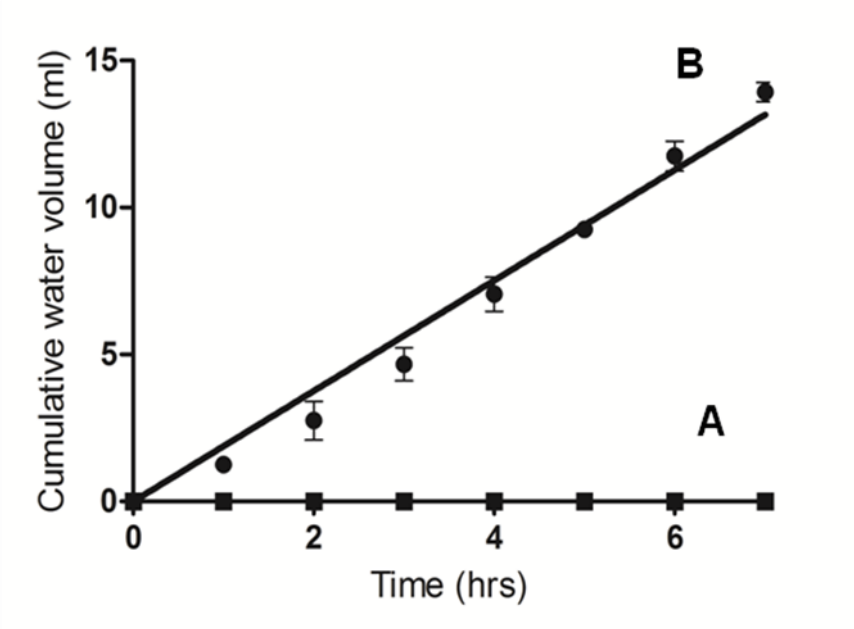

Fig. 3.7: Water permeation across PLGA, 1.25 and 2.5% PVA-PLGA hollow fibre membranes (A) and across 5% PVA-PLGA hollow fibres (B). Data represent the mean ± SD (n =4) and were fitted with linear regression (polynomial) using GraphPad Prism software. y=1.8801x. R^2=0.98.

A good hydraulic permeability is an important parameter in the design of hollow fibres for bioreactor applications, as water-based solutions, such as cell culture media, need to able to move across the scaffold to ensure a continuous provision of nutrients to and removal of waste from the cells, which is of great importance especially for highly metabolic organs. From the results above, it can be then concluded that 5% PVA-PLGA blended hollow fibres are the only membranes among the three different PVA-PLGA hollow fibres that allowed for water permeation and therefore the most suitable membranes to be used in bioreactor devices.

On the basis of the pure water flux findings, permeability of 5% PVA–PLGA membranes to BSA was assessed. This experiment was performed by D. Parker, undergraduate project student in the research group [249]. BSA, being an important component of serum, was used as a model protein for the study of the permeability of the hollow fibre membranes to proteins. Over a period of two hours, there was no significant difference in feed, permeate or retentate concentrations which all remained around the feed concentration of 100 µg/ml (fig. 3.8). Thus, there was no solute rejection nor any fouling due to protein adsorption that would reduce flux

[252]; the BSA flux was found to be constant with time at $0.18\times10^{-3} \pm 1\times10^{-5}$ kg m^{-2} s^{-1} after the 2 h wetting period.

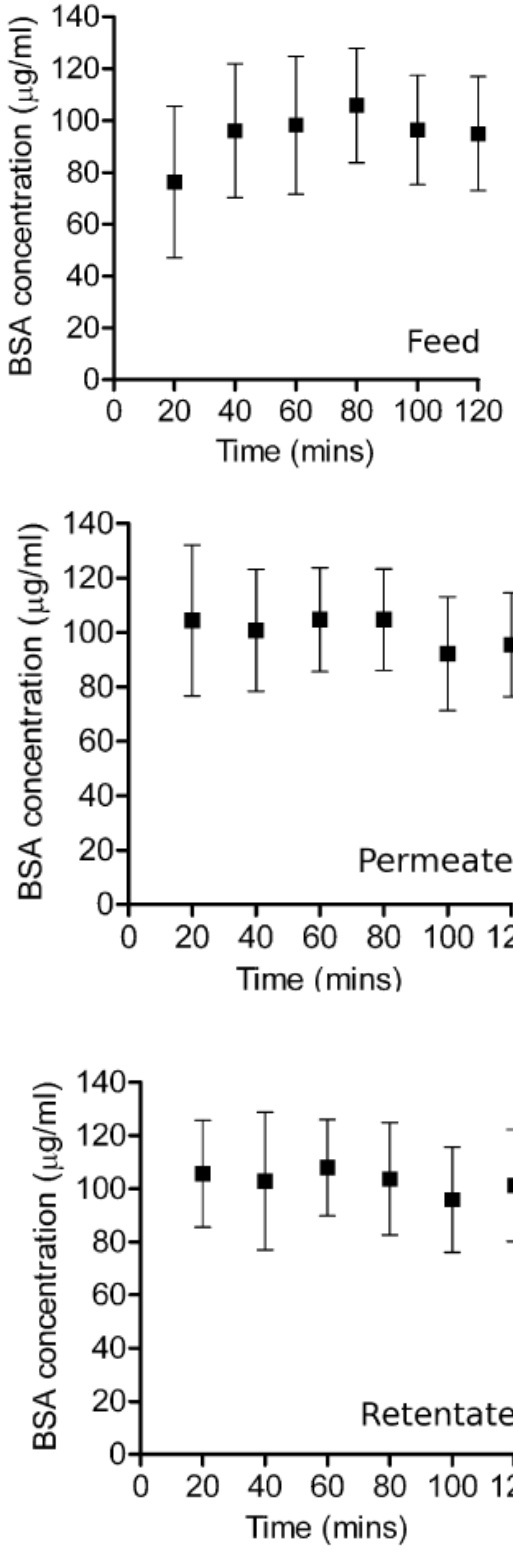

Fig. 3.8: Permeation of 100 µg/ml BSA solution across 5% PVA-PLGA hollow fibres. Concentration of BSA in the feed solution (A), permeate (B) and retentate (C). Data represent the mean ± SD (n=4). From [249].

Previous reports suggest three mechanisms for fouling in microfiltration membranes: (1) internal fouling by pore narrowing, (2) blocking of pores by protein aggregates and (3) formation of protein deposit on the membrane surface [253]. Among these three, the most likely mechanism for BSA fouling is internal deposition of protein molecules, since the pore size is within the microfiltration range, leading to pore narrowing and hence flux reduction [252]. Due to the large pore size of the 5% PVA–PLGA microfiltration membranes, multi-layered deposition of BSA would be required to add significant resistance to permeation for fouling to be observed; BSA has molecular dimensions of 14 nm × 4 nm × 4 nm [254] and the 5% PVA–PLGA membranes have been found to have an average pore size of 1.1 μm, two orders of magnitude greater than the largest dimension of the BSA molecule. Therefore, it is unlikely the BSA fouling will occur in 5% PVA-PLGA blended membranes.

This result is very promising, as, although it does not give a value for the molecular weight cut-off (MWCO) of the PVA-PLGA hollow fibre, it can give a first indication of a range of molecular weights that are allowed to pass across the blended membrane, *i.e.*, molecules up to 66 kDa (BSA molecular weight) can be transported from the extracellular space into the lumen of the fibre and vice versa. BSA, being an important component of cell culture medium, was a good model protein to be used for permeability experiments. These results indicate that 5% PVA-PLGA hollow fibres exhibit increased porosity, pore size and hydrophilicity not only for better cell adhesion and hydraulic permeability, but also for higher mass transfer of proteins and nutrients across the scaffold, characteristics which make them a potential good scaffold for organ tissue engineering applications.

However, a problem associated with the flux of nutrients through the pores of the membrane is given by the convective force through the pores, which might affect cell adhesion on the outer surface of the fibre. The calculation of the convective force through a pore of diameter 1.1 μm of 5% PVA-PLGA membranes gives a value of 84.25 pN. Taking into account that forces required to make the cells adhere to a surface have mean values ranging from 10 to 160 pN [255, 256] further investigation should be carried out in order to verify whether this force might cause detachment of the cells from the outer surface of the hollow fibre.

3.3 Treatment of membranes with sodium hypochlorite

Treatment of hollow fibres with 5% sodium hypochlorite (NaOCl) for 24 hours was performed in an attempt to optimise their properties, especially their permeability. Morphology, mechanical properties, hydrophilicity and permeability of the fibres were studied in order to determine its effect.

3.3.1 Morphology and pore size

Treatment with 5% sodium hypochlorite (NaOCl) had a considerable effect on the morphology of the outer and inner surfaces of the PVA-PLGA fibres. After 60 minutes incubation with NaOCl pore openings could be already observed on the outer and inner surfaces of 5% PVA-PLGA fibres (fig. 3.9). The effect of sodium hypochlorite increased with increasing treatment duration: in fact the skin layer of the membranes treated with sodium hypochlorite for 24 hours had disappeared and the surfaces appeared evenly porous, with increased pore size and porosity (fig. 3.10 A-I) and large macrovoids in the central core (fig. 3.10 L-N). Since the skin layer provides resistance to mass transfer, removal of the skin has the potential to increase the mass transport through the membrane, and also to unveil the porous interior, leading to a significant increase in surface area.

The morphological changes observed in the fibres are probably a result of the oxidative degradation induced by sodium hypochlorite: sodium hypochlorite is known to be an oxidising agent and has been shown to induce degradation of polymeric membranes by oxidation of hydroxyl and ether functions and C-H bonds of polymers. Furthermore, oxidation of alcohols by NaOCl has been previously reported [257]. Therefore OH groups of PVA are oxidised by NaOCl to carbonyl groups, and this oxidation results in the degradation of the outer and inner membrane surfaces, thus leaving a highly porous surface and larger pores. These data confirm previous experiments on polyethersulphone membranes that showed how hypochlorite treatment affected performance and surface properties of the membrane as it led to a significant degradation of the membrane surface leaving bigger pores [245].

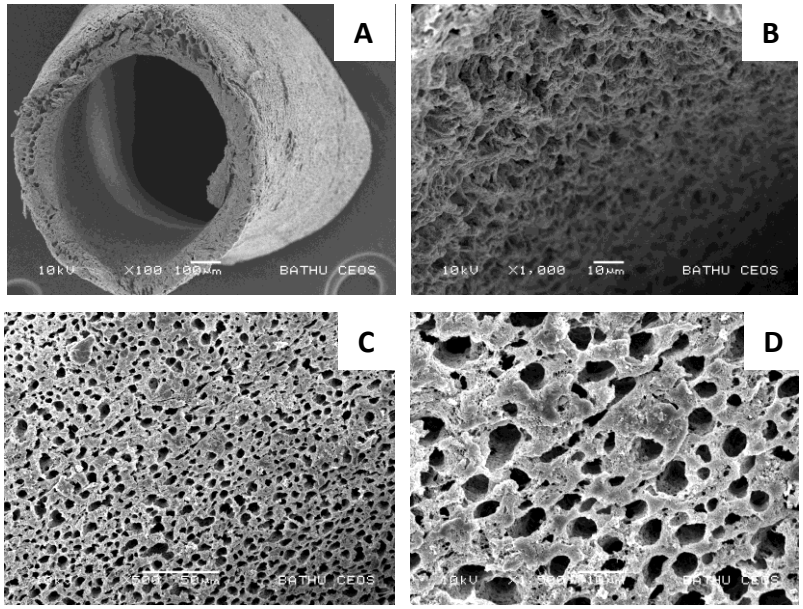

Fig. 3.9: Cross section (A), inner (B) and outer (C, D) surfaces of 5% PVA-PLGA hollow fibres treated for 60 minutes with 5% NaOCl.

Surprisingly, treatment of pure PLGA fibres with NaOCl did not have the same effect than that on blended fibres, as after 24 hours the skin was still not removed (fig. 3.11 D, E) and only a few cracks could be noticed on the outer surface (fig 3.11.F). Also, in the central core, finger-like pores were observed (fig. 3.11 A-C), compared to the large macrovoids present in PVA-PLGA membranes. It can be hypothesized that the addition of PVA allows for more oxidation sites by NaOCl and therefore to a more rapid action, or that the phenomena is enhanced by the thermodynamic changes occurring after the addition of PVA. It can be concluded that the mild oxidising properties of NaOCl are enhanced when PVA is present.

The exact value of pore size of NaOCl treated fibres could not be obtained by gas permeation analysis because the fibres split as a result of the flow of nitrogen gas inside the lumen at increasing pressures.

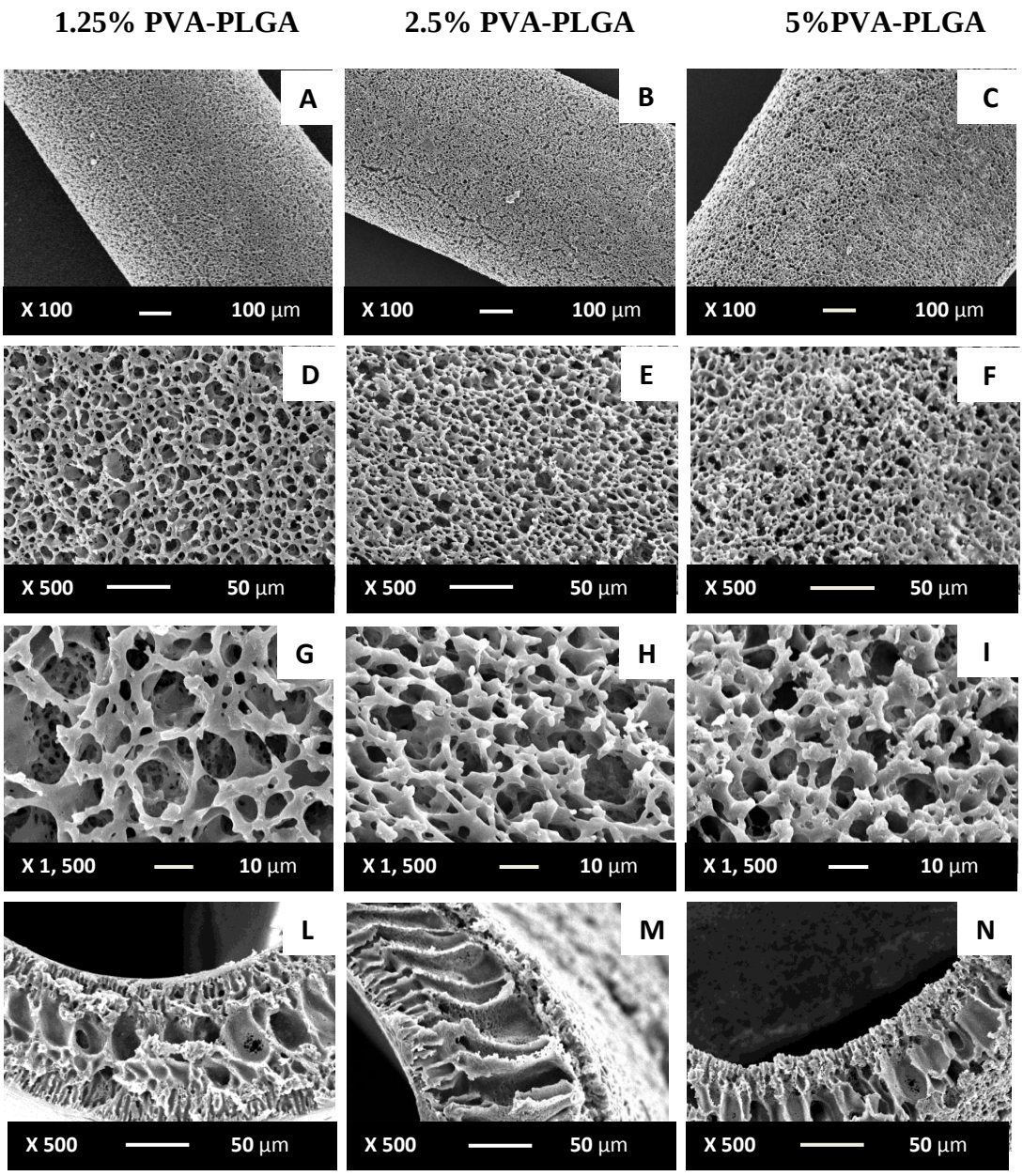

Fig. 3.10: Outer surface (A-I) and cross-section (L-N) of 1.25, 2.5 and 5% PVA-PLGA blended membranes treated for 24 hrs with 5% NaOCl.

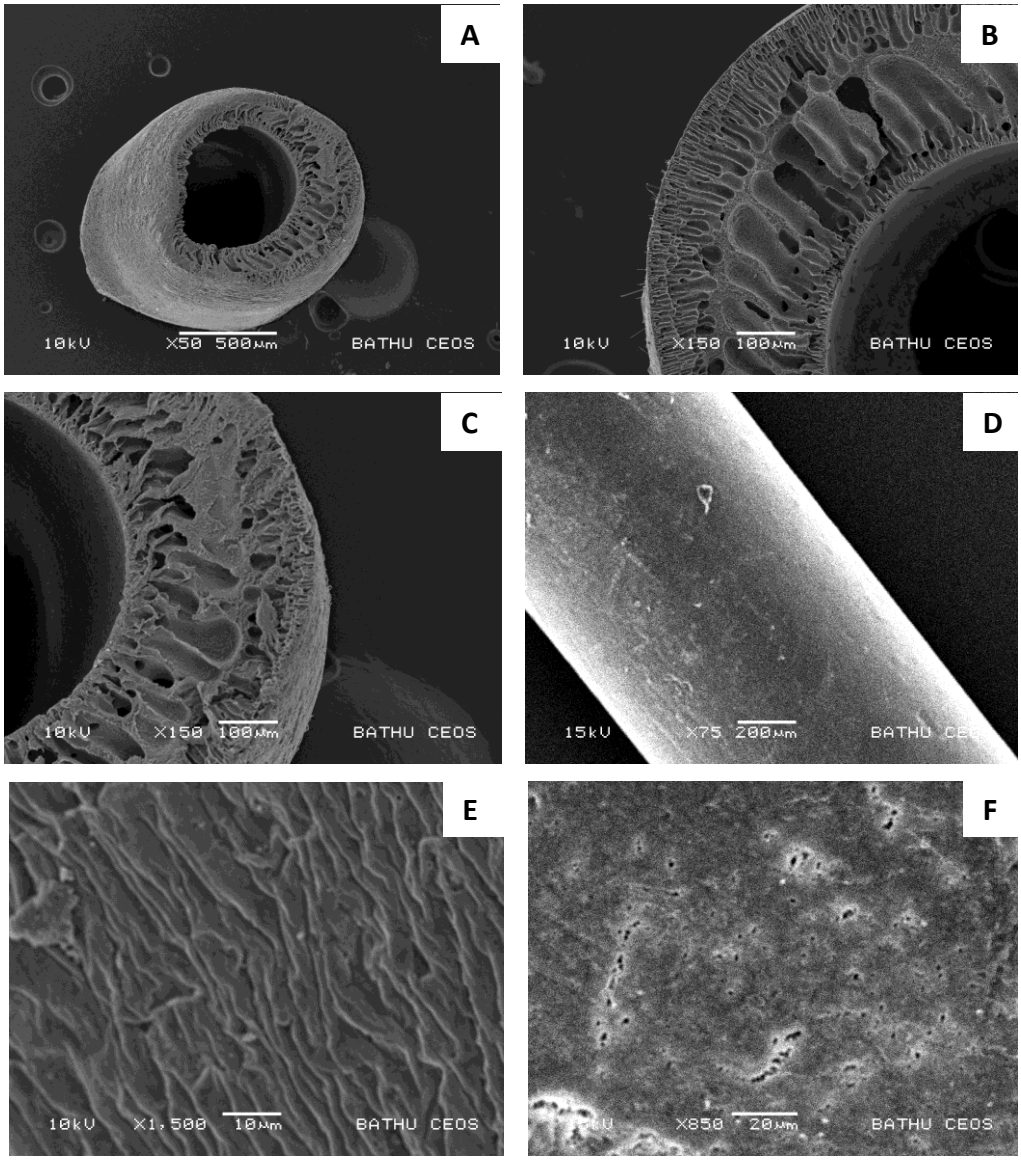

Fig. 3.11: Cross section (A-C), and outer surface (D-F) of PLGA fibres treated with NaOCl for 24 hrs.

3.3.2 Mechanical properties

The addition of PVA in the polymer solution led to a decrease in mechanical strength of the fibres correspondent with the increase of PVA content. When fibres were subsequently treated with sodium hypochlorite, a further decrease was observed (fig. 3.13, table 3.2). These results correspond with the removal of the skin and the increased porosity of the membranes caused by the oxidation with NaOCl. There are no examples in literature of PLGA scaffolds treated with NaOCl, since it has been mostly used in chemical engineering applications rather than tissue engineering. However, from previous studies, it could be hypothesised that NaOCl helps the

complete removal of the remaining PVA in the membrane, leading to a further increase in pore size and therefore to a further decrease in the mechanical properties of the fibres [248].

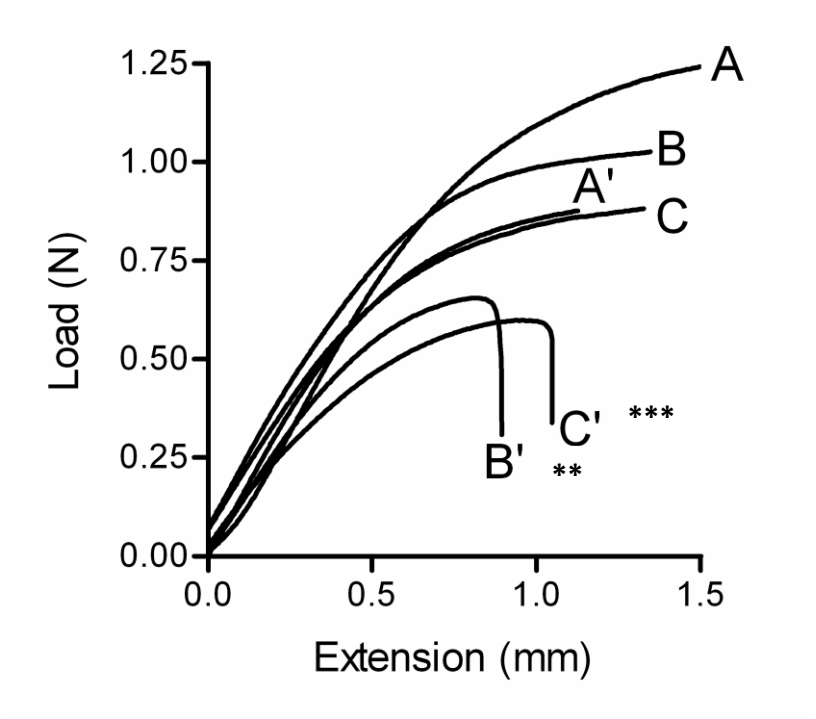

Fig. 3.12: Load displacement curves of 1.25% (A'), 2.5% (B') and 5% (C') PVA-PLGA hollow fibre membranes treated with 5% NaOCl for 24 hours compared to untreated 1.25% (A), 2.5% (B) and 5% (C) PVA-PLGA hollow fibres. **P<0.01, *** P<0.001. One-way analysis of variance (one-way ANOVA) was used to test significant differences between multiple samples.

Table 3.2 Young's Modulus, tensile strength at break and yield strength of NaOCl treated PVA-PLGA fibres compared to untreated fibres. Data represents the mean ± standard deviation (n= 4) *P<0.05, *** P < 0.001. One-way analysis of variance (one-way ANOVA) was used to test significant differences between multiple samples.

Fibre type	Young's modulus (MPa)	Tensile strength at break (MPa)	Yield strength (MPa)
PVA1.25%+NaOCl	88 ±5.20***	1.78 ±0.04***	1.39 ±0.01
PVA 2.5%+ NaOCl	68 ±5.06***	0.98 ±0.22***	0.82 ±0.30*
PVA 5% + NaOCl	58 ±0.93***	0.95 ±0.21***	0.82 ±0.12
(PVA1.25%)	106 ±4.00	2.77 ±0.15	1.43±0.03
(PVA2.5%)	101 ±3.40	2.08 ±0.08	1.2±0.41
(PVA5%)	75 ±9.50	1.68 ±0.09	1.05±0.03

3.3.3 Hydrophilicity and hydraulic permeability

Blending of PLGA with PVA showed an increase in hydrophilicity and hydraulic permeability of PLGA hollow fibres. PVA-PLGA blended fibres subsequently treated with NaOCl showed an even lower contact angle (down to 37° ± 1.7 for 5% PVA-PLGA membranes) (fig. 3.13), decreasing linearly with the increase of PVA concentration, suggesting that NaOCl may also contribute to improve the hydrophilicity of the membranes. A decrease in contact angle was also observed by Susanto and colleagues after treatment of polyethersulphone membranes with NaOCl [243, 245]. However, the increase of the hydrophilicity of PVA-PLGA after treatment with NaOCl requires further investigation, since the pores of the treated membranes are significantly bigger, and the water drop might infiltrate into the fibres giving unreliable results.

Treatment of polyethersulphone membranes with NaOCl has recently been shown to increase permeability and water flux across the membrane, a phenomena which is much more evident when the membrane is blended with a hydrophilic additive, as the additive is decomposed by NaOCl [243, 246]. Furthermore, the capacity of NaOCl to remove proteins deposited on or inside the membrane as shown by previous works [243, 244, 246] would be very important to solve mass transfer issues, still crucial for

tissue engineering applications. However, despite an initial significant increase in water flux across NaOCl-treated fibres, NaOCl treatment resulted in a significant reduction in mechanical strength with the treated fibres splitting after only 2-3 hours with water flow inside the lumen. This was probably caused by the increased porosity and pore size resulting from the skin removal from the outer surface, which were detrimental for the mechanical integrity of the fibres. Therefore treatment of PLGA membranes with NaOCl is not suited for tissue engineering applications and was no longer considered in this project.

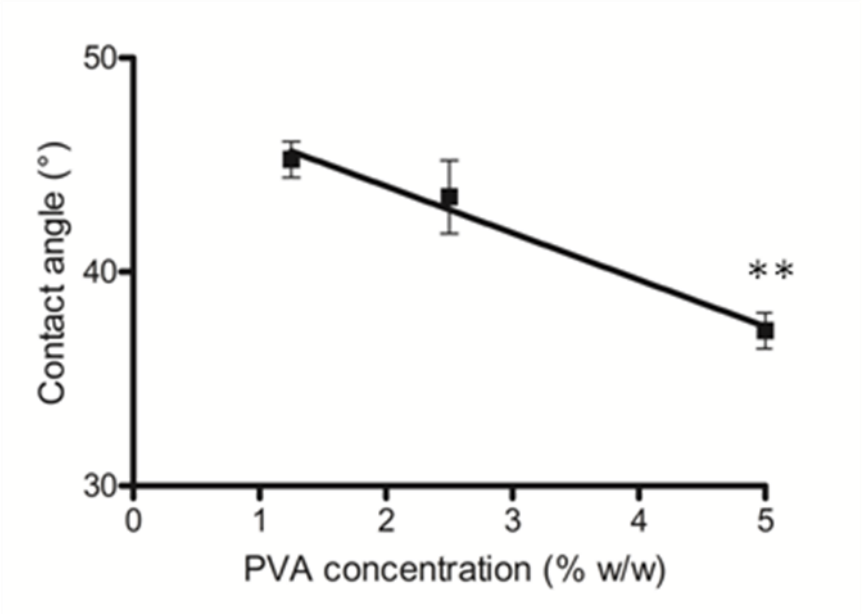

Fig. 3.13: Water contact angle values for PVA-PLGA flat sheet membranes treated with 5% NaOCl for 24 hours. Data represent the mean ± SD (n=4) and were fitted with linear regression using GraphPad Prism software. y= -2.186x + 48.38. R^2 = 0.9847 **P< 0.0.1. One-way analysis of variance (one-way ANOVA) was used to test significant differences between multiple samples.

3.4 Conclusions

One of the major limitations in the use of PLGA as tissue engineering scaffolds in bioreactor devices is its hydrophobic character, which results in low wettability and permeability of water and protein through the scaffold. In this project, blended PVA-PLGA hollow fibre membranes were fabricated to allow wetting without the use of a wetting agent, and to improve protein permeation.

The addition of PVA to PLGA spinning dopes resulted in asymmetric porous hollow fibre membranes with mean pore sizes increasing linearly from 0.54 μm for PLGA to 1.1 μm for 5% PVA–PLGA, and porosity increasing from 0.46 to 0.77. An exponential decrease in water contact angle from 64º to 50º indicates that PVA improves hydrophilicity of PLGA hollow fibre membranes. Pure water flux was only obtained with 5% PVA–PLGA fibres, and these fibres were shown to be permeable to BSA, with no solute rejection or reduced flux or pore size due to fouling. A decrease in mechanical strength from 109 to 75 MPa was seen, however this did not prove detrimental in handling the fibres.

Pure PLGA and blended PVA-PLGA hollow fibres were also treated with sodium hypochlorite in order to improve the properties of the membranes. NaOCl caused the removal of the skin from the inner and outer surface of the fibre, increased pore size, and possibly increased hydrophilicity. However, this proved to be detrimental for the mechanical integrity of the fibres.

It can be concluded that the addition of 5% PVA to PLGA spinning dopes improves the PLGA hollow fibre membrane scaffold properties because it allows for wetting without an additional wetting agent and is necessary for pure water flux and protein permeation, while treatment of hollow fibres with NaOCl negatively affects the mechanical integrity of the fibres, making them not suitable for tissue engineering applications.

4. Cell adhesion and proliferation on PVA-PLGA blended membranes

4.1 Introduction

It has been demonstrated that cell adhesion, spreading and proliferation on biomaterial surface are determined by many material properties, including surface roughness and topography, chemical composition, wettability, surface charge and surface treatments [258]. These parameters have to be considered in the design and fabrication of a scaffold.

The source of the adhesive force at the interface cell-surface is given by the ligand-receptor bonds (typically protein-protein or protein-carbohydrate non-covalent interactions). However, the flow of medium exerts a disruptive (counteradhesive) force on the cells. For the cells to be adhesive to the surface this disrupting force must be balanced by the opposite adhesive force applied by the cells, *i.e.* the sum of the forces must be zero ($\Sigma |F| = 0$) . It is thought that about 10-20 ligand-receptor bonds are enough to encounter the disruptive force. The relative strength of these competing forces (the disruptive hydrodynamic force and the adhesive force) dictates the adhesion strength of the cells to the surface [259].

The results presented in chapter 3 showed that 5% PVA-PLGA blended membranes exhibited increased porosity, pore size, hydrophilicity, hydraulic and protein permeability compared to pure PLGA scaffolds. Blended membranes exhibited a moderate hydrophilic character, with a contact angle of 50 degrees, compared to the more hydrophobic pure PLGA membranes, for which an angle of 64 degrees was measured. The increased hydrophilicity of the blended membrane was shown to allow for higher mass transfer of nutrients compared to PLGA, which in contrast did not allow for adequate hydraulic and protein permeation across the membrane. PVA-PLGA membranes, being more hydrophilic, tend to be more easily wetted by aqueous solutions, and to exhibit a lower protein adsorption, compared to hydrophobic PLGA (see section 3.2.5), thus allowing for a higher permeation of nutrients across the scaffold. The improved wettability of PVA-PLGA membrane

should be also favorable for cell adhesion and for their even distribution on the membrane compared to the hydrophobic PLGA. Hydrophobic surfaces in fact possess high interfacial free energy in aqueous solutions, which tend to unfavourably influence the initial stage of cell contact with the biomaterial. However, in contrast, some other studies have shown that hydrophobic materials, by adsorbing adhesive proteins present in the serum (*e.g.* fibronectin and vitronectin) of cell culture medium, would facilitate the adhesion and proliferation of the cells on the scaffold [260].

Therefore, to examine cell attachment and proliferation on the novel membranes, rat mesenchymal stem cells (MSCs) and human osteosarcoma cell line (MG63s) were seeded on pure PLGA and blended PVA-PLGA membranes. Tissue culture plastic was used as control. PLGA and PVA-PLGA flat sheets were used for the tests instead of hollow fibres for the ease of membrane seeding and observation with the microscope. Medium was changed every 48 hours and samples of cells seeded on both pure PLGA and blended PVA-PLGA flat sheet membranes were collected every 24 hours in a 96 hour time period and analysed qualitatively with fluorescence microscopy and quantitatively with the Pico Green dsDNA quantitation assay.

4.2 Adhesion and proliferation of MSCs to PLGA and to 5% PVA-PLGA flat sheets

4.2.1 Qualitative analysis

Figures 4.1-4.7 show the live staining of rat MSCs attached to pure PLGA and to 5% PVA-PLGA blended flat sheet membranes after 24, 48, 72 and 96 hours seeding. Tissue culture plastic was used as control. Fig. 4.1 shows the seeding of cells on tissue culture plastic. 24 hours after seeding several cells appeared to have adhered to the surface of the well but they are not homogeneously distributed (fig. 4.1 A). The cells presented a rounded morphology, indicating that there is not a particularly high affinity between the cells and the surface of the well. At 48 hours after seeding most cells still presented a rounded morphology (fig. 4.1 B) but after 72 hours they spread on the surface of the flat sheet with many of them exhibiting a flat large morphology

with some spindle-like cells and some polygonal cells. At 96 hours the surface was mostly covered with cells (fig. 4.1 D) except from some empty areas, and the cells exhibited both spindle like and polygonal morphology (fig. 4.2 A, B). MSCs usually have a more spindle like morphology when they retain a high differentiation capacity, with a polygonal shape when they are losing their ability to differentiate. Mesenchymal stem cells are defined as fibroblast-like cells with regard to their morphology, and in fact their morphology is so similar to that of fibroblasts that it is impossible to distinguish these two cell types by morphological analysis [261, 262]. Fig. 4.3 A shows a picture of mesenchymal stem cells and fig. 4.3 B one of fibroblasts. From the two pictures it can be observed how similar is the morphology of the two cell types. However, the cells exhibiting a more polygonal morphology might also be stem cells spontaneously differentiating in osteoblasts. In fact, as can be seen in fig. 4.3 C, osteoblasts have a polygonal morphology, and it would not be surprising the presence of some osteoblasts within the stem cells as mesenchymal stem cells can spontaneously differentiate into osteoblasts, especially when cultured at high densities [263].

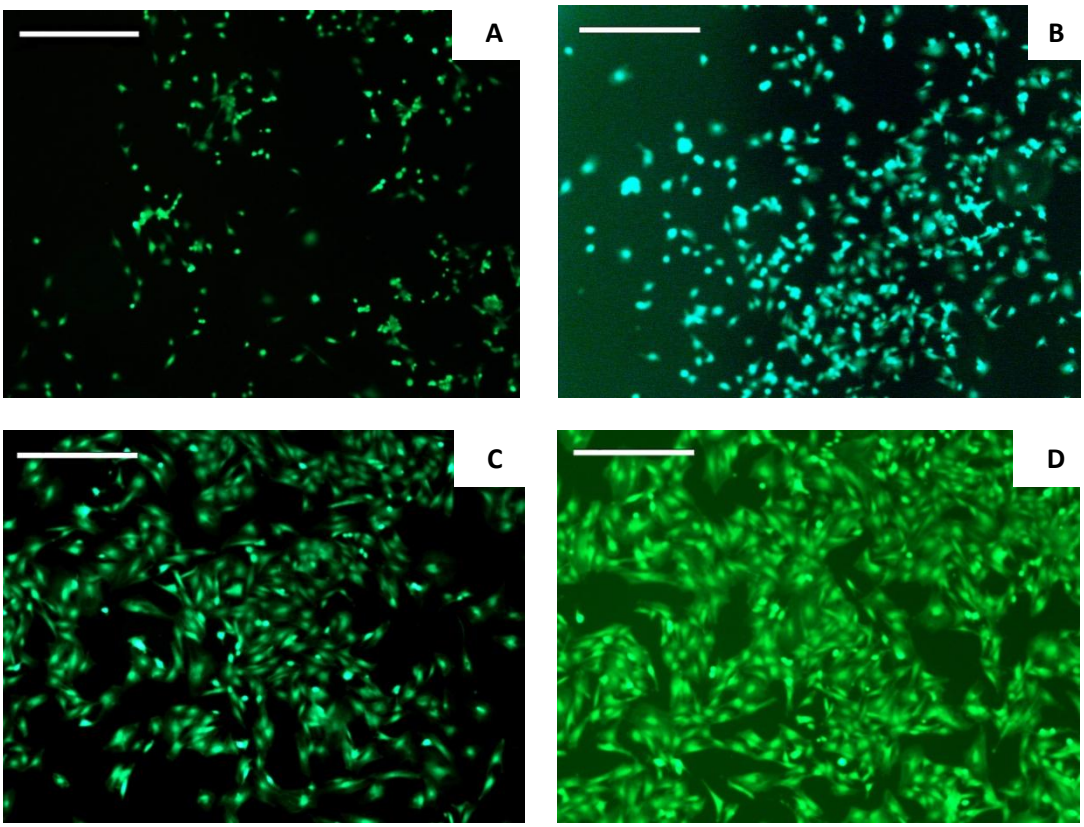

Fig. 4.1: 5X magnification of rat MSCs on tissue culture plastic at 24 (A), 48 (B), 72 (C) and 96 (D) hours after cell seeding. Cells were stained with Vybrant CFDA SE Cell Tracer kit and analysed by fluorescence microscopy. Scale bar: 500 µm.

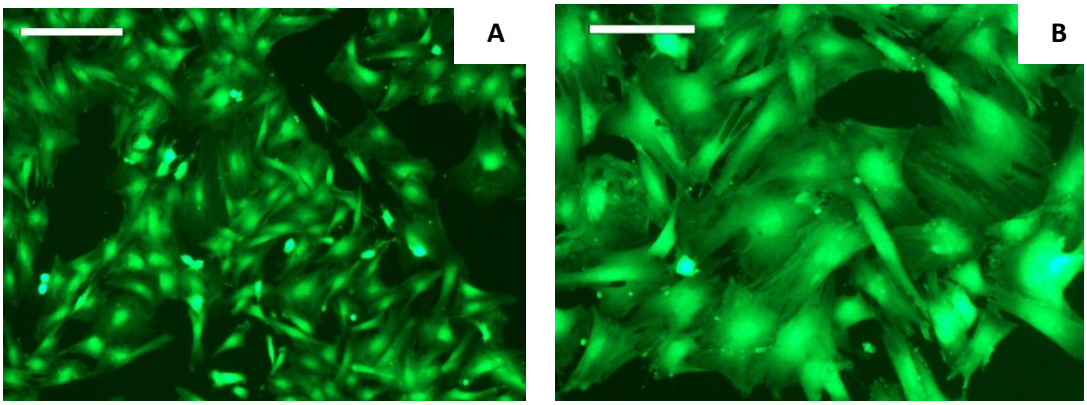

Fig. 4.2: 10 X (A, scale bar: 200 µm) and 20X (B, scale bar: 100 µm) magnification of rMSCs on tissue culture plastic 96 hours after cell seeding. Cells were stained with Vybrant CFDA SE Cell Tracer kit and analysed by fluorescence microscopy.

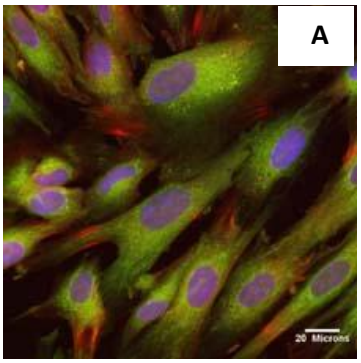

B

Image removed due to copyright reasons

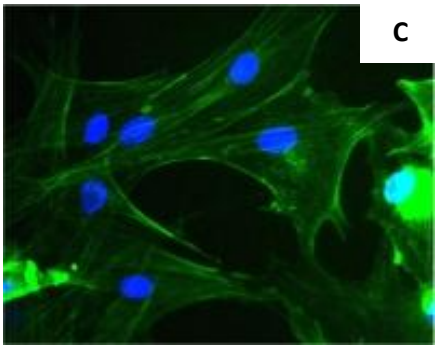

Fig. 4.3: Typical morphology of bone marrow mesenchymal stem cells (A, from [264], with permission from the author), of fibroblasts (B, from [265]), and osteoblasts (C, from [266], with permission from the author).

When the rMSCs were seeded on pure PLGA flat sheets, it was observed that after 24 hours cells had attached in clumps to the material (fig. 4.4 A) and, in contrast to tissue culture plastic had already started spreading on its surface (fig. 4.4 B, 4.5A) indicating high affinity between the cells and the scaffold. After 48 hours cells appeared to have covered most of the material surface (fig. 4.4 C), probably thanks to its porosity, indicated by the black circles, which might have facilitated cell adhesion to the flat sheet. Cells continued spreading, showing their mesenchymal stem cell morphology (fig. 4.5 B). This is visible as well after 72 hours (fig. 4.4 E- F, fig. 4.5 C), while at 96 hours a very dense cell layer was observed (fig. 4.4 G, H). When comparing the attachment of the cells to tissue culture plastic, it can be noticed that MSCs seem to exhibit a higher affinity to PLGA than tissue culture plastic, as can be observed at 48 and 72 hours.

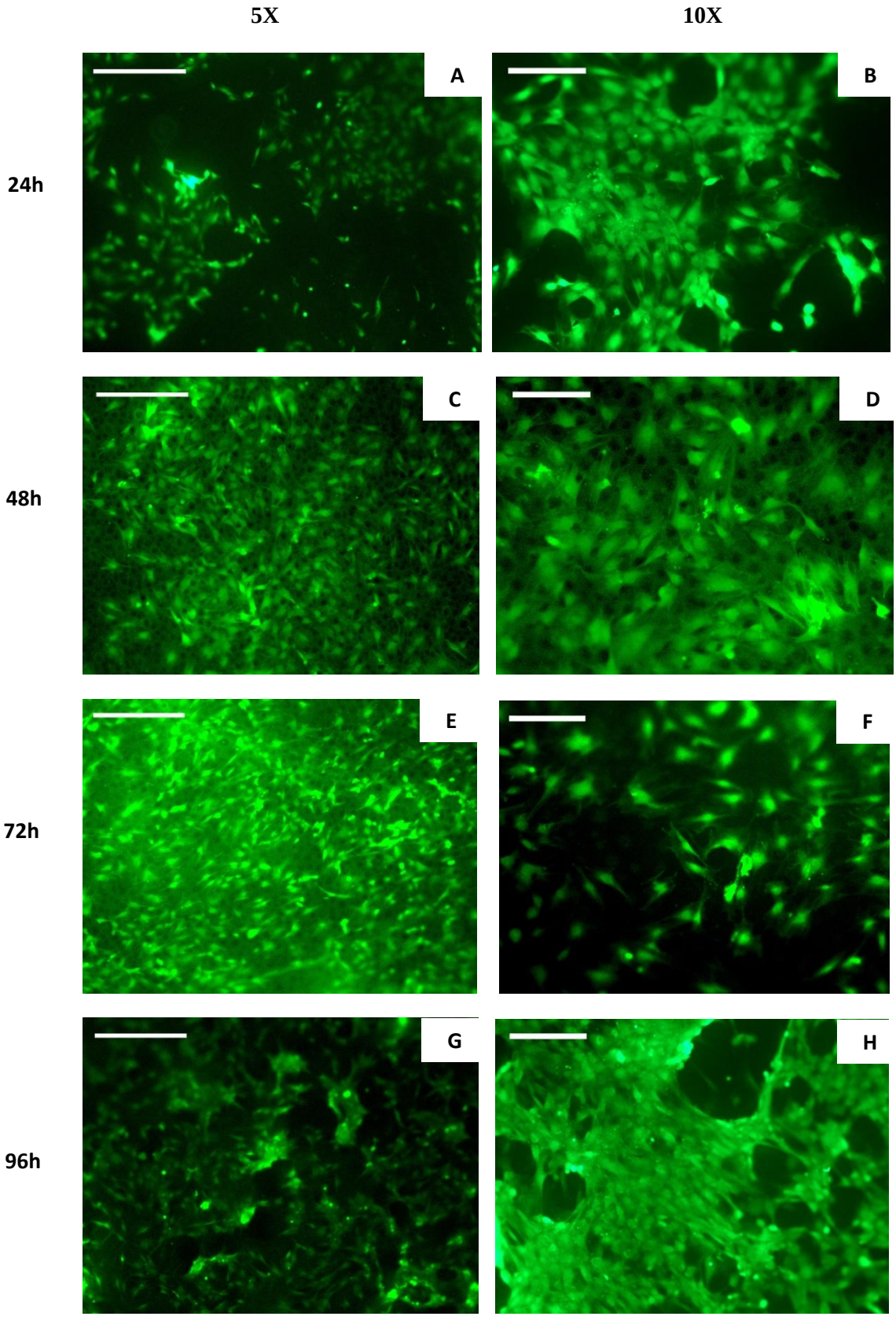

Fig. 4.4: 5X (scale bar: 500 µm) and 10X (scale bar: 200 µm) magnification of rMSCs proliferation on PLGA flat sheets at 24, 48, 72 and 96 hours after cell seeding. Cells were stained with Vybrant CFDA SE Cell Tracer kit and analysed by fluorescence microscopy.

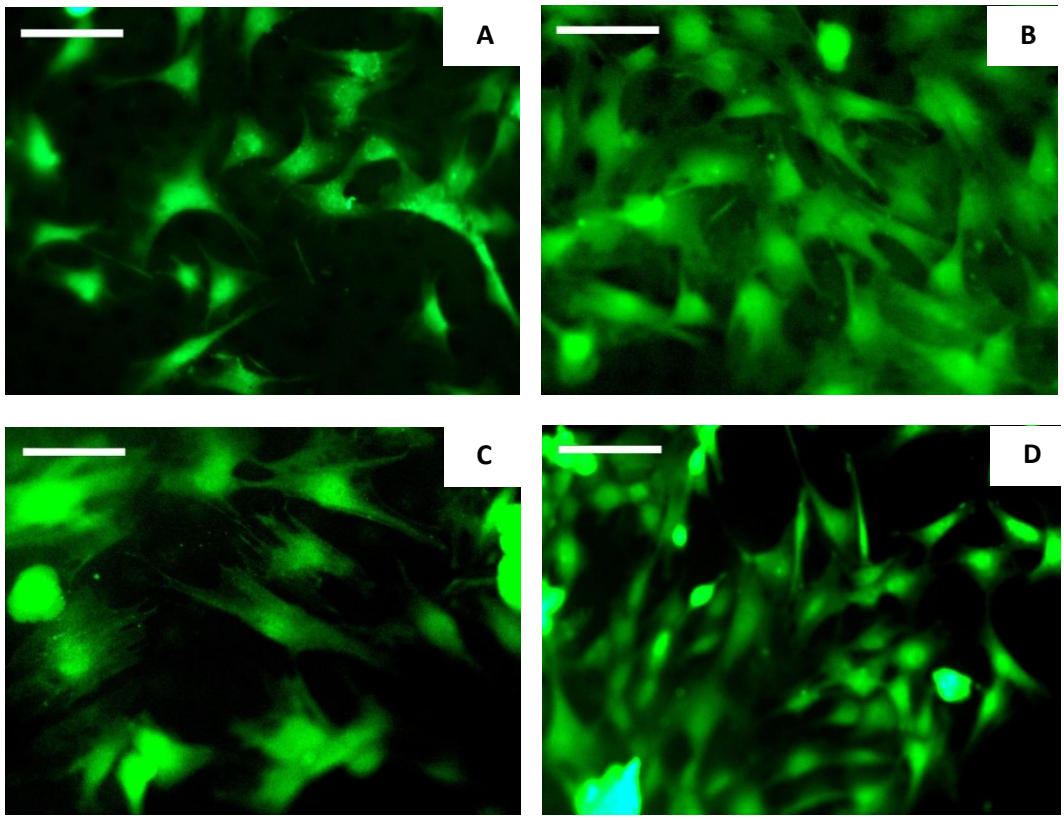

Fig. 4.5: 20X magnification (scale bar: 100 µm) of rMSCs attachment and proliferation on PLGA flat sheets at 24 (A), 48 (B), 72 (C) and 96 (D) hours after cell seeding. Cells were stained with Vybrant CFDA SE Cell Tracer kit and analysed by fluorescence microscopy.

On the contrary, when mesenchymal stem cells were seeded on 5% PVA-PLGA flat sheets, they showed much lower affinity to the material compared to pure PLGA. In fact after 24 hours very few cells attached to the surface of the scaffold and exhibited a rounded morphology, indicating a low affinity to the material (fig. 4.6 A). After 48 hours they started spreading (fig. 4.6 B) and after 72 and 96 hours the surface of the flat sheet still appeared mostly empty with some areas with cell clusters that had continued spreading (fig. 4.6 B and C, and fig. 4.7 A and B).

This result was not expected, since the improved hydrophilicity obtained with the addition of PVA to PLGA should have facilitated cell adhesion to the material, as described by the previous study from Oh SH *et al* [147]. However, there are two conflicting theories about whether it is more appropriate to use hydrophilic or hydrophobic materials to increase cell attachment. Some studies have shown that hydrophilic materials, being more wettable by aqueous cell culture media, increased the affinity of cells and therefore facilitated the adhesion of the cells to the surface of

the scaffold [123, 267-270]. In contrast, other studies have shown that hydrophobic materials, by enhancing adsorption of adhesive proteins through hydrophobic interactions, could improve cell adhesion [260, 271, 272]. It was found that hydrophobic materials adsorbed more fibronectin, collagen I and vitronectin than hydrophilic materials, thus increasing cell affinity to the scaffold [260]. More specifically, there are conflicting results regarding mesenchymal stem cells attachment on hydrophilic and hydrophobic materials. Several studies have shown that highly hydrophilic materials enhance MSC adhesion and proliferation compared to hydrophobic ones [267, 268, 273-276], while other studies reported a better MSC attachment on hydrophobic or even super-hydrophobic surfaces [260, 271]. From these examples it is clear that it is still not well understood whether mesenchymal stem cells prefer hydrophobic or hydrophilic materials.

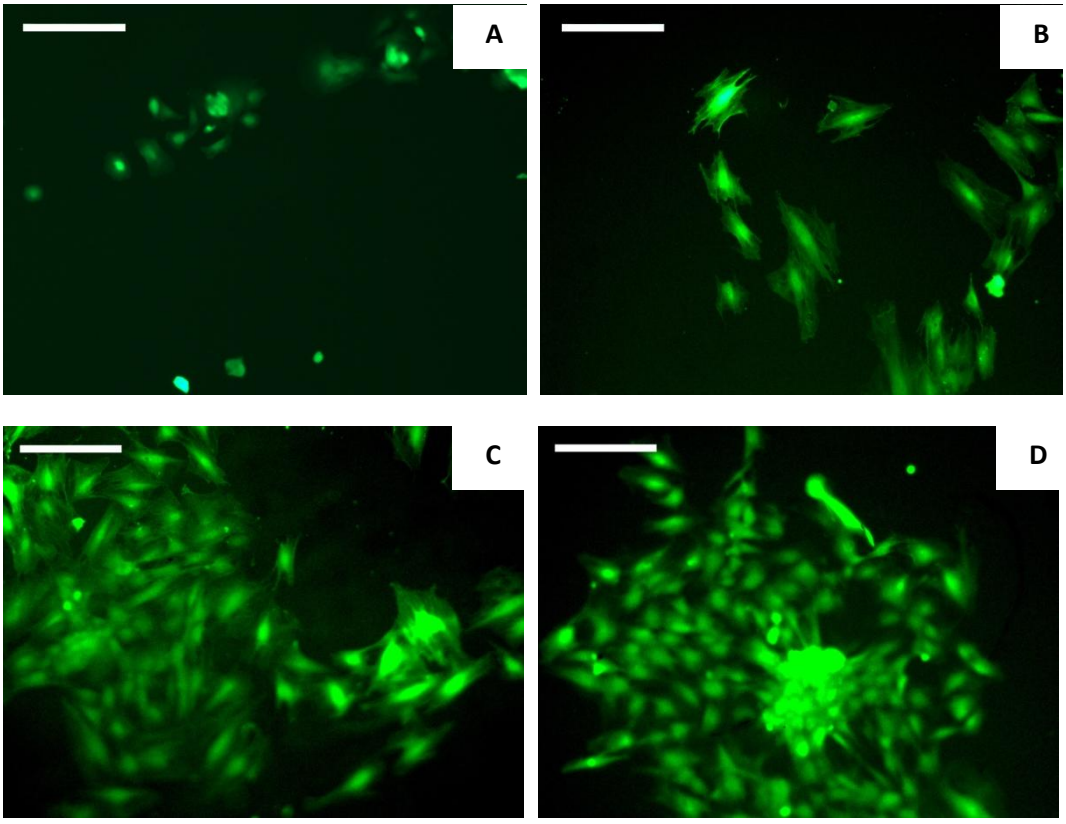

Fig. 4.6: 10X magnification (scale bar: 200 µm) of rMSCs attachment and proliferation on 5% PVA-PLGA flat sheets at 24 (A), 48 (B), 72 (C) and 96 (D) hours after cell seeding. Cells were stained with Vybrant CFDA SE Cell Tracer kit and analysed by fluorescence microscopy.

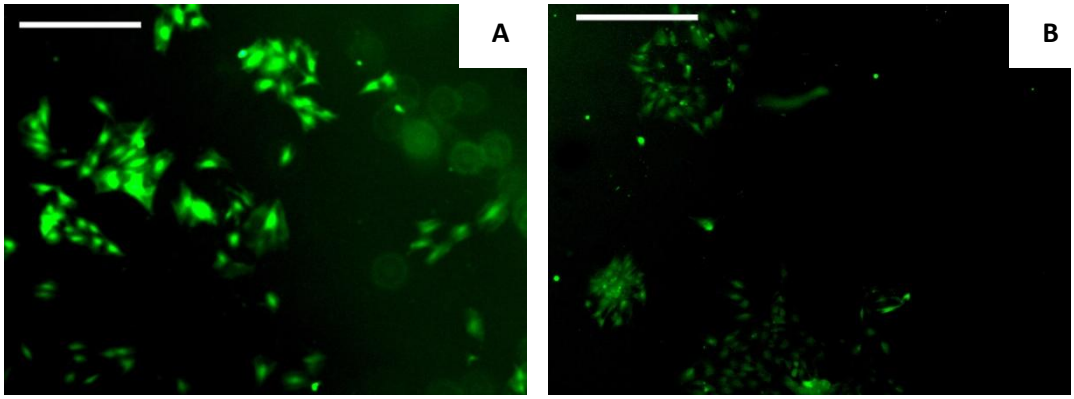

Fig. 4.7: 5X magnification (scale bar: 500 µm) of rMSCs attachment and proliferation on 5% PVA-PLGA flat sheets at 72 (A) and 96 (B) hours after cell seeding. Cells were stained with Vybrant CFDA SE Cell Tracer kit and analysed by fluorescence microscopy.

The latter theory could explain the data obtained in this experiment. The serum present in cell culture medium contains some adhesive proteins such as vitronectin and fibronectin, which contain the RGD sequence recognised by cell-surface integrin receptors. The binding of these adhesive proteins to integrins facilitates cell adhesion to the surface and is followed by a series of structural changes in the cells, such as cell spreading and cytoskeletal reorganisation. PLGA, being a hydrophobic material, might have enhanced the adsorption of these adhesive serum proteins and therefore mesenchymal stem cell attachment [277]. Furthermore, vitronectin provides factors that help the cells to spread out, and this might explain why cells had spread on PLGA surfaces after 24 hours. On the contrary, the more hydrophilic PVA-PLGA membranes are less likely to adsorb proteins. For example, in section 3.2.5 it was shown that BSA could pass through the pores of the membrane without being adsorbed on the material surface. PVA-PLGA might also have reduced vitronectin and fibronectin adsorption, thus reducing cell adhesion and spreading to the membrane surface.

However, since the use of pure PLGA was shown to be unsuitable for bioreactor applications because of its hydrophobic character (section 3.2.5), further strategies, such as immobilising adhesive proteins *e.g.* fibronectin, collagen, vitronectin, or peptide ligands (*e.g.* the RGD sequence) on the surface of PVA-PLGA blended membranes or blending the polymer solution with ECM proteins (*e.g.* collagen) could be attempted in order to allow the use of PVA-PLGA hollow fibres as

membranes that would accomplish the dual task of supporting the adhesion and proliferation of MSCs and, at the same time, of ensuring a good mass transfer of nutrients to and waste from the cells.

4.2.2 Quantitative analysis

To quantify the mesenchymal stem cell attachment and proliferation on PLGA and PVA-PLGA flat sheets, the Pico Green assay was performed, which measured the number of stem cells present on tissue culture plastic, PLGA and 5% PLGA-PVA over 96 hours, following seeding at a density of 10,000 cells/well.

A mass balance equation to describe cell growth limited by nutrients depletion is given by the Monod model [278, 279]:

$$\frac{dN}{dt} = N(\mu - D)$$

where N is the number of cells in the system, D the death or dilution rate, μ the steady state growth rate, assuming that the growth of the cells follow the Michaelis-Menten saturation curve:

$$\mu = \mu_{\max}\left(\frac{R}{k_R + R}\right)$$

where R is the nutrient concentration, μ_{max} is the maximum growth rate and k_R is the half-saturation constant.

As can be seen from fig. 4.8, a higher cell number on PLGA and tissue culture plastic was observed after 24 hour seeding compared to PVA-PLGA, with around 15,000 ± 4597 cells attached to plastic wells and around 16,500 ± 3670 to PLGA, while around 8,500 ± 4857 to 5% PVA-PLGA. These first data indicate that MSCs have adhered on tissue culture plastic and PLGA membranes but not on 5% PVA-PLGA membranes since the number of cells measured after 24 hours was lower than the seeding density (10,000 cells/well). When these data are compared with the qualitative analysis of the live cell staining, an even lower number of attached cells would probably be expected, since the majority of the membrane was without cells, with very few MSCs attached. This discrepancy between the qualitative and quantitative analysis might be due to the fact that Pico Green measures the DNA of every cell, while live staining only stains live cells. Therefore there may have been

8,500 cells attached to the membrane, but many of them were dead after 24 hours, and not detected by live staining.

Beyond 24 hours, while cells continued to proliferate on tissue culture plastic and on PLGA membranes, there was very little proliferation on 5% PVA-PLGA membranes, with around 13,500 ± 4782 cells measured at 48 h and a decrease down to 12,000± 4818 cells at 96 hours. These data confirm the qualitative analysis since very few cells were observed on 5% PVA-PLGA membranes at all the time points while cell proliferation was clearly visible for cells seeded on PLGA and on plastic wells.
Also, while the number of MSCs measured is very similar for PLGA and controls up to 48 hours, at 72 hours more cells had proliferated on PLGA (around 50,000 cells ± 416) than on controls (around 39,000 ± 2041 cells), further increasing after 96 hours. In fact the MSCs number had nearly doubled on PLGA flat sheets after 96 hours, with about 93,000 ± 8235 cells against about 53,000 ± 2835 cells on tissue culture plastic.

These data confirm the high affinity of mesenchymal stem cells to PLGA and reinforce the hypothesis that MSCs prefer hydrophobic environments to hydrophilic ones, as shown by the low adhesion and proliferation of cells on 5% PVA-PLGA flat sheets.

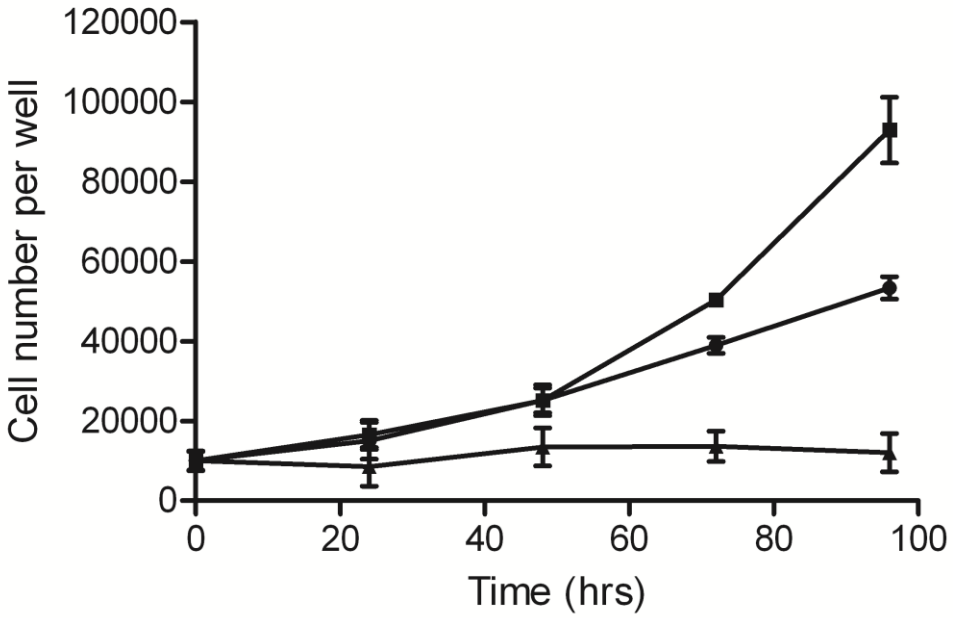

Fig. 4.8: Pico Green quantitative analysis of MSCs proliferation on tissue culture plastic (●), PLGA (■) and 5% PVA-PLGA (▲) flat sheet membranes. Data represent the mean ± SD (n = 3).

4.3 Adhesion and proliferation of MG63 cells to PLGA and to 5%PVA-PLGA flat sheets

4.3.1 Qualitative analysis

In order to investigate the suitability of 5% PVA-PLGA membranes as a scaffold for other cell types, MG63 osteosarcoma cells were seeded and their morphology compared to cells seeded on PLGA and on tissue culture plastic (controls). Fig.4.9 demonstrates that after 24 hour seeding, cells had adhered on plastic (A) and already started spreading (B). After 48 and 72 hours cells continued proliferating as can be observed in fig. 4.9 C- F where most of the well area is covered by cells. Cells exhibited a spindle-like morphology, indicating that the cells had spread on the surface of tissue culture plastic. At 96 hours cells had proliferated to a degree that a dense layer of cells had nearly entirely covered the well (fig. 4.9 G).

In contrast, few cells adhered to PLGA membranes after 24 hour seeding and they still presented a rounded morphology (fig. 4.10 A, B), indicating low affinity of MG63s for PLGA. At 48 and 72 hours after seeding, the few cells that were observed on the surface of the membrane still presented a rounded morphology (fig. 4.10 C-F). At 96 hours the cells did not evenly cover the membrane surface growing in clumps, and leaving many areas without cells. They still had not spread and presented a rounded morphology (fig. 4.10 G, H).

In contrast, after 24 hour seeding on 5% PVA-PLGA flat sheets, cells adhering to the membrane looked more evenly distributed compared to PLGA (fig. 4.11 A, B). They still presented a rounded morphology, but they appeared more spread at 48 hours (fig. 4.11 C, D). At 72 hours cells continued spreading (fig. 4.11 E, F), and the elongated morphology is more evident at 96 hours (fig. 4.11 H), although few live cells were observed on the membrane (fig. 4.11 G). It can be seen that MG63s behaved quite differently from MSCs on these surfaces, as the stem cells showed higher affinity to PLGA compared to tissue culture plastic and to PVA-PLGA, while MG63s seem to have a higher affinity to tissue culture plastic than to pure or blended PLGA membranes. But, most importantly, MG63s started spreading after 48 hours and appeared to be more evenly distributed on blended membranes compared to pure PLGA ones, while very few MSCs adhered in clumps to PVA-PLGA membranes maintaining a round shape even after 96 hours. The reason for the better spreading and distribution of MG63s on 5% PVA-PLGA membranes compared to MSCs might be due to the fact that MG63s have a higher affinity to hydrophilic environments and therefore they are more likely to adhere to hydrophilic materials rather than hydrophobic ones, such as PLGA. This is confirmed by recent studies that showed how osteoblastic-like cells, including MG63s, formed a homogeneous layer on super-hydrophilic materials, while grew in clumps on super-hydrophobic ones [280]. Further studies on MG63s indicated a lower proliferation and higher apoptosis of cells on hydrophobic surfaces compared to hydrophilic ones [281].

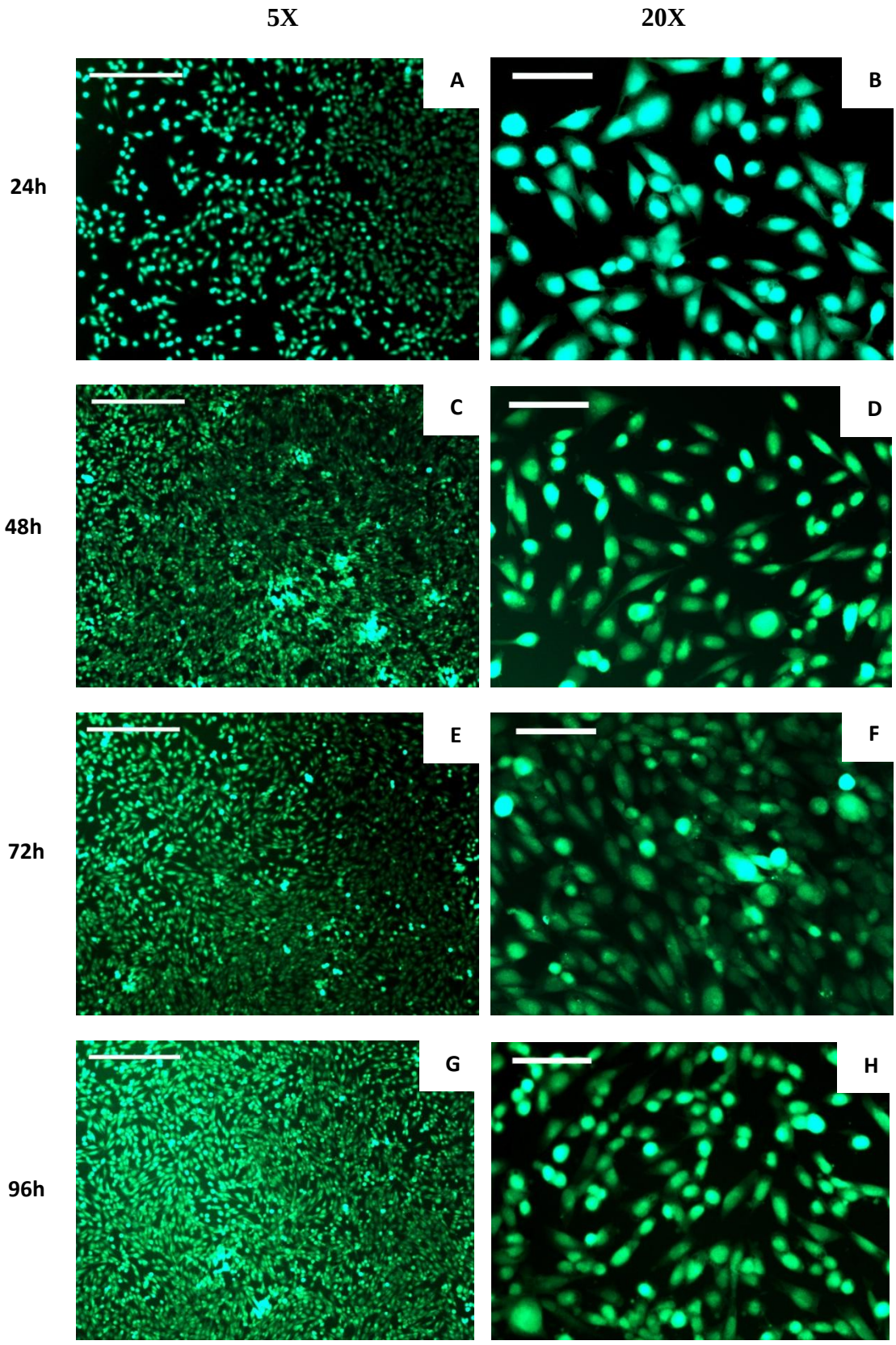

Fig. 4.9: 5X (scale bar: 500 µm) and 20X (scale bar: 100 µm) magnification of MG63 cells on tissue culture plastic at 24, 48, 72 and 96 hours after cell seeding. Cells were stained with Vybrant CFDA SE Cell Tracer kit and analysed by fluorescence microscopy.

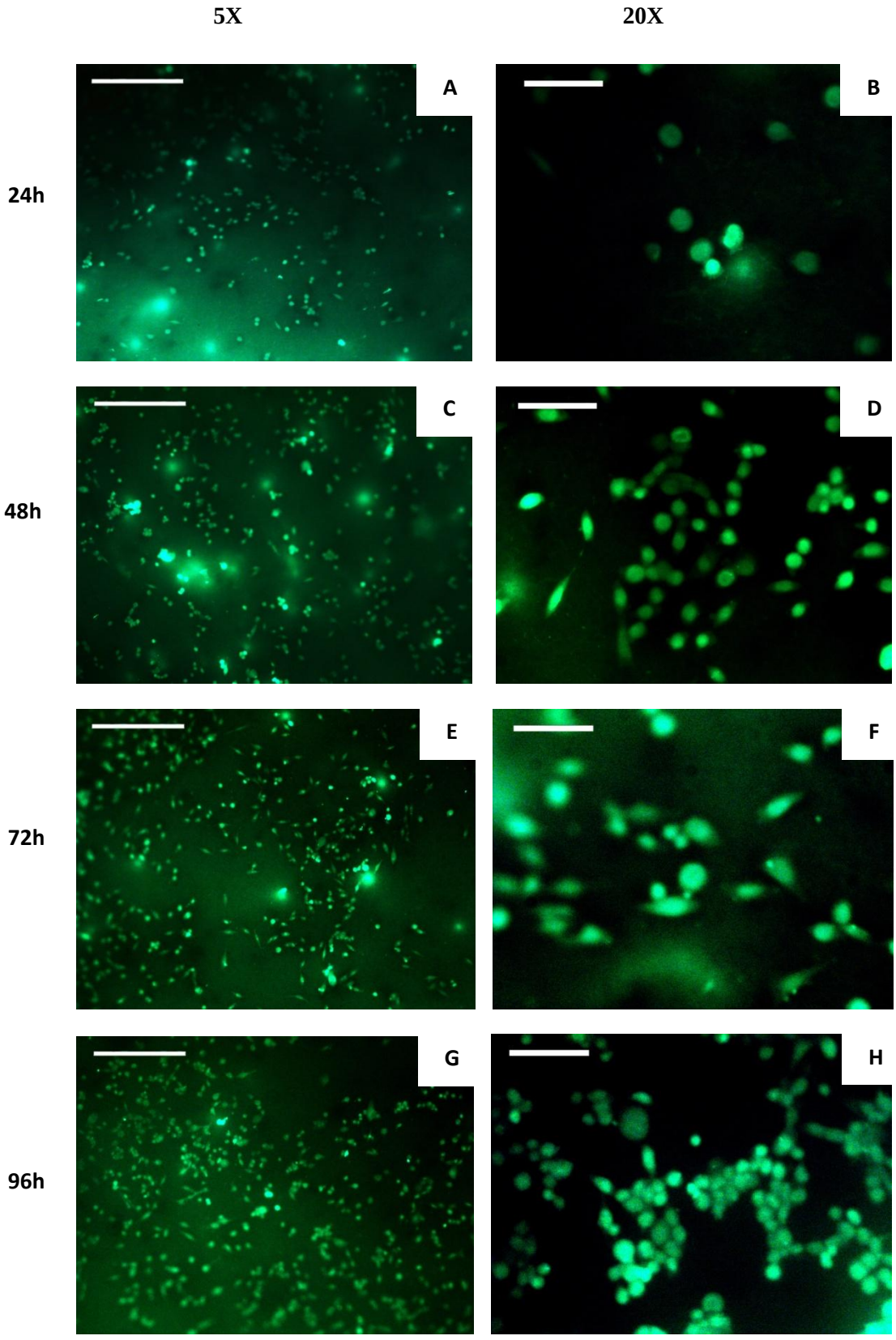

Fig. 4.10: 5X (scale bar: 500 µm) and 20X (scale bar: 100 µm) magnification of MG63 cells on PLGA flat sheets at 24, 48, 72 and 96 hours after cell seeding. Cells were stained with Vybrant CFDA SE Cell Tracer kit and analysed by fluorescence microscopy.

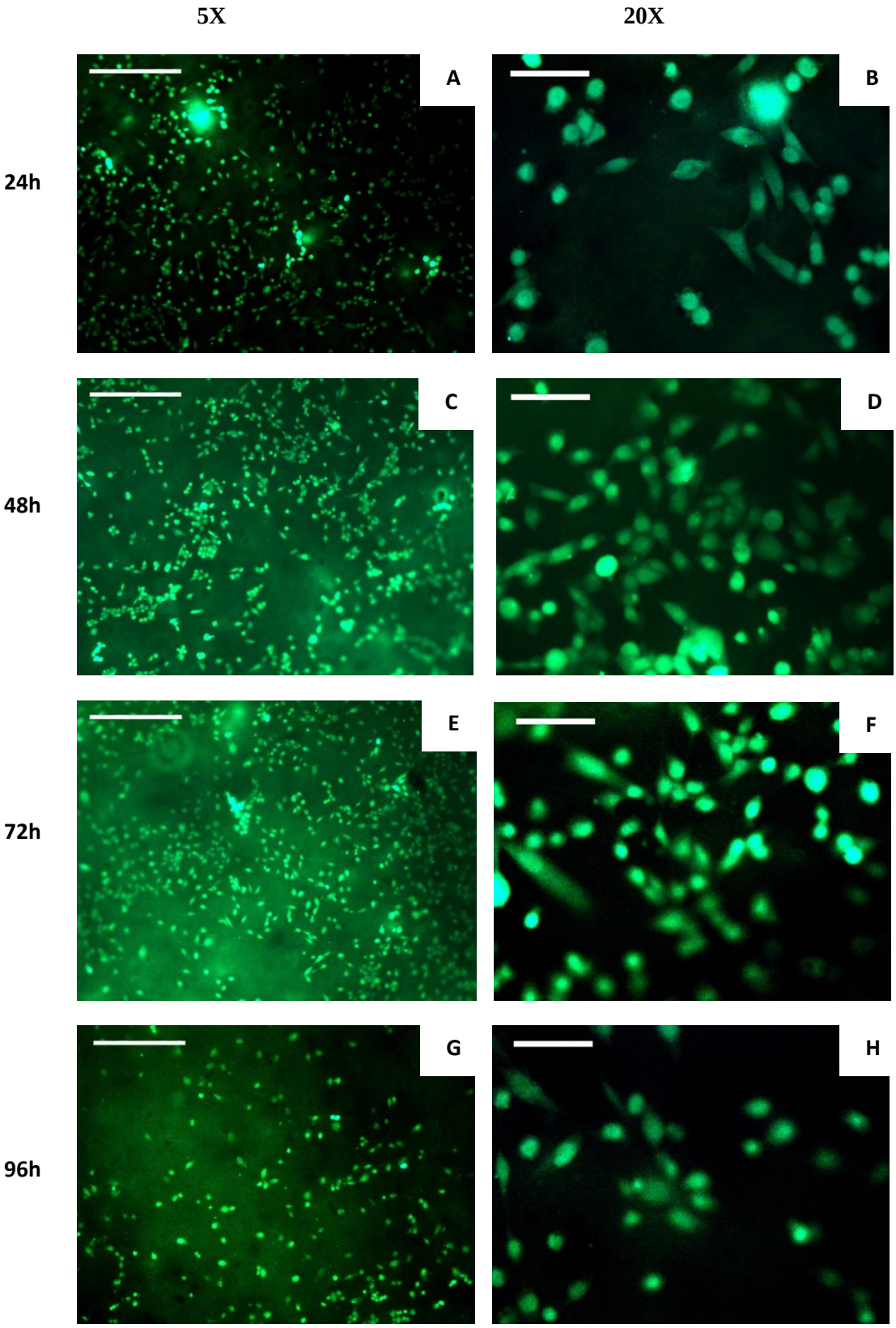

Fig. 4.11: 5X (scale bar: 500 µm) and 20X (scale bar: 100 µm) magnification of MG63 on 5% PVA-PLGA flat sheets at 24, 48, 72 and 96 hours after cell seeding. Cells were stained with Vybrant CFDA SE Cell Tracer kit and analysed by fluorescence microscopy.

4.3.2 Quantitative analysis

In fig. 4.12 the number of MG63s that have adhered and proliferated on tissue culture plastic, PLGA and 5% PVA-PLGA membranes is shown. It can be seen that after 24 hours the number of cells present in plastic wells is already three times higher (around 69,000 ± 7221 cells per well) than the seeding density (26,690 cells per well), while the number measured for both the membranes is very similar with around 42,000 cells per well. Beyond 24 hours, a continuous increase in the number of cells on plastic wells was observed, with around 300,000 ± 27146 cells per well present in tissue culture plastic after 96 hours. These results confirm the visual observation of cell adhesion, spreading and proliferation obtained by fluorescence microscopy, where MG63s seemed to have a high affinity to tissue culture plastic, appearing spread 24 hours after seeding and proliferating until confluent.

As with the qualitative analysis, the quantitative analysis shows that MG63s adhered and proliferated on both PLGA and PVA-PLGA to a minor degree. However, after 72 hours, only about 63,000 cells per well were measured on PLGA flat sheets and 57,000 ± 6108 on 5% PVA-PLGA, while the images obtained from live staining suggested a higher proliferation of cells on blended membranes than on pure PLGA membranes after this time. At 96 hours the number of cells measured on PLGA is lower than that on PVA-PLGA flat sheets, with about 80,000 cells compared to 94,000 on blended membranes, as expected from the trend of results obtained with live staining. However, the high error bar observed for the PVA-PLGA measurements suggests that there is no significant difference in cell adhesion and proliferation on pure PLGA and PVA-PLGA membranes.

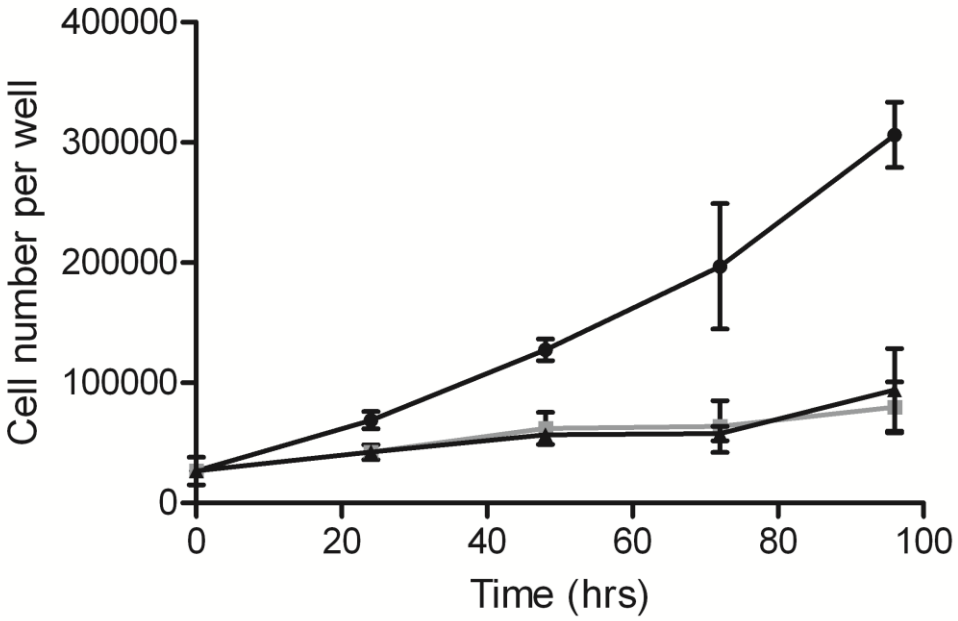

Fig. 4.12: Pico Green quantitative analysis of MG63s adhesion and proliferation on tissue culture plastic, (●), PLGA (■) and 5% PVA-PLGA (▲) flat sheet membranes. Data represent the mean ± SD (n = 3).

4.4 Conclusions

5% PVA-PLGA flat sheet membranes have been tested for cell attachment and proliferation of rat MSCs and MG63 cells in comparison to pure PLGA membranes and tissue culture plastic. The results obtained in these experiments indicate a different affinity of the two cell types to the different materials. Qualitative and quantitative analysis of rat mesenchymal stem cell attachment and proliferation indicated that MSCs adhered, spread and proliferated more on hydrophobic PLGA membranes compared to hydrophilic blended PVA-PLGA membranes and to tissue culture plastic. In contrast, MG63s adhered, spread and proliferated better on tissue culture plastic than on the two membrane types. However, although there is no significant difference between the number of MG63s that adhered to pure PLGA and to blended PVA-PLGA membranes, MG63s appeared to be more spread and more evenly distributed on the hydrophilic blended membranes than on pure PLGA ones, suggesting that MG63s might have higher affinity for hydrophilic environments.

Despite a higher mesenchymal cell affinity for PLGA compared to PVA-PLGA, PLGA is not suitable for employment in hollow fibre bioreactor devices as its hydrophobicity does not allow an appropriate mass transfer of nutrients across the membrane, which is extremely important especially for the *in vitro* reconstruction of highly metabolic organs. In contrast, PVA-PLGA hollow fibre membranes are suitable for employment in bioreactors thanks to their hydrophilic character which allows a higher wettability and therefore a higher permeability of nutrients across the membranes. Hence further strategies should be investigated in order to improve cell attachment on blended membranes, such as modifying the scaffolds with adhesive proteins or peptide ligands (e.g. RGD sequence), or blending the polymer solution with ECM adhesive proteins thus possibly obtaining a membrane which would accomplish the double function of being a good scaffold for cells and at the same time allowing the passage of molecules across the pores without adsorbing them at the material surface.

5. Human hepatocyte growth factor release by cell lines and its application in a 5% PVA-PLGA hollow fibre bioreactor

5.1 Introduction

In chapter 3 a 5% PVA-PLGA hollow fibre bioreactor was shown to allow BSA permeation across the fibre membrane without protein adsorption. In order to demonstrate the applicability of this novel system to tissue engineering, it was necessary to show that functionally relevant proteins could also permeate across the pores of the 5% PVA-PLGA hollow fibres. More specifically, the permeation of hepatocyte growth factor (HGF), an important growth factor involved in liver development and regeneration, was analysed in order to test the system for a potential application in liver tissue engineering.

5.1.1 The liver and liver tissue engineering

Liver is the largest organ of the human body and can be considered a large scale biochemical reactor, as it plays a central role in the metabolism, *i.e.*, the sum of the physical and chemical processes through which living matter is produced, maintained and destroyed, and where energy is produced for liver and all other organs [101]. At a macroscopic level it consists of two main lobes, left and right. Each lobe contains many thousands of units called hepatic lobules that are the structural and functional units of the liver. Each lobule has a central terminal hepatic venule (central vein), and at each corner of the lobule there is a portal triad which contain branches of the hepatic artery, tributaries of the hepatic portal vein and the bile collector ducts [101] [4](fig. 5.1). Incoming blood flows into the liver via the portal triads, passes across the plates of liver cells extending between the portal triads and the central vein, and leaves the liver via the central vein [4]. The intrahepatic circulation consists of sinusoids, which are small capillaries with walls lined by layers of endothelial cells that are not continuous but perforated by small holes (fenestrae) [101] and separated

from the hepatocyte compartment by a thin extracellular matrix region called the space of Disse [3].

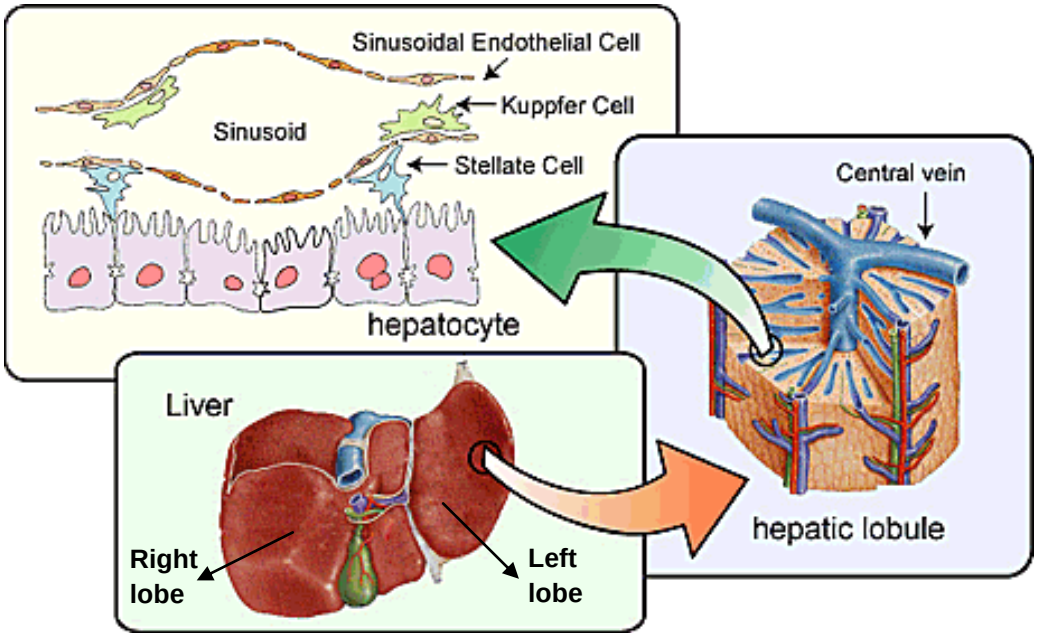

Fig. 5.1: Structure of liver and cell types that constitute it. Adapted from: [282] with permission from the author.

Five different cell types occupy nearly the 80% of the liver volume, whereas the remaining 20% is occupied by ECM components and by extracellular space, *e.g.* space of Disse. Hepatocytes represent the 65% of the liver cells and accomplish the majority of specific hepatic functions:

- Formation of glycogen
- Transformation of lipids in carbohydrates
- Removal of hormones and toxins
- Iron deposit
- Formation of red blood cells and heparin
- Drugs metabolism
- Synthesis of plasma proteins, e.g. albumin
- Synthesis of all 12 non-essential amino-acids
- Urea and bile production

By convenction liver is divided into three zones: zone 1 (periportal), zone 2 (midacinar) and zone 3 (pericentral) [4]. Hepatocytes have subsequently

morphological and functional variations according to the zone in which they are found (zonation).[3]: the smallest cells are located in zone 1 and the largest cells are located in zone 3, cell division potential is maximal periportally and negligible pericentrally and specific genes are expressed in specific zones. Therefore a precise microarchitecture allows the liver to carry out its many different functions [3]. The wall of sinusoids consists mainly of a single layer of endothelial cells, which regulate the hepatic circulation by means of synthesis and release of cytokines. Other cells of the sinusoids are pit cells, Kupffer cells and stellate cells. Pit cells are lymphoid cells attached to the luminal surface and are liver-specific natural killer cells. Kupffer cells form part of the sinusoid lining and are the hepatic macrophages as they can phagocitate bacteria and other materials present in the blood. Stellate cells reside in the space of Disse and are mainly responsible for the production and secretion of extracellular matrix proteins [283, 284].

Although the liver is an organ with an incredible regeneration capacity after acute injury (it can regenerate from as little as 25% of its tissue), when the normal regeneration process is compromised, the damaged liver is unable to perform its normal physiological roles due to irreversible and irreparable damage. This condition is called liver failure [285]. According to the British Liver Trust, liver disease is the 5th "big killer" in the UK, with more than 15,000 deaths in 2007, and a death rate increasing year by year, with a death rate doubled since 1991. There is no cure for liver failure at present, and orthotopic liver transplantation is the only clinically proven effective treatment for patients with endstage liver disease [286]. As the demand for liver transplantation increases, there is an increasing divergence between the number of patients waiting for transplantation and the number of available organs. This scarcity of donor organs results in most patients dying while waiting for a transplantation [286], therefore suggesting that liver transplantation procedures alone will probably never be able to meet the increasing demand [3]. Furthermore, liver transplantation is one of the most expensive surgical procedures, with costs increasing year by year. It is clear that alternative therapy strategies are needed and tissue engineering could provide a therapy for patients without need of liver transplantation.

One of the first aspects that need to be considered for the *in vitro* reconstruction of liver is represented by the delivery of the hepatocyte growth factor (HGF) to the

cells. Experiments conducted in the past on mice lacking of HGF proved that the hepatocyte growth factor is essential for liver development: embryos lacking of HGF presented livers severely reduced in size compared to wild type embryos, with hepatocytes abnormal in morphology, reduced in number, and with frequent signs of apoptosis [287, 288]. Similarly to liver development, HGF is among the most important growth factors involved in liver regeneration, being a strong mitogen for hepatocytes. It is present in large quantities in the matrix of liver, lungs, spleen, placenta, brain [289] and in liver is mostly produced by the stellate cells and also by endothelial cells. HGF acts by binding with high affinity to tyrosine kinase receptor c-met and activates MAP kinases, leading to the expression of regeneration genes [290]. The fact that HGF is involved in liver regeneration is confirmed by many factors: HGF levels in plasma increase after partial hepatectomy, it causes a strong mitogenic response of hepatocytes in culture, HGF injection in portal vein of normal rats and mice causes proliferation of hepatocytes and enlargement of the liver, its receptor c-met is activated after partial hepatectomy, and the knock-out of the receptor is associated with lower or no regeneration. For its important role during liver specification, HGF is widely employed to differentiate stem cells into hepatocytes [213, 291-293], and was used for the same purpose in this project.

5.1.2 Introduction to the experimental work

Fig. 5.2 represents an overview of the system employed to achieve the aim of this project: medium with liver-specific factors flows inside the lumen of the fibre, and these factors permeate across the pores of the membrane, thus reaching the stem cells on the outside of the fibre and differentiating them into hepatocytes.

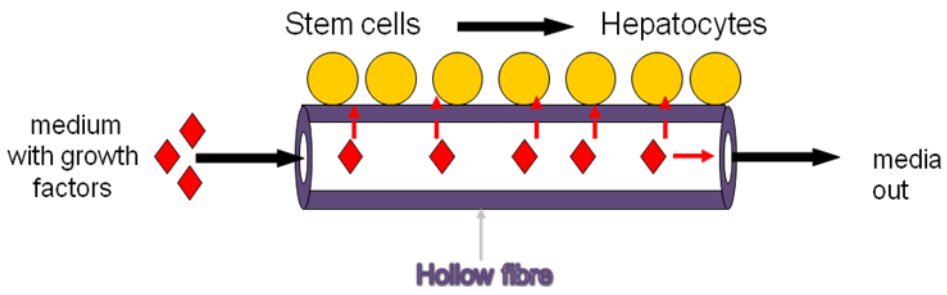

Fig. 5.2: Schematic representation of the system employed to achieve the aims of the project.

For the reasons outlined above, HGF was chosen as the liver-specific factor to be analysed for this project. However, due to the high cost of commercial HGF, an inexpensive system to generate a continuous supply of HGF was investigated.

It is known from the literature that some cell lines have the capacity to secrete HGF into the cell culture medium: the human leukaemia cell line HL60 as stated by Nishino et al [294], Matsumoto et al [240], Inaba et al [239] and the human osteosarcoma cell line MG63, as described by Taichman et al [295]. According to Inaba and colleagues, HL60 releases HGF in cell culture medium under stimulation by 12-O-tetradecanoylphorbol (TPA) and/or dibutyryl cyclic adenosine-monophosphate (dbcAMP), while Matsumoto and colleagues found that heparin induces the release of HGF from HL60s. According to Taichman, MG63 cells spontaneously secreted HGF without the need of any external stimulation. The use of a cell line secreting HGF would allow for the realization of a "cell factory" continuously "producing" the growth factor into the medium. The use of HL60s as cell factory was attractive as, being non-adherent cells, they would allow the realisation of a system consisting of a hollow fibre bioreactor where stem cells were seeded on the outer surface of the membrane and HL60s flowed inside the lumen of the fibre, continuously releasing the HGF into the culture medium. The hollow fibre membrane would therefore constitute a selective barrier which would maintain the two cell types separate, but would allow the continuous passage of HGF from the lumen of the membrane to the outer surface, where mesenchymal stem cells had been seeded.

On the basis of these findings, HL60s and MG63s were tested for their capacity to secrete the HGF in cell culture medium. HL60 cells were also analysed for their viability and metabolic activity when pumped inside the lumen of the bioreactor at two different flow rates: 2 ml/min and 4 ml/min, in order to see whether an increasing shear stress had any negative effect on the cells.

Cell-secreted HGF was then circulated inside the lumen of the 5% PVA-PLGA hollow fibre bioreactor in order to verify the permeability of the novel membrane to the protein and the stability of the growth factor in dynamic environment.

5.2 Proliferation and metabolic activity of HL60s in the single fibre hollow fibre bioreactor

Before testing the capacity of HL60s to secrete HGF when circulated within the hollow fibre bioreactor, the cells were stained with trypan blue and analysed with a MTT assay in order to see whether the shear stress caused by the flow inside the lumen of the hollow fibre might affect their viability and metabolic activity, as this could affect also their efficiency in the secretion of HGF. The single fibre hollow fibre bioreactor was therefore tested to see whether it could recreate a suitable dynamic environment for the HL60 cell line. The hollow fibre in fact would reproduce a blood vessel in the lumen of which blood cells, included HL60s, could circulate, thus reproducing an *in vitro* environment closer to that *in vivo* compared to the static tissue culture flask.

The value of Reynolds number (a dimensionless number that gives a measure of the ratio of intertial forces to viscous forces in a given flow condition, and is used to determine whether the flow will be laminar or turbulent) calculated at the flow rate of 5ml/min inside the hollow fibre is 189, which indicates that the flow inside the hollow fibre is laminar. Laminar flow actually occurs at low Reynolds numbers (< 2100), and is characterized by smooth, constant fluid motion, low flow velocity and high viscosity, while at values > 2100 the flow is turbulent, characterised by high flow velocities and low viscosities, and dominated by inertial forces, which tend to produce random eddies and vortices, which are deleterious for cell integrity. The calculation of the shear stress at the wall at a volumetric flow rate of 5 ml/min, *i.e.* a mean axial velocity of 0.165 m/s gave a value of 1.165 Pa, which is within a physiological range in blood vessels (0.1-1.2 Pa is the physiological range of shear stress experienced by vascular cells) [296-298].

Given the high cell volumes that would have been required for the experiment, flow rates higher than 5 ml/min were not considered.

Fig. 5.3 and 5.4 show the metabolic activity per cell when HL60s were pumped inside the lumen of the hollow fibre in the single fibre bioreactor for 24 and 48 hours, at flow rates of 2 ml/min and 4 ml/min. From the graphs it can be noticed that the metabolic activity per cell was between 1.1 and 1.3 times higher in the samples cultured in the bioreactors at both flow rates rather than in a static environment. This was particularly evident when cells were pumped at a flow rate of 2 ml/min for 48

hours (fig. 5.3 B), where the cells cultured inside the bioreactor showed an absorbance/cell of $9x10^{-6}$ compared to $7x10^{6}$ of controls. Also their viability in the bioreactor was excellent, with 99% of cells viable except for those kept at 4 ml/min after 48 hours, which showed a survival rate of 84%. These preliminary results suggested that the shear stress created by the flow seemed to have a positive influence on HL60s' metabolic activity and confirm the findings of McDowell and Papoutsakis, who reported 85% or higher viability of HL60s cultured in a stirred tank bioreactor and an increase in the cell line metabolic activity [299]. The results obtained with this experiment confirm that the shear stress induced by the laminar flow did not cause cell death and, on the contrary, stimulated HL60s metabolic activity compared to static culture systems.

However, in the system used for the experiment the sample of cells extracted for the analysis might not give an accurate indication of the number and proliferation of the cells, as some cells might have accumulated in some parts of the system, *e.g.* inside the connections at the inlet or outlet of the bioreactor, or those at the inlet or outlet of the reservoir. Furthermore, another aspect of the experiment that might have caused inaccuracies in the results is given by the fact that the cells, being more dense than the medium, might have settled on the bottom of the feed bottle. As a consequence the cells analysed might not be representative of all the cells inside the system, especially after 48 hour, and therefore this aspect should be improved. For example, a magnetic stirrer could be inserted in the feed bottle in order to continuously mix the cells inside the reservoir. Also, in order to obtain more accurate results on the cell density and metabolic parameters, inline probes could be used which would allow the real time monitoring of cell density and metabolic activity without the need for sampling. For example, real time sensors for oxygen, glucose or lactate could give accurate online values for the metabolism of cells, while laser turbidity probes, light based probes or radio-frequency impedance probes would allow the real time measurement of cell density over time.

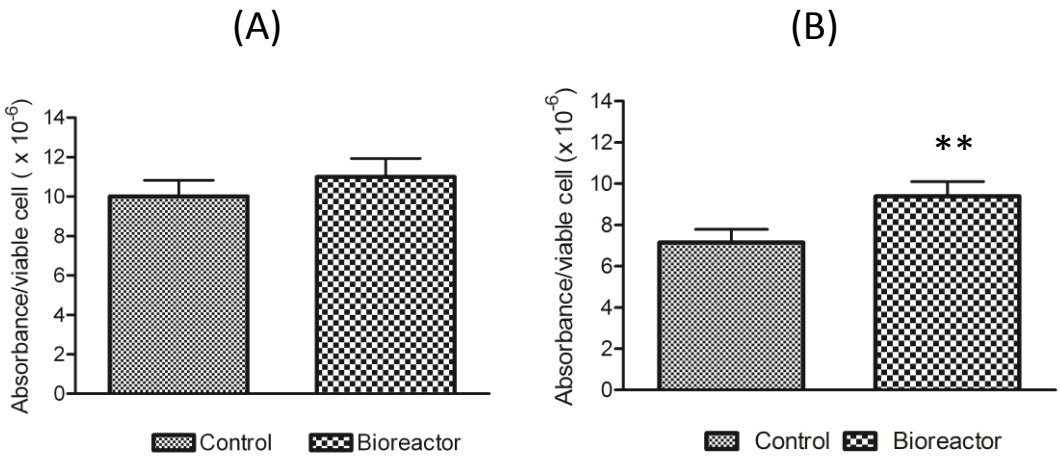

Fig. 5.3: Metabolic activity per cell shown as function of absorbance in the MTT assay for HL60 cells pumped into the hollow fibre for 24 (A) and 48 hours (B) at a flow rate of 2 ml/min (bioreactor), compared to cells grown in static flasks (control). Data represent the mean ± SD (n= 4). ** $P < 0.01$.

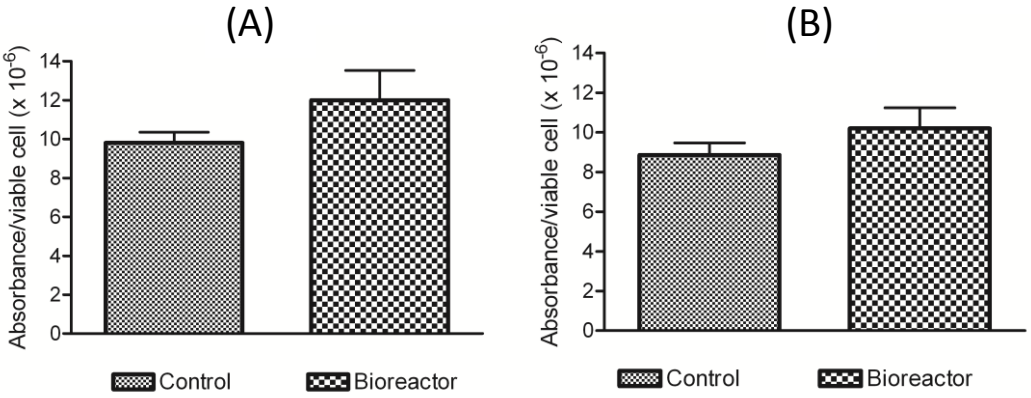

Fig. 5.4: Metabolic activity per cell shown as function of absorbance in the MTT assay for HL60 cells pumped into the hollow fibre for 24 (A) and 48 hours (B) at a flow rate of 4 ml/min, compared to cells grown in static flasks (control). Data represent the mean ± SD (n= 4).

In addition to the shear stress caused by the flow of cells inside the hollow fibre, the shear stress caused by the pulsatile flow of the peristaltic pump should be considered when checking the integrity, viability and metabolic activity of HL60 cells circulated inside the hollow fibre bioreactor. Peristaltic pumps produce alternatively high and low fluid flow rates, and this might be negatively affecting the viability of cells. However, the pulsatile nature of blood flow through the vascular network generates wall shear stress and therefore the peristaltic pump is a valid tool to simulate the fluid shear stress found *in vivo*, provided that the shear stress generated is within

physiological range [300]. Therefore the peristaltic pump used in this project was a useful tool for the circulation of human leukaemia cells (HL60s) inside the hollow fibre membrane, thus simulating circulation occurring *in vivo*.

5.3 Secretion of HGF by the HL60 cell line

Following the confirmation of the suitability of the single fibre bioreactor for HL60 culture, the cell line was tested to verify the release of HGF when stimulated with some specific inducers, more specifically TPA, cAMP and heparin as described by Nishino et al [294], Matsumoto *et al* [240], Inaba *et al* [239]. They reported about 16 ng/ml of HGF secreted in the medium, and 20 ng/ml are needed for the differentiation of MSCs into hepatocytes, according to the protocol of Snykers *et al* [213]. A two-fold concentrator could be used in order to obtain the concentration of HGF required for the differentiation of stem cells. Since TPA was prepared in DMSO, cells were also treated with DMSO to check whether the compound had any effect on the release of HGF. The concentration of HGF secreted in the cell culture medium was measured by ELISA.

As can be seen in fig. 5.5, in contrast with the findings in the literature, neither inducers alone nor the combination of them gave a significant amount of HGF released in medium. However, there are differences between the different treatments, with TPA being the most effective inducer of HGF release with 0.227± 0.59 ng/ml, followed by DMSO with 0.078± 0.2 ng/ml. In addition, the HGF levels found in cell culture medium after stimulation of HL60s with TPA or with dbcAMP were significantly lower than those reported by Inaba and colleagues. They detected about 16 ng/ml of HGF when HL60s were stimulated by TPA alone and 7 ng/ml when stimulated with dbcAMP. In contrast, our results were 0.227± 0.059 ng/ml for stimulation with TPA and 0.036± 0.65 ng/ml for stimulation with dbcAMP, using the same conditions reported in the work by Inaba et al. Following correspondence with the author of the paper, we had confirmation that no other group could reproduce the secretion of HGF by HL60s published in that paper, a reply which led us to reflect about the reliability of those experiments.

Heparin appeared not to have any effect on stimulation of HGF secretion, but, on the contrary it seemed to inhibit the release of the protein, since the levels of HGF detected after treatment of the cells with heparin were null, lower than controls in contrast with the findings of Matsumoto et al, who reported 15.9 ng/ml of HGF secreted by HL60s when stimulated by 1 μg/ml of heparin. Furthermore, no HGF was detected when heparin was combined to TPA and dbcAMP, suggesting that heparin had an inhibitory effect on the release of HGF from HL60s. It is worthy of note that the size of the error bars in this experiment are significantly higher than the average values of concentrations detected. This is an indication that the ELISA kit used for the measurement of HGF concentration is not sufficiently sensitive at such lower protein concentrations.

It can be concluded that the treatment of HL60s with dbcAMP, TPA, heparin or the combination of the three of them did not lead to HGF secretion by HL60s. After investigating whether another suspension culture secreting HGF was reported in the literature, no other suspension cell line was found. The initial plan of realising a co-culture system which consisted of a suspension cell line which circulated inside the lumen of the hollow fibre and continuously secreted HGF for the differentiation of the adherent stem cells, was therefore abandoned.

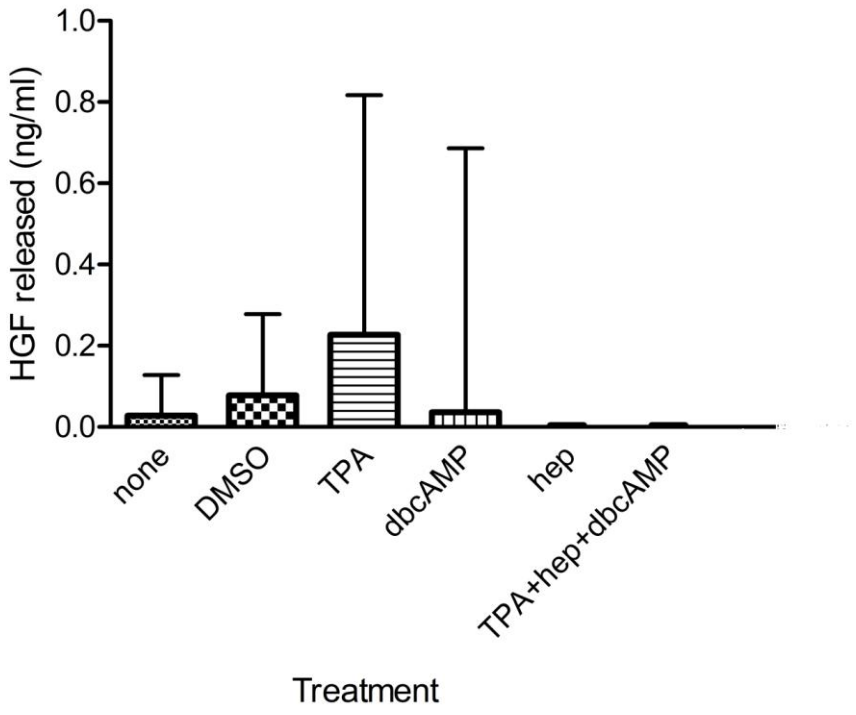

Fig. 5.5: HGF released by HL60s when stimulated by DMSO, TPA, dbcAMP, heparin and a combination of TPA, heparin and dbcAMP. Data represent the mean ± SD (n= 4). The concentration of HGF released by HL60 cells was measured by ELISA.

5.4 Secretion of HGF by the MG63 human osteosarcoma cell line

Given the lack of secretion of HGF from HL60s, another cell line capable of releasing HGF in cell culture medium was investigated. It has been reported that the human osteosarcoma cell line MG63 is able to spontaneously secrete HGF into cell culture medium without any external stimulation [295]. Therefore MG63s were seeded at a concentration of 10,000 cells/ml and incubated for three days at 37º C in order to check whether they were capable of releasing HGF into the cell culture medium.

In this project 8.3 ng/ml of HGF released in the supernatant were measured by ELISA after culturing the cells for three days at a density of 10,000 cells/ml, confirming the data shown in the work of Taichman and colleagues, that reported 15.5 ng/ml of HGF secreted following a twofold concentration of the culture medium. This result is promising, as MG63s could be used a cell factory for HGF

production without the need of expensive commercial HGF. In order to achieve the maximum level of HGF secreted into cell culture media, MG63s were seeded at different densities to see whether the HGF released was increased at increasing cell densities. From fig. 5.6 it can be observed that the concentration of HGF increased at increasing cell density, but at densities higher than 100,000 cells/ml it plateaued. This might be explained by the loss of metabolic activity of the cells at such high seeding densities due to the higher uptake of nutrients by the increased number of cells, and the less metabolically active cells probably secreted lower levels of HGF. Therefore from this graph it can be understood that cell densities between 75,000 and 100,000 cells/ml gave the highest possible concentration of HGF released. MG63 cells, thanks to their ability to secrete HGF at the concentration required for the differentiation of stem cells into hepatocytes, were chosen as the "HGF factory cells" instead of HL60s. It is worth of note that another advantage in using MG63 cells instead of HL60s is given by the fact that MG63s do not require any stimulation with an external chemical compound to release HGF, such as TPA, dbcAMP or heparin in the case of HL60s, but on the contrary they release it spontaneously.

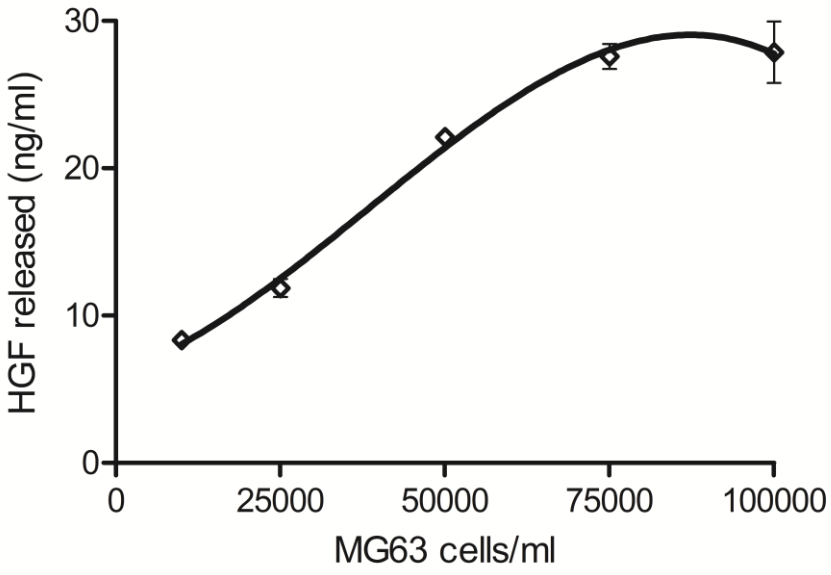

Fig. 5.6: HGF released by MG63s cells seeded at different concentrations after three days from seeding. Data represent the mean ± standard deviation (n= 4) and were fitted with non-linear regression (polynomial of third order) using GraphPad Prism software.

5.5 Comparison of commercial and cell-released HGF behaviour in static and dynamic environment

Mechanical forces generated by the fluid flow inside the bioreactor, *i.e.* shear stress, can cause protein denaturation which would lead to loss of product in the system [301]. Therefore commercial HGF and HGF released by MG63 cells were both tested in static condition or circulated for three hours to analyse whether there was any difference between the natural and commercial growth factor and whether the dynamic forces caused by the flow might affect the stability and integrity of the protein. The concentration of biologically active HGF was then determined by ELISA as described in section 2.9.3 and expressed as a percentage of the initial concentration.

In fig. 5.7 A, the concentration of commercial HGF in static conditions can be observed. The concentration of HGF remained roughly 100% (allowing for experimental error) for the first two hours and then decreased slightly to 93%. This slight decrease in concentration might be due either to degradation of the protein over time, or more likely, to experimental error as, for example, in some previous time points the concentrations measured were slightly higher than the initial 2 ng/ml. One explanation for the decrease in concentration could be that many globular proteins are not very stable in aqueous solutions and are easily subjected to denaturation, which can lead to protein aggregation and thereby loss of product [301]. An experiment considering a longer time span would be useful in order to understand whether the protein started degrading after two hours. In fig. 5.7 B the concentration of commercial HGF circulated continuously for three hours was measured. In contrast to static environment, the concentration of HGF dropped down exponentially with time and after only three hours its concentration was reduced to 35.65% from that at time zero. This might be due to a combination of factors: there might be spontaneous degradation of the protein over time, or the growth factor might have bound to the tubing, which could explain the continuous drop of concentration with the continuous recycling of the solution. However, the most probable cause that might have affected the stability of the protein is represented by the shear forces caused by the flow. It is known that shear stress can have negative effects on protein stability, as proteins exposed to flow might undergo irreversible unfolding [302]

which can result in protein aggregation and loss of product [303-306]. This result indicates that the HGF might be very sensitive to shear stress even at physiological values; 0.1-1.2 Pa is the physiological range of shear stress experienced by vascular cells while 1.5 Pa can be considered the threeshold value for physiological shear stress because arteries exposed to chronic increased blood flow change their diameter to maintain the mean shear stress magnitude at approximately 1.5–2.0 Pa [296-298]. This might explain the rapid loss of 65% of protein in only 3 hours. These results indicate that the commercial HGF purchased from R&D for the project is not suitable for use in dynamic environments, like in bioreactors, and therefore not suitable to be used for this project.

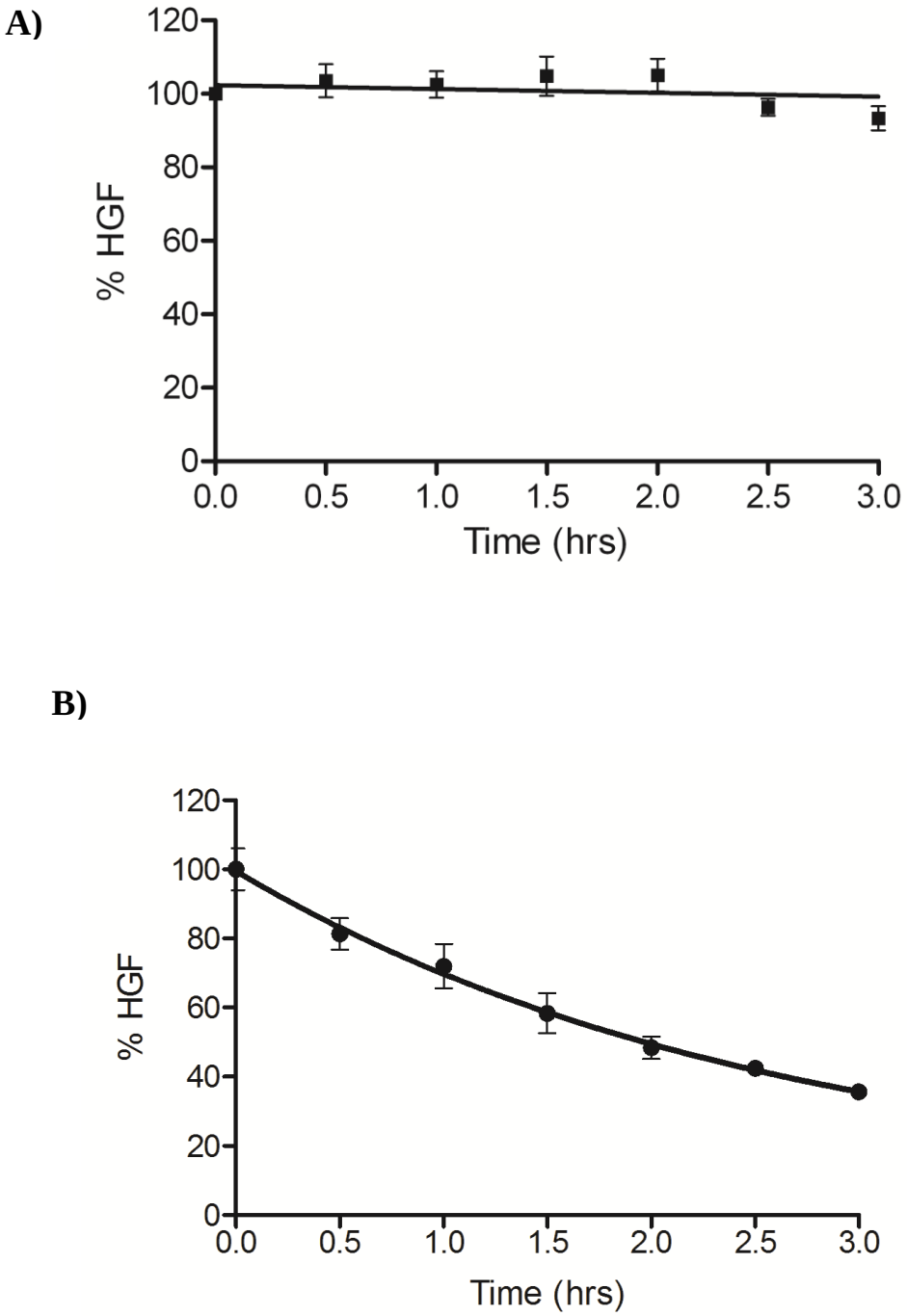

Fig. 5.7: Concentration of commercial HGF (expressed as % of the initial concentration of HGF: 2 ng/ml) over time in static conditions (A) and when circulated continuously inside plastic tubings at a rate of 2.5 ml/min (B). Data represent the mean ± SD of three samples (n=3). Data in graph A were fitted with linear regression, and data in graph B were fitted with non-linear regression (one phase exponential decay) using GraphPad Prism software.

When the same experiment was performed with HGF released by MG63 cells, the result was surprisingly different (fig. 5.8). In fact, under static conditions, the concentration of the protein remained stable for the whole three hours with very few variations among the different samples (indicated by the small error bars) (fig. 5.8 A), and, in contrast to the commercial HGF, it remained stable even in dynamic conditions, with no loss of active protein after three hours (fig. 5.8 B). An explanation for the different behaviour between the native and commercial protein could be that human HGF purchased from R&D is a recombinant protein generated by alternative splicing in *spodoptera frugiperda* by baculovirus infection and lacks some domains of the native protein. In fact it consists of a 60 kDa α and of a 30 kDa β chain, while the native HGF has a 69 kDa α and a 34 kDa β chain. Therefore the commercial protein might be unstable compared to the native HGF secreted by MG63s because some post-translational modifications normally occurring in eukaryotes after native protein synthesis might not have occurred in the recombinant protein. In fact, the use of insect cells as an expression system, although has been shown to express higher protein levels and to be safer compared to mammalian cell systems, presents some disadvantages, *e.g.* the inability of properly processing proteins that are initially synthesised as larger inactive precursor proteins (*e.g.* hormones, growth factors, metalloproteases) [301]. When considering the proteolytic cleavage of different protein precursors, it has been found that although mammalian secretion signals are accurately processed in insect cells, other proteolytic cleavage sites are insufficiently or not at all recognised in insect cell cultures [307]. More specifically, the pro-HGF was cleaved non specifically when produced by *Sf-9* cells [308]. Furthermore, although the N-linked glycosylation sites are the same in mammalian and insect cells, insect cells are not capable of processing the mature oligosaccharides to the forms found in mammalian cells [307, 309, 310]. Finally, the commercial protein during purification is deprived of its natural environment such as stabilizing lipids, lipoproteins and/or proteins, and that might also affect its stability [301]. All these reasons might explain the instability and rapid degradation of commercial HGF when exposed to fluid flow. This result is very important, as HGF secreted by MG63, thanks to its stability in a dynamic environment, could be used in a bioreactor system and, given the high proliferation rate of MG63 cells, large amount of the protein could be continuously available for the stem cells in the

bioreactor in order to differentiate them into hepatocytes or, subsequently, to maintain their state differentiated.

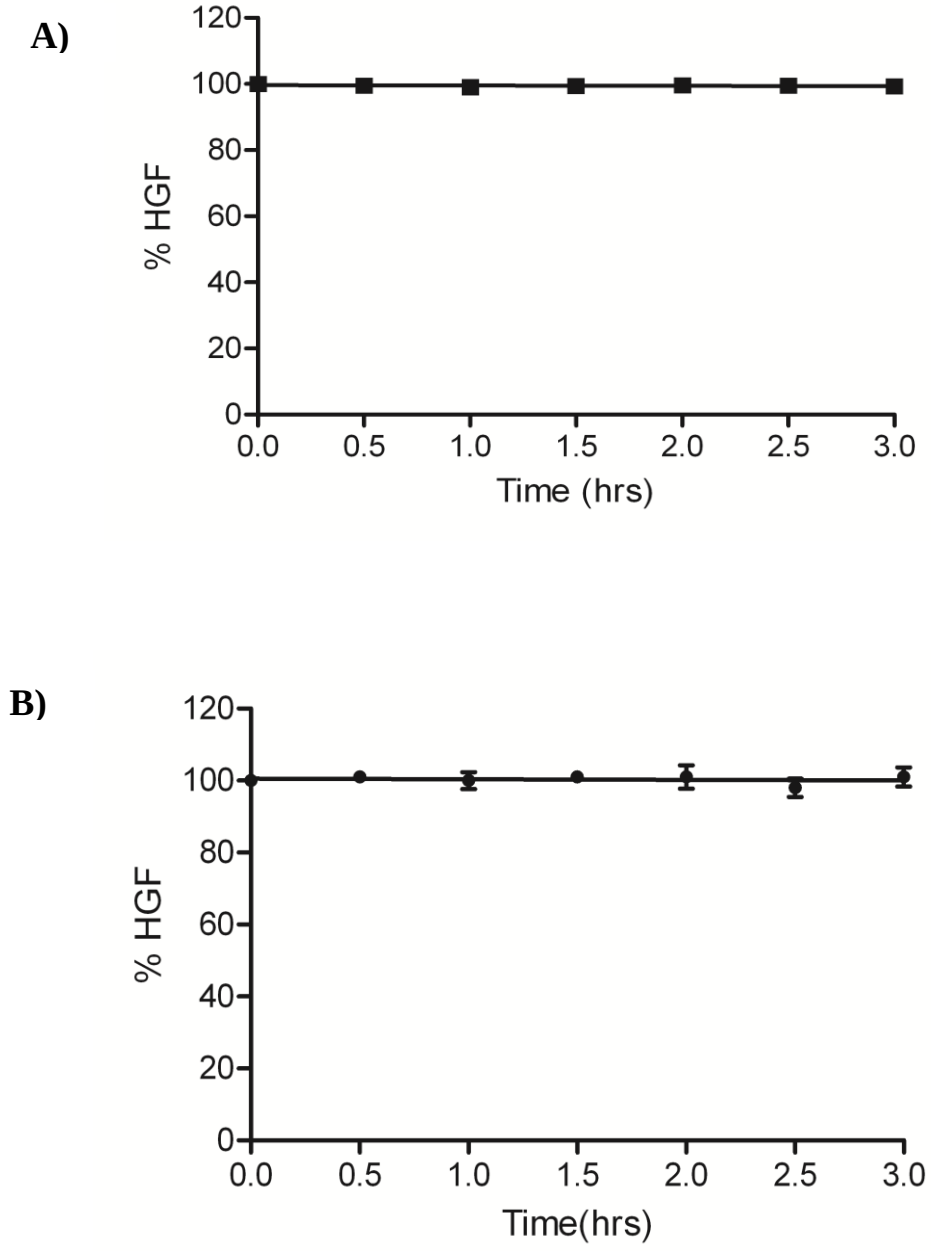

Fig. 5.8: Concentration of HGF secreted by MG63s (expressed as % of the initial concentration of HGF: 2.5 ng/ml) over time in static conditions (A) and when circulated continuously inside plastic tubings at a rate of 2 ml/min (B). Data represent the mean ± SD of three samples (n= 3). Data were fitted with linear regression, using GraphPad Prism software.

5.6 Permeation of HGF secreted by MG63 across 5% PVA-PLGA blended hollow fibres

Mass transfer is one of the fundamental parameters to be considered in tissue and organ engineering strategies. Without an appropriate transfer of nutrients to the cells the *in vitro* tissue/organ reconstruction would fail. Therefore a membrane that allows an appropriate transfer of nutrients to the cells must be employed. In Section 3.2.5 it was shown that 5% PVA-PLGA hollow fibre membranes, thanks to their increased hydrophilicity, allowed a higher hydraulic and BSA permeability with no protein adsorption, when inserted in a single fibre hollow fibre bioreactor. However, several proteins should be analysed in order to prove that the 5% PVA-PLGA hollow fibre bioreactor is a suitable system for organ/tissue engineering. Among these, HGF (80 kDa compared to 66 kDa for BSA) is the first candidate that needs to be tested in this project since it must be continuously available to mesenchymal stem cells in order to differentiate them into hepatocytes and to maintain their state differentiated. Therefore HGF must not only be stable when exposed to the flow generated by the pump, but must also permeate through the pores of the membrane without being absorbed. HGF was therefore circulated inside the lumen of the hollow fibre within the single fibre bioreactor system and the permeability of PVA-PLGA blended membranes to the growth factor was tested. Given the rapid loss of protein during circulation, it was impossible to detect a reasonable amount of commercial HGF after permeation through the hollow fibre membrane. Therefore, only the data obtained from the permeation of HGF released by MG63 are shown.

Fig. 5.9 A- C represent the concentration of HGF from MG63 (expressed as a w/v % of the initial concentration of HGF) in the feed, permeate and retentate respectively, when 8 ng/ml of HGF were circulated for 3 hours through a hollow fibre bioreactor with a 5% PVA-PLGA hollow fibre membrane. From fig. 5.9 A it can be seen that the concentration of HGF in the feed solution was stable over time, as expected, and variations from 100% were only due to experimental error. In fig. 5.9 B it can be observed that the concentration of HGF in the permeate decreased in the first hour and then remained stable for another hour and started decreasing again in the third hour. This decrease in concentration could be caused by several different reasons: denaturation of the protein while permeating through the pores of the fibre, partial

rejection of the protein from the pores or fouling, which can be caused either by internal deposition of protein molecules, by blocking of pores by protein aggregates, or by formation of protein deposits on the membrane surface (concentration polarisation) [253]. From fig. 5.9 C it can be seen that the concentration of the retentate did not remain stable over time but decreased after two hours. Therefore in the first hour, a decrease in the concentration in the permeate, but not in the retentate was observed, which suggests that fouling might have occurred. However, in the third hour a decrease both in permeate and in retentate occurred, which might suggest that HGF underwent denaturation/degradation. However, despite a decrease in HGF concentration in the permeate, 81% of the initial concentration was still present after three hours, which is a promising result for an application of the MG63-secreted HGF to bioreactor technology, as this native HGF not only appeared to be stable in a dynamic environment and not sensitive to shear forces caused by the flow, but also could permeate across the pores of the 5% PVA-PLGA hollow fibre membranes without significant loss of protein in the first three hours. Further studies should be performed in order to understand the mechanism of fouling occurring in the first hour of permeation, and to investigate which is the cause that has led to a further decrease in concentration during the third hour of experiment.

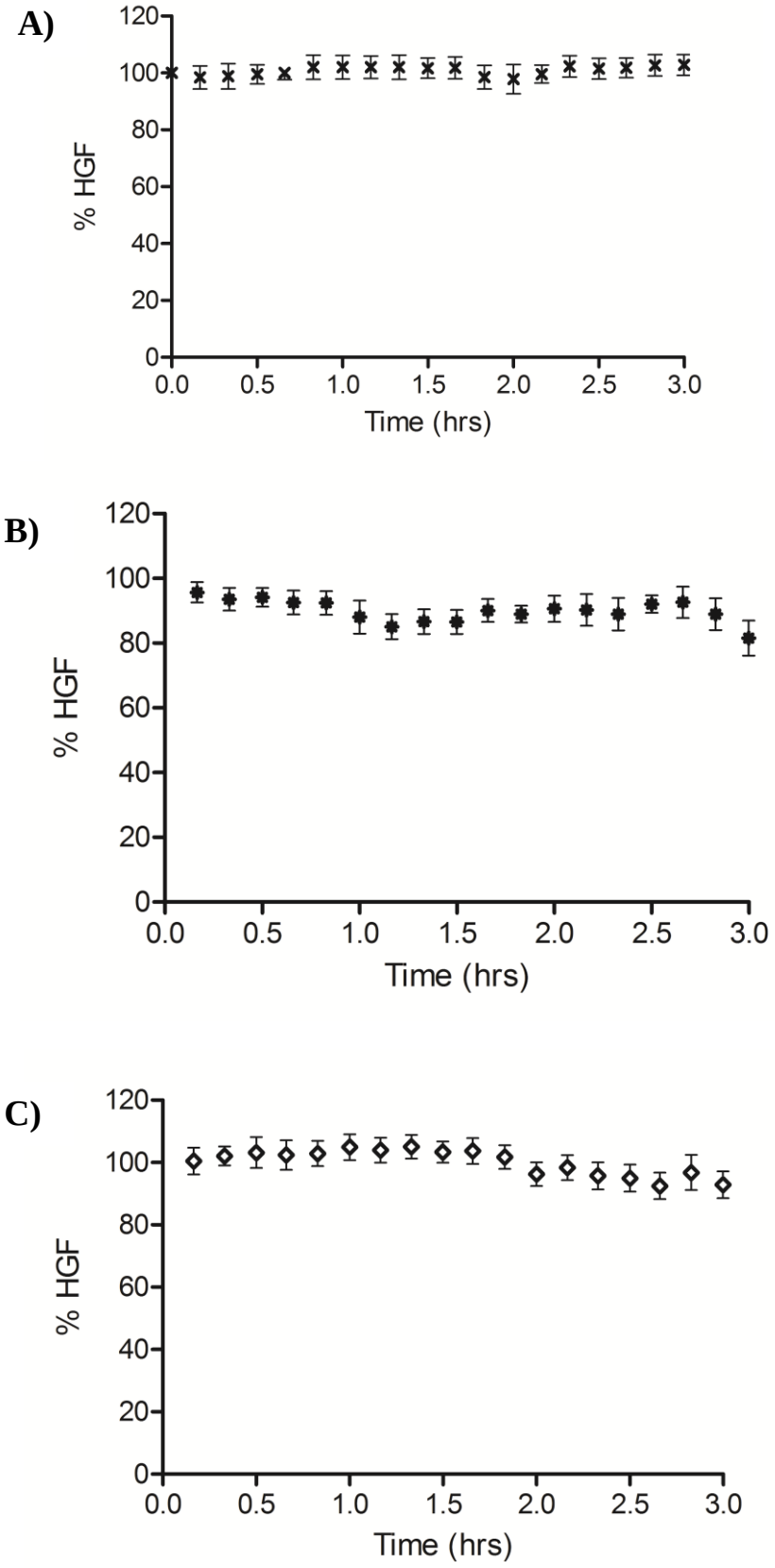

Fig. 5.9: Concentration of HGF (expressed as a % of the initial concentration [8 ng/ml] of HGF in the feed solution at time 0) in the feed solution (A), permeate (B) and retentate (C) solutions over 3 hours circulation at a flow rate of 2.5 ml/min. Data represent the mean ± SD of three samples (n= 3).

5.7 Conclusions

The initial aim of this project was to realise a co-culture system consisting of a suspension cell line which circulated inside the lumen of the hollow fibre and continuously secreted HGF for the differentiation of the stem cells seeded on the outer surface of the membrane. Among cell lines secreting HGF, HL60 cells were chosen in first place for their characteristic of growing in suspension, which was appropriate for achieving the realisation of the system.

The single fibre hollow fibre bioreactor has been shown to be suitable for the culture of the HL60 cell line since the shear stress induced by the laminar flow did not affect cell viability and, on the contrary, stimulated HL60 metabolic activity compared to static culture systems. However, treatment of HL60s with dbcAMP, TPA, heparin or the combination of the three of them did not lead to HGF secretion, so this cell line was abandoned. Another cell line, adherent MG63 cells, thanks to their ability to spontaneously secrete HGF with no need of any external stimulation, and at a concentration required for the differentiation of stem cells into hepatocytes, were chosen as the "HGF factory cells" instead of HL60s.

MG63-derived HGF, has been shown to be stable in a dynamic environment, as opposed to commercial HGF which degraded rapidly when exposed to the flow of the bioreactor. Furthermore, it permeated across the pores of the 5% PVA-PLGA hollow fibre membranes without significant loss of protein in the first three hours. Therefore, MG63-secreted HGF appears to be suitable for use in a bioreactor system and in particular, in the system employed in this project to differentiate stem cells into hepatocytes. In particular, when considering the fact that stem cells need to be exposed to the growth factors for several days or weeks in order to differentiate, a system where MG63 cells, thanks to their high proliferation rate, can continuously release large amounts of the protein would be very advantageous over traditional systems that employ commercial HGF. In this novel system, not only would HGF be continuously available for the stem cells, thus allowing higher differentiation efficiency and the maintenance of their differentiated state, but also the cost of the process would be greatly reduced: this system would allow in fact for the cost-free production of a protein for the whole time required for the differentiation, thus

circumventing the high costs associated with the prolonged treatment of cells with commercial HGF. Finally, it is worth noting that this system where MG63 cell line secretes HGF is only one example of a system that could be used for the production of many other growth factors: if a cell line is found to secrete the protein of interest, it could be used as a cell factory producing the protein for the differentiation of stem cells in lineages other than liver, thus making this system suitable for regeneration of many different tissues.

6 Differentiation of stem cells towards the hepatic lineage with MG63-secreted HGF

6.1 Cell sources for liver regeneration

Table 6.1 gives a summary of the characteristics of various cell sources available for liver regeneration. At present it is clear that the ideal hepatic cell for liver regeneration is still not available, although progress has been made in understanding liver cell proliferation and differentiation [311]. As a consequence of a lack of donor organs for liver transplantation, the supply of primary human hepatocytes (which would be the ideal hepatocellular source) is limited. On the contrary, there is an unlimited availability of primary mammalian hepatocytes, especially porcine hepatocytes. However, porcine xenografts elicit a severe humoral and cellular immunologic response in humans [312, 313]. Another possible risk is the transmission of viral pathogens from the xenograft donor to the recipient [7, 314]. In addition to these risks, it must be taken into consideration that the proteins released by porcine hepatocytes do not carry out the same functions of human hepatocytes, and that, irrespectively of their source, primary hepatocytes are difficult to maintain in culture as they rapidly lose their differentiated function in vitro [7].

Due to their potential for unlimited expansion, several human hepatocyte cell lines such as HepG2 (human hepatoblastoma) [315], the HepG2 derived C3A [316], HepLiu (SV40 immortalised) [317], and immortalised human fetal human hepatocytes [318] have been developed via different systems, *e.g.* via spontaneous transformation [319] or via retroviral transfection of SV40 large-T antigen gene [320] as alternative to human primary hepatocytes. However, it has been shown that these cell lines tend to lose critical functions, *e.g.* drug and ammonia metabolism, in vitro, compared to primary hepatocytes [7, 321]. Furthermore, a risk correlated with the use of immortalized cell lines is the potential risk of transmission of tumorigenic products from the bioartificial liver system into the patient's circulation [286].

Therefore, alternative cell sources for liver cell-based therapies have been investigated. Among them, stem cells are receiving a considerable interest from researchers for liver regeneration strategies, thanks to their differentiation capacity and to their self-renewal capacity, which would allow for the production of a large amount of cells, in contrast to the scarce availability of hepatocytes. Human embryonic stem cells might be an attractive source for human hepatocytes because of their indefinite proliferation *in vitro* and their capacity to differentiate into almost all cell types. Embryonic stem cells have been shown to differentiate into functional hepatocytes upon stimulation with FGF-4 and HGF [291] and to improve liver function in mice when employed in bioartificial liver assist devices [322] However, the differentiation efficiency was found to be rather low [323]; furthermore, the transplantation of these cells into the patient presents safety issues related to their potential of forming tumours and to their immunogenicity in allogenic setting. Finally, the ethical concerns surrounding the use of embryonic stem cells make difficult at present a possible clinical application. New immunocompatible pluripotent cells like induced pluripotent stem cells (iPSCs) could be an alternative to ethical problems associated with the use of human embryos, but long-term studies must still be carried out in order to fully characterise them and eliminate any potential safety concern about their use [324].

Adult stem cells are at present a valid alternative to embryonic stem cells as they do not imply the destruction of a human embryo and they are not tumorigenic and not immunogenic. Nevertheless, the existence of adult liver stem cells is still debated, although there is evidence of the presence of such stem/progenitor cells in adult liver [325-327].

Tissues other than liver are also being considered as they contain adult stem cells which were found to have the capacity to differentiate into hepatocytes. In the past, the developmental paradigm was that adult stem cells were, in contrast to embryonic ones, committed to a specific cell fate. At present, new discoveries on stem cell plasticity have challenged the canonical developmental hierarchy [40]. Hematopoietic stem cells, for example, are adult stem cells found in the bone marrow which give raise mainly to blood cells, but they also can contribute to completely different tissues such as liver [45]. There is also evidence that human foetal pancreas cells can differentiate into hepatocytes when treated with FGF-2 and dexamethasone

[328]. Mesenchymal stem cells are another population of adult stem cells abundant in the bone marrow and adipose tissue, that can differentiate into bone, cartilage and adipose cells, but have also been found to differentiate into hepatocytes under specific induction with cytokines or growth factors [213, 241, 292, 293] or when co-cultured with foetal liver cells [183]. More recent protocols of differentiation of mesenchymal stem cells into the hepatic lineage with growth factors try to mimic nature and the cells are exposed to liver specific factors in time sequence that resembles that occurring during liver development. Snykers *et al*. for example, reported that mesenchymal stem cells differentiated toward the hepatic lineage with a higher efficiency when cells were exposed to liver-specific factors in a time-sequence that mimicked the *in vivo* liver embryogenesis (FGF-4 to induce endoderm, followed by HGF, insulin-transferrin-selenium, dexamethason and trichostatin A to induce liver specification), compared to those treated with a "cocktail" of the all factors at the same time-points [213, 241]. Mesenchymal stem cells therefore seem to be an attractive stem cell type to be used for liver tissue engineering, and for their potential clinical applications, and for these reasons they were employed in the present work.

However, although stem cells have a great potential for liver regeneration strategies, many challenges remain. In fact, although hepatocytes are the only cell type secreting albumin, it should be demonstrated that the stem cell derived hepatocyte expresses also the other hepatocyte-specific genes and also that their expression levels are comparable to those of primary hepatocytes [329]. Other challenges include the ability of triggering and enhancing differentiation and also the stabilisation of the hepatocytes functions [3]. A qualitative as well as quantitative analysis of hepatocyte marker expression is then needed in order to prove the effective differentiation of stem cells into functional hepatocytes.

Table 6.1: Characteristics of various cell sources available for liver regeneration. From [330]

Cell source	Supply	Liver-specific function	Host compatibility	Other risks to patients
Primary Human Hepatocytes	Scarce	Generally unstable	Excellent	Small
Stem-cell derived human hepatocytes	Unlimited	Low efficiency of differentiation to hepatocytes	Excellent	Small
Immortalised human hepatocytes	Unlimited	Function poorly characterised	Excellent	Transmission of tumorigenic products
Human hepatoma cell line	Unlimited	Reduced level compared to primary cells	Excellent	Transmission of tumorigenic products
Primary xenogenic (porcine) hepatocytes	Unlimited	Can express high levels but generally decreases over time	Metabolic mismatch, potential severe immune complications	Transmission of zoonoses

6.2 Introduction to the experimental work

In this project, rat mesenchymal stem cells were chosen as the cell source for liver regeneration. The many advantages in the use of mesenchymal stem cells include their plasticity (*i.e.* their ability to differentiate into lineages other than their tissue of origin), their non-tumourigenicity and non-immunogenicity, and also their ethical approval. The strategy used to differentiate MSCs consisted in exposing the cells to a sequence of liver-specific growth factors that mimic that occurring during liver development. This strategy, if combined to the culture of cells within the hollow fibre bioreactor, was supposed to mimic more closely nature, thus possibly leading to an improvement of the efficiency of differentiation.
Before describing the experimental work, it is worth mentioning that the system used for the differentiation of mesenchymal stem cells assumes that the cells are 100% confluent, and, when they will be seeded on the outer surface of hollow fibre membranes, they will evenly adhere to the membrane which presents pores of 1.1 μm average size and an overall porosity of 0.77.

Once verified by flow cytometry the identity of mesenchymal stem cells, the culture was treated with a sequential exposure of liver-specific factors that mimicked the *in vivo* liver embryogenesis, as shown by Snykers *et al* [213]. Although the protocol from Snykers *et al* was followed with regard to which specific liver factors were added to the cell culture and the time sequence in which they were provided to the cells, the novelty of this experiment consists of the use of HGF released by a cell line instead of commercial HGF. MSC differentiation into the hepatic lineage was analysed either by tracking the morphological changes occurring in cell cultures every three days, and by immunofluorescence to see whether the cells expressed three specific hepatic markers: albumin, UGT and transferrin. Cells treated with cell-secreted HGF were compared to those treated with commercial HGF in order to check whether there was any difference in the differentiation efficiency between the two treatments.

In sections 5.4- 5.6 it was demonstrated that the MG63 cell line has the ability to secrete human HGF in the cell culture medium without need of specific inducers, and that the growth factor secreted is stable when exposed to the flow created inside a

hollow fibre bioreactor and can permeate across 5% PVA-PLGA hollow fibre membranes without significant loss of protein after three hour experiment.

Therefore MG63 secreted-HGF was tested to see whether the native protein was able to induce differentiation of mesenchymal stem cells into hepatocytes. It is known that mesenchymal stem cells can differentiate into hepatocytes upon induction with specific cytokines and growth factors [213, 241, 292, 293]. Mesenchymal stem cells treated with MG63 released HGF were compared with MSCs treated with commercial HGF to see whether any difference in morphology and/or hepatic marker expression had occurred.

6.3 Confirmation of mesenchymal stem cells markers

Prior to differentiation into the hepatic lineage, mesenchymal stem cells extracted from Wistar rats were analysed by flow cytometry to check whether they expressed some of the mesenchymal stem cell markers. More specifically, one negative (CD45) and two positive (CD44 and CD90) MSC markers were analysed.

The anti-rat CD45 marker is a monoclonal antibody to the rat CD45 antigen that recognizes a monomorphic determinant of the rat leukocyte common antigen (L-CA). The CD45 antigen is expressed on leukocytes: T-cells, B-cells, monocytes, macrophages, and granulocytes [331]. CD45 is not expressed on mesenchymal stem cells and therefore is commonly tested as negative marker for MSCs [332]. The anti-rat CD44 marker is a monoclonal antibody that recognises an epitope on the cell surface antigen CD44. It is an adhesion molecule expressed on most leukocytes (except a sub population of B cells), endothelial cells, hepatocytes, and MSCs [333-335]. Furthermore, many cancer cells express high levels of CD44. [336, 337]. Anti-rat CD90 monoclonal antibody recognizes the Thy 1.1 antigenic determinant, designated CD90 on rat as well as mouse cells. This particular determinant has been defined to be monomorphic within rats but polymorphic in the mouse. The Thy-1 antigen is found on a variety of cell types including thymocytes, neuronal cells, mesenchymal stem cells, hematopoietic stem cells, T and immature B cells, endothelial cells and connective tissue [338-341]. Mouse IgG1 and IgG2 isotype control antibodies were used as negative controls in order to estimate non-specific binding of the antibodies to the cells, and therefore to assess the level of background

staining in flow cytometric analysis. In the scatter plots of the cells, a gate was used to select the live MSC population based on cellular size (forward scatter, FSC) and granularity (side scatter, SSC) (see appendix).

Fig. 6.1 and 6.2 show the expression of CD44 and CD45 antigens respectively on the surface of rat MSCs. IgG2a isotype mouse anti-rat control antibody conjugated with fluorescein isothiocyanate (FITC) was used as a negative control for these antigens. The red histograms represent the fluorescence emission of cells expressing the marker, while the white ones that of the IgG2 controls. Data were subsequently normalised to the number of events in order to compare the pairs of histograms. It can be observed that the populations of live cells labelled with IgG2a control antibody emitted minimal fluorescence, as shown by the white histograms located at the left of the diagram, with mean fluorescence emission of 81, while the red histogram representing the fluorescence emission of the population labelled with CD44 mouse anti-rat antibody (fig. 6.1) was slightly shifted to the right compared to the controls, with a mean fluorescence emission of 213, suggesting these cells were weakly positive for CD44. In contrast, the histogram representing the population of cells labelled with CD45 FITC conjugated antibody (fig. 6.2) overlapped with that of IgG2 controls, which also emitted a minimal fluorescence value of 81. This result suggested that these cells were negative for CD45.

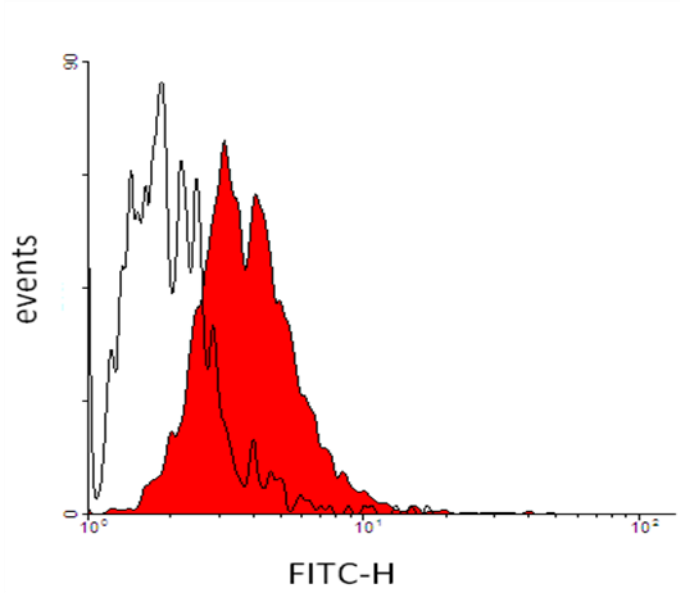

Fig. 6.1: Flow cytometry analysis of the CD44 cell surface marker (red histogram), compared to negative control IgG2 (white histogram). Data are expressed as FITC fluorescence intensity emission. Fluorescence values were normalised to the number of events in order to compare the two histograms.

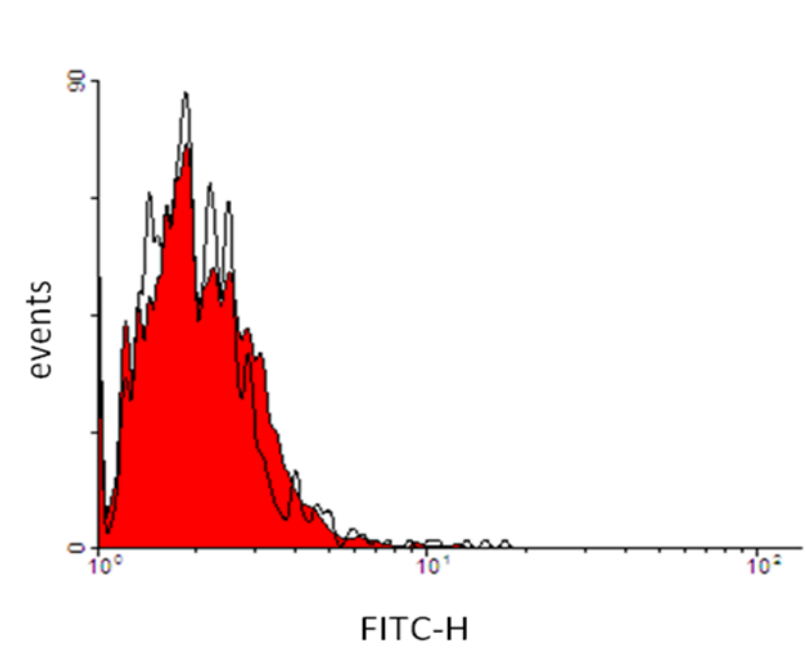

Fig. 6.2: Flow cytometry analysis of the CD45 cell marker (red histogram), compared to negative control (white histogram) IgG2. Data are expressed as FITC fluorescence intensity emission. Fluorescence values were normalised to the number of events in order to compare the two histograms.

Fig. 6.3 shows the expression of the CD90 antigen on the surface of rat MSCs. The IgG1 isotype mouse anti-rat control antibody conjugated to phycoerythrin (PE) was

used as negative control for CD90. Data were subsequently normalised to the number of events in order to compare the two histograms. It can be observed that the populations of live cells labelled with IgG1 control antibody emitted minimal fluorescent signal with mean value of 143, as shown by the histogram located at the left of the diagram, while the population labelled with PE-conjugated CD90 mouse anti-rat antibody emitted a strong fluorescent signal with a mean value of 30,227 and the histogram was shifted to the right compared to the controls, suggesting that the cells were positive for CD90.

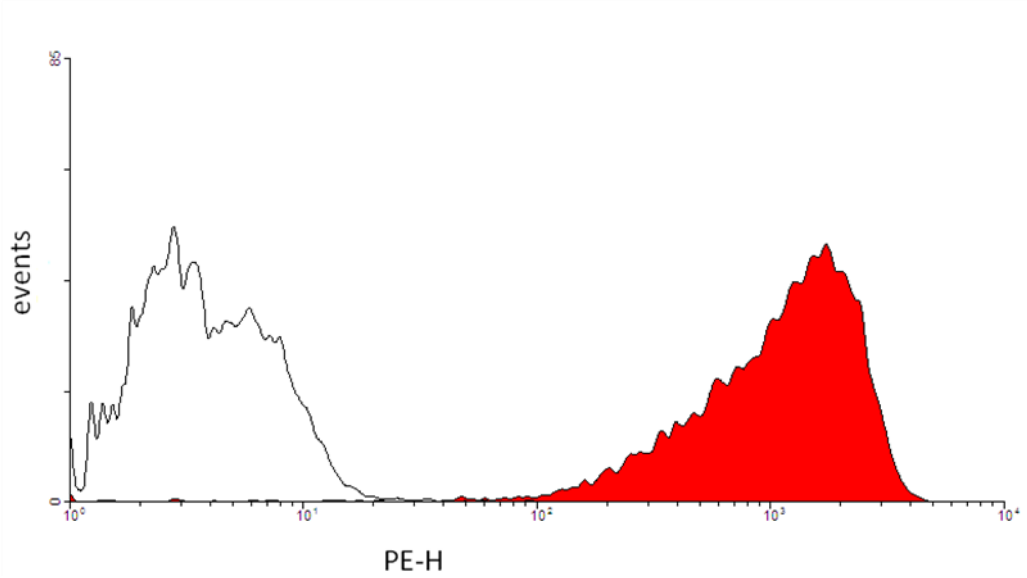

Fig. 6.3: Flow cytometry analysis of the CD90 cell surface marker (red histogram), compared to negative control (white histogram) IgG1. Data are expressed as PE fluorescence intensity emission. Fluorescence values were normalised to the number of events in order to compare the two histograms.

The flow cytometry analysis conducted on these three markers suggests that the technique used to isolate MSCs from rat bone marrow was successful, as cells were positive for CD44 and CD90 and negative for CD45, as indicated in the literature. However, more markers should be analysed in order to confirm the mesenchymal stem cell identity of the population.

Although rat MSCs resulted positive for both CD44 and CD90 surface markers, as expected, the difference in expression between the two markers is probably due to the different fluorochrome conjugated to the two antibodies: PE in fact usually has a stronger signal than FITC, because it has a maximum emission peak at 575 nm

against 518 nm of FITC, and it is more photostable than FITC [342], thus probably for this reason cells labelled with CD90 antibody conjugated to PE emitted a stronger fluorescent signal than those labelled with CD44 antibody conjugated to FITC, that resulted only weakly positive to CD44.

.

6.4 MSC differentiation

Once confirmed the identity of MSCs, the culture was exposed to liver-specific factors in a sequential manner, as shown by Snykers *et al* [213, 241]. According to the authors, the hepatic differentiation of MSCs was more effective when cells were exposed to liver-specific factors in a time-sequence that mimicked the *in vivo* liver embryogenesis, compared to those treated with a "cocktail" of the all factors at the same time-points. Following the protocol of Snykers *et al*, (fig.6.4) cells were expanded and when confluent, they were treated for 3 days with fibroblast growth factor 4 (FGF-4), a growth factor that stimulates the endoderm specification. On the third day, medium was changed and replaced with fresh medium containing hepatocyte growth factor (HGF). Two experiments were carried out in parallel: cells were treated with commercial HGF or with MG63-derived HGF, in order to check any potential difference in morphology and hepatic marker expression between the two treatments. From the 6^{th} to 18^{th} day cells were treated with a cocktail of HGF, insulin-transferrin-sodium selenite (which contains three important growth factors to stimulate cell growth: insulin, transferrin, selenium), dexamethasone (an anti-infammatory gluticorticoid which regulates cell survival, proliferation and differentiation, [182, 343, 344]) and trichostatin A (a *Streptomyces* metabolite which was shown to increase MSCs differentiation into the hepatic lineage [241]).

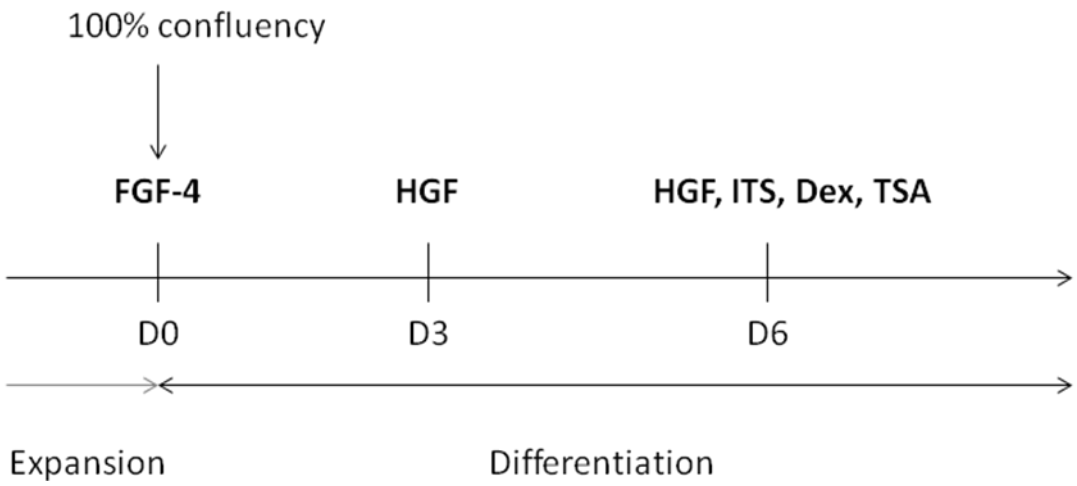

Fig. 6.4: Schematic representation of the protocol used to differentiate MSCs into hepatocytes. MSCs at 100% confluency were exposed to liver specific factors in a time-dependent order that reflects their secretion pattern during *in vivo* liver embryogenesis. Adapted from [213].

MSC differentiation into the hepatic lineage was analysed by tracking the morphological changes occurring in cell cultures every three days, and by immunofluorescence to see whether the cells expressed three specific hepatic markers: albumin, UGT and transferrin. Oil Red O staining was also performed on the cultures in order to detect the potential differentiation of stem cells into the adipogenic lineage.

6.4.1 Morphological analysis

Potential morphological changes were observed from the 14th day of cell treatment with the differentiation medium. MSCs treated with commercial HGF were almost confluent but some dense structures within the culture can be observed (***** in fig. 6.5): they might be areas of mineralization, of bone formation, indicating that differentiation of some MSCs into osteogenic lineage had occurred. However, this cannot be confirmed as a specific staining to detect the presence of mineralization, such as von Kossa should have been performed. However, the potential differentiation of mensenchymal stem cells into bone cells would not be surprising as MSCs can spontaneously differentiate into osteoblasts. Therefore, from a first visual analysis it can be noticed that a non homogeneous population of cells was observed

after 14 days culture consisting of a mixture of mesenchymal stem cells and cells potentially differentiating into the osteogenic lineage.

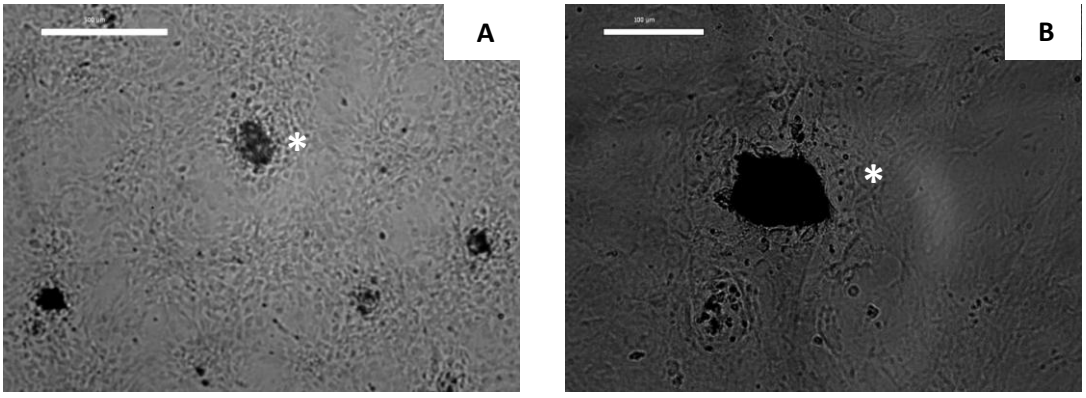

Fig. 6.5: Phase contrast microscopy images of MSCs treated with commercial HGF for 14 days. Scale bars: A) 500 µm; B) 100 µm. *= bone nodules.

Similarly to MSCs treated with commercial HGF, cells treated with MG63-derived HGF exhibited several dark areas that resemble bone nodules formation (* in fig. 6.6) which represent the first areas of ossification. An example of a bone nodule is shown in fig. 6.7. This differentiation might be due either to the spontaneous differentiation of MSCs into osteoblasts or also by the fact that MG63s, being a cell line derived from human osteosarcoma, might have released some osteogenic factors in the medium. For example, MG63s have the ability to secrete osteocalcin [345], TGF-β and prostaglandin E2 [346], which might have induced stem cells to differentiate into osteoblasts.

This suggests that HGF should be purified from the MG63-released supernatant in order to discard the other proteins or factors that are not liver tissue-specific and that might negatively interfere with the induction of stem cell differentiation into the hepatic lineage. A first attempt could be done by filtering the supernatant through a membrane with a molecular weight cutoff as close as possible to 80kDa in a centrifugal tube. The molecules with MW lower than 80 kDa would pass through the filters of the membrane while HGF would be retained. The retained supernatant could be then used to differentiate the stem cells into hepatocytes. In case this method still results in non-specific differentiation of cells, liquid chromatography could be a valid alternative to purify the HGF from the medium.

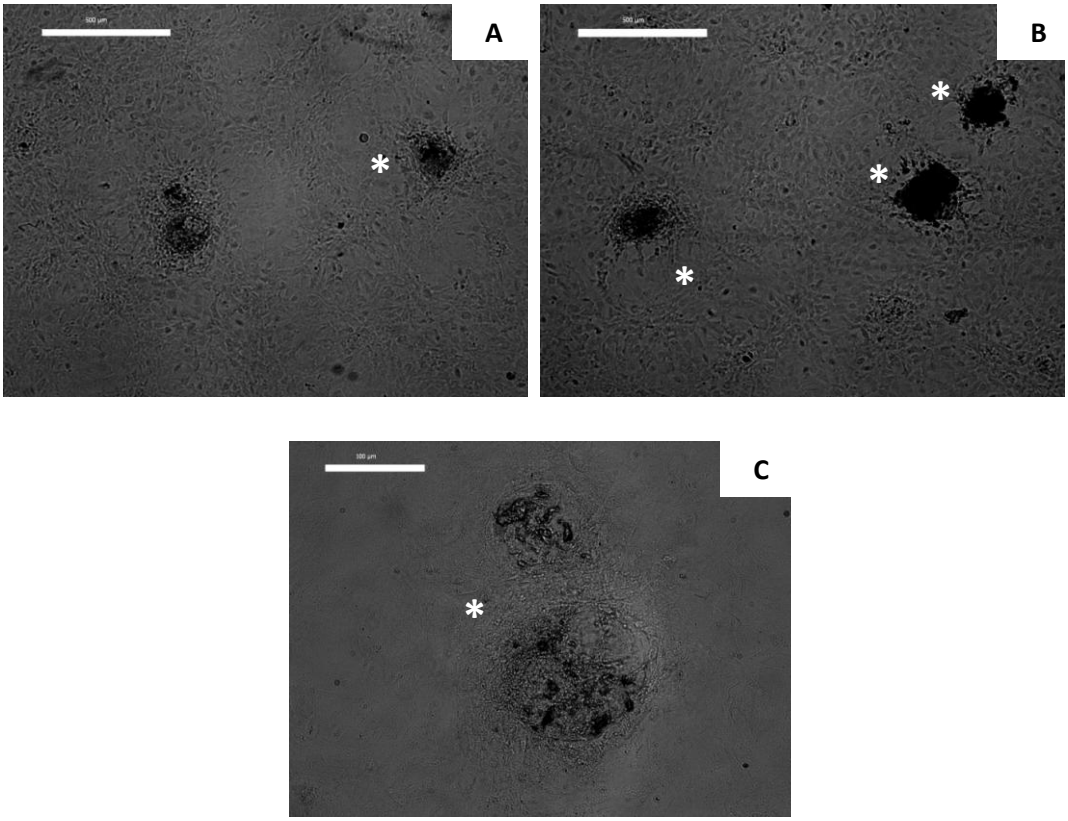

Fig. 6.6: Phase contrast microscopy images of MSCs treated with HGF from MG63s for 14 days. *****= bone nodule. Scale bars: A) 500 µm; B) 200 µm; C) 100 µm.

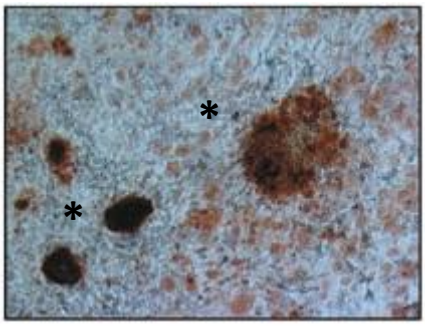

Fig. 6.7: Alizarin red stained osteoblastic cultures showing bone nodules (*) formation. From [347].

At day 17 a significant change in the morphology of the cells was observed. In fig. 6.8 and 6.9 the cells treated with commercial and MG63-secreted HGF, respectively, are displayed. Given the high density of the cells, especially those treated with commercial HGF, it is difficult to determine the morphology and the type of cell, however, it is very likely that the cell population is not homogeneous, and in fig. 6.9

A some structures resembling bone nodules can be observed among the other cells. At a first glance, cells exhibit bigger nuclei (arrows in fig. 6.8 B) and a more polygonal shape, which might indicate that the cells are losing their stem cell properties and might have or be in process of differentiating into the osteoblastic lineage: high mesenchymal stem cell densities have in fact been shown to induce higher chondrogenic and osteogenic differentiation rates due to soluble factors produced by and to signals from the neighbouring cells [180, 181, 185].

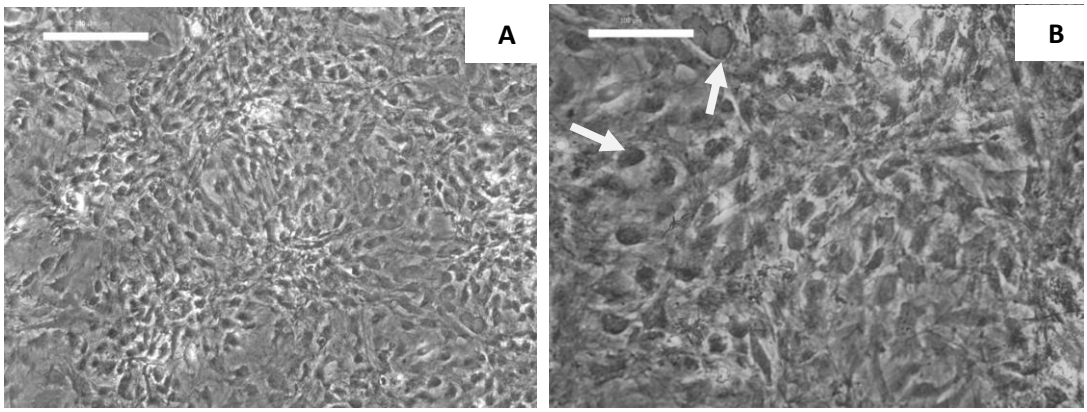

Fig. 6.8: Phase contrast microscopy images of MSCs treated with commercial HGF after 17 day culture. Scale bars: A) 200 µm; B) 100 µm.

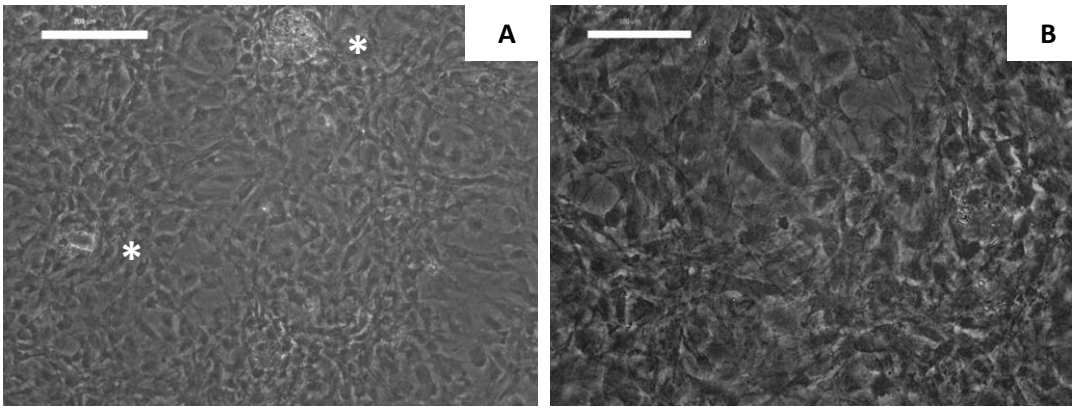

Fig. 6.9: Phase contrast microscopy images of MSCs treated with HGF released by MG63s after 17 day culture. *****= bone nodule. Scale bars: A) 200 µm; B) 100 µm.

6.4.2 Oil Red O staining

Oil Red O staining was performed at day 18 on mesenchymal stem cells treated with commercial and MG63 released HGF to check whether any cells had undergone adipogenic differentiation. In fig. 6.10 Oil Red O staining of MG63 cells, which were used as negative control, is displayed. In this figure nuclei of MG63s are stained blue by haematoxylin staining, and the cytoplasm is weakly stained red/pink, probably due to the non-specific background staining with Oil Red O. In MSCs treated with commercial HGF (fig. 6.11 and 6.12) some intensely red stained areas can be observed, which might be representing lipidic drops. However, it is not clear whether the staining was successful as in cells treated with HGF released by MG63s the red areas resemble more a residue of dye remaining after the washing rather than a specific staining, as can be noticed from the many randomly distributed red spots (fig. 6.12 A, B, C). Therefore it cannot be concluded whether any differentiation of mesenchymal stem cells into adipocytes had occurred.

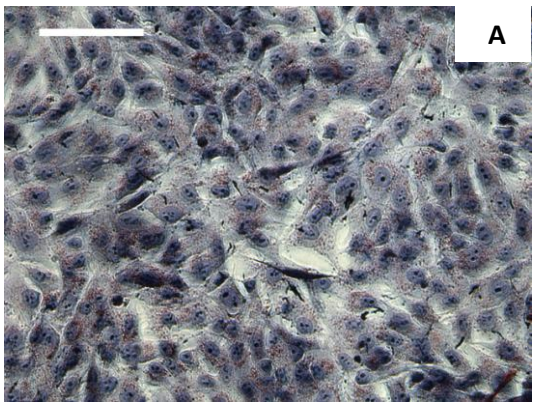

Fig. 6.10: Oil Red O staining of MG63s (negative control). Scale bar: 100µm.

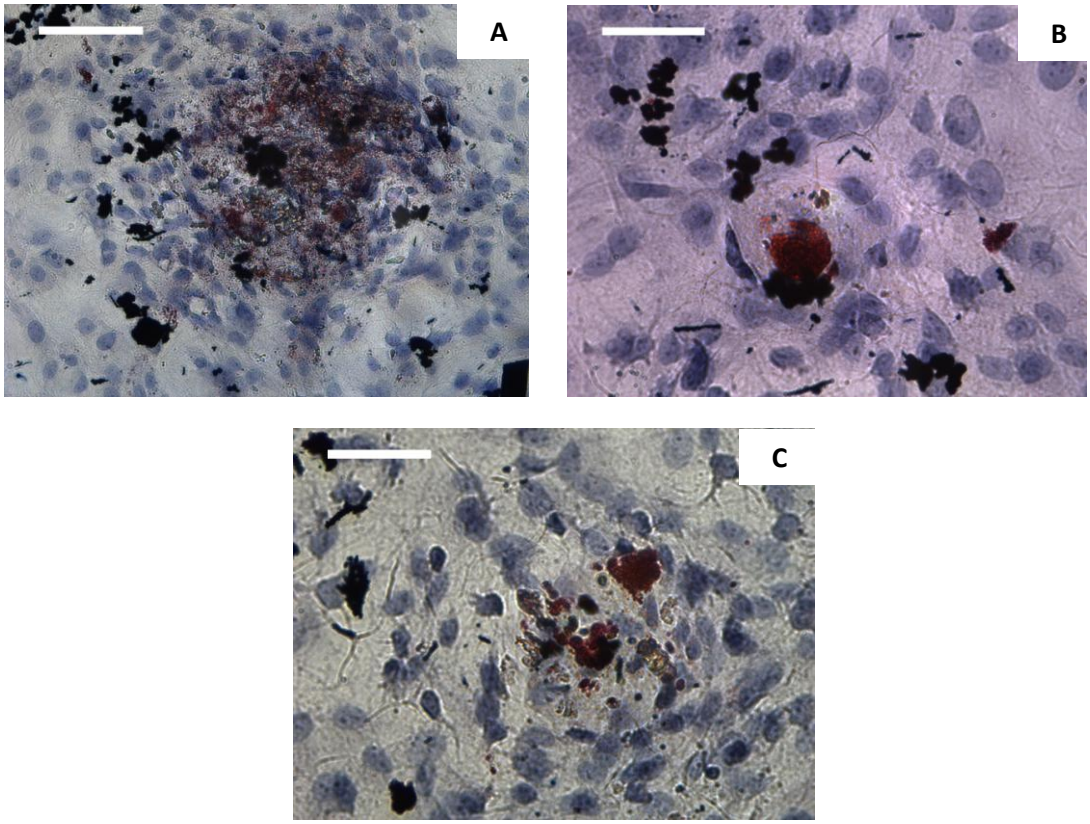

Fig. 6.11: Oil Red O staining of MSCs treated with commercial HGF after 18 day culture. Scale bars: A) 100 µm; B) and C) 50 µm.

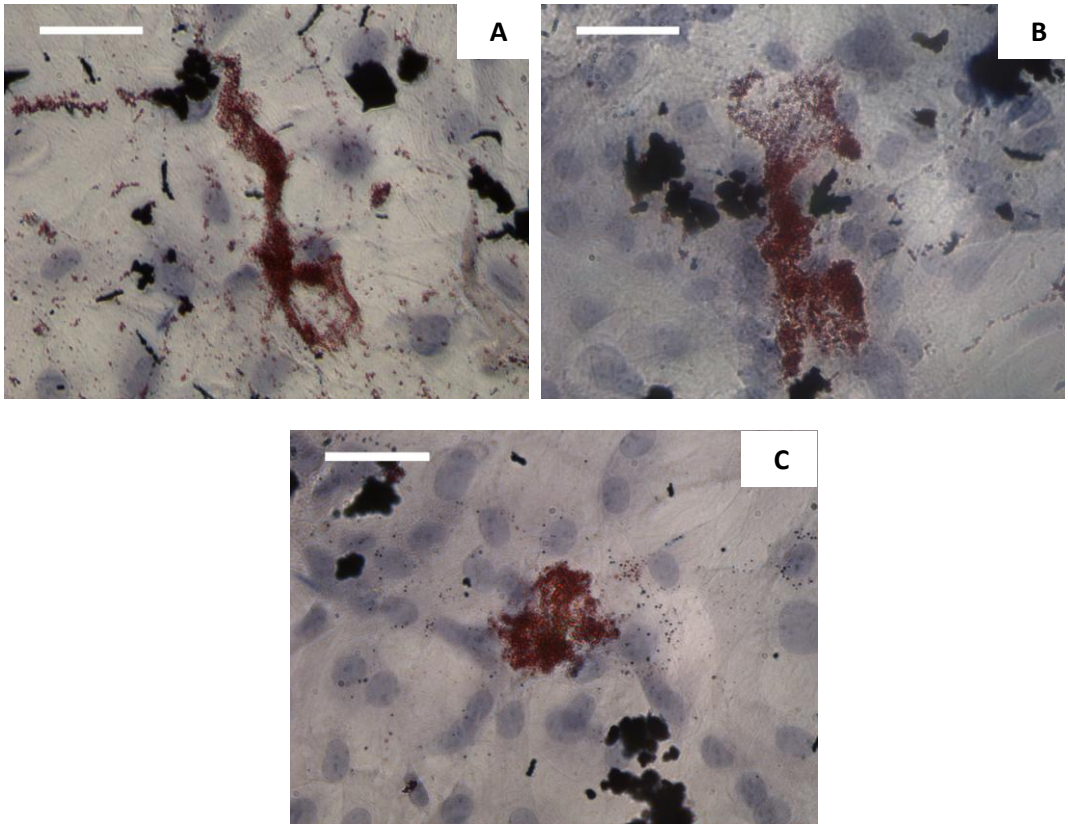

Fig. 6.12: Oil Red O staining of MSCs treated with MG63-derived HGF after 18 day culture. Scale bar: 50μm.

6.4.3 Liver markers

The expression of three liver specific markers, albumin (a plasma protein synthesised by the liver), UDP-Glucuronosyltransferase (UGT, an important enzyme expressed in liver for drug metabolism and elimination of foreign and endogenous substances) and transferrin (a plasma protein synthesised by the liver for iron delivery) was analysed by immunofluorescence. MG63 cells were used as negative controls and the HepG2 cell line as positive controls. From the analysis of positive controls, albumin and UGT, but not transferrin, were expressed by the HepG2 cell line. This last result was not expected as according to the literature, HepG2 cells express transferrin [348] However, from the analysis of the immunofluorescence staining of MG63 cells, the negative control, although transferrin was not expressed, albumin and UGT were highly expressed in MG63s. Undifferentiated MSCs treated with HGF were also positive for UGT and albumin, but negative for transferrin. This result confirms that a problem with the antibodies or during one of the steps of the immunostaining had

occurred, as transferrin was not even expressed in positive controls and albumin and UGT were expressed in all the samples, even in negative controls. This suggests that the results of the immunofluorescence staining of MSCs treated with HGF are unreliable. However, from UGT immunofluorescence images (fig. 6.13), it is possible to notice some morphological features of the cells. Most of the well is occupied by cells that have a morphology that resembles that of mesenchymal stem cells, as an indication that cells had not differentiated, but among these cells there are some clusters of bigger cells that lost the elongated shape to assume a more polygonal morphology. These cells exhibit large nuclei, and sometimes two nuclei are visible, probably indicating that the cells were undergoing division. Some of the cells also exhibit cytoplasmic projections, possibly filopodia (fig. 6.13). These cells had also spread extensively on the surface of the well, reaching about 100 µm in diameter. These cells might just be undifferentiated mesenchymal stem cells that had changed their morphology, as when kept in culture for many passages they usually lose their elongated shape and acquire a more polygonal morphology. Given the polygonal morphology and the large cytoplasm and nuclei of some of these cells (see fig. 6.13 A- D), it could be hypothesized that they might be osteoblasts, which would not be surprising as mesenchymal stem cells tend to spontaneously differentiate at high cell densities [263].

Given their large size and high spreading, these cells cannot be classified as hepatocytes as they usually exhibit a more compact morphology and an average diameter of about 20 µm [349]. In fig. 6.14 the morphology of hepatocytes can be observed. It can be noticed that cells in fig. 6.13 present a more spread morphology while hepatocytes possess a more defined, compact polygonal morphology.

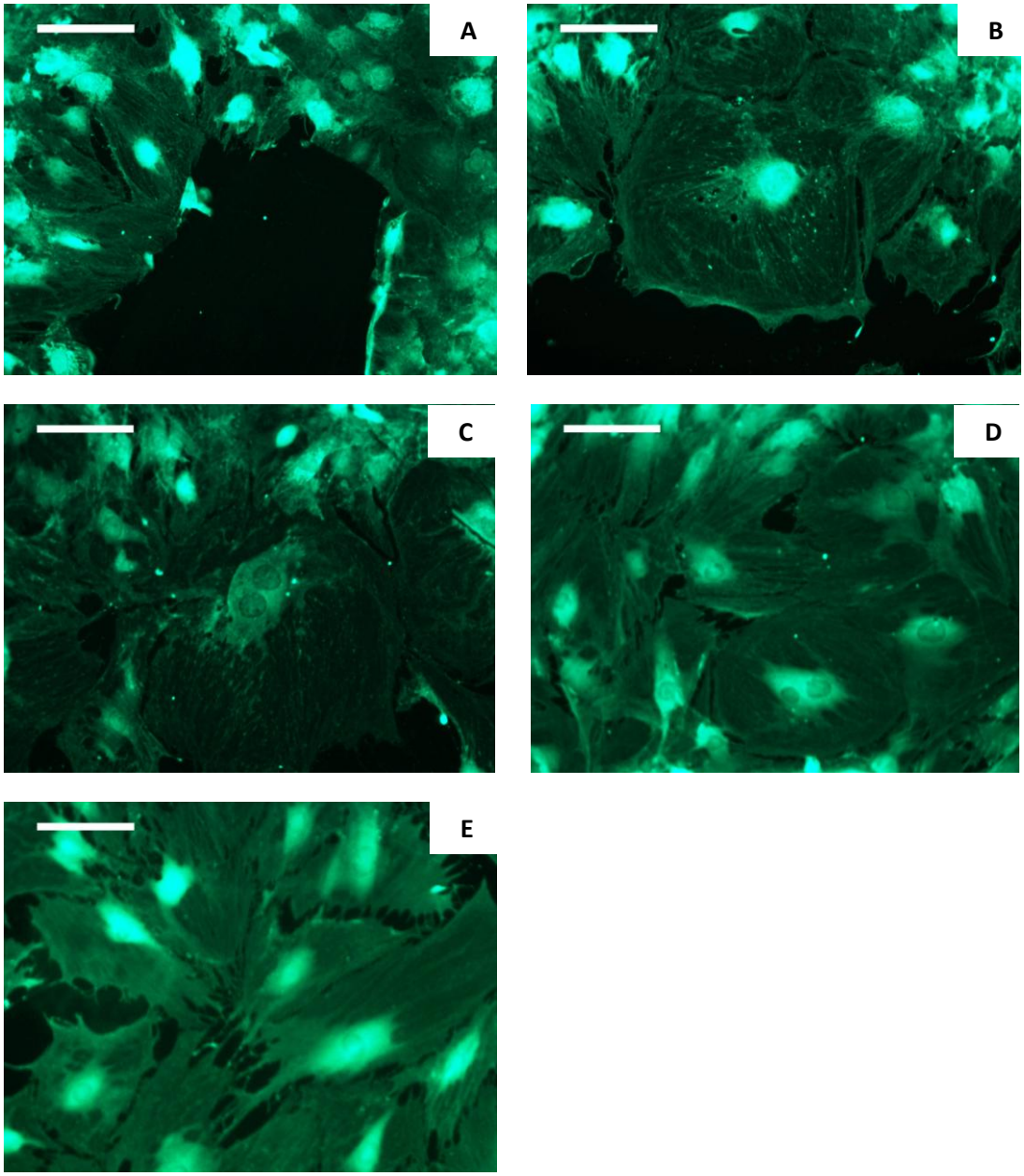

Fig. 6.13: Immunostaining of MSCs treated with HGF from MG63s after 18 days culture. Scale bar: 100 µm.

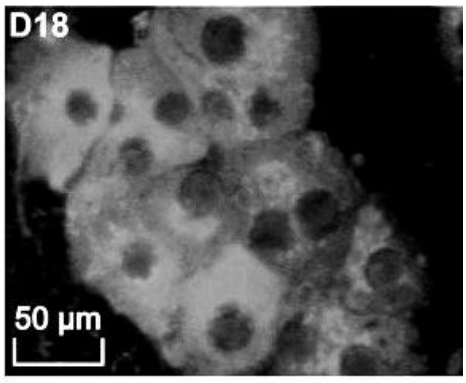

Fig. 6.14: Morphology of hepatocytes. From [213].

Given the unreliable results obtained with the controls, further repeats should be performed in order to clarify the effect of MG63-released HGF on the stem cells. Currently it can only be concluded that a heterogeneous population of cells was observed, and that their morphology did not resemble that of hepatocytes.

If this prediction is correct, then the treatment of MSCs with HGF released by MG63s did not lead to the differentiation of stem cells into hepatocytes. Also, the morphology of the cells treated with commercial and MG63-secreted HGF is very similar, thus suggesting that the treatment of MSCs with hepatogenic growth factors and cytokines in a sequential manner that resembled embryonic liver development did not stimulate the cells to differentiate into hepatocytes, in contrast with the findings of Snykers *et al.*, that reported a homogenous populations of hepatocytes after 18 days sequential exposure of rat bone marrow mesenchymal stem cells to specific hepatogenic factors. More hepatogenic growth factors and cytokines might be required in order to achieve mesenchymal stem cell differentiation, such as nicotinamide [350], oncostatin, EGF [351].

In contrast, the problem might arise from the intrinsic nature of mesenchymal stem cells, as being adult stem cells, they might be already committed to a more specific lineage and therefore it would be more difficult to successfully differentiate them into hepatocytes only by addition of hepatogenic growth factors. The fact that the several successful examples of hepatic differentiation of MSCs arise from protocols where stem cells where co-cultured with primary hepatocytes [183, 352-354], might suggest that mesenchymal stem cells would require further signals provided by primary hepatocytes other than the artificial addition of growth factors in order to become committed to the hepatic lineage.

6.5 Conclusions

In this chapter, HGF secreted by MG63 cells was employed to differentiate rat mesenchymal stem cells into the hepatic lineage. The flow cytometry analysis conducted on the cells extracted from rat bone marrow suggests that the technique used to isolate MSCs was successful, as cells were positive for CD44 and CD90 and

negative for CD45, as indicated in the literature. However, more markers should be analysed in order to confirm the mesenchymal stem cell identity of the population. Treatment of MSCs with HGF released by MG63s seemed not to lead to the differentiation of these cells into hepatocytes when liver specific growth factors were added in a sequence-dependent manner that reflected liver development. Further liver specific growth factors or co-culture with primary hepatocytes might be needed in order to achieve an efficient differentiation of mesenchymal stem cells towards the hepatic lineage. Since commercial HGF was also unsuccessful in inducing hepatic differentiation of mesenchymal stem cells, this suggests that MG63-derived HGF could potentially be used for stem cell differentiation but a deeper understanding of the signals involved in stem cell differentiation and in liver development is required in order to improve the differentiation protocol.

However, given the unreliable results obtained with the controls, the experiment should be repeated in order to confirm this prediction.

7. Conclusions and future work

The present work has contributed to the field of tissue engineering with two major novelties: the development of more hydrophilic PVA-PLGA blended hollow fibre membranes for higher transfer of nutrients to the cells, and the realisation of a system where a growth factor continuously secreted by a cell line is more stable in dynamic environment than the commercial protein.

In section 7.1 a summary of the main findings of this work is presented with final conclusions, while section 7.2 outlines the future work that could lead to further advances in tissue engineering and regenerative medicine.

7.1 Conclusions

The addition of PVA to PLGA polymer solution has been shown to improve the porosity, pore size and hydrophilicity of PLGA hollow fibre membranes. These characteristics were believed to facilitate the transfer of nutrients across the membrane. Among the three different fibres compositions, only 5% PVA–PLGA fibres showed to be permeable to water, and this suggested that they are the only suitable fibres to be employed in bioreactor devices. These fibres were also shown to be permeable to the model protein BSA, with no solute rejection, reduced flux or pore size due to fouling, thus confirming their permeability to large molecules and suitability for bioreactor devices applications.

Subsequent treatment of PVA-PLGA hollow fibres with NaOCl caused the removal of the skin from the inner and outer surface of the fibre, and an increase of pore size, which could potentially lead to an increase in the scaffold surface area and mass transport through the membrane. However, this treatment negatively affected the mechanical integrity of the fibres, making them unsuitable for tissue engineering applications.

Since increasing membrane hydrophilicity should also increase wettability by cell culture medium, it was expected that the novel 5% PVA-PLGA membranes would facilitate cell attachment in comparison to pure PLGA membranes. Two cell types were analysed for their ability to adhere and proliferate on polymer flat sheets: mesenchymal stem cells (MSCs) and osteosarcoma cell line MG63. The results

obtained from the qualitative and quantitative analysis of cell adhesion and proliferation indicated a different affinity of the two cell types to the different materials and were in contrast to our expectations. The analysis conducted on rat mesenchymal stem cell attachment and proliferation indicated that MSCs adhered, spread and proliferated more on hydrophobic PLGA membranes compared to hydrophilic blended PVA-PLGA membranes and to tissue culture plastic, used as control. In contrast, MG63s adhered, spread and proliferated better on tissue culture plastic than on the two membrane types. The unexpected results obtained indicated that the addition of 5% PVA to PLGA did not improve cell attachment and, therefore, other strategies should be attempted in order to obtain a membrane that allows the mass transfer of nutrients but at the same time facilitates cell attachment.

The second part of the project focused on a novel system for the inexpensive and continuous production of hepatocyte growth factor to be used in the bioreactor for the differentiation of stem cells toward the hepatic lineage. The novel strategy pursued in this project consisted of the production of HGF by a cell line. Two cell lines, the HL60 suspension cell line and the MG63 adherent cell line, were tested for their ability to secrete hepatocyte growth factor into cell culture medium. HL60 cells were chosen in first place for their characteristic of growing in suspension, which would have allowed their continuous circulation inside the lumen of the hollow fibre. The single fibre hollow fibre bioreactor has been shown to be suitable for the culture of HL60 cell line since the shear stress induced by the laminar flow did not affect cell viability and, on the contrary, stimulated HL60s metabolic activity compared to static culture systems. However, in contrast with the literature, treatment of HL60s with dbcAMP, TPA, heparin or the combination of the three of them did not lead to HGF secretion by these cells. In contrast, MG63 cells spontaneously secreted HGF without external stimulation as indicated by the literature and, furthermore, showed the ability to secrete the growth factors at different concentrations according to the cell seeding density. Furthermore, MG63-derived HGF has been shown to be stable in a dynamic environment, as opposed to commercial HGF which degraded rapidly when exposed to the flow of the bioreactor. MG63-derived HGF also permeated across the pores of the 5% PVA-PLGA hollow fibre membranes without significant loss of protein in the first three hours of circulation. These promising results would possibly allow the realisation of the system described in section 1.10 (Aims and objectives),

where a growth factor would be continuously available for the stem cells in order to promote their differentiation and for the maintenance of their differentiated state.
Hence, with these positive results utilising MG63-secreted HGF, the growth factor was selected for the subsequent studies on the differentiation of MSCs into the hepatic lineage via liver specific factors. After confirmation by flow cytometric analysis of the identity of mesenchymal stem cells extracted from rat bone marrow, liver specific growth factors were added to the cells in a sequence resembling liver development. Results showed that treatment of MSCs with HGF released by MG63s did not lead to the differentiation of the stem cells into hepatocytes. Additionally, MSCs treated with commercial HGF failed to differentiate, suggesting that the unsuccessful outcome might not be due to the growth factor itself but to the differentiation protocol used which might not be efficient for the differentiation of the stem cells. Further liver specific growth factors or co-culture with primary hepatocytes might be needed in order to achieve an efficient differentiation of mesenchymal stem cells towards the hepatic lineage.

In conclusion, the present work has succeeded in developing a hollow fibre bioreactor system that allows an appropriate mass transfer of proteins across the scaffold for an adequate provision of nutrients to the cells and therefore for improved *in vitro* tissue formation. The novel PVA-PLGA hollow fibre membranes represent an advance over pure PLGA fibres for their improved permeability to water and proteins.

The other important success of this project is represented by the "cell-factory" strategy to produce large amounts of proteins for the differentiation of stem cells, but also for other purposes. The successful production of HGF by MG63 cell line represents an example of cell factory that can be applied to other proteins thus expanding the applicability of the system for the reconstruction of different tissues.
However, the project failed in developing a suitable scaffold for the stem cells and in the differentiation of stem cells into hepatocytes. Therefore future work should focus on improving stem cell attachment and differentiation. The next section describes the short- and long-term work that is required in order to achieve all the goals of the project.

7.2 Future work

7.2.1 Short-term work

- **Hollow fibres membranes**

PVA-PLGA hollow fibres have been characterised for their morphology, pore size, porosity, mechanical properties and hydrophilicity. However, further studies need to be carried out to characterise the membranes. Firstly, degradation studies of the blended membranes should be performed. The study should investigate the degradation of the fibres by assessing the changes in mass, volume, porosity, pore size and intrinsic viscosity at different times, temperatures, pH.

PVA-PLGA hollow fibres have also been shown to be permeable to BSA without adsorption of the protein, and to HGF, without significant loss of protein concentration in the first three hours of experiment. Further studies should be carried out in order to investigate the mechanism by which loss of protein occurred, for example whether the protein had been adsorbed by the membrane or degraded by means of a very sensitive protein assay. Also the experiments should be performed for a longer period of time in order to verify the permeability of the membrane over a longer timeframe for a potential clinical application. Furthermore, the permeation of other proteins and molecules of different molecular sizes across the blended membranes need to be tested in order to obtain a more complete characterisation of the membrane in terms of permeability and for the determination of the molecular weight cut-off.

Treatment of PVA-PLGA hollow fibres with 5% NaOCl has been shown to cause significant loss of mechanical strength of the fibres. However, since the treatment caused the removal of the outer skin of the fibre, which would potentially increase the mass transfer across the membrane, it could be performed at a lower concentration of NaOCl in order to see whether it could improve the porosity with no significant decrease in the mechanical strength.

- **Cell attachment**

In chapter 4, mesenchymal stem cells and MG63 cells were seeded on 5% PVA-PLGA flat sheet in order to verify whether the improved hydrophilicity of the

membrane lead to higher cell attachment to the scaffold. Since PVA-PLGA scaffold did not show good cell attachment, strategies such as immobilising adhesive proteins *e.g.* fibronectin, collagen, vitronectin, or bioactive peptide ligands (*e.g.* the RGD sequence) on the surface of PVA-PLGA blended membranes could be investigated. Additionally, the polymer solution could be blended with ECM proteins prior to scaffold fabrication in order to improve cell adhesion, as these strategies have been shown to increase cell adhesion onto PLGA scaffolds [355-358].

Since the project aims towards the differentiation of mesenchymal stem cells into the hepatic lineage, hepatocytes should also be seeded as well on the membranes to determine their suitability as a scaffold for this cell type.

- **HGF and stem cell differentiation**

In chapter 5, HGF released by MG63 was shown to be stable in a dynamic environment when circulated for 3 hours. The experiment should be repeated for a longer time in order to verify for how long the protein is stable in dynamic culture.
The analysis of three stem cells markers in chapter 6 showed that the cells extracted from rat bone marrow were mesenchymal stem cells. However, further markers should be tested, and more specifically, CD14, CD31 and CD34 [359] as negative markers, and CD29, CD73, CD105, CD 166 as positive mesenchymal stem cells markers [241, 359].
The differentiation protocol used in this research was unable to induce differentiation of mesenchymal stem cells into hepatocytes. Therefore a new protocol that employs further liver specific factors, *e.g.* oncostatin and EGF [178, 182, 207, 208], in addition to those already attempted, should be investigated.

7.2.2 Long term work

The single fibre hollow fibre bioreactor is a novel design that represents a simplified model of a multiple hollow fibre bioreactor. The aim of the design is to investigate the main components and parameters of the hollow fibre bioreactor, *i.e.* the membrane, the mechanical forces acting within the system, the cell behaviour in dynamic culture systems, and the mass transfer across the membrane. The ultimate

goal is to obtain a complete characterisation of the system for the development of a functional hollow fibre bioreactor to be employed in the clinic.

The main studies that need to be performed on the single fibre bioreactor and that would provide a step forward towards the development of a functional multiple fibre bioreactor are described below.

- **Bioreactor design**

The first aspect that has to be considered is the recreation of a suitable environment for the cells, therefore key parameters like temperature, oxygen concentration, pH and media flow rates need to be measured and controlled in order to be maintained at values that mimic the *in vivo* conditions. Since different tissues have different metabolic requirements, the parameters should be modulated according to the tissue or organ that will be reconstructed *in vitro*. Furthermore, since it is known that mechanical forces, *e.g.* shear stress and hydrostatic pressure, can improve or accelerate tissue regeneration *in vitro* [360-362], studies should be carried out in order to understand the contributions that these mechanical forces could make towards tissue regeneration. Mathematical modelling studies might be helpful in order to study these parameters prior to the experiments. Finally, the biomaterial used for the fabrication of the hollow fibres could be selected according to the cell type that will be seeded on it, thus adapting the system to the *in vitro* reconstruction of different tissues.

- **Cell factory system**

This thesis has shown that a cell line capable of releasing a growth factor can be used as a cell factory for the continuous and inexpensive production of hepatocyte growth factor that could potentially be used to direct stem cell differentiation toward the hepatic lineage. The most important aspect of this system is that it can be used for the production of different proteins: a cell line can be engineered to produce the growth factor of choice which can be used for the differentiation of stem cells toward different lineages, and therefore for the *in vitro* reconstruction of different tissues.

- **Stem cell cultures in the hollow fibre bioreactor**

Stem cell biology is a relatively new field of research that has a great potential for the advance in the field of tissue engineering. However, intensive investigation is still

needed for a complete understanding of the mechanisms of their differentiation into a specific lineage, and of their behaviour in dynamic culture systems. Further studies need to be carried out to investigate whether mechanical forces *e.g.* shear stress might have any negative effect on stem cell attachment to the biomaterial or on stem cell viability and metabolic activity. Furthermore, the bioreactor should be tested for its ability to expand the number of stem cells as this parameter is very important when considering future clinical applications.

Other studies should focus on the effect of specific mechanical forces that could direct the differentiation of stem cells into specific lineages, and on whether the differentiation protocols used for static cultures will be still efficient when the cells will be cultured in dynamic systems. Moreover, further studies should investigate whether the cells would maintain the differentiated state in the long term as it would be important for a future clinical application.

- **Clinical application**

Once a complete understanding of the key bioreactor parameters and an efficient differentiation of the stem cells have been achieved, it will be possible to develop a multiple fibre bioreactor for the *in vitro* reconstruction of tissues or organs. In order to translate these findings to clinical applications, large-scale robust and totally controlled culture systems capable of expanding and differentiating stem cells, as fast and pure as possible, are needed. The first issue to be considered is the number of cells that need to be cultured in the system in order to obtain the minimum mass required to regenerate a functional tissue if implanted into the patient. The issue of the number of cells needed is related to the surface area of the fibres that will support the growth of the cells, and to the size of the bioreactor that will need to contain a specific volume of culture medium required by the cells to be kept viable and metabolically active.

Once the system has been set up and the cells within the bioreactor exhibit all the specific functions of a given tissue, the system will be suitable for being tested in an *in vivo* setting. Several *in vivo* studies will be needed before a clinical application will effectively be attempted. First, the *in vivo* degradation of the biomaterial with the cells should be analysed in order to study the relationship between the degradation rate of the scaffold and the generation of a functional tissue. Furthermore, the ability

of the cells to repopulate the damaged tissue once implanted *in vivo* should be investigated. Alternatively, the system could be used to differentiate stem cells that could then be used for cell-based therapies.

Finally, in the case of stem cell-derived tissues, it will be necessary to investigate whether the newly differentiated cells maintain their differentiated state once implanted *in vivo,* as their potential dedifferentiation might cause several safety concerns as the cells might develop into tumours within the body of the patient. Also, since the current systems to differentiate stem cells do not produce a completely homogeneous population of differentiated cells, monitoring the differentiation state of the cells during the scale-up process and selecting the differentiated cells from the immature ones is another challenge that researchers have to face in the near future.

As can be seen from this section, the research presented in this thesis is only the beginning of many years of studies aiming to understand all the mechanisms for tissue regeneration in order to realise a perfectly functional and safe tissue that can be clinically effective.

In conclusion, this research has succeeded in developing a hollow fibre bioreactor system which allows an improved transfer of nutrients to cells and that, therefore, would be suitable for tissue engineering applications, especially for the *in vitro* reconstruction of highly metabolic tissues. This work also succeeded in developing a cell factory system for the continuous and inexpensive production of proteins that could be used for the differentiation of stem cells for tissue engineering, regenerative medicine or cell therapy applications. These two main developments have the potential to bring significant contribution the fields of tissue engineering and regenerative medicine.

References

1. Langer, R. and J.P. Vacanti, *Tissue engineering.* Science, 1993. **260**(5110): p. 920-926.
2. Saxena, A.K., *Tissue engineering and regenerative medicine research perspectives for pediatric surgery.* Pediatric Surgery International. **26**(6): p. 557-573.
3. *Principles of tissue engineering*. third ed, ed. R. Lanza, Langer, R., Vacanti J. 2007, Burlington, MA, USA: Elsevier Academic Press.
4. Atala, A., Lanza R., Thomson J., Nerem R., *Principles of regenerative medicine*. first ed. 2008, Burlington, MA, USA: Academic Press.
5. Humes, H.D. and M.S. Szczypka, *Advances in cell therapy for renal failure.* Transplant Immunology, 2004. **12**(3-4): p. 219-227.
6. Polak, J.M. and A.E. Bishop, *Stem cells and tissue engineering: Past, present, and future.* Skeletal Development and Remodeling in Health, Disease, and Aging, 2006. **1068**: p. 352-366.
7. Gerlach, J.C., K. Zedinger, and J.F. Patzer, *Bioartificial liver systems: why, what, whither?* Regenerative Medicine, 2008. **3**(4): p. 575-595.
8. Aejaz, H.M., A.K. Aleem, N. Parveen, M.N. Khaja, M.L. Narusu, and C.M. Habibullah, *Stem cell therapy - Present status.* Transplantation Proceedings, 2007. **39**(3): p. 694-699.
9. Murry, C.E. and G. Keller, *Differentiation of embryonic stem cells to clinically relevant populations: Lessons from embryonic development.* Cell, 2008. **132**(4): p. 661-680.
10. Zhang, S.C., M. Wernig, I.D. Duncan, O. Brustle, and J.A. Thomson, *In vitro differentiation of transplantable neural precursors from human embryonic stem cells.* Nature Biotechnology, 2001. **19**(12): p. 1129-1133.
11. He, J.Q., Y. Ma, Y. Lee, J.A. Thomson, and T.J. Kamp, *Human embryonic stem cells develop into multiple types of cardiac myocytes - Action potential characterization.* Circulation Research, 2003. **93**(1): p. 32-39.
12. Chadwick, K., L.S. Wang, L. Li, P. Menendez, B. Murdoch, A. Rouleau, and M. Bhatia, *Cytokines and BMP-4 promote hematopoietic differentiation of human embryonic stem cells.* Blood, 2003. **102**(3): p. 906-915.
13. Assady, S., G. Maor, M. Amit, J. Itskovitz-Eldor, K.L. Skorecki, and M. Tzukerman, *Insulin production by human embryonic stem cells.* Diabetes, 2001. **50**(8): p. 1691-1697.
14. Rambhatla, L., C.P. Chiu, P. Kundu, Y. Peng, and M.K. Carpenter, *Generation of hepatocyte-like cells from human embryonic stem cells.* Cell Transplantation, 2003. **12**(1): p. 1-11.
15. Geijsen, N., M. Horoschak, K. Kim, J. Gribnau, K. Eggan, and G.Q. Daley, *Derivation of embryonic germ cells and male gametes from embryonic stem cells.* Nature, 2004. **427**(6970): p. 148-154.
16. Stem Cells For Hope. 2010 [cited 25-06-2010]; Available from: http://www.stemcellsforhope.com/Stem%20Cell%20Therapy.htm.
17. Perrier, A.L., V. Tabar, T. Barberi, M.E. Rubio, J. Bruses, N. Topf, N.L. Harrison, and L. Studer, *Derivation of midbrain dopamine neurons from human embryonic stem cells.* Proc Natl Acad Sci U S A, 2004. **101**(34): p. 12543-12548.

18. Vodyanik, M.A., J.A. Bork, J.A. Thomson, and Slukvin, II, *Human embryonic stem cell-derived CD34(+) cells: efficient production in the coculture with OP9 stromal cells and analysis of lymphohematopoietic potential.* Blood, 2005. **105**(2): p. 617-626.
19. Gerrard, L., L. Rodgers, and W. Cui, *Differentiation of human embryonic stem cells to neural lineages in adherent culture by blocking bone morphogenetic protein signaling.* Stem Cells, 2005. **23**(9): p. 1234-1241.
20. Xu, R.H., X. Chen, D.S. Li, R. Li, G.C. Addicks, C. Glennon, T.P. Zwaka, and J.A. Thomson, *BMP4 initiates human embryonic stem cell differentiation to trophoblast.* Nature Biotechnology, 2002. **20**(12): p. 1261-1264.
21. Dawson, E., G. Mapili, K. Erickson, S. Taqvi, and K. Roy, *Biomaterials for stem cell differentiation.* Advanced Drug Delivery Reviews, 2008. **60**(2): p. 215-228.
22. Drukker, M., G. Katz, A. Urbach, M. Schuldiner, G. Markel, J. Itskovitz-Eldor, B. Reubinoff, O. Mandelboim, and N. Benvenisty, *Characterization of the expression of MHC proteins in human embryonic stem cells.* Proc Natl Acad Sci U S A, 2002. **99**(15): p. 9864-9869.
23. Colman, A. and A. Kind, *Therapeutic cloning: concepts and practicalities.* Trends in Biotechnology, 2000. **18**(5): p. 192-196.
24. Stacey, G.N., F. Cobo, A. Nieto, P. Talavera, L. Healy, and A. Concha, *The development of 'feeder' cells for the preparation of clinical grade hES cell lines: Challenges and solutions.* Journal of Biotechnology, 2006. **125**(4): p. 583-588.
25. Hovatta, O. and H. Skottman, *Feeder-free derivation of human embryonic stem-cell lines.* Lancet, 2005. **365**(9471): p. 1601-1603.
26. Levenberg, S., N.F. Huang, E. Lavik, A.B. Rogers, J. Itskovitz-Eldor, and R. Langer, *Differentiation of human embryonic stem cells on three-dimensional polymer scaffolds.* Proc Natl Acad Sci U S A, 2003. **100**(22): p. 12741-12746.
27. Gerecht, S., J.A. Burdick, L.S. Ferreira, S.A. Townsend, R. Langer, and G. Vunjak-Novakovic, *Hyaluronic acid hydrogel for controlled self-renewal and differentiation of human embryonic stem cells.* Proc Natl Acad Sci U S A, 2007. **104**(27): p. 11298-11303.
28. Maguire, T., E. Novik, R. Schloss, and M. Yarmush, *Alginate-PLL microencapsulation: Effect on the differentiation of embryonic stem cells into hepatocytes.* Biotechnology and Bioengineering, 2006. **93**(3): p. 581-591.
29. Nur-E-Kamal, A., Ahmed, I., Kamal, J.M., Schindler, M., Meiners, S. , *Three dimensional nanofibrillar surfaces promote self-renewal in mouse embryonic stem cells.* Stem Cells, 2006. **24**(2): p. 426-433.
30. Chung, Y., I. Klimanskaya, S. Becker, J. Marh, S.J. Lu, J. Johnson, L. Meisner, and R. Lanza, *Embryonic and extraembryonic stem cell lines derived from single mouse blastomeres.* Nature, 2006. **439**(7073): p. 216-219.
31. Burke, Z.D., S. Thowfeequ, M. Peran, and D. Tosh, *Stem cells in the adult pancreas and liver.* Biochemical Journal, 2007. **404**: p. 169-178.
32. Edwards, R.G., *Stem cells today: B1. Bone marrow stem cells.* Reproductive Biomedicine Online, 2004. **9**(5): p. 541-583.
33. Asahara, T., T. Murohara, A. Sullivan, M. Silver, R. vanderZee, T. Li, B. Witzenbichler, G. Schatteman, and J.M. Isner, *Isolation of putative progenitor endothelial cells for angiogenesis.* Science, 1997. **275**(5302): p. 964-967.

34. Steindler, D.A. and D.W. Pincus, *Stem cells and neuropoiesis in the adult human brain.* Lancet, 2002. **359**(9311): p. 1047-1054.
35. Zuk, P.A., M. Zhu, H. Mizuno, J. Huang, J.W. Futrell, A.J. Katz, P. Benhaim, H.P. Lorenz, and M.H. Hedrick, *Multilineage cells from human adipose tissue: Implications for cell-based therapies.* Tissue Engineering, 2001. **7**(2): p. 211-228.
36. Tosh, D. and A. Strain, *Liver stem cells - prospects for clinical use.* J Hepatol, 2005. **42**: p. S75-S84.
37. Alessandri, G., S. Pagano, A. Bez, A. Benetti, S. Pozzi, G. Iannolo, M. Baronio, G. Invernici, A. Caruso, C. Muneretto, G. Bisleri, and E. Parati, *Isolation and culture of human muscle-derived stem cells able to differentiate into myogenic and neurogenic cell lineages.* Lancet, 2004. **364**(9448): p. 1872-1883.
38. Zulewski, H., E.J. Abraham, M.J. Gerlach, P.B. Daniel, W. Moritz, B. Muller, M. Vallejo, M.K. Thomas, and J.F. Habener, *Multipotential nestin-positive stem cells isolated from adult pancreatic islets differentiate ex vivo into pancreatic endocrine, exocrine, and hepatic phenotypes.* Diabetes, 2001. **50**(3): p. 521-533.
39. Benito, A.I., M.A. Diaz, M. Gonzalez-Vicent, J. Sevilla, and L. Madero, *Hematopoietic stem cell transplantation using umbilical cord blood progenitors: review of current clinical results.* Bone Marrow Transplantation, 2004. **33**(7): p. 675-690.
40. Snykers, S., J. De Kock, V. Rogiers, and T. Vanhaecke, *In Vitro Differentiation of Embryonic and Adult Stem Cells into Hepatocytes: State of the Art.* Stem Cells, 2009. **27**(3): p. 577-605.
41. Balsam, L.B., A.J. Wagers, J.L. Christensen, T. Kofidis, I.L. Weissman, and R.C. Robbins, *Haematopoietic stem cells adopt mature haematopoietic fates in ischaemic myocardium.* Nature, 2004. **428**(6983): p. 668-673.
42. Corbel, S.Y., A. Lee, L. Yi, J. Duenas, T.R. Brazelton, H.M. Blau, and F.M.V. Rossi, *Contribution of hematopoietic stem cells to skeletal muscle.* Nature Medicine, 2003. **9**(12): p. 1528-1532.
43. Orlic, D., J. Kajstura, S. Chimenti, I. Jakoniuk, S.M. Anderson, B.S. Li, J. Pickel, R. McKay, B. Nadal-Ginard, D.M. Bodine, A. Leri, and P. Anversa, *Bone marrow cells regenerate infarcted myocardium.* Nature, 2001. **410**(6829): p. 701-705.
44. Petersen, B.E., W.C. Bowen, K.D. Patrene, W.M. Mars, A.K. Sullivan, N. Murase, S.S. Boggs, J.S. Greenberger, and J.P. Goff, *Bone marrow as a potential source of hepatic oval cells.* Science, 1999. **284**(5417): p. 1168-1170.
45. Lagasse, E., H. Connors, M. Al-Dhalimy, M. Reitsma, M. Dohse, L. Osborne, X. Wang, M. Finegold, I.L. Weissman, and M. Grompe, *Purified hematopoietic stem cells can differentiate into hepatocytes in vivo.* Nature Medicine, 2000. **6**(11): p. 1229-1234.
46. Wagers, A.J., R.I. Sherwood, J.L. Christensen, and I.L. Weissman, *Little evidence for developmental plasticity of adult hematopoietic stem cells.* Science, 2002. **297**(5590): p. 2256-2259.
47. Alvarez-Dolado, M., R. Pardal, J.M. Garcia-Vardugo, J.R. Fike, H.O. Lee, K. Pfeffer, C. Lois, S.J. Morrison, and A. Alvarez-Buylla, *Fusion of bone-marrow-derived cells with Purkinje neurons, cardiomyocytes and hepatocytes.* Nature, 2003. **425**(6961): p. 968-973.

48. Ianus, A., G.G. Holz, N.D. Theise, and M.A. Hussain, *In vivo derivation of glucose-competent pancreatic endocrine cells from bone marrow without evidence of cell fusion.* Journal of Clinical Investigation, 2003. **111**(6): p. 843-850.
49. Kale, S., A. Karihaloo, P.R. Clark, M. Kashgarian, D.S. Krause, and L.G. Cantley, *Bone marrow stem cells contribute to repair of the ischemically injured renal tubule.* Journal of Clinical Investigation, 2003. **112**(1): p. 42-49.
50. Brazelton, T.R., F.M.V. Rossi, G.I. Keshet, and H.M. Blau, *From marrow to brain: Expression of neuronal phenotypes in adult mice.* Science, 2000. **290**(5497): p. 1775-1779.
51. Mezey, E., K.J. Chandross, G. Harta, R.A. Maki, and S.R. McKercher, *Turning blood into brain: Cells bearing neuronal antigens generated in vivo from bone marrow.* Science, 2000. **290**(5497): p. 1779-1782.
52. Yamada, S., K. Terada, Y. Ueno, T. Sugiyama, M. Seno, and I. Kojima, *Differentiation of adult hepatic stem-like cells into pancreatic endocrine cells.* Cell Transplantation, 2005. **14**(9): p. 647-653.
53. Zalzman, M., L. Anker-Kitai, and S. Efrat, *Differentiation of human liver-derived, insulin-producing cells toward the beta-cell phenotype.* Diabetes, 2005. **54**(9): p. 2568-2575.
54. Dabeva, M.D. and D.A. Shafritz, *Hepatic stem cells and liver repopulation.* Seminars in Liver Disease, 2003. **23**(4): p. 349-361.
55. Winslow, T. 2001 [cited 2010 25-06-2010]; Available from: http://teresewinslow.com/.
56. Aggarwal, S. and M.F. Pittenger, *Human mesenchymal stem cells modulate allogeneic immune cell responses.* Blood, 2005. **105**(4): p. 1815-1822.
57. Lee, O.K., T.K. Kuo, W.M. Chen, K.D. Lee, S.L. Hsieh, and T.H. Chen, *Isolation of multipotent mesenchymal stem cells from umbilical cord blood.* Blood, 2004. **103**(5): p. 1669-1675.
58. in't Anker, P.S., S.A. Scherjon, C. Kleijburg-van der Keur, G. de Groot-Swings, F.H.J. Claas, W.E. Fibbe, and H.H.H. Kanhai, *Isolation of mesenchymal stem cells of fetal or maternal origin from human placenta.* Stem Cells, 2004. **22**(7): p. 1338-1345.
59. Zuk, P.A., M. Zhu, P. Ashjian, D.A. De Ugarte, J.I. Huang, H. Mizuno, Z.C. Alfonso, J.K. Fraser, P. Benhaim, and M.H. Hedrick, *Human adipose tissue is a source of multipotent stem cells.* Molecular Biology of the Cell, 2002. **13**(12): p. 4279-4295.
60. Ashjian, P.H., A.S. Elbarbary, B. Edmonds, D. DeUgarte, M. Zhu, P.A. Zuk, H.P. Lorenz, P. Benhaim, and M.H. Hedrick, *In vitro differentiation of human processed lipoaspirate cells into early neural progenitors.* Plastic and Reconstructive Surgery, 2003. **111**(6): p. 1922-1931.
61. Huang, J.I., P.A. Zuk, N.F. Jones, M. Zhu, H.P. Lorenz, M.H. Hedrick, and P. Benhaim, *Chondrogenic potential of multipotential cells from human adipose tissue.* Plastic and Reconstructive Surgery, 2004. **113**(2): p. 585-594.
62. Pitchford, S.C., R.C. Furze, C.P. Jones, A.M. Wengner, and S.M. Rankin, *Differential Mobilization of Subsets of Progenitor Cells from the Bone Marrow.* Cell Stem Cell, 2009. **4**(1): p. 62-72.
63. Wakitani, S., M. Nawata, K. Tensho, T. Okabe, H. Machida, and H. Ohgushi, *Repair of articular cartilage defects in the patello-femoral joint with autologous bone marrow mesenchymal cell transplantation: three case*

reports involving nine defects in five knees. Journal of Tissue Engineering and Regenerative Medicine, 2007. **1**(1): p. 74-79.
64. Centeno, C.J., D. Busse, J. Kisiday, C. Keohan, M. Freeman, and D. Karli, *Regeneration of meniscus cartilage in a knee treated with percutaneously implanted autologous mesenchymal stem cells.* Medical Hypotheses, 2008. **71**(6): p. 900-908.
65. Centeno, C.J., D. Busse, J. Kisiday, C. Keohan, M. Freeman, and D. Karli, *Increased Knee Cartilage Volume in Degenerative Joint Disease using Percutaneously Implanted, Autologous Mesenchymal Stem Cells.* Pain Physician, 2008. **11**(3): p. 343-353.
66. Macchiarini, P., P. Jungebluth, T. Go, M.A. Asnaghi, L.E. Rees, T.A. Cogan, A. Dodson, J. Martorell, S. Bellini, P.P. Parnigotto, S.C. Dickinson, A.P. Hollander, S. Mantero, M.T. Conconi, and M.A. Birchall, *Clinical transplantation of a tissue-engineered airway.* Lancet, 2008. **372**(9655): p. 2023-2030.
67. Story C., L.d., *The promise and the challenge of stem cell research.* 2007.
68. Takahashi, K. and S. Yamanaka, *Induction of pluripotent stem cells from mouse embryonic and adult fibroblast cultures by defined factors.* Cell, 2006. **126**(4): p. 663-676.
69. Nakagawa, M., M. Koyanagi, K. Tanabe, K. Takahashi, T. Ichisaka, T. Aoi, K. Okita, Y. Mochiduki, N. Takizawa, and S. Yamanaka, *Generation of induced pluripotent stem cells without Myc from mouse and human fibroblasts.* Nature Biotechnology, 2008. **26**(1): p. 101-106.
70. Huangfu D, O.K., Maehr R, Guo W, Eijkelenboom A, Chen S, Muhlestein W, Melton DA, *Induction of pluripotent stem cells from primary human fibroblasts with only Oct4 and Sox2.* Nature Biotechnology 2008. **26**: p. 1269 - 1275
71. Aoi, T., K. Yae, M. Nakagawa, T. Ichisaka, K. Okita, K. Takahashi, T. Chiba, and S. Yamanaka, *Generation of pluripotent stem cells from adult mouse liver and stomach cells.* Science, 2008. **321**(5889): p. 699-702.
72. Kim, J.B., V. Sebastiano, G.M. Wu, M.J. Arauzo-Bravo, P. Sasse, L. Gentile, K. Ko, D. Ruau, M. Ehrich, D. van den Boom, J. Meyer, K. Hubner, C. Bernemann, C. Ortmeier, M. Zenke, B.K. Fleischmann, H. Zaehres, and H.R. Scholer, *Oct4-Induced Pluripotency in Adult Neural Stem Cells.* Cell, 2009. **136**(3): p. 411-419.
73. Yamanaka, S., *Ekiden to iPS Cells.* Nature Medicine, 2009. **15**(10): p. 1145-1148.
74. Lowry, W.E. and K. Plath, *The many ways to make an iPS cell.* Nature Biotechnology, 2008. **26**(11): p. 1246-1248.
75. Stadtfeld, M., M. Nagaya, J. Utikal, G. Weir, and K. Hochedlinger, *Induced Pluripotent Stem Cells Generated Without Viral Integration.* Science, 2008. **322**(5903): p. 945-949.
76. Okita, K., T. Ichisaka, and S. Yamanaka, *Generation of germline-competent induced pluripotent stem cells.* Nature, 2007. **448**(7151): p. 313-U1.
77. Vierbuchen, T., Ostermeier, A., P. Pang, Z., Kokubu, Y., C. Su¨dhof, T., Wernig, M., *Direct conversion of fibroblasts to functional neurons by defined factors.* Nature, 2010(10.1038).
78. *Definitions in biomaterials: proceedings of a consensus conference of the european society for biomaterials, Chester, England, March 3-5 1986*, ed. D.F. Williams. 1987: Elsevier.

79. *ASTM:F2150:HISTORICAL STANDARD:F2150-01 Standard guide for characterization and testing of biomaterial scaffolds used in tissue engineered medical products*, west conshohocken, PA: ASTM international
80. *The biomedical engineering handbook. [Vol. 1], Biomedical engineering fundamentals*. 3rd ed, ed. B. J.D. Vol. 1. 2006, Boca Raton, Fla: CRC Press, Taylor & Francis Group.
81. Rozga, J., *Liver support technology - an update.* Xenotransplantation, 2006. **13**(5): p. 380-389.
82. Bini, T.B., S.J. Gao, T.C. Tan, S. Wang, A. Lim, L.B. Hai, and S. Ramakrishna, *Electrospun poly(L-lactide-co-glycolide) biodegradable polymer nanofibre tubes for peripheral nerve regeneration.* Nanotechnology, 2004. **15**(11): p. 1459-1464.
83. Wang, W., S. Itoh, K. Konno, T. Kikkawa, S. Ichinose, K. Sakai, T. Ohkuma, and K. Watabe, *Effects of Schwann cell alignment along the oriented electrospun chitosan nanofibers on nerve regeneration.* Journal of Biomedical Materials Research Part A, 2009. **91A**(4): p. 994-1005.
84. Yang, S.F., K.F. Leong, Z.H. Du, and C.K. Chua, *The design of scaffolds for use in tissue engineering. Part 1. Traditional factors.* Tissue Engineering, 2001. **7**(6): p. 679-689.
85. Seidlits, S.K., Z.Z. Khaing, R.R. Petersen, J.D. Nickels, J.E. Vanscoy, J.B. Shear, and C.E. Schmidt, *The effects of hyaluronic acid hydrogels with tunable mechanical properties on neural progenitor cell differentiation.* Biomaterials. **31**(14): p. 3930-3940.
86. Suri, S. and C.E. Schmidt, *Cell-Laden Hydrogel Constructs of Hyaluronic Acid, Collagen, and Laminin for Neural Tissue Engineering.* Tissue Engineering Part A. **16**(5): p. 1703-1716.
87. Wang, L. and J.P. Stegemann, *Thermogelling chitosan and collagen composite hydrogels initiated with beta-glycerophosphate for bone tissue engineering.* Biomaterials. **31**(14).
88. Wang, F., Z. Li, M. Khan, K. Tamama, P. Kuppusamy, W.R. Wagner, C.K. Sen, and J. Guan, *Injectable, rapid gelling and highly flexible hydrogel composites as growth factor and cell carriers.* Acta Biomater. **6**(6): p. 1978-91.
89. Elisseeff, J., K. Anseth, D. Sims, W. McIntosh, M. Randolph, and R. Langer, *Transdermal photopolymerization for minimally invasive implantation.* Proc Natl Acad Sci U S A, 1999. **96**(6): p. 3104-3107.
90. Chung, H.J. and T.G. Park, *Surface engineered and drug releasing pre-fabricated scaffolds for tissue engineering.* Advanced Drug Delivery Reviews, 2007. **59**(4-5): p. 249-262.
91. Barbetta, A., A. Gumiero, R. Pecci, R. Bedini, and M. Dentini, *Gas-in-Liquid Foam Templating as a Method for the Production of Highly Porous Scaffolds.* Biomacromolecules, 2009. **10**(12).
92. Ellis, M.J. and J.B. Chaudhuri, *Poly(lactic-co-glycolic acid) hollow fibre membranes for use as a tissue engineering scaffold.* Biotechnology and Bioengineering, 2007. **96**(1): p. 177-187.
93. Venugopal, J., M.P. Prabhakaran, Y.Z. Zhang, S. Low, A.T. Choon, and S. Ramakrishna, *Biomimetic hydroxyapatite-containing composite nanofibrous substrates for bone tissue engineering.* Philosophical Transactions of the Royal Society a-Mathematical Physical and Engineering Sciences. **368**(1917): p. 2065-2081.

94. Colton, C.K., *Implantable biohybrid artificial organs* Cell Transplantation, 1995. **4**(4): p. 415-436.
95. Malda, J., T.B.F. Woodfield, F. van der Vloodt, F.K. Kooy, D.E. Martens, J. Tramper, C.A. van Blitterswijk, and J. Riesle, *The effect of PEGT/PBT scaffold architecture on oxygen gradients in tissue engineered cartilaginous constructs.* Biomaterials, 2004. **25**(26): p. 5773-5780.
96. Thomson, R.C., M.C. Wake, M.J. Yaszemski, and A.G. Mikos, *Biodegradable polymer scaffolds to regenerate organs.* Biopolymers Ii, 1995. **122**: p. 245-274.
97. Kim, B.S., C.E. Baez, and A. Atala, *Biomaterials for tissue engineering.* World Journal of Urology, 2000. **18**(1): p. 2-9.
98. Wake, M.C., C.W. Patrick, and A.G. Mikos, *Pore morphology effects on the fibrovascular tissue-growth in porous polymer substrates* Cell Transplantation, 1994. **3**(4): p. 339-343.
99. Yannas, I.V., *Facts and theories of induced organ regeneration.* Regenerative Medicine I: Theories, Models and Methods, 2005. **93**: p. 1-38.
100. Karageorgiou, V. and D. Kaplan, *Porosity of 3D biornaterial scaffolds and osteogenesis.* Biomaterials, 2005. **26**(27): p. 5474-5491.
101. *The biomedical engineering handbook. [Vol. 3], Tissue engineering and artificial organs* ed. J.D. Bronzino. 2006, Boca Raton, Fla: CRC Press, Taylor & Francis Group.
102. Grayson, W.L., P.H.G. Chao, D. Marolt, D.L. Kaplan, and G. Vunjak-Novakovic, *Engineering custom-designed osteochondral tissue grafts.* Trends in Biotechnology, 2008. **26**(4): p. 181-189.
103. Petrini, P., S. Fare, A. Piva, and M.C. Tanzi, *Design, synthesis and properties of polyurethane hydrogels for tissue engineering.* Journal of Materials Science-Materials in Medicine, 2003. **14**(8): p. 683-686.
104. Hu, W.J., J.W. Eaton, and L.P. Tang, *Molecular basis of biomaterial-mediated foreign body reactions.* Blood, 2001. **98**(4): p. 1231-1238.
105. Mikos, A.G., M.D. Lyman, L.E. Freed, and R. Langer, *Wetting of poly(L-lactic acid) and poly(DL-lactic-co-glycolic acid) foams for tissue culture.* Biomaterials, 1994. **15**(1): p. 55-8.
106. Nuttelman, C.R., D.J. Mortisen, S.M. Henry, and K.S. Anseth, *Attachment of fibronectin to poly(vinyl alcohol) hydrogels promotes NIH3T3 cell adhesion, proliferation, and migration.* Journal of Biomedical Materials Research, 2001. **57**(2): p. 217-223.
107. Hersel, U., C. Dahmen, and H. Kessler, *RGD modified polymers: biomaterials for stimulated cell adhesion and beyond.* Biomaterials, 2003. **24**(24): p. 4385-4415.
108. Flemming, R.G., C.J. Murphy, G.A. Abrams, S.L. Goodman, and P.F. Nealey, *Effects of synthetic micro- and nano-structured surfaces on cell behavior.* Biomaterials, 1999. **20**(6): p. 573-588.
109. Park, G.E., M.A. Pattison, K. Park, and T.J. Webster, *Accelerated chondrocyte functions on NaOH-treated PLGA scaffolds.* Biomaterials, 2005. **26**(16): p. 3075-3082.
110. Woo, K.M., V.J. Chen, and P.X. Ma, *Nano-fibrous scaffolding architecture enhances protein adsorption and cell attachment.* Bioinspired Nanoscale Hybrid Systems, 2003. **735**: p. 69-73.
111. Shin, M., O. Ishii, T. Sueda, and J.P. Vacanti, *Contractile cardiac grafts using a novel nanofibrous mesh.* Biomaterials, 2004. **25**(17): p. 3717-3723.

112. Lee, K.Y., E. Alsberg, and D.J. Mooney, *Degradable and injectable poly(aldehyde guluronate) hydrogels for bone tissue engineering.* Journal of Biomedical Materials Research, 2001. **56**(2): p. 228-233.
113. Ferrer, M.-H., *Development and Characterisation of completely degradable composite tissue engineering scaffolds*. 2007.
114. Rajendran, *Engineering Physics*. 2009, New Delhi: TataMc-Graw Hill Publishing company Ltd.
115. Vert, M., S.M. Li, G. Spenlehauer, and P. Guerin, *Bioresorbability and biocompatibility of aliphatic polyesters* Journal of Materials Science-Materials in Medicine, 1992. **3**(6): p. 432-446.
116. Reed, A.M. and D.K. Gilding, *Biodegradable polymers for use in surgery-poly(glycolic)-poly(lactic acid) homo and co-polymers. 2. In vitro degradation* Polymer, 1981. **22**(4): p. 494-498.
117. Vainionpaa, S., J. Kilpikari, J. Laiho, P. Helevirta, P. Rokkanen, and P. Tormala, *Strength and strength retention in vitro, of absorbable, self-reinforced polyglycolide (PGA) rods for fracture fixation* Biomaterials, 1987. **8**(1): p. 46-48.
118. Bostman, O.M., *Absorbable implants for the fixation of fractures* Journal of Bone and Joint Surgery-American Volume, 1991. **73A**(1): p. 148-153.
119. Catiker, E., *Degradation of PLA, PLGA homo- and copolymers in the presence of serum albumin: a spectroscopic investigation* Polymer International, 2000. **49**(7): p. 728-734.
120. Intra, J., *Pulsatile release of biomolecules from polydimethylsiloxane (PDMS) chips with hydrolytically degradable seals* Journal of Controlled Release, 2008. **127**(3).
121. Lu, L., S.J. Peter, M.D. Lyman, H.L. Lai, S.M. Leite, J.A. Tamada, S. Uyama, J.P. Vacanti, R. Langer, and A.G. Mikos, *In vitro and in vivo degradation of porous poly(DL-lactic-co-glycolic acid) foams.* Biomaterials, 2000. **21**(18): p. 1837-1845.
122. Middleton, J.C. and A.J. Tipton, *Synthetic biodegradable polymers as orthopedic devices.* Biomaterials, 2000. **21**(23): p. 2335-2346.
123. Oh, S.H., S.G. Kang, and J.H. Lee, *Degradation behavior of hydrophilized PLGA scaffolds prepared by melt-molding particulate-leaching method: Comparison with control hydrophobic one.* Journal of Materials Science-Materials in Medicine, 2006. **17**(2): p. 131-137.
124. Leung, L., C. Chan, S. Baek, and H. Naguib, *Comparison of morphology and mechanical properties of PLGA bioscaffolds.* Biomedical Materials, 2008. **3**(2).
125. Pamula, E. and E. Menaszek, *In vitro and in vivo degradation of poly(L-lactide-co-glycolide) films and scaffolds.* Journal of Materials Science-Materials in Medicine, 2008. **19**(5): p. 2063-2070.
126. Moshfeghian, A., J. Tillman, and S.V. Madihally, *Characterization of emulsified chitosan-PLGA matrices formed using controlled-rate freezing and lyophilization technique.* Journal of Biomedical Materials Research Part A, 2006. **79A**(2): p. 418-430.
127. Ge, Z.G., L.S. Wang, B.C. Heng, X.F. Tian, K. Lu, V.T.W. Fan, J.F. Yeo, T. Cao, and E. Tan, *Proliferation and Differentiation of Human Osteoblasts within 3D printed Poly-Lactic-co-Glycolic Acid Scaffolds.* Journal of Biomaterials Applications, 2009. **23**(6): p. 533-547.

128. Shearer, H., M.J. Ellis, S.P. Perera, and J.B. Chaudhuri, *Effects of common sterilization methods on the structure and properties of poly(D,L lactic-co-glycolic acid) scaffolds.* Tissue Eng, 2006. **12**(10): p. 2717-27.
129. Gao, J., L. Niklason, and R. Langer, *Surface hydrolysis of poly(glycolic acid) meshes increases the seeding density of vascular smooth muscle cells.* J Biomed Mater Res, 1998. **42**(3): p. 417-24.
130. Bhati, R.S., D.P. Mukherjee, K.J. McCarthy, S.H. Rogers, D.F. Smith, and S.W. Shalaby, *The growth of chondrocytes into a fibronectin-coated biodegradable scaffold.* J Biomed Mater Res, 2001. **56**(1): p. 74-82.
131. Wu, S.R., G.S. Sheu, and S.S. Shyu, *Kevlar fiber-epoxy adhesion and its effect on composite mechanical and fracture properties by plasma and chemical treatment.* Journal of Applied Polymer Science, 1996. **62**(9): p. 1347-1360.
132. Cai, Q., J. Yang, J. Bei, and S. Wang, *A novel porous cells scaffold made of polylactide-dextran blend by combining phase-separation and particle-leaching techniques.* Biomaterials, 2002. **23**(23): p. 4483-92.
133. Uragami, T., Y. Naito, and M. Sugihara, *Studies on Synthesis and Permeability of Special Polymer Membranes .39. Permeation Characteristics and Structure of Polymer Blend Membranes from Poly(Vinylidene Fluoride) and Poly(Ethylene Glycol).* Polymer Bulletin, 1981. **4**(10): p. 617-622.
134. Yin, X.L., H.B. Cheng, X. Wang, and Y.X. Yao, *Morphology and properties of hollow-fiber membrane made by PAN mixing with small amount of PVDF.* Journal of Membrane Science, 1998. **146**(2): p. 179-184.
135. Giusti, P., L. Lazzeri, M.G. Cascone, and M. Seggiani, *Blends of Synthetic and Natural Polymers as Special Performance Materials.* Macromolecular Symposia, 1995. **100**: p. 81-87.
136. Koyano, T., N. Minoura, and M. Nagura, *Preparation of poly(vinyl alcohol)-blended hydrogels with an inhibition effect for cell attachment and their permeation properties of vitamin B-12 and dissolved oxygen.* Kobunshi Ronbunshu, 1998. **55**(6): p. 305-313.
137. Lin, W.J. and C.H. Lu, *Characterization and permeation of microporous poly (epsilon-caprolactone) films.* Journal of Membrane Science, 2002. **198**(1): p. 109-118.
138. Solak, E.K., G. Asman, P. Camurlu, and O. Sanli, *Sorption, diffusion, and pervaporation characteristics of dimethylformamide/water mixtures using sodium alginate/polyvinyl pyrrolidone blend membranes.* Vacuum, 2008. **82**(6): p. 579-587.
139. Sanli, O., E. Orhan, and G. Asman, *Release of salicylic acid through poly(vinyl alcohol/poly(vinyl pyrrolidone) and poly(vinyl alcohol-g-N-vinyl-2-pyrrolidone) membranes.* Journal of Applied Polymer Science, 2006. **102**(2): p. 1244-1253.
140. Wan, L.S., Z.K. Xu, X.J. Huang, A.F. Che, and Z.G. Wang, *A novel process for the post-treatment of polyacrylonitrile-based membranes: Performance improvement and possible mechanism.* Journal of Membrane Science, 2006. **277**(1-2): p. 157-164.
141. Qin, J.J., Y. Li, L.S. Lee, and H. Lee, *Cellulose acetate hollow fiber ultrafiltration membranes made from CA/PVP 360 K/NMP/water.* Journal of Membrane Science, 2003. **218**(1-2): p. 173-183.

142. Qin, J.J., F.S. Wong, Y. Li, and Y.T. Liu, *A high flux ultrafiltration membrane spun from PSU/PVP (K90)/DMF/1,2-propanediol.* Journal of Membrane Science, 2003. **211**(1): p. 139-147.
143. Svang-Ariyaskul, A., R.Y.M. Huang, P.L. Douglas, R. Pal, X. Feng, P. Chen, and L. Liu, *Blended chitosan and polyvinyl alcohol membranes for the pervaporation dehydration of isopropanol.* Journal of Membrane Science, 2006. **280**(1-2): p. 815-823.
144. Bahrami, S.B., S.S. Kordestani, H. Mirzadeh, and P. Mansoori, *Poly(vinyl alcohol) - Chitosan blends: Preparation, mechanical and physical properties.* Iranian Polymer Journal, 2003. **12**(2): p. 139-146.
145. Paul, W. and C.P. Sharma, *Polyetherurethaneurea Reinforced Poly(Vinyl Alcohol) Dialysis Membranes - Studies on Permeability and Mechanical Strength.* Bulletin of Materials Science, 1994. **17**(6): p. 1065-1070.
146. Nakatsuka, S. and A.L. Andrady, *Permeability of Vitamin-B12 in Chitosan Membranes - Effect of Cross-Linking and Blending with Poly(Vinyl Alcohol) on Permeability.* Journal of Applied Polymer Science, 1992. **44**(1): p. 17-28.
147. Oh, S.H., S.G. Kang, E.S. Kim, S.H. Cho, and J.H. Lee, *Fabrication and characterization of hydrophilic poly(lactic-co-glycolic acid)/poly(vinyl alcohol) blend cell scaffolds by melt-molding particulate-leaching method.* Biomaterials, 2003. **24**(22): p. 4011-4021.
148. Holland, B.H., JN, *The effect of polymerisation conditions on the kinetics and mechanisms of thermal degradation of PMMA* Polymer degradation and stability, 2002. **77**(3): p. 435-439.
149. Vijayalakshmi, S.M., G, *Photodegradation of poly(vinyl alcohol) under UV and pulsed-laser irradiation in aqueous solution* Journal of applied polymer science, 2006. **102**(2).
150. Qin, X.H. and S.Y. Wang, *Electrospun nanofibers from crosslinked poly(vinyl alcohol) and its filtration efficiency.* Journal of Applied Polymer Science, 2008. **109**(2): p. 951-956.
151. Luadthong, C., A. Tachaprutinun, and S.P. Wanichwecharungruang, *Synthesis and characterization of micro/nanoparticles of poly(vinylalcohol-co-vinylcinnamate) derivatives.* European Polymer Journal, 2008. **44**(5): p. 1285-1295.
152. Yue, Y.M., K. Xu, X.G. Liu, Q. Chen, X. Sheng, and P.X. Wang, *Preparation and characterization of interpenetration polymer network films based on poly(vinyl alcohol) and poly(acrylic acid) for drug delivery.* Journal of Applied Polymer Science, 2008. **108**(6): p. 3836-3842.
153. Grayson, W.L., T.P. Martens, G.M. Eng, M. Radisic, and G. Vunjak-Novakovic, *Biomimetic approach to tissue engineering.* Seminars in Cell & Developmental Biology, 2009. **20**(6): p. 665-673.
154. Bancroft, G.N., V.I. Sikavitsas, and A.G. Mikos, *Design of a flow perfusion bioreactor system for bone tissue-engineering applications.* Tissue Engineering, 2003. **9**(3): p. 549-554.
155. Godara, P., C.D. McFarland, and R.E. Nordon, *Design of bioreactors for mesenchymal stem cell tissue engineering.* Journal of Chemical Technology and Biotechnology, 2008. **83**(4): p. 408-420.
156. Martin, Y. and P. Vermette, *Bioreactors for tissue mass culture: Design, characterization, and recent advances.* Biomaterials, 2005. **26**(35): p. 7481-7503.

157. Chen, X., H. Xu, C. Wan, M. McCaigue, and G. Li, *Bioreactor expansion of human adult bone marrow-derived mesenchymal stem cells.* Stem Cells, 2006. **24**(9): p. 2052-2059.
158. Vunjak-Novakovic, G., I. Martin, B. Obradovic, S. Treppo, A.J. Grodzinsky, R. Langer, and L.E. Freed, *Bioreactor cultivation conditions modulate the composition and mechanical properties of tissue-engineered cartilage.* Journal of Orthopaedic Research, 1999. **17**(1): p. 130-138.
159. Granet, C., N. Laroche, L. Vico, C. Alexandre, and M.H. Lafage-Proust, *Rotating-wall vessels, promising bioreactors for osteoblastic cell culture: comparison with other 3D conditions.* Medical & Biological Engineering & Computing, 1998. **36**(4): p. 513-519.
160. Lelkes, P.I., D.L. Galvan, G.T. Hayman, T.J. Goodwin, D.Y. Chatman, S. Cherian, R.M.G. Garcia, and B.R. Unsworth, *Simulated microgravity conditions enhance differentiation of cultured PC12 cells towards the neuroendocrine phenotype.* In Vitro Cellular & Developmental Biology-Animal, 1998. **34**(4): p. 316-325.
161. Chang, T.T. and M. Hughes-Fulford, *Monolayer and Spheroid Culture of Human Liver Hepatocellular Carcinoma Cell Line Cells Demonstrate Distinct Global Gene Expression Patterns and Functional Phenotypes.* Tissue Engineering Part A, 2009. **15**(3): p. 559-567.
162. Frye, C.A. and C.W. Patrick, *Three-dimensional adipose tissue model using low shear bioreactors.* In Vitro Cellular & Developmental Biology-Animal, 2006. **42**(5-6): p. 109-114.
163. Frerich, B., K. Zuckmantel, K. Winter, S. Muller-Durwald, and A. Hemprich, *Maturation of capillary-like structures in a tube-like construct in perfusion and rotation culture.* International Journal of Oral and Maxillofacial Surgery, 2008. **37**(5): p. 459-466.
164. Carrier, R.L., M. Papadaki, M. Rupnick, F.J. Schoen, N. Bursac, R. Langer, L.E. Freed, and G. Vunjak-Novakovic, *Cardiac tissue engineering: Cell seeding, cultivation parameters, and tissue construct characterization.* Biotechnology and Bioengineering, 1999. **64**(5): p. 580-589.
165. Chen, H.C. and Y.C. Hu, *Bioreactors for tissue engineering.* Biotechnology Letters, 2006. **28**: p. 1415-1423.
166. Hammond, T.G. and J.M. Hammond, *Optimized suspension culture: the rotating-wall vessel.* American Journal of Physiology-Renal Physiology, 2001. **281**(1): p. F12-F25.
167. Powers, M.J., K. Domansky, M.R. Kaazempur-Mofrad, A. Kalezi, A. Capitano, A. Upadhyaya, P. Kurzawski, K.E. Wack, D.B. Stolz, R. Kamm, and L.G. Griffith, *A microfabricated array bioreactor for perfused 3D liver culture.* Biotechnology and Bioengineering, 2002. **78**(3): p. 257-269.
168. Martin, I., D. Wendt, and M. Heberer, *The role of bioreactors in tissue engineering.* Trends in Biotechnology, 2004. **22**(2): p. 80-86.
169. Chaudhuri, J. and M. Al-Rubeai, *Bioreactors for tissue engineeering : principles, design and operation*. 2005, Dordrecht: Springer. viii, 375 p.
170. Jackson, L.R., L.J. Trudel, and N.S. Lipman, *Small-scale monoclonal antibody production in vitro: Methods and resources.* Lab Animal, 1999. **28**(3): p. 38-+.
171. Malone, C.C., P.M. Schiltz, A.D. Mackintosh, L.D. Beutel, F.S. Heinemann, and R.O. Dillman, *Characterization of human tumor-infiltrating lymphocytes*

expanded in hollow-fiber bioreactors for immunotherapy of cancer. Cancer Biotherapy and Radiopharmaceuticals, 2001. **16**(5): p. 381-390.
172. Pan, D., D.F. Stroncek, and C.B. Whitley, *Improved gene transfer and normalized enzyme levels in primitive hematopoietic progenitors from patients with mucopolysaccharidosis type I using a bioreactor.* Journal of Gene Medicine, 2004. **6**(12): p. 1293-1303.
173. Dewar, V., P. Voet, F. Denamur, and J. Smal, *Industrial implementation of in vitro production of monoclonal antibodies.* Ilar Journal, 2005. **46**(3): p. 307-313.
174. Gardner, T.A., S.C. Ko, L. Yang, J.J.S. Cadwell, L.W.K. Chung, and C. Kao, *Serum-free recombinant production of adenovirus using a hollow fiber capillary system.* Biotechniques, 2001. **30**(2): p. 422-+.
175. Bowry, S.K., *Dialysis membranes today.* International Journal of Artificial Organs, 2002. **25**(5): p. 447-460.
176. Abu-Absi, S.F., G. Seth, R.A. Narayanan, K. Groehler, P. Lai, M.L. Anderson, T. Sielaff, and W.S. Hu, *Characterization of a hollow fiber bioartificial liver device.* Artificial Organs, 2005. **29**(5): p. 419-422.
177. Haque, M.A., M. Nagaoka, B. Hexig, and T. Akaike, *Artificial extracellular matrix for embryonic stem cell cultures: a new frontier of nanobiomaterials.* Science and Technology of Advanced Materials. **11**(1).
178. Moore, R.N., A. Dasgupta, N. Rajaei, M.L. Yarmush, M. Toner, L. Larue, and P.V. Moghe, *Enhanced Differentiation of Embryonic Stem Cells Using Co-Cultivation With Hepatocytes.* Biotechnology and Bioengineering, 2008. **101**(6): p. 1332-1343.
179. Albrecht, D.R., G.H. Underhill, T.B. Wassermann, R.L. Sah, and S.N. Bhatia, *Probing the role of multicellular organization in three-dimensional microenvironments.* Nature Methods, 2006. **3**(5): p. 369-375.
180. Shav, D. and S. Einav, *The effect of mechanical loads in the differentiation of precursor cells into mature cells.* Analysis of Cardiac Development: From Embryo to Old Age. **1188**: p. 25-31.
181. Kim, B.S., K.S. Kang, and S.K. Kang, *Soluble factors from ASCs effectively direct control of chondrogenic fate.* Cell Proliferation. **43**(3): p. 249-261.
182. Moore, R.N. and P.V. Moghe, *Expedited growth factor-mediated specification of human embryonic stem cells toward the hepatic lineage.* Stem Cell Research, 2009. **3**(1): p. 51-62.
183. Lange, C., H. Bruns, D. Kluth, A.R. Zander, and H.C. Fiegel, *Hepatocytic differentiation of mesenchymal stem cells in cocultures with fetal liver cells.* World Journal of Gastroenterology, 2006. **12**(15): p. 2394-2397.
184. Mitaka, T., F. Sato, T. Mizuguchi, T. Yokono, and Y. Mochizuki, *Reconstruction of hepatic organoid by rat small hepatocytes and hepatic nonparenchymal cells.* Hepatology, 1999. **29**(1): p. 111-125.
185. Csaki, C., U. Matis, A. Mobasheri, and M. Shakibaei, *Co-culture of canine mesenchymal stem cells with primary bone-derived osteoblasts promotes osteogenic differentiation.* Histochemistry and Cell Biology, 2009. **131**(2): p. 251-266.
186. Buytaert-Hoefen, K.A., E. Alvarez, and C.R. Freed, *Generation of tyrosine hydroxylase positive neurons from human embryonic stem cells after coculture with cellular substrates and exposure to GDNF.* Stem Cells, 2004. **22**(5): p. 669-674.

187. Abouelfetouh, A., T. Kondoh, K. Ehara, and E. Kohmura, *Morphological differentiation of bone marrow stromal cells into neuron-like cells after co-culture with hippocampal slice.* Brain Research, 2004. **1029**(1): p. 114-119.
188. Wislet-Gendebien, S., G. Hans, P. Leprince, J.M. Rigo, G. Moonen, and B. Rogister, *Plasticity of cultured mesenchymal stem cells: Switch from nestin-positive to excitable neuron-like phenotype.* Stem Cells, 2005. **23**(3): p. 392-402.
189. Coleman, B., J.B. Fallon, L.N. Pettingill, M.G. de Silva, and R.K. Shepherd, *Auditory hair cell explant co-cultures promote the differentiation of stem cells into bipolar neurons.* Experimental Cell Research, 2007. **313**(2): p. 232-243.
190. Kawasaki, H., K. Mizuseki, S. Nishikawa, S. Kaneko, Y. Kuwana, S. Nakanishi, and Y. Sasai, *Induction of midbrain dopaminergic neurons from ES cells by stromal cell-derived inducing activity.* Neuron, 2000. **28**(1): p. 31-40.
191. Morizane, A., J. Takahashi, Y. Takagi, Y. Sasai, and N. Hashimoto, *Optimal conditions for in vivo induction of dopaminergic neurons from embryonic stem cells through stromal cell-derived inducing activity.* Journal of Neuroscience Research, 2002. **69**(6): p. 934-939.
192. Liu, J., J. Huang, T.X. Lin, C.X. Zhang, and X.B. Yin, *Cell-to-cell contact induces human adipose tissue-derived stromal cells to differentiate into urothelium-like cells in vitro.* Biochemical and Biophysical Research Communications, 2009. **390**(3): p. 931-936.
193. Chai, C. and K.W. Leong, *Biomaterials approach to expand and direct differentiation of stem cells.* Molecular Therapy, 2007. **15**(3): p. 467-480.
194. Ehring, B., K. Biber, T.M. Upton, D. Plosky, M. Pykett, and M. Rosenzweig, *Expansion of HPCs from cord blood in a novel 3D matrix.* Cytotherapy, 2003. **5**(6): p. 490-499.
195. Willerth, S.M., T.E. Faxel, D.I. Gottlieb, and S.E. Sakiyama-Elbert, *The effects of soluble growth factors on embryonic stem cell differentiation inside of fibrin scaffolds.* Stem Cells, 2007. **25**(9): p. 2235-2244.
196. Im, G.I., *Chondrogenesis from mesenchymal stem cells derived from adipose tissue on the fibrin scaffold.* Current Applied Physics, 2005. **5**(5): p. 438-443.
197. Kim, H.S., J.B. Lim, Y.H. Min, S.T. Lee, C.J. Lyu, E.S. Kim, and H.O. Kim, *Ex vivo expansion of human umbilical cord blood CD34(+) cells in a collagen bead-containing 3-dimensional culture system.* International Journal of Hematology, 2003. **78**(2): p. 126-132.
198. Meinel, L., S. Hofmann, V. Karageorgiou, L. Zichner, R. Langer, D. Kaplan, and G. Vunjak-Novakovic, *Engineering cartilage-like tissue using human mesenchymal stem cells and silk protein scaffolds.* Biotechnology and Bioengineering, 2004. **88**(3): p. 379-391.
199. Taqvi, S. and K. Roy, *Influence of scaffold physical properties and stromal cell coculture on hematopoietic differentiation of mouse embryonic stem cells.* Biomaterials, 2006. **27**(36): p. 6024-6031.
200. Li, W.J., R. Tuli, X.X. Huang, P. Laquerriere, and R.S. Tuan, *Multilineage differentiation of human mesenchymal stem cells in a three-dimensional nanofibrous scaffold.* Biomaterials, 2005. **26**(25): p. 5158-5166.
201. Kang X., X.Y., Powell H.M., James Lee L., Belury M.A., Lanutti J.J., Kniss D.A., *Adipogenesis of murine embryonic stem cells in a three-dimensional culture system using electrospun polymer scaffolds.* Biomaterials, 2007. **28**: p. 450-458.

202. Hwang, N.S., M.S. Kim, S. Sampattavanich, J.H. Baek, Z.J. Zhang, and J. Elisseeff, *Effects of three-dimensional culture and growth factors on the chondrogenic differentiation of murine embryonic stem cells.* Stem Cells, 2006. **24**(2): p. 284-291.
203. Curran, J.M., R. Chen, R. Stokes, E. Irvine, D. Graham, E. Gubbins, D. Delaney, N. Amro, R. Sanedrin, H. Jamil, and J.A. Hunt, *Nanoscale definition of substrate materials to direct human adult stem cells towards tissue specific populations.* Journal of Materials Science-Materials in Medicine. **21**(3): p. 1021-1029.
204. Yilgor, P., N. Hasirci, and V. Hasirci, *Sequential BMP-2/BMP-7 delivery from polyester nanocapsules.* Journal of Biomedical Materials Research Part A. **93A**(2): p. 528-536.
205. Weiss, S., T. Hennig, R. Bock, E. Steck, and W. Richter, *Impact of Growth Factors and PTHrP on Early and Late Chondrogenic Differentiation of Human Mesenchymal Stem Cells.* Journal of Cellular Physiology. **223**(1): p. 84-93.
206. Huppert, S.S. and M.A. Magnuson, *New Complexity in Differentiating Stem Cells Toward Hepatic and Pancreatic Fates.* Science Signaling, 2009. **2**(83).
207. Guguen-Guillouzo, C., A. Corlu, and A. Guillouzo, *Stem cell-derived hepatocytes and their use in toxicology.* Toxicology. **270**(1): p. 3-9.
208. Touboul, T., N.R.F. Hannan, S. Corbineau, A. Martinez, C. Martinet, S. Branchereau, S. Mainot, H. Strick-Marchand, R. Pedersen, J. Di Santo, A. Weber, and L. Vallier, *Generation of Functional Hepatocytes from Human Embryonic Stem Cells Under Chemically Defined Conditions that Recapitulate Liver Development.* Hepatology. **51**(5): p. 1754-1765.
209. Stern, C.D., *Neural induction: old problem, new findings, yet more questions.* Development, 2005. **132**(9): p. 2007-2021.
210. Cohen, M.A., P. Itsykson, and B.E. Reubinoff, *The role of FGF-signaling in early neural specification of human embryonic stem cells.* Developmental Biology. **340**(2): p. 450-458.
211. Sun, J.Q., W.H. Zhou, B. Sha, and Y. Yang, *Ischemia induced neural stem cell proliferation and differentiation in neonatal rat involved vascular endothelial growth factor and transforming growth factor-beta pathways.* Brain & Development. **32**(3): p. 191-200.
212. Vazin, T., K.G. Becker, J. Chen, C.E. Spivak, C.R. Lupica, Y.Q. Zhang, L. Worden, and W.J. Freed, *A Novel Combination of Factors, Termed SPIE, which Promotes Dopaminergic Neuron Differentiation from Human Embryonic Stem Cells.* Plos One, 2009. **4**(8).
213. Snykers, S., T. Vanhaecke, P. Papeleu, A. Luttun, Y.H. Jiang, Y. Vander Heyden, C. Verfaillie, and V. Rogiers, *Sequential exposure to cytokines reflecting embryogenesis: The key for in vitro differentiation of adult bone marrow stem cells into functional hepatocyte-like cells.* Toxicological Sciences, 2006. **94**(2): p. 330-341.
214. Raiche, A.T. and D.A. Puleo, *In vitro effects of combined and sequential delivery of two bone growth factors.* Biomaterials, 2004. **25**(4): p. 677-685.
215. Yilgor, P., K. Tuzlakoglu, R.L. Reis, N. Hasirci, and V. Hasirci, *Incorporation of a sequential BMP-2/BMP-7 delivery system into chitosan-based scaffolds for bone tissue engineering.* Biomaterials, 2009. **30**(21): p. 3551-3559.

216. Park, J., E. Lim, S. Back, H. Na, Y. Park, and K. Sun, *Nerve regeneration following spinal cord injury using matrix metalloproteinase-sensitive, hyaluronic acid-based biomimetic hydrogel scaffold containing brain-derived neurotrophic factor.* Journal of Biomedical Materials Research Part A. **93A**(3): p. 1091-1099.
217. Sahoo, S., L.T. Ang, J.C.H. Goh, and S.L. Toh, *Growth factor delivery through electrospun nanofibers in scaffolds for tissue engineering applications.* Journal of Biomedical Materials Research Part A. **93A**(4): p. 1539-1550.
218. Jeon, O., S.J. Song, H.S. Yang, S.H. Bhang, S.W. Kang, M.A. Sung, J.H. Lee, and B.S. Kim, *Long-term delivery enhances in vivo osteogenic efficacy of bone morphogenetic protein-2 compared to short-term delivery.* Biochemical and Biophysical Research Communications, 2008. **369**(2): p. 774-780.
219. Wei, G.B., Q.M. Jin, W.V. Giannobile, and P.X. Ma, *The enhancement of osteogenesis by nano-fibrous scaffolds incorporating rhBMP-7 nanospheres.* Biomaterials, 2007. **28**(12): p. 2087-2096.
220. Tzeng, S.Y. and E.B. Lavik, *Photopolymerizable nanoarray hydrogels deliver CNTF and promote differentiation of neural stem cells.* Soft Matter. **6**(10): p. 2208-2215.
221. Hay, D.C., D. Zhao, A. Ross, R. Mandalam, J. Lebkowski, and W. Cui, *Direct differentiation of human embryonic stem cells to hepatocyte-like cells exhibiting functional activities.* Cloning and Stem Cells, 2007. **9**(1): p. 51-62.
222. Choi, K.-H., B.H. Choi, S.R. Park, B.J. Kim, and B.-H. Min, *The chondrogenic differentiation of mesenchymal stem cells on an extracellular matrix scaffold derived from porcine chondrocytes.* Biomaterials. **31**(20): p. 5355-65.
223. Andrade-Zaldivar, H., L. Santos, and A.D. Rodriguez, *Expansion of human hematopoietic stem cells for transplantation: trends and perspectives.* Cytotechnology, 2008. **56**(3): p. 151-160.
224. Zhao, F., R. Chella, and T. Ma, *Effects of shear stress on 3-D human mesenchymal stem cell construct development in a perfusion bioreactor system: Experiments and hydrodynamic modeling.* Biotechnology and Bioengineering, 2007. **96**(3): p. 584-595.
225. Fehrer, C., R. Brunauer, G. Laschober, H. Unterluggauer, S. Reitinger, F. Kloss, C. Gully, R. Gassner, and G. Lepperdinger, *Reduced oxygen tension attenuates differentiation capacity of human mesenchymal stem cells and prolongs their lifespan.* Aging Cell, 2007. **6**: p. 745-757.
226. Zhao, F. and T. Ma, *Perfusion bioreactor system for human mesenchymal stem cell tissue engineering: Dynamic cell seeding and construct development.* Biotechnology and Bioengineering, 2005. **91**(4): p. 482-493.
227. Dang, S.M., S. Gerecht-Nir, J. Chen, J. Itskovitz-Eldor, and P.W. Zandstra, *Controlled, scalable embryonic stem cell differentiation culture.* Stem Cells, 2004. **22**(3): p. 275-282.
228. Bauwens, C., T. Yin, S. Dang, R. Peerani, and P.W. Zandstra, *Development of a perfusion fed bioreactor for embryonic stem cell-derived cardiomyocyte generation: Oxygen-mediated enhancement of cardiomyocyte output.* Biotechnology and Bioengineering, 2005. **90**(4): p. 452-461.
229. Gerecht-Nir, S., S. Cohen, and J. Itskovitz-Eldor, *Bioreactor cultivation enhances the efficiency of human embryoid body (hEB) formation and differentiation.* Biotechnology and Bioengineering, 2004. **86**(5): p. 493-502.

230. Azarin, S.M. and S.P. Palecek, *Development of scalable culture systems for human embryonic stem cells.* Biochemical Engineering Journal. **48**(3): p. 378-384.
231. Serra, M., C. Brito, E.M. Costa, M.F.Q. Sousa, and P.M. Alves, *Integrating human stem cell expansion and neuronal differentiation in bioreactors.* Bmc Biotechnology, 2009. **9**.
232. Serra, M., C. Brito, S.B. Leite, E. Gorjup, H. von Briesen, M.J.T. Carrondo, and P.M. Alves, *Stirred bioreactors for the expansion of adult pancreatic stem cells.* Annals of Anatomy-Anatomischer Anzeiger, 2009. **191**(1): p. 104-115.
233. Shearer, H., *Hollow fibre bioreactors for bone tissue engineering*, in *Chemical Engineering*. 2007, Bath: Bath. p. 298.
234. Li, K., J.F. Kong, D.L. Wang, and W.K. Teo, *Tailor-made asymmetric PVDF hollow fibers for soluble gas removal.* Aiche Journal, 1999. **45**(6): p. 1211-1219.
235. Bradford, M.M., *Rapid and Sensitive Method for Quantitation of Microgram Quantities of Protein Utilizing Principle of Protein-Dye Binding.* Analytical Biochemistry, 1976. **72**(1-2): p. 248-254.
236. Collins, S.J., *The HL-60 promyelocytic leukemia-cell line- proliferation, differentiation, and cellular oncogene expression* Blood, 1987. **70**(5): p. 1233-1244.
237. Cho, M.H., K.S. Kim, H.H. Ahn, M.S. Kim, S.H. Kim, G. Khang, B. Lee, and H.B. Lee, *Chitosan gel as an in situ-forming scaffold for rat bone marrow mesenchymal stem cells in vivo.* Tissue Engineering Part A, 2008. **14**(6): p. 1099-1108.
238. Denizot, F. and R. Lang, *Rapid colorimetric assay for cell-growth and survival- modifications to the tetrazolium dye procedure giving improved sensitivity and reliability* Journal of Immunological Methods, 1986. **89**(2): p. 271-277.
239. Inaba, M., H. Koyama, M. Hino, S. Okuno, M. Terada, Y. Nishizawa, T. Nishino, and H. Morii, *Regulation of release of hepatocyte growth factor from Human promyelocytic leukemia-cells, HL-60, by 1,25-dihydroxyvitamin-D(3), 12-O-tetradecanoylphorbol 13-acetate, and dibutyryl cyclic adenosine-monophosphate* Blood, 1993. **82**(1): p. 53-59.
240. Matsumoto, K., H. Tajima, H. Okazaki, and T. Nakamura, *Heparin as an inducer of hepatocyte growth-factor* Journal of Biochemistry, 1993. **114**(6): p. 820-826.
241. Snykers, S., T. Vanhaecke, A. De Becker, P. Papeleu, M. Vinken, I. Van Riet, and V. Rogiers, *Chromatin remodeling agent trichostatin A: a key-factor in the hepatic differentiation of human mesenchymal stem cells derived of adult bone marrow*. Bmc Developmental Biology, 2007. **7**: p. 15.
242. Sutherland, R.M., B. Sordat, J. Bamat, H. Gabbert, B. Bourrat, and W. Muellerklieser, Oxygenation and differentiation in multicellular spheroids of human-colon carcinoma. Cancer Research, 1986. **46**(10): p. 5320-5329.
243. Susanto, H. and M. Ulbricht, *Characteristics, performance and stability of polyethersulfone ultrafiltration membranes prepared by phase separation method using different macromolecular additives.* Journal of Membrane Science, 2009. **327**(1-2): p. 125-135.
244. Caillou, S., C.J.P. Boonaert, J.L. Dewez, and P.G. Rouxhet, *Oxidation of proteins adsorbed on hemodialysis membranes and model materials.* Journal

of Biomedical Materials Research Part B-Applied Biomaterials, 2008. **84B**(1): p. 240-248.
245. Arkhangelsky, E., D. Kuzmenko, and V. Gitis, *Impact of chemical cleaning on properties and functioning of polyethersulfone membranes.* Journal of Membrane Science, 2007. **305**: p. 176-184.
246. Arahman, N., T. Maruyama, T. Sotani, and H. Matsuyama, *Fouling Reduction of a Poly(ether sulfone) Hollow-Fiber Membrane with a Hydrophilic Surfactant Prepared via Non-Solvent-Induced Phase Separation.* Journal of Applied Polymer Science, 2009. **111**(3): p. 1653-1658.
247. Jung, B., J.K. Yoon, B. Kim, and H.W. Rhee, *Effect of molecular weight of polymeric additives on formation, permeation properties and hypochlorite treatment of asymmetric polyacrylonitrile membranes.* Journal of Membrane Science, 2004. **243**(1-2): p. 45-57.
248. Xu, Z.L., T.S. Chung, and Y. Huang, *Effect of polyvinylpyrrolidone molecular weights on morphology, oil/water separation, mechanical and thermal properties of polyetherimide/polyvinylpyrrolidone hollow fiber membranes.* Journal of Applied Polymer Science, 1999. **74**(9): p. 2220-2233.
249. Meneghello, G., D.J. Parker, B.J. Ainsworth, S.P. Perera, J.B. Chaudhuri, M.J. Ellis, and P.A. De Bank, *Fabrication and characterization of poly(lactic-co-glycolic acid)/polyvinyl alcohol blended hollow fibre membranes for tissue engineering applications.* Journal of Membrane Science, 2009. **344**(1-2): p. 55-61.
250. Mulder, M., *Basic Principles of Membrane Technology*. 1990: Kluwer Academic Publishers.
251. Hong, P.D., C.M. Chou, and C.H. He, *Solvent effects on aggregation behavior of polyvinyl alcohol solutions.* Polymer, 2001. **42**(14): p. 6105-6112.
252. Kelly, S.T. and A.L. Zydney, *Mechanisms for Bsa Fouling during Microfiltration.* Journal of Membrane Science, 1995. **107**(1-2): p. 115-127.
253. Persson, A., A.S. Jonsson, and G. Zacchi, *Transmission of BSA during cross-flow microfiltration: influence of pH and salt concentration.* Journal of Membrane Science, 2003. **223**(1-2): p. 11-21.
254. Nakamura, K. and K. Matsumoto, *Properties of protein adsorption onto pore surface during microfiltration: Effects of solution environment and membrane hydrophobicity*. Journal of Membrane Science, 2006. **280**(1-2): p. 363-374.
255. Mantero, S.P., D; Vesentini, S; Montevecchi, F M, *Endothelial cell adhesion force estimation at the nanoscale.* . J Appl Biomater Biomech, 2005. **3**(1): p. 42-9
256. Lehenkari, P.H., MA, *Single integrin molecule adhesion forces in intact cells measured by atomic force microscopy* Biochemical and Biophysical Research Communications, 1999. **259**(3): p. 645-650.
257. Simon, A.N., LD; Le-Clech, P; Khan, SJ; Drewes, JE, *Effects of membrane degradation on the removal of pharmaceutically active compounds (PhACs) by NF/RO filtration processes* Journal of Membrane Science, 2009. **340**(1-2): p. 16-25.
258. Jiao, Y.P. and F.Z. Cui, *Surface modification of polyester biomaterials for tissue engineering.* Biomedical Materials, 2007. **2**(4): p. R24-R37.
259. Tees, D.G., DJ, *Leukocyte adhesion: An exquisite balance of hydrodynamic and molecular forces* News in physiological sciences, 2003. **18**: p. 186-190.
260. Ji GZ, W.X., Chen G, *Growth of Human Umbilical Cord Wharton's Jelly-Derived Mesenchymal Stem Cells on the Terpolyester Poly(3-*

hydroxybutyrate-co-3-hydroxyvalerateco-3-hydroxyhexanoate). Journal of Biomaterials Science-Polymer Edition, 2009. **20**: p. 325-339.
261. Haniffa, M.A., X.N. Wang, U. Holtick, M. Rae, J.D. Isaacs, A.M. Dickinson, C.M.U. Hilkens, and M.P. Collin, *Adult human fibroblasts are potent immunoregulatory cells and functionally equivalent to mesenchymal stem cells.* Journal of Immunology, 2007. **179**(3): p. 1595-1604.
262. Haniffa, M.A., M.P. Collin, C.D. Buckley, and F. Dazzi, *Mesenchymal stem cells: the fibroblasts' new clothes?* Haematologica-the Hematology Journal, 2009. **94**(2): p. 258-263.
263. Miltenyi Biotec. 2009 [cited 27-06-2010]; Available from: http://www.miltenyibiotec.com/download/datasheets/625/DS130-092-291-867.pdf.
264. CET. 2010 cited 26-06-2010]; Available from: http://celleng-tech.com/index/bmsc.html.
265. Hamamatsu Corporation. 2010 [cited 26-06-2010]; Available from: http://www.cimaging.net/applications/examples/fibroblast.php.
266. Thompson, M. 2010 [cited 26-06-2010]; Available from: www.eng.ox.ac.uk/obme/images/flexcell_obs.jpg.
267. Lee, K.H., G.H. Kwon, S.J. Shin, J.Y. Baek, D.K. Han, Y. Park, and S.H. Lee, *Hydrophilic electrospun polyurethane nanofiber matrices for hMSC culture in a microfluidic cell chip.* Journal of Biomedical Materials Research Part A, 2009. **90A**(2): p. 619-628.
268. Barrias, C.C., M.C.L. Martins, G. Almeida-Porada, M.A. Barbosa, and P.L. Granja, *The correlation between the adsorption of adhesive proteins and cell behaviour on hydroxyl-methyl mixed self-assembled monolayers.* Biomaterials, 2009. **30**(3): p. 307-316.
269. Nisbet, D.R., L.M.Y. Yu, T. Zahir, J.S. Forsythe, and M.S. Shoichet, *Characterization of neural stem cells on electrospun poly(epsilon-caprolactone) submicron scaffolds: evaluating their potential in neural tissue engineering.* Journal of Biomaterials Science-Polymer Edition, 2008. **19**(5): p. 623-634.
270. Gomathi, N., D. Mishra, T.K. Maiti, and S. Neogi, *Enhanced Cell Adhesion to Helium Plasma-Treated Polypropylene.* Journal of Adhesion Science and Technology, 2009. **23**(13-14): p. 1861-1874.
271. Bauer, S., J. Park, K. von der Mark, and P. Schmuki, *Improved attachment of mesenchymal stem cells on super-hydrophobic TiO2 nanotubes.* Acta Biomaterialia, 2008. **4**(5): p. 1576-1582.
272. Lee, J.H., G. Khang, J.W. Lee, and H.B. Lee, *Interaction of different types of cells on polymer surfaces with wettability gradient.* Journal of Colloid and Interface Science, 1998. **205**(2): p. 323-330.
273. Yoon, H., S.H. Ahn, and G.H. Kim, *Three-Dimensional Polycaprolactone Hierarchical Scaffolds Supplemented with Natural Biomaterials to Enhance Mesenchymal Stem Cell Proliferation.* Macromolecular Rapid Communications, 2009. **30**(19): p. 1632-1637.
274. Rentsch, B., A. Hofmann, A. Breier, C. Rentsch, and D. Scharnweber, *Embroidered and Surface Modified Polycaprolactone-Co-Lactide Scaffolds as Bone Substitute: In Vitro Characterization.* Annals of Biomedical Engineering, 2009. **37**(10): p. 2118-2128.
275. Yu, B.Y., S.W. Hu, Y.M. Sun, Y.T. Lee, and T.H. Young, *Modulating the Activities of Human Mesenchymal Stem Cells (hMSCs) and C3A/HepG2*

Hepatoma Cells by Modifying the Surface Characteristics of Poly(3-hydroxybutyrate-co-3-hydroxyhexnoate) (PHBHHx). Journal of Biomaterials Science-Polymer Edition, 2009. **20**(9): p. 1275-1293.
276. Curran, J.M., Z. Tang, and J.A. Hunt, *PLGA doping of PCL affects the plastic potential of human mesenchymal stem cells, both in the presence and absence of biological stimuli.* Journal of Biomedical Materials Research Part A, 2009. **89A**(1): p. 1-12.
277. Chastain, S.R., A.K. Kundu, S. Dhar, J.W. Calvert, and A.J. Putnam, *Adhesion of mesenchymal stem cells to polymer scaffolds occurs via distinct ECM ligands and controls their osteogenic differentiation.* Journal of Biomedical Materials Research Part A, 2006. **78A**(1): p. 73-85.
278. Haefner, J., *Modeling Biological Systems: Principles and Applications, Second Edition*. 2005, New York: Springer,. 480.
279. Siegwart P, C.J., Male K, Luong JHT, Perrier M, Kamen A, *Adaptive control at low glucose concentration of HEK-293 cell serum-free cultures* Biotechnology Progress, 1999. **15**(4): p. 608-616.
280. Lim, J.Y., M.C. Shaughnessy, Z.Y. Zhou, H. Noh, E.A. Vogler, and H.J. Donahue, *Surface energy effects on osteoblast spatial growth and mineralization.* Biomaterials, 2008. **29**(12): p. 1776-1784.
281. Chang, E.J., H.H. Kim, J.E. Huh, I.A. Kim, J.S. Ko, C.P. Chung, and H.M. Kim, *Low proliferation and high apoptosis of osteoblastic cells on hydrophobic surface are associated with defective Ras signaling.* Experimental Cell Research, 2005. **303**(1): p. 197-206.
282. http://i.ehow.com/images/GlobalPhoto/Articles/5106552/237258-main_Full.jpg.
283. Scanlon, V.C.S., T., *Essentials of anatomy and physiology*. 2003, Philadelphia: F.A. Davis Co.
284. Wheather P.R. , B.H.G., Lancaster P., *Colour atlas of histology*. 1985, Harlow Longman.
285. Palsson B, H.J., Plonsey R, Bronzno JD, *Tissue Engineering*. 2003, Boca Raton: CRC Press.
286. Tilles, A.W., F. Berthiaume, M.L. Yarmush, R.G. Tompkins, and M. Toner, *Bioengineering of liver assist devices.* J Hepatobiliary Pancreat Surg, 2002. **9**(6): p. 686-96.
287. Kinoshita, T. and A. Miyajima, *Cytokine regulation of liver development.* Biochimica Et Biophysica Acta-Molecular Cell Research, 2002. **1592**(3): p. 303-312.
288. Schmidt, C., F. Bladt, S. Goedecke, V. Brinkmann, W. Zschiesche, M. Sharpe, E. Gherardi, and C. Birchmeier, *Scatter factor/hepatocyte growth-factor is essential for liver development* Nature, 1995. **373**(6516): p. 699-702.
289. Michalopoulos, G.K., *Liver regeneration.* Journal of Cellular Physiology, 2007. **213**: p. 286-300.
290. LaBrecque, *Liver regeneration: A picture emerges from the puzzle.* Am J Gastroenterol, 1994. **89**: p. (supplement) S86.
291. Schwartz, R.E., J.L. Linehan, M.S. Painschab, W.S. Hu, C.M. Verfaillie, and D.S. Kaufman, *Defined conditions for development of functional hepatic cells from human embryonic stem cells.* Stem Cells and Development, 2005. **14**(6): p. 643-655.
292. Hong, S.H., E.J. Gang, J.A. Jeong, C.Y. Ahn, S.H. Hwang, I.H. Yang, H.K. Park, H. Han, and H. Kim, *In vitro differentiation of human umbilical cord*

blood-derived mesenchymal stem cells'into hepatocyte-like cells. Biochemical and Biophysical Research Communications, 2005. **330**(4): p. 1153-1161.
293. Ong, S.Y., H. Dai, and K.W. Leong, *Inducing hepatic differentiation of human mesenchymal stem cells in pellet culture.* Biomaterials, 2006. **27**(22): p. 4087-4097.
294. Nishino, T., N. Kaise, Y. Sindo, N. Nishino, T. Nishida, S. Yasuda, and Y. Masui, *Promyelocytic leukemia-cell line, HL-60, produces human hepatocyte growth factor* Biochemical and Biophysical Research Communications, 1991. **181**(1): p. 323-330.
295. Taichman, R.S., M.J. Reilly, R.S. Verma, K. Ehrenman, and S.G. Emerson, *Hepatocyte growth factor is secreted by osteoblasts and cooperatively permits the survival of haematopoietic progenitors.* British Journal of Haematology, 2001. **112**(2): p. 438-448.
296. Lesman, A., Y. Blinder, and S. Levenberg, *Modeling of Flow-Induced Shear Stress Applied on 3D Cellular Scaffolds: Implications for Vascular Tissue Engineering.* Biotechnology and Bioengineering, 2010. **105**(3): p. 645-654.
297. Groen, H.C., F.J.H. Gijsen, A. van der Lugt, M.S. Ferguson, T.S. Hatsukami, A.F.W. van der Steen, C. Yuan, and J.J. Wentzel, *Plaque rupture in the carotid artery is localized at the high shear stress region - A case report.* Stroke, 2007. **38**(8): p. 2379-2381.
298. Sakamoto, N., T. Ohashi, and M. Sato, *Effect of fluid shear stress on migration of vascular smooth muscle cells in cocultured model.* Annals of Biomedical Engineering, 2006. **34**(3): p. 408-415.
299. McDowell, C.L. and E.T. Papoutsakis, *Increased agitation intensity increases CD13 receptor surface content and mRNA levels, and alters the metabolism of HL60 cells cultured in stirred tank bioreactors.* Biotechnology and Bioengineering, 1998. **60**(2): p. 239-250.
300. White, C.F., JA, *The shear stress of it all: the cell membrane and mechanochemical transduction* Philosophical transactions of the royal society B-biological sciences 2007. **362**(1484): p. 1459-1467.
301. L&K-Biosciences. *The L&K process guide- protein stability*. 2010 26-06-2010 [cited; Available from: http://www.lk-processguide.com/proteinstability.php.
302. Ashton, L., J. Dusting, E. Imomoh, S. Balabani, and E.W. Blanch, *Shear-Induced Unfolding of Lysozyme Monitored In Situ.* Biophysical Journal, 2009. **96**(10): p. 4231-4236.
303. Kiese, S., A. Papppenberger, W. Friess, and H.C. Mahler, *Shaken, not stirred: Mechanical stress testing of an IgG1 antibody.* Journal of Pharmaceutical Sciences, 2008. **97**(10): p. 4347-4366.
304. Szymczak, P. and M. Cieplak, *Proteins in a shear flow.* Journal of Chemical Physics, 2007. **127**.
305. Biddlecombe, J.G., A.V. Craig, H. Zhang, S. Uddin, S. Mulot, B.C. Fish, and D.G. Bracewell, *Determining antibody stability: Creation of solid-liquid interfacial effects within a high shear environment.* Biotechnology Progress, 2007. **23**(5): p. 1218-1222.
306. Cromwell, M.E.M., E. Hilario, and F. Jacobson, *Protein aggregation and bioprocessing.* Aaps Journal, 2006. **8**(3): p. E572-E579.
307. Verma, R., E. Boleti, and A.J.T. George, *Antibody engineering: Comparison of bacterial, yeast, insect and mammalian expression systems.* Journal of Immunological Methods, 1998. **216**(1-2): p. 165-181.

308. Wang, M.Y., Y.H. Yang, H.S. Lee, and S.Y. Lai, *Production of functional hepatocyte growth factor (HGF) in insect cells infected with an HGF-recombinant baculovirus in a serum-free medium.* Biotechnology Progress, 2000. **16**(2): p. 146-151.
309. Jarvis, D.L., *Baculovirus-insect cell expression systems* Guide to Protein Purification, Second Edition, 2009. **466**: p. 191-222.
310. Brondyk, W.H., *Selecting an appropriate method for expressing a recombinant protein* Guide to Protein Purification, Second Edition, 2009. **466**: p. 131-147.
311. Chamuleau, R.A., T. Deurholt, and R. Hoekstra, *Which are the right cells to be used in a bioartificial liver?* Metab Brain Dis, 2005. **20**(4): p. 327-35.
312. Baquerizo, A., A. Mhoyan, A. Kearns-Jonker, W.S. Arnaout, C. Shackleton, R.W. Busuttil, A.A. Demetriou, and D.V. Cramer, *Characterization of human xenoreactive antibodies in liver failure patients exposed to pig hepatocytes after bioartificial liver treatment - An ex vivo model of pig to human xenotransplantation.* Transplantation, 1999. **67**(1): p. 5-18.
313. van de Kerkhove, M.P., M.R. Germans, T. Deurholt, R. Hoekstra, D.H. Joziasse, A.C. van Wijk, T.M. van Gulik, R.A. Chamuleau, and A. Roos, *Evidence for Galalpha(1-3)Gal expression on primary porcine hepatocytes: implications for bioartificial liver systems.* J Hepatol, 2005. **42**(4): p. 541-7.
314. Fishman, J.A. and C. Patience, *Xenotransplantation: infectious risk revisited.* Am J Transplant, 2004. **4**(9): p. 1383-90.
315. Kelly, J.H. and G.J. Darlington, *Modulation of the liver specific phenotype in the human hepatoblastoma line HEP-G2.* In Vitro Cellular & Developmental Biology, 1989. **25**(2): p. 217-222.
316. Wang, L.S., J.H. Sun, L. Li, D. Mears, M. Horvat, and A.G.R. Sheil, *Comparison of porcine hepatocytes with human hepatoma (C3A) cells for use in a bioartificial liver support system.* Cell Transplantation, 1998. **7**(5): p. 459-468.
317. Liu, J., J. Pan, S. Naik, H. Santangini, D. Trenkler, N. Thompson, A. Rifai, J.R. Chowdhury, and H.O. Jauregui, *Characterization and evaluation of detoxification functions of a nontumorigenic immortalized porcine hepatocyte cell line (HepLiu).* Cell Transplantation, 1999. **8**(3): p. 219-232.
318. Yoon, J.H., N.V.S. Lee, J.S. Lee, J.B. Park, and C.Y. Kim, *Development of a non-transformed human liver cell line with differentiated-hepatocyte and urea-synthetic functions: applicable for bioartificial liver.* International Journal of Artificial Organs, 1999. **22**(11): p. 769-777.
319. Kobayashi, N., M. Miyazaki, K. Fukaya, Y. Inoue, M. Sakaguchi, T. Uemura, H. Noguchi, A. Kondo, N. Tanaka, and M. Namba, *Transplantation of highly differentiated immortalized human hepatocytes to treat acute liver failure.* Transplantation, 2000. **69**(2): p. 202-207.
320. Kobayashi, N., T. Okitsu, S. Nakaji, and N. Tanaka, *Hybrid bioartificial liver: establishing a reversibly immortalized human hepatocyte line and developing a bioartificial liver for practical use.* J Artif Organs, 2003. **6**(4): p. 236-44.
321. Cascio, S.M., *Novel strategies for immortalization of human hepatocytes.* Artif Organs, 2001. **25**(7): p. 529-38.
322. Soto-Gutierrez, A., N. Kobayashi, J.D. Rivas-Carrillo, N. Navarro-Alvarez, D.B. Zhao, T. Okitsu, H. Noguchi, H. Basma, Y. Tabata, Y. Chen, K. Tanaka, M. Narushima, A. Miki, T. Ueda, H.S. Jun, J.W. Yoon, J. Lebkowski, N.

Tanaka, and I.J. Fox, *Reversal of mouse hepatic failure using an implanted liver-assist device containing ES cell-derived hepatocytes.* Nature Biotechnology, 2006. **24**(11): p. 1412-1419.
323. Amano, T., M. Gertsenstein, A. Nagy, H. Kurihara, and H. Suzuki, *Nuclear transfer reprogramming does not improve the low developmental potency of embryonic stem cells induced by long-term culture.* Reproduction, 2006. **132**(2): p. 257-263.
324. Metallo, C.M., S.M. Azarin, L. Ji, J.J. de Pablo, and S.P. Palecek, *Engineering tissue from human embryonic stem cells.* Journal of Cellular and Molecular Medicine, 2008. **12**(3): p. 709-729.
325. Theise, N.D., R. Saxena, B.C. Portmann, S.N. Thung, H. Yee, L. Chiriboga, A. Kumar, and J.M. Crawford, *The canals of Hering and hepatic stem cells in humans.* Hepatology, 1999. **30**(6): p. 1425-33.
326. Dabeva, M.D., S.G. Hwang, S.R. Vasa, E. Hurston, P.M. Novikoff, D.C. Hixson, S. Gupta, and D.A. Shafritz, *Differentiation of pancreatic epithelial progenitor cells into hepatocytes following transplantation into rat liver.* Proc Natl Acad Sci U S A, 1997. **94**(14): p. 7356-61.
327. Li, W.L., J. Su, Y.C. Yao, X.R. Tao, Y.B. Yan, H.Y. Yu, X.M. Wang, J.X. Li, Y.J. Yang, J.T.Y. Lau, and Y.P. Hu, *Isolation and characterization of bipotent liver progenitor cells from adult mouse.* Stem Cells, 2006. **24**(2): p. 322-332.
328. Sumitran-Holgersson, S., G. Nowak, S. Thowfeequ, S. Begum, M. Joshi, M. Jaksch, A. Kjaeldgaard, C. Jorns, B.G. Ericzon, and D. Tosh, *Generation of Hepatocyte-Like Cells From In Vitro Transdifferentiated Human Fetal Pancreas.* Cell Transplantation, 2009. **18**(2): p. 183-193.
329. Santin, M., *Strategies in regenerative medicine: integrating biology with materials design* ed. S. M. 2009, New York ; London Springer.
330. Chan, C., F. Berthiaume, B.D. Nath, A.W. Tilles, M. Toner, and M.L. Yarmush, *Hepatic tissue engineering for adjunct and temporary liver support: Critical technologies.* Liver Transplantation, 2004. **10**(11): p. 1331-1342.
331. Trowbridge, I.S. and M.L. Thomas, *CD45 - an emerging role as a protein-tyrosine-phosphatase required for lymphocyte-activation and development* Annual Review of Immunology, 1994. **12**: p. 85-116.
332. Chamberlain, G., J. Fox, B. Ashton, and J. Middleton, *Concise review: Mesenchymal stem cells: Their phenotype, differentiation capacity, immunological features, and potential for homing.* Stem Cells, 2007. **25**: p. 2739-2749.
333. Jackson, D.G., *Immunological functions of hyaluronan and its receptors in the lymphatics.* Immunological Reviews, 2009. **230**: p. 216-231.
334. Yovchev, M., P. Grozdanov, H. Zhou, C. Guha, and M. Dabeva, *Identification of adult rat hepatic progenitor cells that can reconstitute the liver.* Faseb Journal, 2007. **21**(5): p. A70-A70.
335. Boumaza, I., S. Srinivasan, W.T. Witt, C. Feghali-Bostwick, Y.F. Dai, A. Garcia-Ocana, and M. Feili-Hariri, *Autologous bone marrow-derived rat mesenchymal stem cells promote PDX-1 and insulin expression in the islets, alter T cell cytokine pattern and preserve regulatory T cells in the periphery and induce sustained normoglycemia.* Journal of Autoimmunity, 2009. **32**(1): p. 33-42.

336. Toole, B.P., *Hyaluronan-CD44 Interactions in Cancer: Paradoxes and Possibilities.* Clinical Cancer Research, 2009. **15**(24): p. 7462-7468.
337. Hwang-Verslues, W.W., W.H. Kuo, P.H. Chang, C.C. Pan, H.H. Wang, S.T. Tsai, Y.M. Jeng, J.Y. Shew, J.T. Kung, C.H. Chen, E. Lee, K.J. Chang, and W.H. Lee, *Multiple Lineages of Human Breast Cancer Stem/Progenitor Cells Identified by Profiling with Stem Cell Markers.* Plos One, 2009. **4**(12).
338. Immunotools. 2010 [cited 25-06-2010]; Available from: www.immunotools.com.
339. Schugar, R.C., S.M. Chirieleison, K.E. Wescoe, B.T. Schmidt, Y. Askew, J.J. Nance, J.M. Evron, B. Peault, and B.M. Deasy, *High Harvest Yield, High Expansion, and Phenotype Stability of CD146 Mesenchymal Stromal Cells from Whole Primitive Human Umbilical Cord Tissue.* Journal of Biomedicine and Biotechnology, 2009.
340. Wetzel, A., T. Wetzig, U.F. Haustein, M. Sticherling, U. Anderegg, J.C. Simon, and A. Saalbach, *Increased neutrophil adherence in psoriasis: Role of the human endothelial cell receptor Thy-1 (CD90).* Journal of Investigative Dermatology, 2006. **126**(2): p. 441-452.
341. Kisselbach, L., M. Merges, A. Bossie, and A. Boyd, *CD90 Expression on human primary cells and elimination of contaminating fibroblasts from cell cultures.* Cytotechnology, 2009. **59**(1): p. 31-44.
342. AbDSerotech. [cited 2010 25-06-2010]; Available from: www.abdserotec.com/uploads/Flow-Cytometry.pdf.
343. Kon, J., N. Ichinohe, H. Ooe, Q. Chen, K. Sasaki, and T. Mitaka, *Thy1-Positive Cells Have Bipotential Ability to Differentiate into Hepatocytes and Biliary Epithelial Cells in Galactosamine-induced Rat Liver Regeneration.* American Journal of Pathology, 2009. **175**(6): p. 2362-2371.
344. Boku, S., S. Nakagawa, T. Masuda, H. Nishikawa, A. Kato, Y. Kitaichi, T. Inoue, and T. Koyama, *Glucocorticoids and Lithium Reciprocally Regulate the Proliferation of Adult Dentate Gyrus-Derived Neural Precursor Cells Through GSK-3 beta and beta-Catenin/TCF Pathway.* Neuropsychopharmacology, 2009. **34**(3): p. 805-815.
345. Lincks, J., B.D. Boyan, C.R. Blanchard, C.H. Lohmann, Y. Liu, D.L. Cochran, D.D. Dean, and Z. Schwartz, *Response of MG63 osteoblast-like cells to titanium and titanium alloy is dependent on surface roughness and composition.* Biomaterials, 1998. **19**(23): p. 2219-2232.
346. Lohmann, C.H., L.F. Bonewald, M.A. Sisk, V.L. Sylvia, D.L. Cochran, D.D. Dean, B.D. Boyan, and Z. Schwartz, *Maturation state determines the response of osteogenic cells to surface roughness and 1,25-dihydroxyvitamin D-3.* Journal of Bone and Mineral Research, 2000. **15**(6): p. 1169-1180.
347. Stewart, T.L., P. Roschger, B.M. Misof, V. Mann, P. Fratzl, K. Klaushofer, R. Aspden, and S.H. Ralston, *Association of COLIA1 Sp1 alleles with defective bone nodule formation in vitro and abnormal bone mineralization in vivo.* Calcified Tissue International, 2005. **77**(2): p. 113-118.
348. Fosset, C., R. Danzeisen, L. Gambling, B.A. McGaw, and H.J. McArdle, *Cu loading alters expression of non-IRE regulated, but not IRE regulated, Fe dependent proteins in HepG2 cells.* Journal of Inorganic Biochemistry, 2009. **103**(5): p. 709-716.
349. Wanson, J.C., P. Drochmans, C. May, W. Penasse, and A. Popowski, *Isolation of centrolobular and perilobular hepatocytes after phenobarbital treatment* Journal of Cell Biology, 1975. **66**(1): p. 23-41.

350. Chivu, M., S.O. Dima, C.I. Stancu, C. Dobrea, V. Uscatescu, L.G. Necula, C. Bleotu, C. Tanase, R. Albulescu, C. Ardeleanu, and I. Popescu, *In vitro hepatic differentiation of human bone marrow mesenchymal stem cells under differential exposure to liver-specific factors.* Translational Research, 2009. **154**(3): p. 122-132.
351. Xie, C., Y.B. Zheng, H.P. Zhu, L. Peng, and Z.L. Gao, *Human bone marrow mesenchymal stem cells are resistant to HBV infection during differentiation into hepatocytes in vivo and in vitro.* Cell Biology International, 2009. **33**(4): p. 493-500.
352. Gu, J.Y., X.L. Shi, Y. Zhang, X.H. Chu, H.L. Hang, and Y.T. Ding, *Establishment of a three-dimensional co-culture system by porcine hepatocytes and bone marrow mesenchymal stem cells in vitro.* Hepatology Research, 2009. **39**(4): p. 398-407.
353. Li, T.Z., S.H. Shin, H.H. Cho, J.H. Kim, and H. Suh, *Growth Factor-Free Cultured Rat Bone Marrow Derived Mesenchymal Stem Cells towards Hepatic Progenitor Cell Differentiation.* Biotechnology and Bioprocess Engineering, 2008. **13**(6): p. 659-665.
354. Luk, J.M., P.P. Wang, C.K. Lee, J.H. Wang, and S.T. Fan, *Hepatic potential of bone marrow stromal cells: Development of in vitro co-culture and intra-portal transplantation models.* Journal of Immunological Methods, 2005. **305**(1): p. 39-47.
355. Park, K.S., S.M. Kim, M.S. Kim, I. Lee, J.M. Rhee, H.B. Lee, and G. Khang, *Effect of cell-adhesive-molecule-coated poly(lactide-co-glycolide) film on the cellular Behaviors of olfactory ensheathing cells and Schwann cells.* Journal of Applied Polymer Science, 2008. **107**(2): p. 1243-1251.
356. Furth, M.E., A. Atala, and M.E. Van Dyke, *Smart biomaterials design for tissue engineering and regenerative medicine.* Biomaterials, 2007. **28**(34): p. 5068-5073.
357. Matsuda, C., M. Takagi, T. Hattori, S. Wakitani, and T. Yoshida, *Differentiation of human bone marrow mesenchymal stem cells to chondrocytes for construction of three-dimensional cartilage tissue.* Cytotechnology, 2005. **47**(1-3): p. 11-17.
358. Dai, W.D., N. Kawazoe, X.T. Lin, J. Dong, and G.P. Chen, *The influence of structural design of PLGA/collagen hybrid scaffolds in cartilage tissue engineering.* Biomaterials. **31**(8): p. 2141-2152.
359. Liu, F., Y. Akiyama, S. Tai, K. Maruyama, Y. Kawaguchi, K. Muramatsu, and K. Yamaguchi, *Changes in the expression of CD106, osteogenic genes, and transcription factors involved in the osteogenic differentiation of human bone marrow mesenchymal stem cells.* Journal of Bone and Mineral Metabolism, 2008. **26**(4): p. 312-320.
360. Mauck, R.L., M.A. Soltz, C.C.B. Wang, D.D. Wong, P.H.G. Chao, W.B. Valhmu, C.T. Hung, and G.A. Ateshian, *Functional tissue engineering of articular cartilage through dynamic loading of chondrocyte-seeded agarose gels.* Journal of Biomechanical Engineering-Transactions of the Asme, 2000. **122**(3): p. 252-260.
361. Powell, C.A., B.L. Smiley, J. Mills, and H.H. Vandenburgh, *Mechanical stimulation improves tissue-engineered human skeletal muscle.* American Journal of Physiology-Cell Physiology, 2002. **283**(5): p. C1557-C1565.
362. Pazzano, D., K.A. Mercier, J.M. Moran, S.S. Fong, D.D. DiBiasio, J.X. Rulfs, S.S. Kohles, and L.J. Bonassar, *Comparison of chondrogensis in static and*

perfused bioreactor culture. Biotechnology Progress, 2000. **16**(5): p. 893-896.

Appendix

Flow cytometry dot plots

FSC: forward scatter, provides information on cell size

SSC: side scatter, provides information on cell granularity

P1: population of live cells

Dot plot for IgG2 control FITC conjugated

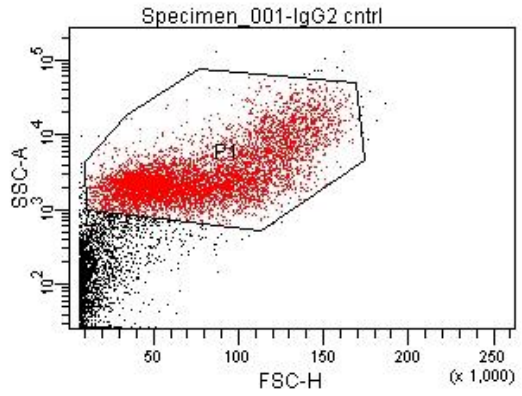

Specimen Name: Specimen_001
Tube Name: igG2F

Population	#Events	%Total	FITC-H Mean	PE-H Mean
All Events	1,070	100.0	89	172
P1	588	55.0	81	155

Dot plot for CD44 marker, FITC conjugated

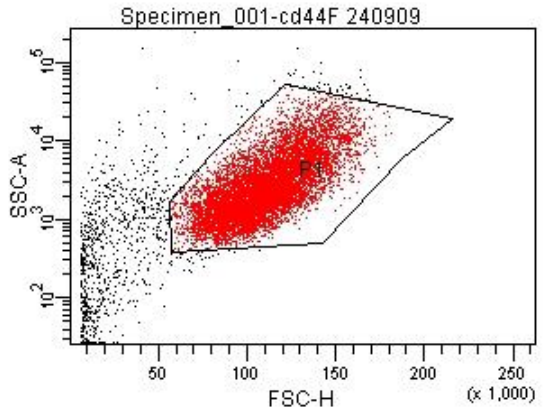

Specimen Name: Specimen_001
Tube Name: cd44F 240909

Population	#Events	%Total	FITC-H Mean	PE-H Mean
All Events	10,000	100.0	210	182
P1	9,053	90.5	213	182

Dot plot for CD45 marker, FITC conjugated

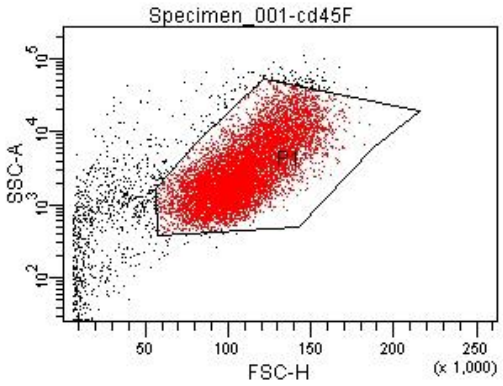

Specimen Name: Specimen_001
Tube Name: cd45F

Population	#Events	%Total	FITC-H Mean	PE-H Mean
All Events	10,000	100.0	90	106
P1	8,986	89.9	81	96

Dot plot for IgG1 control PE conjugated

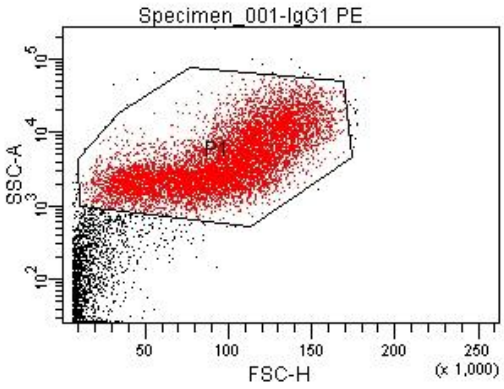

Specimen Name: Specimen_001
Tube Name: IgG1 PE

Population	#Events	%Total	FITC-H Mean	PE-H Mean
All Events	10,000	100.0	64	130
P1	8,167	81.7	73	143

Dot plot for CD90 marker, PE conjugated

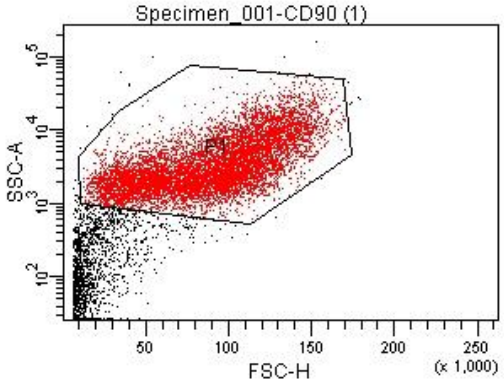

Specimen Name: Specimen_001
Tube Name: CD90 (1)

Population	#Events	%Total	FITC-H Mean	PE-H Mean
All Events	10,000	100.0	167	25,290
P1	8,154	81.5	195	30,227